UNIVERSITY OF MEDICINE AND HEALTH SCIENCES

Royal College of Surgeons in Ireland

repository@rcsi.com

The role of the anorectic neuropeptide CART in breast cancer

AUTHOR(S)

Brian Mooney

CITATION

Mooney, Brian (2018): The role of the anorectic neuropeptide CART in breast cancer. Royal College of Surgeons in Ireland. Thesis. https://doi.org/10.25419/rcsi.10802597.v1

DOI

10.25419/rcsi.10802597.v1

LICENCE

CC BY-NC-SA 4.0

This work is made available under the above open licence by RCSI and has been printed from https://repository.rcsi.com. For more information please contact repository@rcsi.com

URL

https://repository.rcsi.com/articles/thesis/The_role_of_the_anorectic_neuropeptide_CART_in_breast_cancer/10802597/1

The role of the anorectic neuropeptide CART in breast cancer

Brian Mooney, BSc

Department of Molecular and Cellular Therapeutics

A thesis submitted to the school of Postgraduate Studies, Faculty of Medicine and Health Sciences, Royal College of Surgeons in Ireland, in fulfilment of the degree of Doctor of Philosophy

Supervisor: Dr Darran O'Connor

Co-Supervisor: Dr Triona Ni Chonghaile

May 2018

Candidate Thesis Declaration

I declare that this thesis, which I submit to RCSI for examination in consideration of the award of a higher degree (Doctor of Philosophy) is my own personal effort. Where any of the content presented is the result of input or data from a related collaborative research programme this is duly acknowledged in the text such that it is possible to ascertain how much work of the work is my own. I have not already obtained a degree in RCSI or elsewhere on the basis of this work. Furthermore, I took reasonable care to ensure that the work is original, and, to the best of my knowledge, does not breach copyright law, and has not been taken from other sources except where such work has been cited and acknowledged within the text.

Signed

Student number

Date

Figures

Chapter 1

Figure 1.1. Breast cancer was the most commonly diagnosed cancer in women between the years of 2015 and 2017.

Figure 1.2. Progression of a normal duct, to ductal carcinoma in-situ (DCIS), to invasive carcinoma.

Figure 1.3. Advances in the management of cancer with chemotherapy.

Figure 1.4 Various immunotherapeutic agents currently in clinical trials function by disrupting the PD1-PDL1 interaction between T cells and cancer cells, resulting in the recognition and destruction of the cancer cells.

Figure 1.5. Schematic diagram of functional domains contained within ERα.

Figure 1.6. Aromatase inhibitors function by blocking the conversion of pre-estrogen hormones to estrogen.

Figure 1.7. 5-year net survival percentages for breast cancer patients based on stage of cancer.

Figure 1.8. The CART gene contains multiple binding sites for transcriptional regulation.

Figure 1.9. CART has previously been identified to signal through ERK, as well as CREB, putatively via a Gi/Go linked GPCR.

Figure 1.10. Insulin and Leptin can positively influence CART-containing neurons to inhibit food intake.

Figure 1.11. Shcherbina and colleagues demonstrated that silencing of CART had drastic effects on the normal function of pancreatic beta cells.

Chapter 2

Figure 2.1. The diagram above shows how the western blot transfer sandwich is assembled.

Figure 2.2. Diagram showing the principle of chemiluminescent signal generation during western blot analysis.

Figure 2.3. Reactions carried out during the dual luciferase reporter assay

Figure 2.4. Perseus workflow carried out to generate the working matrix, matrix 7.

Figure 2.5. Diagram showing how the optimal transfection conditions were determined using the siGLO transfection control.

Chapter 3

Figure 3.1. CART can alter the function of ERα

Figure 3.2. Typical workflow of a ChIP-seq experiment.

Figure 3.3. CART increases the phosphorylation of ERK, and increases the expression of ERα target genes.

Figure 3.4. Patients in both METABRIC and TCGA datasets with high levels of CART have significantly higher levels of many ERα target genes

Figure 3.5. X-Gal is broken down by active galactosidase to produce blue bacterial colonies, indicating a successful site-directed mutagenesis protocol.

Figure 3.6. Conformation of successful site-directed mutagenesis.

Figure 3.7. Ectopic expression of CMV plasmids in MCF7 cells confirms CART is still expressed following mutating each LXD motif.

Figure 3.8. Introducing mutations into LXD motifs within CART alters ERα function.

Figure 3.9. Cells show an increased expression of CART following treatment with increasing concentrations of doxycycline.

Figure 3.10. Three independent experiments were used for RNA-sequencing analysis.

Figure 3.11. PCA highlights the grouping pattern for each individual treatment group, and each biological replicate.

Figure 3.12. Z-score heatmap reveals 2 distinct clusters, highlighting the 100 significantly upregulated, and 156 significantly downregulated genes, following CART expression.

Figure 3.13. Genes upregulated by CART are mainly involved in biological processes associated with transcription.

Figure 3.14. The molecular function of genes upregulated by CART are mainly involved in function such as DNA binding and transcription.

Figure 3.15. Genes upregulated by CART are associated with tobacco-use disorder and obesity.

Figure 3.16. GSEA of genes significantly upregulated by CART.

Figure 3.17. CART treatment results in an increase of cells in the S and G2/M phases of the cell cycle.

Figure 3.18. Genes downregulated by CART are associated with a wide range of biological processes, such as cell-cell adhesion, glycolysis and NIK/NF-kappaB signalling.

Figure 3.19. Genes downregulated by CART are associated with acquired immunodeficiency syndrome / disease progression.

Figure 3.20. Top 10 genes identified as ERα target genes in the upregulated dataset.

Figure 3.21. Top 10 genes identified as ERα target genes in the downregulated dataset.

Figure 3.22. CART expression results in the significant increase of many genes identified via RNA sequencing.

Figure 3.23. Heatmap of Z-scores for the top 200 genes based on FPKMS difference.

Figure 3.24. GSEA reveals genes which are associated with anti-endocrine resistance, as well as genes which have been characterized as ER target genes.

Figure 3.25. Attempted validation of putative ESR1 target genes, as well as genes associated with anti-endocrine resistance.

Figure 3.26. Cellular response to tamoxifen, but not fulvestrant, is altered in cells expressing CART.

Figure 3.27. Graphical representation of CART signalling in ER+ breast cancer.

Chapter 4

Figure 4.1. Immunoprecipitating a target protein results in interacting partners also becoming purified.

Figure 4.2. CART is not a physical interactor of ERα.

Figure 4.3. Established workflow for mass spectrometry analysis following ERα immunoprecipitation.

Figure 4.4. Western blot analysis of immunoprecipitation samples used for mass spectrometry analysis.

Figure 4.5. Principal component analysis and hierarchical clustering of samples +/- CART expression (D-12 antibody)

Figure 4.6. Volcano plot of identified proteins in ERα immunoprecipitation samples +/- CART expression (D-12 antibody).

Figure 4.7. Principal component analysis and hierarchical clustering of samples +/- 1 nm E2 treatment (D-12 antibody).

Figure 4.8. Volcano plot of identified proteins in ERα immunoprecipitation samples +/- 1 nm E2 treatment (D-12 antibody).

Figure 4.9. Principal component analysis and hierarchical clustering of samples +/- CART expression (F-10 antibody)

Figure 4.10. Volcano plot of identified proteins in ERα immunoprecipitation samples +/- CART expression (F-10 antibody).

Figure 4.11. Principal component analysis and hierarchical clustering of samples +/- 1 nm E2 treatment (F-10 antibody).

Figure 4.12. Volcano plot of identified proteins in ERα immunoprecipitation samples +/- 1 nm E2 treatment (F-10 antibody).

Figure 4.13. There are no common interactors recruited to ERα by CART.

Figure 4.14. Principal component analysis (PCA) shows samples from F-10 antibody group closer with the IgG negative control samples than the D-12 antibody.

Figure 4.15. Proteins significantly recruited to ERα in the presence of CART are members of the “nucleic-acid binding” and “transcription factor” protein classes.

Figure 4.16. Proteins significantly recruited to ERα in the absence of CART are associated with protein transport/trafficking.

Figure 4.17. STRING diagram shows a previously reported interaction between ERα, ARID1A, SIN3B, SKP1 and SMARCD1.

Figure 4.18. HECTD4 and WIZ may be indirect interactors of ERα.

Figure 4.19. Confidence of the supporting data from figure 4.18.

Figure 4.20. Unsuccessful validation of an interaction between ERα, HECTD4 and WIZ.

Figure 4.21. ERα alpha levels are maintained at higher levels when cells are expressing CART.

Figure 4.22. CART expression results in the decreased turnover of ERα.

Figure 4.23. ERα levels in CHX treated cells were normalised to ERα levels in DMSO treated cells, and an increase in stability of ERα was still observed in the absence of estradiol.

Figure 4.24. Co-immunoprecipitation validation of interaction between SMARCD1 and ERα.

Figure 4.25. UNIPROT database highlights the presence of a signal peptide at the beginning of the CART protein.

Figure 4.26. The human protein atlas suggests GLUD1 is only expressed in the mitochondria of cells.

Figure 4.27. The recruitment of chromatin remodelling complexes to ERα may allow for the unwinding of chromatin structures and facilitate DNA binding.

Chapter 5

Figure 5.1. BAF complex subunits are mutated in a subunit, and cancer, specific manner.

Figure 5.2. *In silico* analysis of *SMARCD1* expression in a cohort of breast cancer patients.

Figure 5.3. High expression of *SMARCD1* expression is significantly associated with poor overall survival (OS), and distant metastasis-free survival (DMFS) in breast cancer patients.

Figure 5.4. High expression of *SMARCD1* is significantly associated with worse OS (A) and DMFS (B) in ER+, but not ER-, breast cancer patients.

Figure 5.5. *SMARCD1* copy number status is significantly correlated with worse OS in the TCGA dataset of 1076 breast cancer patients.

Figure 5.6. *SMARCD1* expression significantly correlates with poor survival in unstratified breast cancer patients within the TCGA dataset.

Figure 5.7. High protein expression of SMARCD1 indicates worse OS in the TCGA dataset.

Figure 5.8. High protein expression of SMARCD1 indicates worse OS in p53 mutant breast cancer patients.

Figure 5.9. Optimisation of siRNA transfection conditions using the reverse transfection protocol.

Figure 5.10. The DharmaFect transfection reagent was well tolerated across all concentrations.

Figure 5.11. SMARCD1 expression is decreased upon transfecting 4 individual, non-overlapping, siRNAs targeting SMARCD1.

Figure 5.12. Modulating the expression of *SMARCD1* alters the morphology of Tet-ON T47D cells.

Figure 5.13. SMARCD1 knockdown significantly alters the growth pattern of Tet-ON T47D cells.

Figure 5.14. *SMARCD1* knockdown results in altered expression of *PKIB*, but not *CCND1*.

Figure 5.15. SMARCD1 knockdown results in enhanced expression of certain genes identified via RNA-sequencing.

Figure 5.16. Modulation of SMARCD1 expression in un-induced cells does not sensitize cells to anti-endocrine therapy.

Figure 5.17. Modulation of SMARCD1 expression in DOX-induced cells does not sensitize cells to anti-endocrine therapy.

Figure 5.18. Members of the BAF-chromatin remodelling complex are upregulated in Anti-Endocrine resistant cell-line models.

Chapter 6

Figure 6.1. An overlap in transcription factor binding events is seen between ERα and SMARCB1, as well as between ERα and SMARCC1.

Figure 6.2 Possible models for how ERα interacts with WIZ

Figure 6.3. *HECTD4* expression is significantly higher in ER+ breast cancer, and correlates with poor survival.

Figure 6.4. Possible mechanisms by which CART can promote survival in the tumour microenvironment.

Appendices

Figure 1C. ERE-TATA Luciferase plasmid

Figure 2C. CMV-Renilla plasmid

Figure 3C. CMV6-XL5 (CMV-CART) plasmid

Figure 4C. PLVX-Tet-ON-ADVANCED plasmid

Figure 5C. PLVX-Tight-PURO plasmid

Tables

Chapter 1

Table 1.1. Molecular subtypes based on receptor expression status.

Chapter 2

Table 2.1. Volumes of each reagent needed to prepare 10 ml of an SDS-Polyacrylamide resolving gel.

Table 2.2. Volumes of each reagent needed to prepare 10 ml of an SDS-Polyacrylamide stacking gel

Table 2.3. Times and temperatures used for cDNA synthesis.

Table 2.4 Times and temperatures for qRT-PCR.

Table 2.5. PCR settings for site-directed mutagenesis protocol

Chapter 3

Table 3.1. Reference experiments used for identifying potential ERα target genes

Chapter 4

Table 4.1. Selectable interaction sources, and the representative colour for each source.

Chapter 5

Table 5.1. Subunits of the human BAF complex are either “ATP-ase”, “Core” or “Accessory” subunits.

Appendices

Table 1B. Antibodies used during studies.

Table 2B. Primer sequences used during studies

Table 3B. Primer sequences used to generate LXD-CART mutants

Table 4B. SMARCD1 siRNA sequences

Table 1D. Gene ontology (molecular function) of genes significantly upregulated by CART

Table 2D. Gene ontology (biological process) of genes significantly upregulated by CART

Table 3D. Gene ontology (GAD disease) of genes significantly upregulated by CART

Table 4D. Gene Set Enrichment Analysis (GSEA) of genes significantly upregulated by CART

Table 5D. Gene ontology (molecular function) of genes significantly downregulated by CART (top 20)

Table 6D. Gene ontology (biological process) of genes significantly downregulated by CART (top 20)

Table 7D. Gene ontology (GAD disease) of genes significantly downregulated by CART

Table 8D. GSEA of genes significantly downregulated by CART (top 20)

Table 9D. GSEA of top 200 genes upregulated by CART based on FPKMS difference. Top 50 gene sets are shown

Table 1E - +/- DOX, ERα D-12 antibody. All values are -log2 LFQ

Table 2E. +/- E2, ERα D-12 antibody. All values are -log2 LFQ

Table 3E, +/- DOX, ERα F-10 antibody. All values are -log2 LFQ

Table 4E, +/- E2, ERα F-10 antibody. All values are -log2 LFQ

Abbreviations

1D	One dimensional
ACN	Acetonitrile
AI	Aromatase Inhibitor
AIB1	Amplified in Breast cancer 1
ANOVA	Analysis of Variance
AP1	Activator Protein 1
AP2	Activator Protein 2
APS	Ammonium Persulfate
ARID1A	AT-Rich Interactive Domain-containing protein 1A
BAF	BRG1-associated factors
BCA	Bicinchoninic Acid
BMI	Body Mass Index
BRCA	Breast Cancer Associated gene
BSA	Bovine Serum Albumin
CAMP	Cyclic Adenosine Monophosphate
CAP2	Cyclase Associated Actin Cytoskeleton Regulatory Protein 2
CART	Cocaine-and Amphetamine- Regulated Transcript
CCND1	Cyclin D1
CDK	Cyclin Dependent Kinase
CDNA	Complementary Deoxyribonucleic Acid
ChIP	Chromatin Immunoprecipitation
ChIP-seq	Chromatin Immunoprecipitation Sequencing

CHX	Cycloheximide
CMV	Cytomegalovirus
CNS	Copy Number Status
Co-IP	Co-Immunoprecipitation
CRE	CAMP Responsive Element
CREB	CRE Binding Protein
ctDNA	Circulating Tumour DNA
CTRL	Control
DAVID	Database for Annotation Visualisation and Integrated Discovery
DCIS	Ductal Carcinoma In Situ
DE	Differential Expression
DMEM	Dulbecco's Modified Eagle's Medium
DMFS	Distant Metastasis Free Survival
DMP	Dimethylpirimophosphate
DMSO	Dimethylsulphoxide
DNA	Deoxyribonucleic Acid
DNTP	Deoxynucleotide Triphosphate
DOX	Doxycycline
E2	17β-Estradiol
EDTA	Ethylenediaminetetraacetic Acid
ECL	Enhanced Chemiluminescent
EGFR	Epidermal Growth Factor Receptor
ELF5	E74-linked factor 5
EMT	Epithelial-to-Mesenchymal Transition

EPA	Environmental Protection Agency
ERα	Estrogen Receptor alpha
ERE	Estrogen Responsive Element
ERK	Extracellular signal Related Kinase
ESR1	Estrogen Receptor 1
EtOH	Ethanol
FACS	Fluorescence Activated Cell Sorting
FBS	Fetal Bovine Serum
FDR	False Discovery Rate
FPKMS	Fragments Per Kilobase Per Million reads
GLUD1/2	Glutamate Dehydrogease 1/2
GO	Gene Ontology
GPCR	G-Protein Coupled Receptor
GREB	Growth Regulation by Estrogen in Breast cancer
GSEA	Gene Set Enrichment Analysis
HECTD4	HECT-Domain Containing Protein 4
HER2	Human Epidermal Growth Factor Receptor 2
HCl	Hydrochloric Acid
HPLC	High Performance Liquid Chromatography
HRP	Horseradish Peroxidase
HRT	Hormone Replacement Therapy
HSP90	Heat shock Protein 90
IHC	Immunohistochemistry
IDC	Invasive Ductal Carcinoma

IgG	Immunoglobulin G
ILC	Invasive Lobular Carcinoma
IP	Immunoprecipitation
IP-MS	Immunoprecipitation Mass Spectrometry
LFQ	Label Free Quantification
LCIS	Lobular Carcinoma In Situ
LB	Luria Bertani
MALAT1	Metastasis Associated Lung Adenocarcinoma Transcript 1
MAPK	Mitogen Activated Protein Kinase
METABRIC	Molecular Taxonomy of Breast Cancer International Consortium
MIR	Micro-Ribonucleic Acid
MRNA	Messenger Ribonucleic Acid
MS/MS	Tandem Mass spectrometry
MTT	3-(4,5-dimethylthiazol-2-yl)-2,5-diphenyltetrazolium bromide
MYOF	Myoferlin
NCOR1	Nuclear receptor Corepressor 1
NCRI	National Cancer Registry of Ireland
NPY	Neuropeptide Y
ORF	Open Reading Frame
OS	Overall Survival
PBS	Phosphate Buffered Saline
PCA	Principal component Analysis

PCR	Polymerise Chain Reaction
PD	Parkinson's Disease
PEG	Poly Ethylene Glycol
PGR	Progesterone Receptor
PI	Propidium Iodide
qRT-PCR	Quantitative Real-Time Polymerase Chain Reaction
RFS	Relapse Free Survival
RIN	RNA Integrity Number
RIPA	Radioimmunoprecipitation Assay
RNA	Ribonucleic Acid
RNA-seq	Ribonucleic Acid Sequencing
RPMI	Roswell Park Memorial Institute
RXRA	Retinoid-X Receptor Alpha
SD	Standard Deviation
SDH	Succinate Dehydrogenase
SDS	Sodium Dodecyl Sulphate
SEM	Standard Error of the Mean
SERD	Selective Estrogen Receptor Downregulator
SERM	Selective Estrogen Receptor Modulator
siRNA	Small interfering Ribonucleic Acid
SKP1	S-phase Kinase Protein 1
SMARC	SWI/SNF Related, Matrix Associated, Actin Dependent Regulator of Chromatin
SNP	Single Nucleotide Polymorphism
SRC1	Steroid Receptor Coactivator 1

SWI/SNF	Mating type SwItching and sucrose metabolism (Sucrose Non Fermentable)
TAILORx	Trial Assigning Individualized Options for Treatment
TCGA	The Cancer Genome Atlas
TEMED	Tetraethyaminediethylamine
TET	Tetracycline
TFA	Trifluroacetic Acid
TFF1	Trefoil Factor 1
TMA	Tissue Microarray
VDR	Vitamin-D Receptor
VEH	Vehicle
VEGF	Vascular Epidermal Growth Factor
WIZ	Widely Interspaced Zinc finger motifs
X-Gal	5-Bromo-4-Chloro-Indolyl β-D-Galactopyranoside

Summary

While survival rates for breast cancer patients in Ireland is on the rise, a significant proportion of women will unfortunately succumb to this malicious disease. Previously, we identified high expression of the neuropeptide CART to indicate worse survival, and worse response to tamoxifen, in a subset of breast cancer patients. While the role of CART in other disease states is better understood, the role of CART in breast cancer remains elusive. To this end, we aimed to further our understanding of the role CART plays in estrogen receptor positive (ER+) breast cancer.

Through transcriptomic profiling, we identified a number of genes, both upregulated and downregulated by CART, to be potential genes controlled by the Estrogen Receptor alpha (ERα). Owing to this finding, we hypothesized that CART may alter the binding partners of ERα, and understanding what complexes are recruited to ERα by CART may not only help us understand the role of CART in ER+ breast cancer better, but also potentially identify actionable future targets. Our results indicated that CART may potentially promote an interaction between ERα and two novel ERα interactors, a zinc-finger protein (WIZ) and a poorly understood E3 ligase (HECTD4). Additionally, we identified members of the BAF-chromatin remodelling complex to be significantly enriched interactors in the presence of CART. One identified subunit of this complex, SMARCD1, stood out as a potentially interesting target due to previous research highlighting its importance in nuclear receptor function. Knockdown of SMARCD1 resulted in altered morphology and growth of ER+ breast cancer cells, and caused transcriptional deregulation in a gene-specific manner. While knockdown of SMARCD1 did not further sensitize cells to anti-endocrine therapy, we identified a number of other BAF-complex subunits to be significantly upregulated in cell line models of anti-endocrine resistance.

We suggest that a potential mechanism by which CART indicates worse survival is through altered recruitment of BAF-complex subunits to ERα, and certain members of this complex may be attractive targets worthy of future interrogation.

Acknowledgments

I am thankful to the Irish Cancer Society for their funding of this study, and for their constant support over the last 4 years.

This thesis would not have been possible without the people in which I shared this journey with. First, I am indebted to my supervisor Dr. Darran O'Connor. His constant guidance and support over the last 4 years enabled me to develop as a scientist, and I feel grateful to have had a supervisor that allowed me to pursue my findings as an independent cancer researcher. Next, my co-supervisor Dr. Triona Ni Chonghaile, for her feedback and direction over the last number of years, and for teaching me that sometimes you just have to shake it off.

I was extremely fortunate to work alongside some exceptional cancer researchers, many of which I am proud to call my friends. To Kate, for her unparalleled dedication to training me during my early days in the lab. To Lisa, for being a friend with whom sharing the experience of this PhD made it all the more enjoyable, and at times, all the more bearable. To Sudipto, for mentoring me in the lab, providing me with constructive feedback on my work, and for feeding me when an extra side of lunch was on offer. To all other members of the lab, both past and present; Cami, Laoighse, Bo, Bruce, Emer, Louise, Marta, it was a great experience to share the lab with you all.

To my parents, for their selfless dedication in raising me to pursue my goals, and for teaching me to be ambitious. A special thank you is also in order to my sister Sinead, and my two brothers Paul and Ciaran.

To the house of 211, for providing me with some of the most memorable experiences of my life. May the lawn be well kept always.

And finally, to Sinead. The support you showed over the last 4 years helped keep me going through some of the hardest times of this study. Further, your remarkable ability to remind me of a life outside of the lab has truly been one of a kind.

Table of Contents

Figures 3
Tables 11
Abbreviations 14
Summary 20
Acknowledgments 21
Chapter 1. Introduction 28
1.1 Breast cancer 29
1.1.1 Statistics of breast cancer in Ireland 29
1.1.1 Environmental and genetic risk-factors of breast cancer 30
1.1.2 Histological subtypes of breast cancer 31
1.1.3 Molecular subtypes of breast cancer 33
1.1.5 Treatment regimens and their effectiveness in breast cancers of different histological and molecular subtypes 35
1.1.5.1 Management of breast cancer through surgery 35
1.1.5.2 Radiotherapy 36
1.1.5.3 Chemotherapy 37
1.1.5.4 Targeted-therapy approaches 38
1.1.5.5 Immunotherapy; The future for hard-to-treat breast cancers? 40
1.1.6 Estrogen Receptor positive (ER+) cancer 41
1.1.6.1 ERα structure and function 41
1.1.6.2 Mechanisms of altered tamoxifen response 43
1.1.6.3 Additional anti-endocrine agents 46
1.1.7 A final note on the future of breast cancer detection and treatment 48
1.2 The Cocaine- and Amphetamine–Regulated transcript (CART) 51
1.2.1 *CARTPT* gene structure, processing and regulation 51
1.2.2 Proposed CART signalling mechanisms 53
1.2.3 The function of CART peptides – Drug reward and feeding 54
1.2.4 CART peptides in disease 57
1.2.4.1 Obesity 57
1.2.4.2 *Diabetes mellitus* 58
1.2.4.3 CART peptides as therapeutic strategies for patients with Parkinson's disease and Stroke victims 60
1.2.4.4 CART and cancer 61
1.3 Aims of project 63
Chapter 2. Materials and Methods 64

2.1 Cell culture 65
2.1.1 Cell lines 65
2.1.2 Sub-culturing of cell lines 65
2.1.3 Cryofreezing of cell lines for long-term storage 65
2.1.4 Thawing and re-growing cell lines after long-term cryopreservation 66
2.1.5 Cell counting and seeding 66
2.1.6 Preparation of medium for “hormone-stripped” experiments 67
2.2 Generation of stable-inducible cell lines 67
2.2.1 Safety precautions 67
2.2.2 Principle of tetracycline-induced gene expression systems 67
2.2.3 Preparation of lentiviral particles 68
2.2.4 Transduction of the T47D cell line 68
2.2.5 Secondary virus harvesting and target cell transduction 68
2.2.6 Conformation of successful dual-transduction 69
2.3 In vitro phenotypic assays 69
2.3.1 Propidium iodide staining and cell cycle analysis 69
2.3.2 MTT (3-(4,5-dimethylthiazol-2-yl)-2,5-diphenyltetrazolium bromide) assay 70
2.3.3 Anti-endocrine drug treatments 70
2.3.4 Protein half-life determination 71
2.4 Statistical analysis 71
2.5 Protein extraction and Western blotting 72
2.5.1 Protein extraction 72
2.5.2 Protein quantification and sample preparation for SDS-Polyacryamide Gel Electrophoresis (SDS-PAGE) 72
2.5.3 Polyacrylamide gel preparation 73
2.5.4 One-dimensional gel electrophoresis 75
2.5.5 Western blot 75
2.5.6 Secondary antibody and detection of protein bands 77
2.5.7 Stripping and re-probing of nitrocellulose membrane 78
2.6 RNA isolation and qRT-PCR analysis 78
2.6.1 RNA extraction and quantification 78
2.6.2 cDNA synthesis 79
2.6.3 Quantitative Reverse Transcriptase-PCR (qRT-PCR) 80
2.7 Endogenous protein immunoprecipitation 81
2.7.1 Antibody-bead crosslinking 81
2.7.2 Immunoprecipitation 81

2.8 Bacterial techniques 82
2.8.1 Growing bacteria from glycerol stocks 82
2.8.2 DNA extraction from bacteria cultures 83
2.8.3 Bacteria cell transformation 83
2.9 Site-directed Mutagenesis 83
2.10 Estrogen Responsive Element (ERE)-Dual luciferase reporter assay 84
2.10.1 Principle of ERE-dual luciferase reporter assay 84
2.10.2 Dual transient transfection of ERE-luc and Renilla reporter plasmids 85
2.11 RNA sequencing 86
2.11.1 Experimental design and sample preparation 86
2.11.2 Library preparation and RNA sequencing 87
2.11.3 Data preparation 87
2.11.4 Alignment and processing of trimmed data 87
2.11.5 Differential expression 88
2.11.6 Gene ontology (GO) analysis of differentially expressed genes 88
2.11.7 Heatmap generation 89
2.11.8 Gene Set Enrichment Analysis (GSEA) 89
2.12 Mining of publicly-available ERα ChIP-seq datasets 89
2.13 Mass spectrometry analysis of Immunoprecipitated ERα-protein complexes 90
2.13.1 Experimental design 90
2.13.2 Mass spectrometry immunoprecipitation 90
2.13.2.1 General notes 90
2.13.2.2 Antibody-bead crosslinking 90
2.13.2.3 Preparation of cell lysates for immunoprecipitation 91
2.13.3.4 Immunoprecipitation 92
2.13.3.5 In-solution digestion of proteins 92
2.13.3.6 Acidification of digested peptides 93
2.13.3.7 C18 zip-tip equilibration 94
2.13.3.8 MaxQuant search parameters 95
2.13.3.9 Statistical analysis using Perseus 95
2.13.3.10 STRING and PANTHER analysis for identified proteins 97
2.14 Small interfering RNA (siRNA) techniques 97
2.14.1 siRNA transfection optimisation 97
2.14.2 siRNA transfections 98
2.14.3 Cellular response to anti-endocrine agents following SMARCD1 knockdown ... 99

Chapter 3. Investigating the consequence CART has on the transcriptional landscape of ER+ breast cancer 100
3.1 Introduction 101
3.1.1 CART and cancer 101
3.1.2 The role of LxxLL motifs in nuclear receptor function 101
3.1.3 Transcriptomic profiling 102
3.1.4 Chromatin immunoprecipitation sequencing (ChIP-seq) 103
3.1.3 Aims of chapter 105
3.2 Results 106
3.2.1 Investigating the effect CART has on common ERα target genes 106
3.2.2 An investigation into a potential structure-function relationship between CART and ERα 110
3.2.3 Generation of stable, inducible, T47D cell lines 113
3.2.4 Using the Tet-ON T47D cell line for RNA-sequencing 114
3.2.5 Principal component analysis (PCA) and heatmap generation reveals a number of significantly differentially expressed genes by CART 115
3.2.6 Gene Ontology (GO) analysis of significantly upregulated genes 117
3.2.7 Gene set enrichment analysis (GSEA) of genes significantly upregulated by CART 120
3.2.8. GO analysis of genes significantly downregulated by CART 123
3.2.9 Using publicly available ChIP-seq data to characterize if any differentially expressed genes have previously been shown to contain promoter binding sites for ERα 124
3.2.10 Validation of genes using qRT-PCR 127
3.2.11 Examining the top differentially expressed genes based on FPKMS difference128
3.2.12 Cellular response to anti-endocrine agents 133
3.3 Discussion 135
3.3.1 CART can alter the expression of ERα target genes 135
3.3.2 The role of LxxLL motifs in CART mediated ERα activity 136
3.3.3 Genes significantly upregulated by CART 137
3.3.4 Genes significantly downregulated by CART 138
3.3.5 ERα can bind promotor regions of genes identified in RNA sequencing post treatment with CART 140
3.3.6 CART increases the expression of a subset of genes associated with tamoxifen resistance 141
Chapter 4. Proteomic investigation into the effect of CART on the Estrogen Receptor interactome 143
4.1 Introduction 144

4.1.1 Analysis of protein complexes 144
4.1.2 ERα interaction networks 146
4.1.3 Aims of chapter 148
4.2 Results 149
4.2.1 Investigating if CART is a physical interactor of ERα 149
4.2.2 Mass spectrometry workflow and ERα immunoprecipitation 150
4.2.2 Hierarchical clustering, principal component analysis (PCA) and volcano plot generation of data from ERα D-12 immunoprecipitation 153
4.2.3 Hierarchical clustering, principal component analysis (PCA) and volcano plot generation of data from ERα F-10 immunoprecipitation 159
4.2.4 Comparing common interactors between ERα IP samples using both D-12 and F-10 antibodies 164
4.2.5 Using PANTHER to assign protein class to identified interactors in the presence/absence of CART 167
4.2.6 The STRING interaction database shows previously reported interactions between ERα and proteins identified via mass spectrometry. 170
4.2.7 Using STRING to understand whether WIZ and HECTD4 are direct interactors of ERα 173
4.2.8 Attempted validation of interaction between ERα, HECTD4 and WIZ 175
4.2.9 Investigating the impact CART has on the turnover of ERα 177
4.2.9 Validation of the interaction between SMARCD1 and ERα 181
4.3 Discussion 183
4.3.1 LXD motifs within CART do not allow for an interaction between ERα and CART 183
4.3.2 Detection of ERα interaction networks using two independent antibodies 184
4.3.3 CART putatively promotes an interaction between ERα and the zinc-finger protein WIZ 186
4.3.4 CART putatively promotes an interaction between ERα and the E3 ligase HECTD4 187
4.3.5 CART expression results in the recruitment of chromatin remodelling complexes to ERα 189
Chapter 5. Investigating the therapeutic potential of SMARCD1 in ER+ breast cancer 192
5.1 Introduction 193
5.1.1 The BAF-chromatin remodelling complex 193
5.1.2 Implications of the BAF-chromatin remodelling complex in cancer 195
5.1.3 Aims of chapter 198
5.2 Results 199
5.2.1 *In silico* analysis of SMARCD1 expression 199

5.2.2 Analysis of SMARCD1 expression in a second, independent cohort of breast cancer patients (TCGA dataset) 205
5.2.3 Optimisation of siRNA transfection conditions prior to modulation of SMARCD1 expression 212
5.2.4 Modulating the expression of SMARCD1 using siRNA 214
5.2.5 Investigating the consequence SMARCD1 knockdown has on the growth of ER+ breast cancer cells 217
5.2.6 Does SMARCD1-knockdown prevent CART from driving the expression of ERα target genes? 218
5.2.7 Does SMARCD1-knockdown prevent CART from increasing the expression of potential ERα target genes identified from RNA-sequencing? 220
5.2.8 Does SMARCD1-knockdown sensitize breast cancer cells to anti-endocrine therapy? 222
5.2.9 Investigating whether other BAF-complex proteins may play a role in anti-endocrine resistance 225
5.3 Discussion 227
5.3.1 SMARCD1 as a marker of poor prognosis in breast cancer 227
5.3.2 SMARCD1 as a mediator of breast cancer growth, and ERα function 228
5.3.3 Aberrant expression of BAF-chromatin remodelling complexes in cell-line models of anti-endocrine resistance 231
Chapter 6. General Discussion 234
6.1 Key findings 235
6.2 Future directions 236
6.3 Conclusions 247
Appendices 248
Bibliography 277

Chapter 1. Introduction

1.1 Breast cancer

1.1.1 Statistics of breast cancer in Ireland

Cancer is a collection of diseases which will directly, or indirectly, affect all of us in our lifetime. This year, the National Cancer Registry of Ireland (NCRI) released their report on cancer incidences between the years 2015 and 2017. This report highlighted some truly startling statistics, as well as some trends which gave the indication that our fight against cancer is making some real progress. Between the years 2015 and 2017, an average of 40,570 cancers (or non-invasive tumours) were diagnosed annually (NCRI 2017). The cumulative lifetime risk for both men and woman being diagnosed with cancer was approximately 1 in 3, and 1 in 4, respectively (NCRI 2017). In line with previous reports, breast cancer remains the most commonly diagnosed female malignancy, accounting for roughly 30% of all cancers diagnosed in women (excluding non-melanoma skin cancer) (figure 1.1).

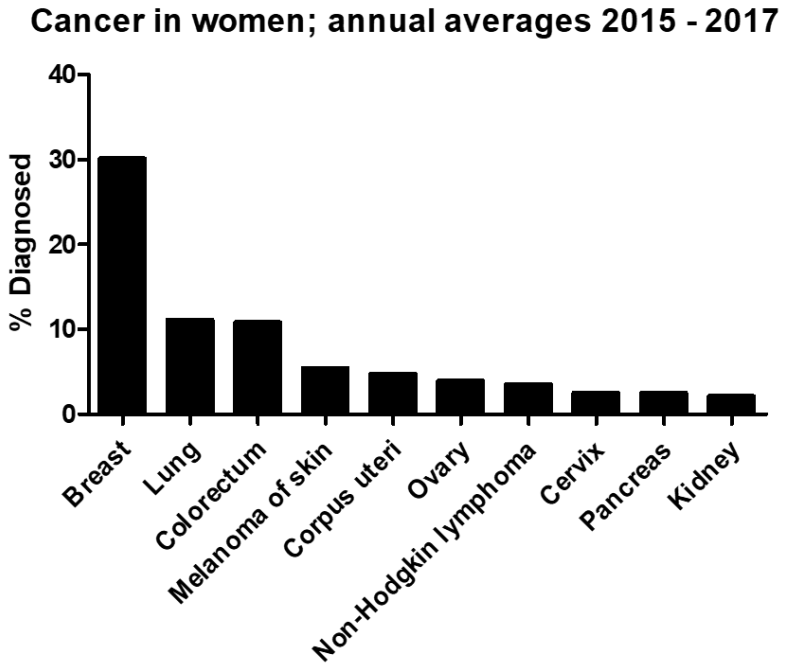

Figure 1.1. Breast cancer was the most commonly diagnosed cancer in women in Ireland between the years of 2015 and 2017.

After breast, the most commonly diagnosed cancers in Irish women were lung (11.1%), colorectum (10.8%), melanoma of skin (5.4%), corpus uteri (4.7%) and ovarian (3.9%) (NCRI 2017). While the incidence of breast cancer is on the rise (1,562 cases reported in the year 1994 to 3,094 cases reported in the year 2015), it is reassuring to know that the five-year average net survival of breast cancer patients is also on the rise (71.6% in the 1994-1998 cohort to 82.9% in the 2010-2014 cohort) (NCRI 2017). It is thought that this increase in breast cancer prevalence coinciding with a decrease in mortality may be due to the fantastic efforts of the national breast screening programme, BreastCheck. Interestingly, two spikes in breast cancer incidence occurred following the years 2000 and 2007, both of which coincided with the two roll-out phases of BreastCheck. This would suggest that, through the great efforts of BreastCheck, more Irish women are having their breast cancers diagnosed at an earlier stage, which is of paramount importance to the patient's prognosis. Indeed, the 5-year net-survival for breast cancer patients based on cancer stage displays truly harrowing statistics. Between the years 2010 – 2014, it was estimated that the 5-year net survival rate for breast cancer patients diagnosed with stage 1 breast cancer was a remarkable 97%, however, this net survival significantly declines as the breast cancer grade increases, with a frightening 5-year net survival rate of only 26% for patients diagnosed with stage 4 breast cancer (NCRI 2017). It is clear, then, that while our efforts in the fight against cancer are certainly resulting in increased survival rates, there is still much work to be done in understanding and eradicating this malicious disease.

1.1.1 Environmental and genetic risk-factors of breast cancer

Through collective research efforts across the globe, we now understand many risk-factors which may be associated with breast cancer. These risk factors can be both environmental, as well as genetic. Many of the environmental risk factors do not specifically predispose individuals to breast cancer, as they are understood to be general cancer risk factors. Examples include smoking, alcohol intake, and poor diet. Obesity is a known risk factor for breast cancer

(Renehan et al., 2010), in both post-menopausal (Morimoto et al., 2002) and pre-menopausal women (Anderson et al., 2012). Exposure to hormones represents a significant risk factor for breast cancer. For example, increased exposure to estrogen in post-menopausal women strongly correlates with increased breast cancer risk (Travis et al., 2003). In 2002, a truly landmark epidemiological study highlighted a strong correlation between childbearing, breastfeeding, and breast cancer (Collaborative group on Hormonal Factors in Breast Cancer. 2002). This research highlighted that breast cancer risk decreased by 4.3% for every 12 months of breastfeeding, and by 7% for each birth, a truly remarkable finding. Further, another study demonstrated that a greater reduction in risk of breast cancer is seen in women who give birth at young ages (20 years) when compared to older ages (Ewertz et al., 1990). Hormone replacement therapy (HRT) is another known risk factor for breast cancer. HRT is often considered for alleviating symptoms of premature/early menopause, however, a study published in 1997 identified HRT as a significant risk factor for breast cancer (Lancet 1997). Further, a recent study has highlighted hormonal contraceptive use is related to increased breast cancer risk (Morch et al., 2017). One of the best understood genetic risk factor of breast cancer is mutations within the BREast Cancer Associated genes 1 and 2 (BRCA1, BRCA2). It is estimated that the average breast cancer risk in BRCA1 and BRCA2 germline mutation carriers by the age of 70 is roughly 65% and 45% respectively (Antoniou et al., 2003). Defects in these genes are thought to impede biological processes such as DNA repair (Petrucelli et al., 2010). Other genetic targets which are associated with increased breast cancer risk include the tumour suppressor protein TP53 (Birch et al., Oncogene 2001) and PTEN (Njiaju et al., 2012), which encodes a member of the PI3-Kinase pathway.

1.1.2 Histological subtypes of breast cancer

Breast cancer is not one disease; it collectively defines a number of cancers of the breast, many of which are distinct from one-another. Histologically, breast cancers are usually stratified into two groups, *in situ* carcinoma, or

invasive carcinoma. *In situ* carcinoma is a breast tumour which has not migrated out of the primary tumour site (see figure 1.2), whereas an invasive carcinoma would be detected in surrounding breast tissue.

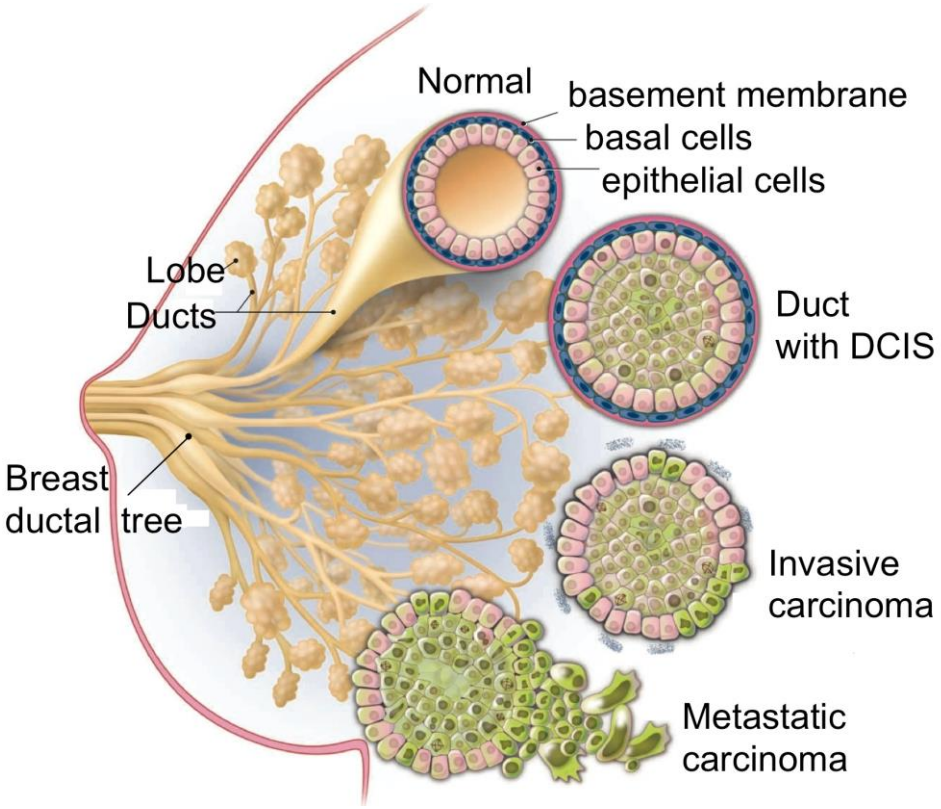

Figure 1.2. Progression of a normal duct, to ductal carcinoma *in situ* (DCIS), to invasive carcinoma.

Image credit: K.Sutliff Science 2014.

The detection of in situ carcinomas is increasing in Ireland (39 cases identified in 1994, up to 365 cases identified in 2015), a trend certainly aided by the BreastCheck screening programme. *In situ* carcinomas are usually subcategorised based on the identified primary tumour site, ductal carcinoma *in situ* (DCIS) or lobular carcinoma *in situ* (LCIS), in which the prevalence of the former is greater. Invasive breast cancers are the most common form of breast cancer diagnosed, with invasive ductal carcinoma (IDC) accounting for roughly 80% of all breast cancer cases, and invasive lobular carcinoma (ILC)

accounting for roughly 10 – 15% of cases in Ireland. While the histological subtyping of breast cancer certainly provides necessary information pertaining to whether surgical resection is a suitable treatment option, the molecular characteristics of the cancer will ultimately provide the necessary information to guide an appropriate treatment regime.

1.1.3 Molecular subtypes of breast cancer

Currently, six distinct molecular subtypes of breast cancer are thought to exist within breast cancer. These are: Basal-like, Claudin-low, HER2-enriched, Luminal A, Luminal B and Normal breast like. Below, table 1.1 highlights the defining traits of each subtype.

Table 1.1. Molecular subtypes based on receptor expression status.

Subtype	Incidence	Receptor status	Proliferative rate	Histological grade	Prognosis
Basal-like	10 – 20%	ER-, PGR-, HER2-	High	High	Poor
Claudin-low	12 – 14%	ER-, PGR-, HER2-	High	High	Poor
HER2	10 – 15%	ER-, PGR-, HER2+	High	High	Poor
Luminal A	50 – 60%	ER+, PGR+, HER2-	Low	Low	Good
Luminal B	10 – 20%	ER+/-, PGR+/-, HER2+/-	High	Intermediate	Intermediate / poor
Normal-like	5 – 10%	ER-/+, HER2-	Low	Low	Intermediate

Table adapted from Eroles et al., 2012.

Luminal cancers are the most common subtype of breast cancer, and can be further classified into luminal A and luminal B. Luminal A breast cancer is the

most common molecular subtype of breast cancer. This molecular subtype of breast cancer expresses both estrogen receptor alpha (ERα) and the progesterone receptor (PGR). Appropriately, this subtype also expresses genes pertaining to ERα activation, such as cyclin D1 (Sotiriou et al., 2003). Luminal A breast cancer is also known to present with a good prognosis, which has been demonstrated in multiple studies (Sorlie et al., 2003, Parker et al., 2009). Luminal B, on the other hand, account for roughly 10 – 20% of breast cancer cases diagnosed. These cancers are typically ER+, PGR+ and HER2+. They express proliferative genes at a higher amount to luminal A breast cancer (Sorlie et al., 2001), and present clinically with a worse prognosis (Parker et al., 2009). Indeed, the proliferative marker Ki67 can be used to distinguish between luminal A and B tumours, with the luminal B subtype typically expressing higher amounts of this proliferative marker (Dowsett et al., 2011).

The HER2-enriched subtype of breast cancer is classified by an overexpression of the HER2 receptor, but also shares some similarities with the basal-like subtype in terms of low ERα and PGR expression, as well as an expression of basal epithelial gene markers (Perou et al., 2000). While HER2 enriched breast cancers typically present with an extremely poor prognosis (Parker et al., 2009) recent advances in targeted therapies for this subtype of breast cancer has shown significant clinical benefit (discussed further in section 1.1.5.5).

The basal-like breast cancer subtype was the fourth molecularly distinct subtype (after luminal A, B and HER2) identified in the landmark study published by Perou and colleagues in the year 2000 (Perou et al., 2000). Basal-like breast cancers typically present with a poor prognosis (Parker et al., 2009), due to their extremely aggressive nature and high metastatic ability associated with epithelial to mesenchymal transition (EMT) (Felipe Lima et al., 2016). Further, the basal-like breast cancer subtype typically presents with high mutational burden of the tumour suppressor protein p53 (Sorlie et al., 2001), and has also been shown to harbour germline BRCA1 mutations (Bosch et al., 2010).

The normal-like breast subtype was initially named so, as they are poorly defined and were grouped into the subtype classification with normal breast samples (Perou et al., 2000). While this subtype is thought to be closely related to the basal-like subtype, the clinical significance of this subtype is still relatively undetermined (Eroles et al., 2012). In fact, a study published in 2010 doubted the existence of this subtype completely, suggesting that the subtype was potentially only identified due to normal breast tissue contamination (Weigelt et al., 2010).

The Claudin-low subtype was identified in 2007 as an additional, molecularly distinct, breast cancer subtype (Herschkowitz et al., 2007). The subtype was defined by low expression of cell-cell adhesion genes (including Claudins), low expression of luminal genes, and high expression of cell markers associated with endothelial cells and lymphocytes. This subtype typically presents with poor prognosis, and was shown to resemble a breast cancer stem-cell like signature (Prat et al., 2010).

1.1.5 Treatment regimens and their effectiveness in breast cancers of different histological and molecular subtypes

1.1.5.1 Management of breast cancer through surgery

The first use of surgery for the management of breast cancer was performed over 100 years ago by Dr. W.S. Halsted (Ann Surg. 1894). The approach was known as a radical mastectomy, which involved the complete removal of the breast. While this remained the standard of surgical breast cancer management for a number of years, findings from trials over the past 50 years have brought this to an end. For example, no clinical benefit was observed when a randomised trial (NSABP B-04) compared radical mastectomy without radiation, to simple mastectomy with radiation and simple mastectomy without radiation (Fisher et al., 2002). Another randomised trial (NSABP B-06) compared mastectomy to lumpectomy alone and lumpectomy with radiation (Fisher et al., 2002). The findings from this trial indicated that lumpectomy with

radiation was more beneficial than mastectomy, and so lumpectomy with radiation is now considered the primary form of surgical management of breast cancer (Fisher et al., 2002, Matsen et al., 2012). Contradictions to the use of lumpectomy with radiation do exist, such as inability to clearly access the tumour, or physical intolerability to radiation therapy. Matsen and colleagues recommend mastectomy for the management of tumour recurrences (Matsen et al., 2012).

Most certainly, surgical procedures such as the mastectomy can have drastic effects on the patient's mental health, which should be an important consideration when discussing surgical options and follow-up care. A study published in 1985 highlighted that patients who received a lumpectomy showed better adaptation to their surgery, were less self-conscious, and were more open about their surgery and sexuality when compared to patients who received a mastectomy (Steinberg et al., 1985).

Finally, in terms of surgical performance based on histological subtypes of breast cancer, ILC can often present with issues in detection due to the poorly defined nature of this cancer. Further, the infiltrative-like growth pattern often makes the tumour area more difficult to define, and therefore may result in a more aggressive surgical regime when compared to the more common IDC (Singletary et al., 2005)

1.1.5.2 Radiotherapy

Radiotherapy involves the use of high energy x-rays to promote cell death of cancer cells contained to a local region. One of the first instances of radiotherapy use for the treatment of breast cancer was in 1896, when Dr. Emil Grubbe attempted to use x-rays to treat a patient with recurrent breast cancer (Wang et al., 2013). Today, adjuvant radiotherapy following lumpectomy (Fisher et al., 2002) as well as mastectomy (Vilarino-Varela et al., 2009) is common in the management of breast cancer due to the acknowledged clinical benefit. Radiotherapy is, however, a local treatment option for the management of breast cancer, and so the benefit of radiotherapy on metastatic/highly advanced breast cancer may be limited.

1.1.5.3 Chemotherapy

In general, chemotherapeutic agents work by targeting fast-dividing cells in the body, such as cancer cells. Surprisingly, one of the first chemotherapeutic agents was derived from mustard gas. A mustard gas derivative was first used in 1943 to treat a patient with non-Hodgkins lymphoma (Goodman et al., 1946), and was initially suggested as a potential treatment option when an accidental release of sulphur mustards resulted in bone marrow and lymph node depletion in individuals exposed to the spill (Krumbhaar et al., 1919, DeVita Jr et al., 2008).

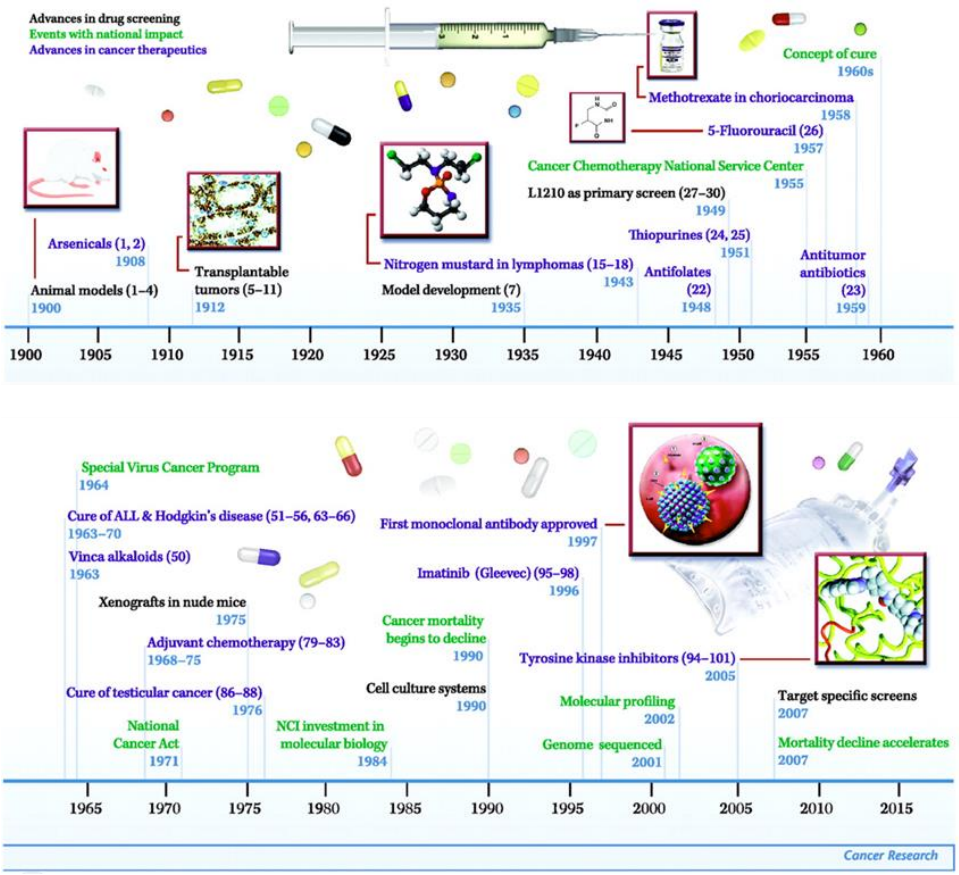

Figure 1.3. Advances in the management of cancer with Chemotherapy. Image sourced from DeVita Jr. et al., 2008.

Chemotherapeutic agents have progressed drastically since the days of nitrogen mustard agents, with a plethora of chemotherapeutic agents now in

use for cancer. Examples of chemotherapeutic treatment regimens include cyclophosphamide, methotrexate, and 5-flurouracil (CMF) as a first-generation chemotherapy regimen, cyclophosphamide, doxorubicin, and 5-flurouracil (CAF/FAC) as a second-generation chemotherapy regimen, and dose dense sequential doxorubicin/cyclophosphamide-paclitaxel (AC-T) as a third-generation chemotherapy regimen (Anampa et al., 2015).

A trend in recent years has been to predict whether chemotherapy is absolutely necessary, due to the knowledge that chemotherapeutic side-effects can be severe in patients. A classic example of a trial performed in breast cancer for predicting whether patients need chemotherapy is the Trial Assigning Individualized Options for Treatment (TAILORx) trial (Sparano et al., 2008) (Sparano et al., 2015). The TAILORx trial utilized the OncotypeDX (Genomic Health) predictive gene signature to assign a recurrence score for ER+, HER2-, node negative breast cancer, in which it was suggested that low-risk breast cancer patients may not benefit from both anti-endocrine therapy and chemotherapy, and may do just as well with anti-endocrine therapy alone. Further, in high risk patients, the use of both anti-endocrine therapy in combination with chemotherapy was recommended (Sparano et al., 2015).

Since basal-like breast cancers typically do not express hormone receptors, chemotherapy is typically the first line of therapeutic intervention for these patients. While the basal-like subtype of breast cancer is typically chemo-sensitive, the relapse rate for patients diagnosed with this aggressive breast cancer is, unfortunately, also higher than other molecular subtypes of breast cancer (Bertucci et al., 2012). Indeed, this highlights a pressing need for identifying targeted therapies for this subtype of breast cancer.

1.1.5.4 Targeted-therapy approaches

The gold-standard of therapeutic cancer care is, undoubtedly, targeted therapeutic approaches. The failed post-coital contraceptive ICI46474 has become arguably the most successful targeted therapeutic identified for breast cancer, known today as tamoxifen (Jordan et al., 1976, 2008). Tamoxifen has been hugely successful, reducing recurrence rates (Lancet 1983) and

improving the survival rates of hormone receptor positive breast cancer patients (Baum et al., 1983). Moreover, results from the “Adjuvant Tamoxifen: Longer against Shorter” (ATLAS) trial indicates longer term tamoxifen treatment results in reduced breast cancer recurrence and mortality (Davies et al., 2013). This study reported a 21.4% cumulative risk of recurrence during years 5 – 14 in women assigned to continue therapy, but this risk increased to 25.1% in controls (Davies et al., 2013). Tamoxifen, which acts by blocking the action of ERα (discussed further in section 1.1.6) is also recommended for ERα negative breast cancer patients which present with PGR positivity due to improved clinical outcome (Fisher et al., 1983). Molecularly, the luminal A subtype of breast cancer is understood to benefit more from tamoxifen versus the luminal B subtype (Tran et al., 2011). Further, a study in 2002 suggested that the benefit of tamoxifen is not as obvious in patients with ILC when compared to patients with IDC, although the authors acknowledge the small sample-size for ILC patients may be a limitation of the study (Jirstrom et al., 2005). Another class of targeted therapies, known as aromatase inhibitors (AIs), provide clinical benefit to ER+ breast cancer by blocking the conversion of pre-estrogen hormones to estrogen. Indeed, results from the “Arimidex, Tamoxifen, Alone or in Combination” ATAC trial indicate AIs provide improved clinical benefit when compared to tamoxifen in post-menopausal breast cancer patients (Howell et al., 2005). Targeted therapies for ER+ breast cancer are discussed further in section 1.1.6.

While the HER2-enriched subtype of breast cancer is associated with poor prognosis (see section 1.1.4), the development of the monoclonal antibody Trastuzumab (Herceptin, Roche) has significantly improved survival in patients diagnosed with this subtype of breast cancer (Baselga et al., 2005). Further, and as mentioned previously, results from the CLEOPATRA trial in HER2+ breast cancer recommended that the targeted therapy trastuzumab should be administered in combination with chemotherapy to maximise clinical benefit (Swain et al., 2013).

Unfortunately, as basal-like breast cancers do not typically express hormone receptors, targeted therapeutic approaches are limited. However, ongoing research has highlighted molecular characteristics in basal-like breast cancer

which may be exploited to achieve clinical benefit. Owing to the knowledge that basal-like breast cancers may harbour mutations resulting in dysfunctional BRCA1/2 genes, investigations to assess whether basal-like breast cancers may benefit from PARP inhibitors are currently ongoing, with data thus far suggesting that BRCA mutant, basal breast cancer patients may indeed benefit from the use of PARP inhibitors (Gelmon et al., 2012), but further research is necessary. The clinical utility of targeting the Epidermal Growth Factor Receptor (EGFR), as well as the Vascular Epidermal Growth Factor (VEGF) is currently under investigation, although results appear moderately conflicting, with some concerns raised regarding treatment-related mortality (Ranpura et al., 2011, O'Reilly et al., 2015). Furthermore, pre-clinical studies have highlighted targeting Cyclin-Dependent Kinases such as CDK4/6 (Liu et al., 2017) and CDK7 (Wang et al., 2015, Li et al., 2017) may provide clinical benefit to patients with basal-like breast cancer, and may be an area worthy of continued investigation.

1.1.5.5 Immunotherapy; The future for hard-to-treat breast cancers?

The field of immunotherapy has quickly grasped the attention of cancer researchers around the globe. Evasion of immune detection by cancer cells is understood to be a defining hallmark of cancer (Hanahan et al., 2011), however, novel immunotherapeutic approaches aim to harness the patient's immune system against the cancer. Indeed, immunotherapeutic intervention has resulted in excellent clinical responses in cancers such as melanoma (Hodi et al., 2010, Wolchok et al., 2013) and renal cell carcinoma (McDermott et al., 2015). It is thought that mutational burden may result in a more robust response from immunotherapeutic agents (Yuan et al., 2016). Data presented at the American Society of Clinical Oncology (ASCO) meeting in 2017 highlighted an estimated pathologic complete response rate of 40% was achieved in triple-negative breast cancer patients in the pembrolizumab treatment arm (Nanda et al., 2017). Further, an estimated pathological complete response of 30%, and 21%, was seen following pembrolizumab treatment in HER2 negative, and hormone-receptor positive/HER2 negative

patients respectively (Nanda et al., 2017). Pembrolizumab, an immunotherapy drug, functions by binding the immune checkpoint protein PD-1 on certain immune cells such as CAR T cells and effector T cells. This binding of PD-1 allows the T cells to recognize the cancerous cells and target them for destruction (June et al., 2017) (figure 1.4). These data pertain to the ongoing I-SPY 2 trial, and highlight a truly remarkable step forward for breast cancer treatment strategies.

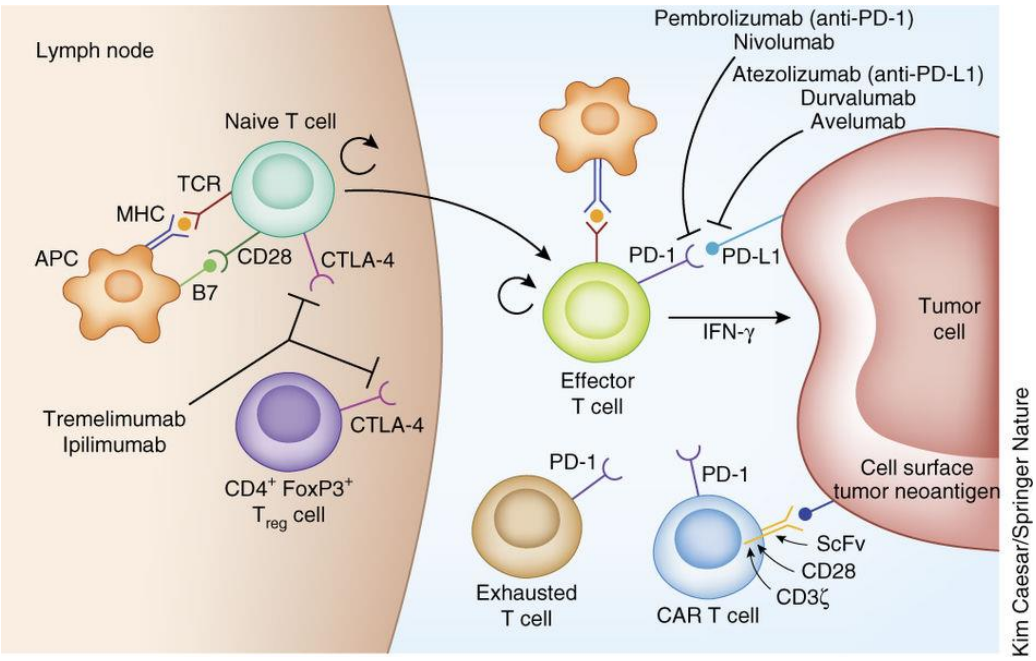

Figure 1.4. Various immunotherapeutic agents currently in clinical trials function by disrupting the PD1-PDL1 interaction between T cells and cancer cells, resulting in the recognition and destruction of the cancer cells.

Image sourced from June et al., 2017.

1.1.6 Estrogen Receptor positive (ER+) cancer

1.1.6.1 ERα structure and function

Breast cancers expressing ERα make up the overwhelming majority of breast cancers diagnosed, with about 80% of breast cancers diagnosed in Ireland

showing an overexpression of ERα. One of the first links between estrogen and its importance for breast cancer growth came in the late 1800's, where Dr. Beatson performed a surgery which involved the removal of the ovaries to suppress breast cancer growth (Beatson. 1896). Over 100 years later, we now understand estrogen is a critical mediator of breast cancer growth, and does so by influencing the activity of ERα. This has resulted in a significant body of work performed in understanding ERα function, and the development of therapeutic strategies for patients with ER+ breast cancer. Estrogen, the female sex hormone, is capable of driving the growth of ER+ breast cancers through activation of ERα. The activation of ERα by estrogen results in dimerization of ERα in the nucleus of the cell, and results in DNA binding events, typically far upstream of estrogen-dependent genes, at specific responsive elements (termed estrogen responsive elements, or EREs). ERα can also be activated through growth factor signalling cascades such as the mitogen-activated protein kinase cascade (MAPK) downstream of growth factor receptors such as EGFR and HER2 (Schiff et al., 2004).

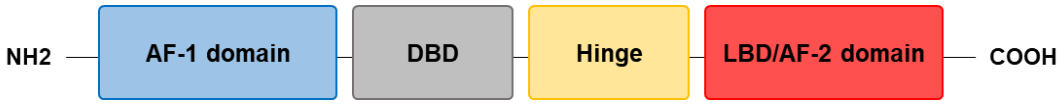

Figure 1.5. Schematic diagram of functional domains contained within ERα.

AF – Activation function, DBD – DNA binding domain, LBD – Ligand binding domain.

Upon binding EREs, transcription complexes comprised of transcriptional coregulators are typically recruited to AF domains on ERα to facilitate transcriptional regulation. The first identified coregulator of ERα is known now as SRC-1 (Steroid Receptor Coactivator-1), and was shown initially to be necessary for the activity of multiple nuclear hormone receptors, including ERα (Onate et al., 1995). The recruitment of coregulator proteins to facilitate ERα function is discussed further in section 5.1 of this study.

The understanding of estrogens role in cancer cell growth has resulted in a huge amount of research in the pharmacological targeting of ERα for the management of breast cancer. The first targeted therapy for cancer, tamoxifen, is known to be effective in ER+ breast cancer patients (see section 1.1.5.4). Tamoxifen can reposition helix 12 within ERα, blocking coactivator recruitment via the AF2 domain, and thus transcription of genes dependent on AF2 activation is repressed (Chang et al., 2012). Resistance to tamoxifen, however, remains a clinically significant issue, with a third of breast cancer patients exhibiting *de novo* resistance to the drug, and over half acquiring resistance over the course of their treatment regime (Viedma-Rodriguez et al., 2014). There are currently multiple mechanisms understood to contribute to altered tamoxifen response, a number of which are briefly discussed below.

1.1.6.2 Mechanisms of altered tamoxifen response

Indeed, the expression of ERα is the first indicator of response to tamoxifen, and lack of ERα expression is thought to be a *de novo* mechanism of resistance to tamoxifen (Dowsett et al., 2003). While a loss of ERα expression during treatment may result in tamoxifen resistance, clinical research has established that this is not a common occurrence in primary tumours (Gutierrez et al., 2005, Osborne et al., 2011). Certainly, identifying underlying reasons why ERα is not expressed in a proportion of breast cancer patients may aid in combating *de novo* resistance of tamoxifen. A study in 2011 highlighted that epigenetic silencing of ERα can be reversed using HDAC inhibitors, and this sensitized tumours to anti-endocrine therapy (Sabnis et al., 2011). Therefore, understanding mechanisms that allow for the re-expression of ERα may aid in establishing tamoxifen sensitivity in patients.

The modification of ERα through post-translational phosphorylation events may represent another mechanism of acquired tamoxifen resistance. Many of the ERα phosphorylation residues which have been extensively studied reside in the AF1 domain of ERα. Phosphorylation of serine-118 was initially demonstrated to contribute to the ligand-independent activation of ERα, and levels of serine-118 phosphorylation were elevated in patients who had

relapsed during their time on tamoxifen (Sarwar et al., 2006). More recently, the implications of serine-118 phosphorylation in terms of response to tamoxifen have demonstrated conflicting results, with studies suggesting serine-118 phosphorylation is associated with both poor response (Chen et al., 2013) as well as good response to tamoxifen (Murphy et al., 2004). Another phosphorylation residue, serine-167, also resides within the AF1 domain of ERα, and has been classified as a marker of tamoxifen response. Serine-167 was detected as a site phosphorylated by overexpression of EGFR or AKT, and while the original data suggested this may infer a tamoxifen resistant phenotype, clinical data is not in agreement with this. For example, one study highlighted that high expression of serine-167 phosphorylated ERα correlated with good clinical outcome in a cohort of breast cancer patients, the majority of which were receiving tamoxifen (Jiang et al., 2007). Interestingly, in 2008, a study identified a relationship between serine-118 and serine-167 phosphorylation, indicating that low serine-118 phosphorylation, and high serine-167 phosphorylation, resulted in improved response to tamoxifen (Yamashita et al., 2008).

Initial investigations into the role ERα mutations play in the response of tamoxifen indicated that ERα mutations were both infrequent, and did not account for tamoxifen resistance in breast tumours (Karnik et al., 1994). However, more recent evidence suggests that ERα is indeed mutated, and many of these mutations may confer altered sensitivity to tamoxifen. In the year 2000, a mutation within ERα (K303R), named a “hypersensitive ERα mutation” was identified in a significant proportion of breast cancer patients within their cohort (Fuqua et al., 2000). It was recently demonstrated that this mutation has been found to alter the coregulator recruitment to ERα, and may confer tamoxifen resistance (Fuqua et al., 2014). Furthermore, in 1997, a constitutively active, mutant, form of ERα was identified, classified by a nonsynonymous mutation to the tyrosine residue at position 537 (Y537N) (Zhang et al., 1997). The Y537N mutation has recently been shown to play a role in ligand-independent activation of ERα (Jeselsohn et al., 2014). This mutation has shown to promote an anti-endocrine resistant (Jeselsohn et al., 2014), as well as responsive (Robinson et al., 2013), phenotype. While

mutations within ERα itself may indeed play a role in anti-endocrine resistance, it is worth mentioning that recent clinical data suggests that these mutations are detected relatively infrequently in primary tumours, and so may not be a key factor of *de novo* resistance (Chang et al., 2012, Robinson et al., 2013). However, while ERα mutational burden appears low in primary tumours, recent research has suggested that mutations occur frequently in metastatic breast cancer (in the range of 30%), and should be considered as an important factor in acquired endocrine resistance (Jeselson et al., 2015, Reinert et al., 2017).

ERα coregulator expression/recruitment certainly plays a role in anti-endocrine resistance. One of the best understood examples of this is the role Amplified-In-Breast cancer 1 (AIB1) plays in acquired tamoxifen resistance. AIB1, a coregulator of ERα function, is understood to be frequently amplified in breast cancer, and is thought the influence the hormone-dependent growth of ER+ breast cancers (List et al., 2001). Furthermore, knockdown of AIB1 has been reported to restore sensitivity to tamoxifen *in vitro* (Su et al., 2008), and that the tamoxifen resistant cell line, LCC2 (Brunner et al., 1993), is dependent on AIB1 for growth (Karmakar et al., 2011). Intriguingly, pre-clinical data appears moderately conflicting, with studies suggesting high expression of AIB1 indicating both better (Alkner et al., 2013, Weiner et al., 2013) and worse (Osborne et al., 2003, Myers et al., 2005) response to tamoxifen. As discussed previously, SRC1 was the first identified coregulator of ERα function (Onate et al., 1995). In 1997, a study published in Molecular Endocrinology highlighted that SRC1 could enhance both estrogen, and tamoxifen, stimulated transcription (Smith et al., 1997). Early studies on SRC1 suggested that high levels of SRC1 may indicate a favourable response to tamoxifen (Berns et al., 1998), however, recently published data suggests that SRC1 may indeed drive a more aggressive, Tamoxifen resistant, phenotype (Redmond et al., 2009, Qin et al., 2009, Walsh et al., 2012). Recent advances in sequencing technologies have allowed for the further identification of novel ERα interactors, many of which have been implemented in altered response to tamoxifen. For example, recent research has identified both GREB1 (Mohammed et al., 2013) and PGR (Mohammed et al., 2015) to be interactors of ERα, and the chromatin-binding events induced by these interactions

indicate good clinical outcome for patients. Further, the identified pioneer factor FOXA1 has been implemented as a crucial factor for tamoxifen response (Badve et al., 2007, Hurtado et al., 2011). Further, and finally, it is not only “co-activator” proteins which may infer a tamoxifen resistance phenotype. Low expression of the “co-repressor” protein NCOR1 has previously been associated with shorter relapse-free survival of patients treated with tamoxifen (Girault et al., 2003).

1.1.6.3 Additional anti-endocrine agents

While tamoxifen remains the dominant treatment option for pre-menopausal women diagnosed with breast cancer, clinical trials have suggested the use of aromatase inhibitors may be significantly more beneficial to post-menopausal breast cancer patients compared to tamoxifen (Howell et al., 2005). Aromatase inhibitors work by preventing the aromatase enzyme from converting pre-estrogen hormones (such as testosterone) to estrogen (figure 1.6). Some examples of aromatase inhibitors include anastrozole, letrozole, and exemestane.

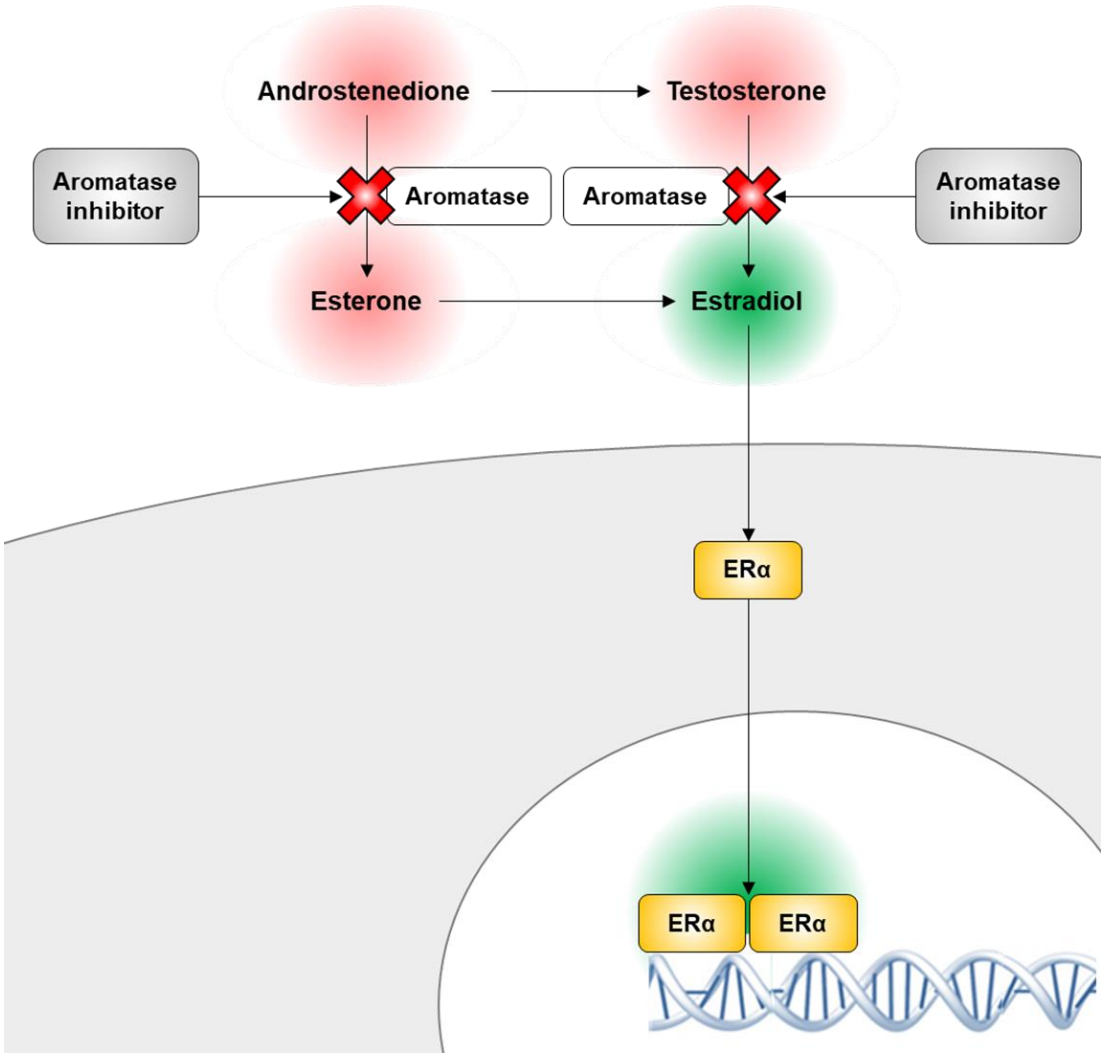

Figure 1.6. Aromatase inhibitors function by blocking the conversion of pre-estrogen hormones to estrogen.

Additionally, it was recently shown that pre-menopausal women treated with aromatase inhibitors plus ovarian suppression showed improved clinical benefit over patients who received tamoxifen (Figg et al., 2014, Pagani et al., 2014).

Fulvestrant (Faslodex; AstraZeneca Pharmaceuticals) is an example of a selective estrogen receptor degrader (SERD). It's mechanism of action is different to that of tamoxifen, in that binding of fulvestrant prevents the translocation of ERα to the nucleus, resulting in its proteasomal degradation. In 2004, a trial was conducted in order to assess the effectiveness of fulvestrant versus tamoxifen. The trial concluded that fulvestrant had similar

efficacy to tamoxifen, was well tolerated, and did not show significant inferiority when compared to tamoxifen (Howell et al., 2004). Fulvestrant has been shown to be as effective as certain aromatase inhibitors (alone or in combination) (Howell et al., 2005, Bergh et al., 2012). A recent trial concluded that 500 mg fulvestrant was more effective than 250 mg fulvestrant (Di Leo et al., 2014), and so it may be interesting to monitor ongoing trials using this higher dose of fulvestrant. For example, the FALCON study, set for completion in February 2018, is investigating high dose fulvestrant in combination with anastrozole (AI) as a first-in line hormonal strategy for breast cancer patients (Ciruelos et al., 2014).

1.1.7 A final note on the future of breast cancer detection and treatment

It would not be an overstatement to say the best biomarker for predicting better survival in patients is, plainly, early detection of their cancer. In figure 1.7, the 5-year net survival for breast cancer patients in Ireland is shown based on the stage of the breast cancer (NCRI 2017). This unequivocally demonstrates that early detection of breast cancer is of paramount importance to a good prognosis.

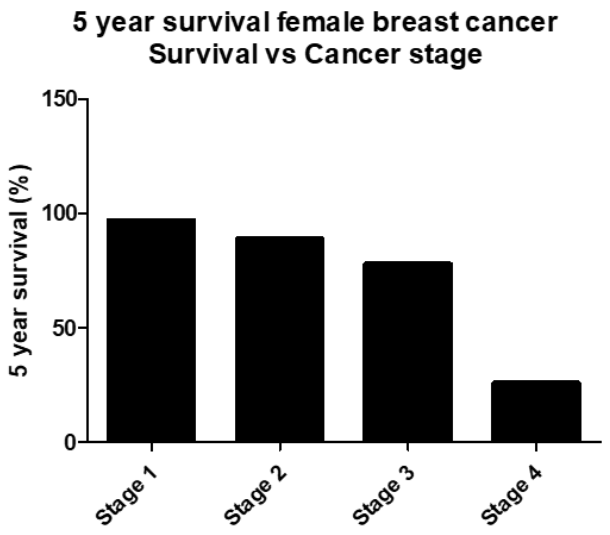

Figure 1.7. 5-year net survival percentages for breast cancer patients based on stage of cancer.

Average survival; Stage 1 – 97%, Stage 2 – 89%, Stage 3 – 78%, Stage 4 – 26%.

The introduction of the BreastCheck national screening programme could be considered a major reason why breast cancer diagnosis increased in Ireland over the last 10 years, yet mortality decreased. It is now estimated that the 5-year net survival for women diagnosed with breast cancer is 82.9%, and while this is among one of the highest 5-year survival rates for cancer in Ireland, research is still vitally important in pushing this 5-year survival even higher.

Some truly ground-breaking research into cell-free circulating-tumour DNA (ctDNA) as an accurate, and early, predictor of cancer recurrence has begun to emerge, with much of this work spearheaded by Professor Richard Marais in the field of melanoma. To date, Marais and colleagues report ctDNA is effective at predicting relapse in melanoma patients some weeks before this is detected in the clinic (Girotti et al., 2016). Further, whole exome sequencing of ctDNA is effective at detecting mechanisms of resistance, tumour evolution, and subclonal responses to therapy (Girotti et al., 2016, Gremel et al., 2016, Lee et al., 2017). This remarkable technique has the potential to truly change how events of relapse, as well as mechanisms of resistance, are identified in

patients, and certainly represents a significant step forward in the management of cancer.

Finally, while research into earlier detection of cancer will be of huge benefit to cancer patients, studies into managing hard-to-treat cancers are still vitally important. As mentioned in section 1.1.5 above, basal-like breast cancer is an extremely aggressive disease with limited treatment options available to patients, however, the implementation of immunotherapy as a viable treatment option may prove to be a huge step forward in the treatment of breast cancer. Preliminary findings from the I-Spy 2 trial suggest the PD-1 therapeutic Pembrolizumab may be an extremely beneficial treatment option for hard-to-treat breast cancers, and the results of this trial will certainly be eagerly anticipated by the cancer community (Nanda et al., 2017).

1.2 The Cocaine- and Amphetamine–Regulated transcript (CART)

1.2.1 *CARTPT* gene structure, processing and regulation

CART (The Cocaine- and Amphetamine-Regulated Transcript) was first discovered in 1995, after administration of cocaine and amphetamine resulted in an upregulation of a previously uncharacterized mRNA transcript in mice (Douglass et al., 1995). Interestingly, the authors of this study characterized a “hydrophobic leader sequence” at the amino terminal of the transcript, leading them to hypothesize that the peptide may be targeted for secretion (Douglass et al., 1995). It is now understood that this leader sequence is a signal peptide, which indeed, is involved in targeting the transcript for secretion. The same group went on to characterize that the CART gene is comprised of 3 exons, 2 introns, and can be mapped to chromosome 5 (Douglass et al., 1996). Following these discoveries, multiple groups began working on CART, with reports highlighting that CART is processed in a tissue-specific manner to produce biologically active peptides (Thim et al., 1999). It is now understood that this tissue-specific processing of CART occurs through pro-hormone convertases (Dey et al., 2003, Stein et al., 2006) with further studies demonstrating that silencing of prohormone convertase expression results in the improper processing of CART (Stein et al., 2006). The best characterized active CART peptides are CART 42-89, and CART 49-89.

Throughout the years of research on CART, many potential regulators of CART expression have been suggested. One of the first studies that showed regulation of CART was published in 1998, whereby mice lacking the gene corresponding to leptin displayed diminished levels of CART (Kristensen et al., 1998). Recently published data is in agreement with this, with a study published in 2016 demonstrating that leptin can regulate the expression of CART in ovarian granulosa cells (Ma et al., 2016). Further, in 2006, CART mRNA and protein expression was found to be upregulated by estradiol under ischemic conditions (Xu et al., 2006). This is important to note, as we have found estradiol does not regulate the expression of CART in breast cancer cells, and so it would appear the expression of CART is tightly regulated across

different tissues (Brennan et al., 2012). A more recent example of this cell/region specific transcription was highlighted in 2016, where a study discovered that nicotine could decrease, increase, or have no effect, on the expression of CART in different areas of the brain (Kaya et al., 2016).

Identified transcription factor binding sites upstream of the CART gene include Cyclic-AMP responsive element (CRE), STAT sites, and AP1 sites (Dominguez et al., 2002). Below, figure 1.8 (taken from Dominguez et al., 2002) highlights the various transcription factor binding sites pertaining to CART, suggesting its transcriptional regulation may involve transcription factors such as CREB and cJUN.

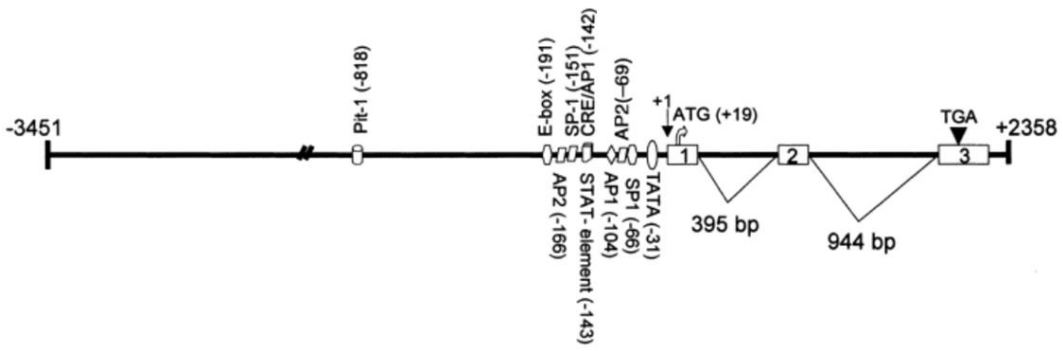

Figure 1.8. The CART gene contains multiple binding sites for transcriptional regulation.

Image sourced from Dominguez et al., 2002.

In 2002, two studies highlighted that CART could indeed be transcribed in a cAMP responsive manner, confirming the CRE site upstream of CART as an active responsive element (Barrett et al., 2002, Dominguez et al., 2002). One of the first studies directly associating CREB with CART expression was published in 2009 (Jones et al., 2009). The authors demonstrated that ionomycin increased intracellular calcium levels, which subsequently resulted in an increased expression of CART mRNA, and increased the levels of phospho-CREB (Jones et al., 2009). In addition, using a mobility shift assay, they demonstrated an increase of a CART-oligo/pCREB protein complex (Jones et al., 2009). Unequivocal proof was published in 2010, where a study

demonstrated, using chromatin immunoprecipitation (ChIP) assays, the presence of both CREB and phospho-CREB (serine-133) binding the proximal promotor region of CART (Rogge et al., 2010).

1.2.2 Proposed CART signalling mechanisms

While the effects of CART are currently under extensive investigation (see section 1.2.3), the mechanisms by which CART controls these functions remain somewhat ambiguous. One of the first studies to confirm CART signalling *in vitro* came in 2005, when the peptide was shown to increase the phosphorylation of extracellular signal related kinase (ERK) in the pituitary-derived AtT20 cell line (Lakatos et al., 2005). Further, this study demonstrated that the MEK inhibitor U0126 was capable of diminishing this phosphorylation event, as was pertussis toxin (Lakatos et al., 2005). The fact that pertussis toxin prevented CART from signalling through ERK lead the authors to suggest CART may signal through a Gi/Go linked G-protein coupled receptor (GPCR) (Lakatos et al., 2005) (figure 1.9).

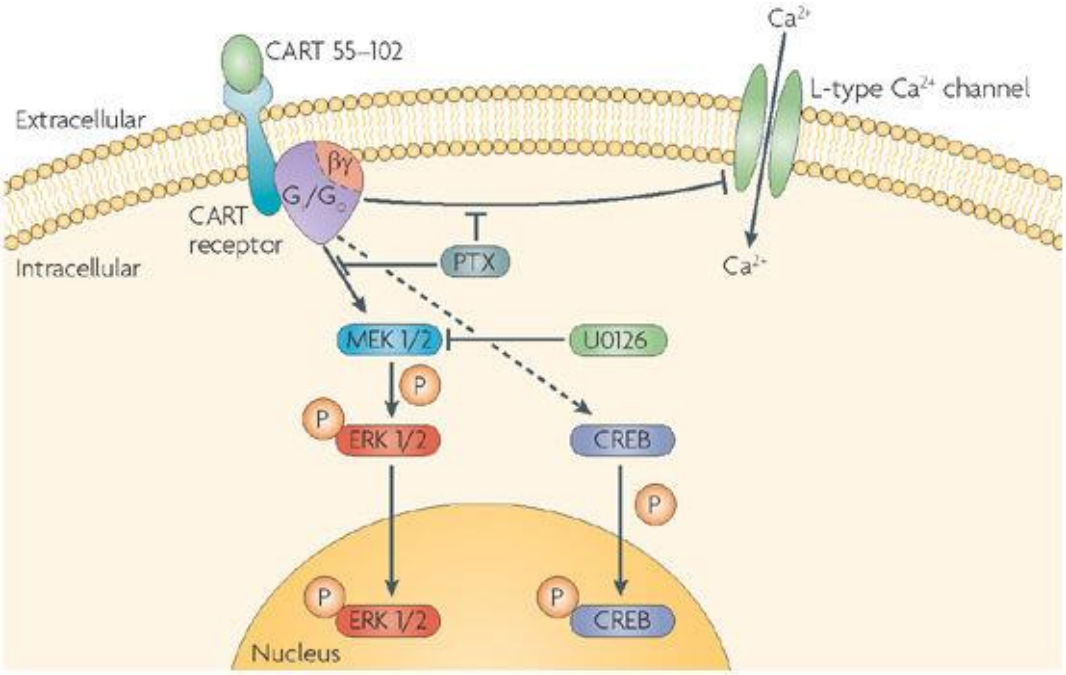

Figure 1.9. CART has previously been identified to signal through ERK, as well as CREB, putatively via a Gi/Go linked GPCR.

Image sourced from Rogge et al., 2008.

Other studies appear to be in agreeance with the hypothesis that CART signals through a Gi/Go GPCR mechanism (Yermolaieva et al., 2001, Lin et al., 2011), however, the exact receptor(s) CART signals through remain unknown, and so additional studies are certainly required to elucidate what receptor(s) CART may signal through.

Multiple suggested pathways in which CART may signal through are beginning to emerge. As mentioned previously, CART was previously shown to signal through ERK, a key component of the Mitogen-Activated Protein Kinase pathway (MAPK) (Lakatos et al., 2005). A number of studies have emerged in agreement with this, demonstrating CART may phosphorylate ERK (Jia et al., 2008, Chiu et al., 2010, Lin et al., 2011, Brennan et al., 2012). Interestingly, a more recent study reported that CART could phosphorylate cJun-amino-terminal kinase (JNK), but not ERK (Nagelova et al., 2014). A potential reason for this may have been that the majority of previous research was carried out using the CART 42-89 peptide, whereas this study used the 49-89 peptide. Finally, a study in 2013 highlighted that CART treatment resulted in the phosphorylation of PKB, FOXO1, ERK and P90RSK under glucotoxic conditions (Sathanoori et al., 2013). The authors suggested that these factors were phosphorylated as a result of CART promoting the proliferation and survival of cells under glucotoxic conditions, as proliferation could be inhibited using agents to block each of these pathways (Sathanoori et al., 2013). There are undoubtedly a number of signalling mechanisms which CART may signal through, however, much work is still needed in order to fully understand these. Primarily, the identification of the receptor(s) in which CART signals through would certainly provide researchers with an invaluable tool for understanding the molecular biology of CART even further.

1.2.3 The function of CART peptides – Drug reward and feeding

As mentioned previously, CART was named due to the knowledge that it's expression was increased in response to cocaine and amphetamines. Much of the early work on CART focused on understanding why CART was increased in response to psychostimulatory drugs. Early studies suggested

that, upon CART administration to the intra-ventral tegmental area of rat brains, locomotor activity was increased (Kimmel et al., 2000). This was followed by a number of studies suggesting that CART, rather than enhancing locomotor activity in the presence of cocaine, actually reduced cocaine-induced locomotor activity (Jaworski et al., 2003, Kim et al., 2003, Jaworski et al., 2007). Further, a study in 2008 demonstrated CART injection into the nucleus accumbens reduced cocaine self-administration in rats, leading the authors to conclude that CART acts to oppose the action of psychostimulants (Jaworski et al., 2008). This hypothesis has since been strengthened by recent studies in agreement that CART functions to oppose the action of psychostimulants (Job et al., 2012, Job et al., 2014). Fascinatingly, a study in 2013 demonstrated that repeated cocaine administration was capable of de-sensitizing rats to the inhibitory effects of CART (Job et al., 2013), suggesting that desensitization to CART can occur following prolonged exposure to psychostimulatory drugs. These studies have firmly cemented CART as a regulator of addiction and drug reward. Given the role of CART in addiction, it is not surprising that recent studies found nicotine to have profound effects on the expression of CART in many areas of the brain (Kaya et al., 2016).

While the role of CART in addiction appears clear, it is worth mentioning that a primary role of CART in the body is regulation of feeding. The role of CART in feeding was first proposed in 1998, where a study highlighted CART was capable of inhibiting food intake (Lambert et al., 1998). Shortly after this, a further study added strength to the hypothesis that CART was a negative regulator of feeding (Kristensen et al., 1998). This study demonstrated that food-deprivation resulted in diminished CART mRNA levels, and leptin could regulate CART levels (Kristensen et al., 1998). Leptin is a well characterized negative-regulator of feeding (Klok et al., 2007), and so in linking the expression of CART with leptin, the hypothesis that CART was a negative regulator of feeding was strengthened substantially. Further research has confirmed that CART can indeed negatively regulate weight gain (Qing et al., 2007, Burghardt et al., 2016), confirming CART as a negative regulator of feeding and weight gain. CART negatively regulating feeding is thought to

involve the inverse relationship between CART and appetite-promoting factors such as neuropeptide-Y (NPY) and ghrelin (Yu et al., 2017) (figure 1.10).

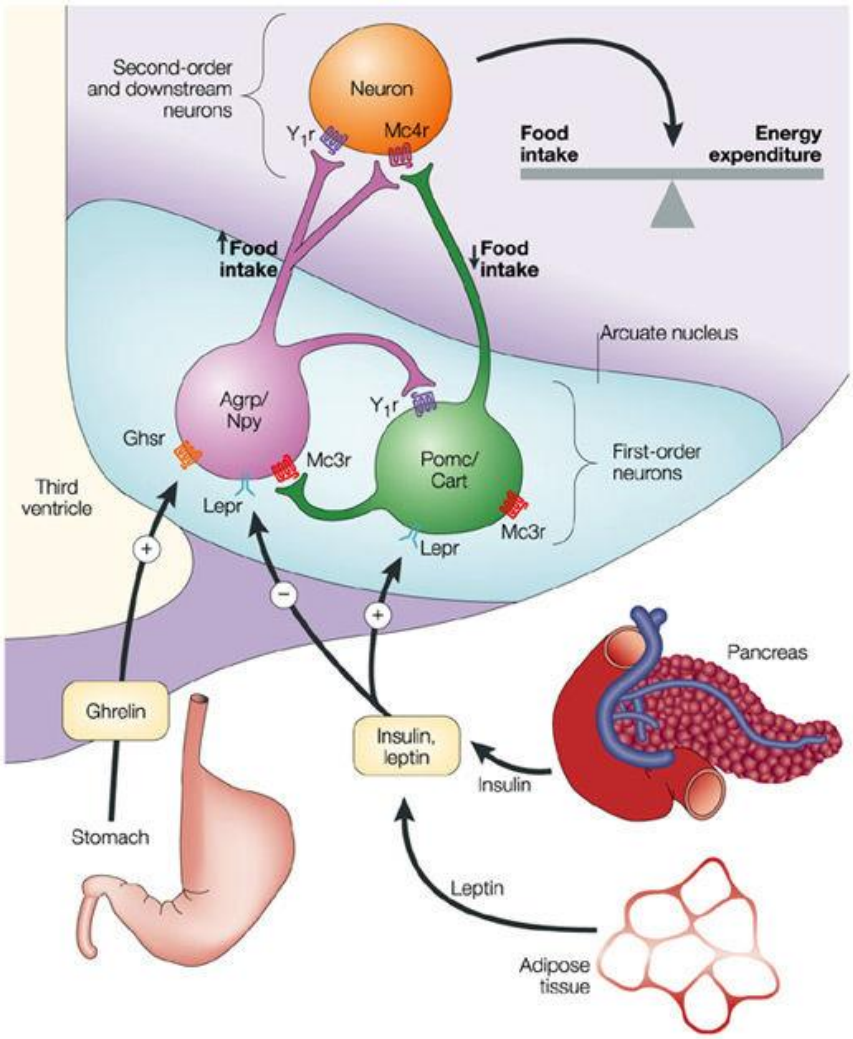

Figure 1.10. Insulin and Leptin can positively influence CART-containing neurons to inhibit food intake.

Image sourced from Barsh et al., 2002.

1.2.4 CART peptides in disease

1.2.4.1 Obesity

Given CART's role as an anorectic neuropeptide, it is not surprising to find that CART has previously been shown to contribute to obesity. As mentioned above, CART is generally accepted to negatively contribute to food intake. Indeed, CART knockout mice have previously been shown to exhibit weight gain (Asnicar et al., 2001), and delivery of CART to obese rats facilitated suppression of weight gain (Qing et al., 2007). One of the first links between CART and obesity in humans was published in 2001, where a missense mutation (L34F) within the N-terminal region of CART was found in a large family of obese subjects (Del Giudice et al., 2001). The authors of this study followed up with another study published in 2006, confirming the L34F mutation within CART resulted in the improper processing and sorting of CART *in vitro* (Yanik et al., 2006). A study published in 2005 suggested a single nucleotide polymorphism (SNP) within the CART gene was significantly associated with obesity, but the functional consequence of this SNP was not fully elucidated (Guerardel et al., 2005). In 2016, a study investigating the anti-obesity effects of Chowiseungcheng-tang (CST, used to treat metabolic disorders) confirmed that the anti-obesity impact of CST was, at least in part, due to an increase in the expression of CART (Ansari et al., 2016).

There are, however, studies which conflict with the aforementioned examples. For example, in 2010, a role for CART as a positive regulator of food intake was proposed from diabetic rat models (Hou et al., 2010). In 2012, a study highlighted that serum CART levels positively correlated with body mass index (BMI) in diabetic and non-diabetic human subjects (Hehir et al., 2012). Furthermore, in 2016, a positive correlation between BMI, and increased levels of CART in ovarian granulosa cells and follicular fluid, was found in female subjects undergoing *in vitro* fertilization (IVF) (Ma et al., 2016). Finally, in 2013, a study confirmed that long-term high fat diet induced the expression of both CART and NPY, however, CART was expressed in the same neurons as NPY (pro-feeding), and the increase in CART had no effect on diet-induced obesity

(Lee et al., 2013). This study highlighted that while CART may be expressed in “NPY neurons”, very few “CART neurons” express NPY. The authors very eloquently suggested that, if the anorectic potential of CART is real, then their rat subjects must be resistant to CART (Lee et al., 2013). This is fascinating given the fact that, while CART is known to increase after administration of cocaine to inhibit locomotor function, previous research has proved that prolonged exposure to cocaine results in desensitization to CART (Job et al., 2013). This raises the intriguing possibility that, in chronic obesity, the human body no longer responds to the anorectic signals of CART, thus CART would still be produced in response to feeding, but would have no effect on satiety (similar to the effects of insulin in type 2 diabetic patients).

1.2.4.2 *Diabetes mellitus*

Diabetes mellitus is characterized by the bodies inability to metabolise glucose. Type 1 diabetes is characterised by the inability of pancreatic beta cells to produce insulin, the hormone responsible for the transport of glucose into the cells, resulting in hyperglycaemia. In contrast, patients with type 2 diabetes still possess the ability to produce insulin, however, it is ineffective at removing glucose from the bloodstream. In 2006, a putative role for CART in diabetes was established (Wierup et al., 2006). The authors stated that the rational for their study was due to previously published research demonstrating CART expression in pancreatic islet cells (Wierup et al., 2004), and that CART deficient mice showed impaired glucose-stimulated insulin secretion and impaired glucose tolerance (Weirup et al., 2005, Weirup et al., 2006). In the study, the authors confirmed CART as a regulator of islet cell hormone secretion, and demonstrated an upregulation of CART in beta-cells of type 2 diabetic rats (Weirup et al., 2006). An impressive study in 2016 highlighted a number of key mechanisms by which CART could contribute to in a model of type 2 diabetes, such as increased glucose secretion, decreased glucagon secretion, and altered glucose homeostasis (Abels et al., 2016). Further, the authors found that CART was expressed at higher levels in islet cells of type 2 diabetic humans and mice (Abels et al., 2016). The most recent studies of

CART in diabetes are in agreement with the aforementioned studies, demonstrating that silencing of CART drastically reduced insulin secretion and a network of transcription factors essential to the normal function of pancreatic beta cells *in vitro* (Shcherbina et al., 2017) (figure 1.11).

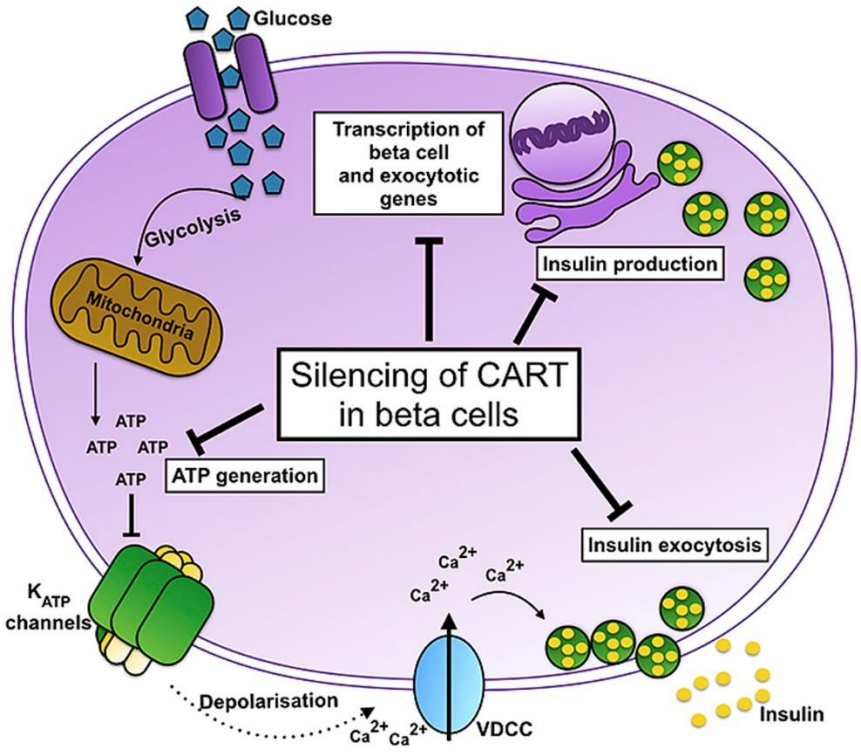

Figure 1.11. Shcherbina and colleagues demonstrated that silencing of CART had drastic effects on the normal function of pancreatic beta cells. Image sourced from Shcherbina et al., 2017.

In addition, it has been demonstrated that CART protects beta cells against glucotoxicity (Sathanoori et al., 2013), a hallmark which may arise in type 2 diabetic patients. Taking the data of all mentioned studies above, this suggests that CART is required for the normal function of beta cells in models of type 2 diabetes, and CART may protect beta cells from glucotoxicity which may be a consequence of type 2 diabetes. The authors of these studies are in agreement that a therapeutic use for CART in enhancing beta cell function

may be of benefit for patients with type 2 diabetes. Interestingly, there is very little studies in the literature for the role of CART in type 1 diabetes. One study published in 2007 demonstrated that serum levels of CART were decreased in models of type 1 diabetes compared to healthy controls (Toyoshima et al., 2007). Given that type 1 diabetes is characterised by an inability for the body to produce insulin, perhaps an investigation into the use of CART as a therapeutic strategy in type 1 diabetes is warranted.

1.2.4.3 CART peptides as therapeutic strategies for patients with Parkinson's disease and Stroke victims

Recent research has highlighted that CART may be an attractive therapeutic strategy for patients suffering from Parkinson's disease (PD). This was first suggested in a study published in 2012 (Mao et al., 2012). The authors suggested that CART could localise to the mitochondria to elicit activating and antioxidative effects, and highlighted that CART administration could improve behaviours exhibited by PD mouse models (Mao et al., 2012). The authors concluded that, through its role as an antioxidant, CART could be beneficial to PD patients, given the understanding that mitochondrial dysfunction is a known contributing factor to PD. In 2016, another study delved further into this hypothesis by testing whether CART could attenuate a PD like condition brought on by treatment with 6-hydroxydopamine, as well as testing whether CART had any effect on the anti-PD effects of levodopa (L-DOPA). Astonishingly, CART was found to significantly diminish the action of 6-hydroxydopamine in inducing a PD like state, and CART could potentiate the anti-PD effects of L-DOPA (Upadhya et al., 2016). The authors suggested that CART may increase dopamine release from intact neurons in models of PD, and this increase in dopamine results in the increased activity of L-DOPA (Upadhya et al., 2016).

One of the first studies to associate CART as a beneficial peptide in stroke victims was published in 2006. The authors confirmed that estradiol could increase the expression of CART using both *in vitro* and *in vivo* models of neural injury (Xu et al., 2006). The authors went on to demonstrate intravenous

administration of CART protected against ischemic brain injury *in vivo* (Xu et al., 2006). A number of studies followed this, all in agreement that CART could protect against ischemic brain injury following an artificial stroke (Chang et al., 2011), and a possible mechanism for this was the pro neuro-regenerative effects promoted by CART (Luo et al., 2013). The most recent studies on CART as a protector against brain injury confirmed CART could facilitate neurite outgrowth of cortical neurons after glucose and oxygen deprivation (Wang et al., 2014), and could induce angiogenesis as a protective mechanism from stroke (Liu et al., 2016). Taken together, these data strongly suggest CART acts in a neuroprotective manner, and may offer a novel therapeutic strategy for alleviating symptoms of neurodegenerative disorders such as PD and stroke.

1.2.4.4 CART and cancer

The role CART plays in cancer remains an elusive, understudied phenomenon. The first study highlighting a potential role for CART in cancer came in 1999, where a study reported high expression of CART in anorectic rat glucagonomas, but not in hypoglycemic insulinomas (Jensen et al., 1999). This study also highlighted that a non-anorectic metastasis of glucagonoma origin retained high expression of CART, and produced high levels of circulating CART (Jensen et al., 1999). Following this, a number of studies emerged highlighting that CART expression can be altered in neuroendocrine cancers (Bech et al., 2008, Jarhult et al., 2010, Landerholm et al., 2011). However, it was not until 2012 that the relationship between CART expression and patient survival came to light (Brennan et al., 2012). In this study, CART was characterized as an independent prognostic factor in ER+, lymph node-negative breast cancer. Furthermore, this study highlighted that CART could alter the function of ERα, and high expression of CART indicated worse response to tamoxifen (Brennan et al., 2012). In the same year, a similar finding was found in patients with small bowel carcinoid tumours (Landerholm et al., 2012). In this study, it was shown that high CART expression correlated with worse survival in patients with small bowel carcinoid tumours. The study

went on to demonstrate CART could increase the growth of colon cancer cells, and increase the expression of cyclin D-1 *in vitro*. Since then, CART has been identified as a potentially useful biomarker for identifying progressive disease in patients with pancreatic neuroendocrine tumours (Ramachandran et al., 2015), and may be associated with breast cancer risk in pre-menopausal women with high indigenous American ancestry (Slattery et al., 2015).

1.3 Aims of project

As discussed in section 1.1 of this study, further research is still needed in order to understand why some women, unfortunately, do not respond to treatment. Current research is gradually elucidating the role CART plays in diseases such as diabetes and obesity, however, the role of CART in cancer remains ambiguous. We previously identified CART to be a prognostic factor in ER+, lymph node-negative breast cancer (Brennan et al., 2012). Further, this research highlighted a role for CART in altering the function of ERα, and high levels of CART indicated worse response to tamoxifen (Brennan et al., 2012). Consequently, we suggest that interrogating the molecular biology of CART in breast cancer may benefit in understanding why CART indicates worse survival in breast cancer patients.

A two-pronged approach has been designed for this study. First, we aim to utilize transcriptomic techniques in order to gain a broad understanding of the effects CART can have on the transcriptional landscape of ER+ breast cancer cells. Next, we aim to investigate the consequence CART has on ERα interacting partners using a mass spectrometry approach. By performing these techniques, we hope to identify key factors which may help in understanding why CART is associated with worse survival in breast cancer patients.

Chapter 2. Materials and Methods

2.1 Cell culture

2.1.1 Cell lines

MCF-7 cells were a kind gift from Professor Robert Clarke of Georgestown University. T-47D and HEK293-T cells were purchased from ATCC. MCF-7 and HEK293-T cell lines were grown in DMEM (Sigma Aldrich, St. Louis, MO, USA), and T-47D cells were grown in RPMI-1640 (Gibco, Thermo Fisher Scientific, Waltham, MA, USA). All medium was supplemented with 10 % (v/v) Fetal Bovine Serum (FBS) (Gibco, Thermo Fisher Scientific, Waltham, MA, USA), 1 % (v/v) penicillin/streptomycin (Gibco, Thermo Fisher Scientific, Waltham, MA, USA), and 1 % (v/v) L-glutamine (Gibco, Thermo Fisher Scientific, Waltham, MA, USA). Cells were routinely checked for mycoplasma contamination. All cell lines were maintained in a cell culture incubator at 37°C in 5% CO_2.

2.1.2 Sub-culturing of cell lines

Once cell lines had reached 75 - 80 % confluency, the medium was removed and cells were washed using sterile phosphate-buffered saline (PBS) (Sigma Aldrich, St. Louis, MO, USA). Once washed, the cell monolayer was covered in 0.05 % trypsin (Gibco, Thermo Fisher Scientific, Waltham, MA, USA) and cells were left to detach at 37°C. Once detachment was confirmed using a light microscope, fresh medium was added at a volume twice that of trypsin to inactivate it. Cells were then seeded into new culture dishes at the appropriate sub-cultivation ratio (usually 1:4 – 1:6).

2.1.3 Cryofreezing of cell lines for long-term storage

An 80% confluent 75 cm^2 growth flask (T-75) (Sarstedt, Nümbrecht, Germany) was used per stock. Once detached from the flask by trypsinisation, the cells were collected in a 15 ml round-bottom tube (Greiner Bio-One, Kremsmünster, Austria) and centrifuged at 300 x g for 3 minutes. The supernatant was

removed, and the cell pellet was re-suspended in 1 ml freezing medium (standard medium with 10% (v/v) sterile-filtered DMSO (Sigma Aldrich, St. Louis, MO, USA) and transferred to a cryo-tube (Greiner Bio-One, Kremsmünster, Austria)). This was then placed into a Mr.Frosty (Nalgene) and the cells were frozen to -80°C. Once frozen, the cells were moved from the -80°C to the liquid nitrogen tank for long-term storage.

2.1.4 Thawing and re-growing cell lines after long-term cryopreservation

Medium was warmed to 37°C in a water bath and 4 ml was aliquoted to a 15 ml round-bottom tube. Cells were removed from freezing and half the tube was immersed in a 37°C water bath until cells were no longer frozen. Cells were transferred to the tube containing pre-warmed growth medium and centrifuged at 300 x g for 3 minutes. Next, the medium was removed, 5 ml fresh growth medium was added to the cell pellet and transferred to a 25 cm^{2} growth flask (T25) (Sarstedt, Nümbrecht, Germany). Once cells achieved a monolayer within this flask, the cells were trypsinised and re-seeded into larger flasks.

2.1.5 Cell counting and seeding

Following detachment from the culture flask, cells were transferred to a sterile 15 ml round-bottom tube and centrifuged at 300 x g for 3 minutes. After centrifugation, the supernatant was removed and the cell pellet was re-suspended in 10 ml fresh growth medium. Ten µl of this suspension was loaded onto one side of a haemocytometer and the total number of cells was counted. All 4 squares of the haemocytometer were counted, and the number was divided by 4 to give an average number of cells loaded. This number was further multiplied by 10,000 to give the number of cells per 1 ml growth medium. From this, cells could be seeded at a known density for each experiment.

2.1.6 Preparation of medium for “hormone-stripped” experiments

For studies completed in the absence of estrogen, phenol-red free derivatives of either DMEM (Sigma Aldrich, St. Louis, MO, USA) or RPMI-1640 (Gibco, Thermo Fisher Scientific, Waltham, MA, USA) were used, due to the knowledge that phenol-red is a weak estrogen mimic. Medium was supplemented with 5 % (v/v) Charcoal/Dextran treated FBS (Hyclone, GE Healthcare, Wauwatsoa, WI, USA), 1 % (v/v) penicillin/streptomycin and 1 % (v/v) L-glutamine. Hereon in, this medium will be referred to as “hormone-stripped medium”.

2.2 Generation of stable-inducible cell lines

2.2.1 Safety precautions

All procedures involving lentiviral particles were carried out in a level 2 biosafety containment laboratory. Handling & disposal procedures of all materials/waste was approved by the Environmental Protection Agency (EPA).

2.2.2 Principle of tetracycline-induced gene expression systems

A lentiviral expression vector containing the CART sequence was generated previously within our lab by ligating the CART sequence into the pLVX-Tight-Puro (Clontech Laboratories, Mountain View, CA, USA) plasmid (re-named pLVX-CART). The Lenti-X^{TM} Tet-ON Advanced system (Clontech Laboratories, Mountain View, CA, USA) was employed in order to create a “tetracycline-inducible” cell line capable of expressing CART in response to a tetracycline. Gene expression is induced following the introduction of a tetracycline derivative such as doxycycline. When doxycycline is introduced into the cell culture medium, the rtTA-Advanced protein binds to the tetracycline response element in the P-tight promotor, facilitating gene expression of CART. This process allows for the controlled expression of

CART under any experimental conditions. Plasmid maps can be found under appendices, section C.

2.2.3 Preparation of lentiviral particles

One day prior to transfection, the HEK293-T cells were plated in a T75 flask (Sarstedt, Nümbrecht, Germany). The next day, cells were transfected with the pLVX-CART plasmid, as well as the necessary lentiviral plasmids. The transfection was carried out using lipofectamine-2000 (Thermo Fisher Scientific, Waltham, MA, USA) as per manufacturers guidelines. The next day, medium was replaced with fresh growth medium for 48 hours, and following this, the medium containing lentiviral particles was collected from the flask and filtered through a 0.45 µm filter (Merck, Kenilworth, NJ, USA).

2.2.4 Transduction of the T47D cell line

Lentiviral-containing medium collected previously was supplemented with polybrene (Chemicon, Merck, Kenilworth, NJ, USA) at a concentration of 10 µg/ml to facilitate lentiviral gene transfer, and added to target cells. Following a 24-hour incubation with the virus, the growth medium was removed and replaced with fresh growth medium containing 2 µg/ml puromycin (Sigma Aldrich, St. Louis, MO, USA). As a control, a non-transduced T47D derivative received growth medium containing this concentration of puromycin. Selection was carried out until no viable cells could be detected in the non-transduced control (1 – 2 weeks was sufficient time for this to occur).

2.2.5 Secondary virus harvesting and target cell transduction

Once the target cells had been transduced with the pLVX-CART plasmid and selection was complete, a second virus was generated using the Tet-ON-ADVANCED plasmid. This was carried out in HEK293-T cells as described previously (section 2.2.3), and target cells were transduced with the harvested virus. Following a 24-hour incubation with the virus, the growth medium was

removed and replaced with fresh growth medium containing 200 µG/ml G-418 (Sigma Aldrich, St. Louis, MO, USA). As described previously (section 2.2.4), a non-transduced derivative of the T47D cell line was also treated with G-418 as a selection control. The concentration of G-418 was incrementally increased to 600 µg/ml on a weekly basis until no viable cells could be detected in the non-transduced cells (4 weeks was sufficient time for this to occur).

2.2.6 Conformation of successful dual-transduction

Following selection, cells were plated in 6 well plates and treated with increasing concentrations of doxycycline (dox) (Sigma Aldrich, St. Louis, MO, USA) for 72 hours. Following this, protein was extracted and Western blot analysis (detailed in section 2.4) was employed to confirm successful CART expression. Cells were hereon renamed Tet-ON T47D cells.

2.3 In vitro phenotypic assays

2.3.1 Propidium iodide staining and cell cycle analysis

Cells were collected by centrifugation at 300 x g and washed with sterile PBS (Sigma Aldrich, St. Louis, MO, USA). Following this, cells were pelleted by centrifugation at 300 x g for 5 minutes, and the pellet was resuspended in 1 ml PBS, and ethanol (Sigma Aldrich, St. Louis, MO, USA) was added dropwise to the suspension over gentle agitation until a final ethanol concentration of 70% was reached. Cells were left on ice for 15 minutes, followed by centrifugation at 300 x g for 5 minutes and the pellet was resuspended in 500 µl propidium iodide staining solution (50 µg/ml propidium iodide (Sigma Aldrich, St. Louis, MO, USA), 0.1 mg/ml RNase A (Sigma Aldrich, St. Louis, MO, USA), 0.05% (v/v) triton X-100 (Sigma Aldrich, St. Louis, MO, USA), in PBS (Sigma Aldrich, St. Louis, MO, USA)). Cells were left to fix for 40 minutes at 37°C, pelleted by centrifugation at 300 x g, and further resuspended in 3 ml PBS. Following this, cells were pelleted for a final time at 300 x g, the supernatant was removed

and the cell pellet was resuspended in 500 µl PBS for flow cytometry. Flow cytometry was performed on a FACScanto machine (BD Biosciences, Qume Drive San Jose, CA, USA), and 10,000 events per run were recorded.

2.3.2 MTT (3-(4,5-dimethylthiazol-2-yl)-2,5-diphenyltetrazolium bromide) assay

4000 cells were seeded per well into a 96 well plate (Sarstedt, Nümbrecht, Germany). The following day, medium was removed and replaced with the given experimental conditions, and cells were incubated at 37°C for the duration of the experiment. On the final day, a stock of thiazol blue tetrazolium bromide (Sigma Aldrich, St. Louis, MO, USA) was prepared at a concentration of 5 mg/ml in sterile PBS, and sterile filtered through a 0.22 µm filter (Merck, Kenilworth, NJ, USA). A total of 20 µl of this solution was added per well, and cells were incubated for at least 3 hours at 37°C in the dark. During this time, viable cells in culture use mitochondrial enzymes (such as mitochondrial reductase) to convert the MTT to purple formazon crystals. Following the incubation, the medium was removed, and purple formazon crystals were dissolved in 200 µl DMSO (Sigma Aldrich, St. Louis, MO, USA). The plate was left on a plate-shaker for 15 minutes, followed by reading at 570 nm on a Victor Wallac Spectrophotometer.

2.3.3 Anti-endocrine drug treatments

Both anti-endocrine agents (4-OH Tamoxifen and Fulvestrant) were purchased from Selleckchem (Selleckchem, Munich, Germany). Both agents were re-suspended in DMSO (Sigma Aldrich, St. Louis, MO, USA) as per manufacturers guidelines (final stock was 50 mM for both drugs), and DMSO was used as the experimental vehicle control in all instances. For drug treatments, cells were seeded in 96 well plates and left to adhere overnight at 37°C. Medium was changed the next day and replaced with medium containing the desired concentration of drug or vehicle control. Once the indicated time

had elapsed, the MTT assay was used to assess cell viability as described in section 2.3.2.

2.3.4 Protein half-life determination

To determine the half-life of the estrogen receptor, a eukaryotic protein-translation inhibitor known as Cycloheximide (CHX) (Sigma Aldrich, St. Louis, MO, USA) was used. Cells were plated in 6 well plates at a density of 200,000 cells per well in full medium. 24 hours later, medium was removed, cells were washed in sterile PBS, and fresh hormone-stripped medium was placed on the cells. 24 hours later, medium was supplemented with 1 µg/ml dox or suitable vehicle control for a further 72 hours. After this, medium was replaced with hormone-stripped medium containing 20 µG/ml CHX or vehicle control (DMSO), as well as 1 nM estradiol or vehicle control (EtOH) for the given time-points. Once each time point had elapsed, medium was removed and cells were washed in sterile PBS. Protein was extracted using radioimmunoprecipitation (RIPA) buffer as detailed in section 2.5.1.

2.4 Statistical analysis

All statistical tests are detailed in figure legends pertaining to the presented data. For statistical analysis between 2 groups, a 1-tailed or 2-tailed students t-test was performed. The 1-tailed t-test was only used when prior experimental knowledge meant the expected trend was already known (for example, validation of genes already deemed statistically significant from RNA-seq). For statistical analysis between more than 2 groups, a one-way or two-way ANOVA was used. The two-way ANOVA was employed when the experiment contained more than 2 or more variables. Multiple comparisons (either Bonferroni or Tukey) were performed following the ANOVA on Graphpad Prism.

2.5 Protein extraction and Western blotting

2.5.1 Protein extraction

Cells were lysed using RIPA buffer. Recipe for RIPA buffer can be found under appendices, section A. RIPA buffer was supplemented with complete mini EDTA free protease inhibitor (Roche Holding AG, Basel, Switzerland), and phosphatase inhibitor cocktail 4 (Sigma Aldrich, St. Louis, MO, USA) as per manufacturers recommended guidelines. Briefly, a sufficient volume of RIPA buffer was used to ensure full coverage of the growth plate. Plates were left on ice for 10 minutes, followed by scraping with a cell scraper (Sarstedt, Nümbrecht, Germany). Cells were collected in an eppendorf tube and left on ice for a further 10 minutes, with vortexing every 2-3 minutes. Collected cells were subsequently centrifuged at 18,000 x g for 20 minutes and the supernatant was retained. For samples where protein and RNA was extracted from the same samples, cells were first trypsinized and centrifuged at 300 x g into a cell pellet. This pellet was re-suspended in PBS and split in half, one half for RNA and the other for protein. These pellets were subsequently centrifuged at 300 x g, and following removal of the PBS, the pellet for protein extraction was resuspended in RIPA buffer and the protein extraction protocol was carried out as mentioned previously. The pellet for RNA was resuspended in TriSure (Bioline, London, UK) and RNA was extracted as per instructions detailed in section 2.6.

2.5.2 Protein quantification and sample preparation for SDS-Polyacryamide Gel Electrophoresis (SDS-PAGE)

Protein samples extracted previously were quantified using the Bicononinc Assay (BCA assay). BCA standards were prepared using Bovine Serum Albumin (Sigma Aldrich, St. Louis, MO, USA) within a concentration range of 2000 µG/ml to 0 µG/ml. 20 µl of each standard was pipetted in technical triplicate into a 96 well plate. 2 µl of protein to be quantified was pipetted into new wells (also in technical triplicate), followed by 18 µl of H_2O to bring the

final volume equal to that of the BCA standards. BCA protein reagent A and B (Thermo Fisher Scientific, Waltham, MA, USA) were mixed at a ratio of 50:1, and 200 µl of the mixture was pipetted into each well of the 96 well plate. The plate was subsequently incubated at 37°C for 15 minutes and read on a Victor Wallac Spectrophotometer at 570 nm. Protein sample concentrations were calculated based on the standard curve generated from the BSA protein standards, and 25 – 50 µg of protein was used per sample. LDS (Thermo Fisher Scientific, Waltham, MA, USA) was mixed with 2-mercaptoethanol (Sigma Aldrich, St. Louis, MO, USA) at a 10:1 ratio and added to the protein sample at a volume 4 times less than the total volume. Samples were then incubated at 100°C for 8 minutes followed by brief centrifugation at 18,000 x g.

2.5.3 Polyacrylamide gel preparation

Polyacrylamide gels were prepared in order to separate proteins based on their size (molecular weight). For high molecular weight proteins, an 8 % gel was used, and for low molecular weight proteins, a 12 % or 15 % gel was used. These gels were prepared using autoclaved water, 30% acrylamide (National Diagnostics), Tris-HCl (Thermo Fisher Scientific, Waltham, MA, USA), sodium dodecylsulfate (SDS) (Thermo Fisher Scientific, Waltham, MA, USA), ammonium persulfate (APS) (Sigma Aldrich, St. Louis, MO, USA) and N-N-N-N-tetraethyaminediethylamine (TEMED) (Sigma Aldrich, St. Louis, MO, USA). The volumes for each percentage gel is detailed below.

Table 2.1. Volumes of each reagent needed to prepare 10 ml of an SDS-polyacrylamide resolving gel.

Reagent	Volume for 8% gel (ml)	Volume for 10% gel (ml)	Volume for 12% gel (ml)	Volume for 15% gel (ml)
Water	4.6	4.0	3.3	2.3
30% acrylamide	2.7	3.3	4.0	5.0
1.5 M Tris-HCl pH 8.8	2.5	2.5	2.5	2.5
10 % SDS	0.1	0.1	0.1	0.1
10 % APS	0.1	0.1	0.1	0.1
TEMED	0.006	0.004	0.004	0.004

Once the resolving gel was cast, a thin layer of isopropanol (Sigma Aldrich, St. Louis, MO, USA) was used to cover the top of the gel to ensure the gel would set evenly. Once the gel was confirmed as set, the layer of isopropanol was removed and a 5 % stacking gel was placed on top of the resolving gel. The volumes for this stacking gel are detailed below.

Table 2.2. Volumes of each reagent needed to prepare 10 ml of an SDS-polyacrylamide stacking gel

Reagent	Volume for 5% stacking gel (ml)
Water	6.8
30% acrylamide	1.7
1.0 M Tris-HCl pH 6.8	1.25
10 % SDS	0.1
10 % APS	0.1
TEMED	0.01

Once the stacking gel was added, a 15 well comb (Bio-Rad Laboratories, Hercules, CA, USA) was placed in the stacking gel and the gel was left to set.

2.5.4 One-dimensional gel electrophoresis

One-dimensional gel electrophoresis was carried out using a mini-PROTEAN tetra vertical electrophoresis cell (Bio-Rad Laboratories, Hercules, CA, USA). Gels were placed into the electrode assembly and into the buffer tank. The buffer tank was filled with 1X running buffer, the recipe for which can be found under appendices, section A. The combs were removed from the gels and samples prepared previously were loaded into the wells. A protein ladder (PageRuler plus pre-stained protein ladder, Thermo Fisher Scientific, Waltham, MA, USA) was used as a marker of protein size. The lid was placed on the buffer tank and connected to a powerpack, and 90 V of power was used to promote migration of the protein samples from the top of the gel to the bottom.

2.5.5 Western blot

Once sufficient protein separation was achieved, the gel was removed from the electrophoresis cassette and into a mini gel holder cassette (Bio-Rad Laboratories, Hercules, CA, USA) as shown in figure 2.1. The gel was placed over a nitrocellulose membrane (GE Healthcare, Wauwatsoa, WI, USA) to facilitate transfer of proteins from gel to membrane. The western blot apparatus was then placed into a buffer tank and filled with 1X transfer buffer, the recipe for which can be found under appendices, section A. An ice pack was placed in the tank to keep the transfer buffer cold, and the transfer was run at 300 mA for 2 hours in the cold room.

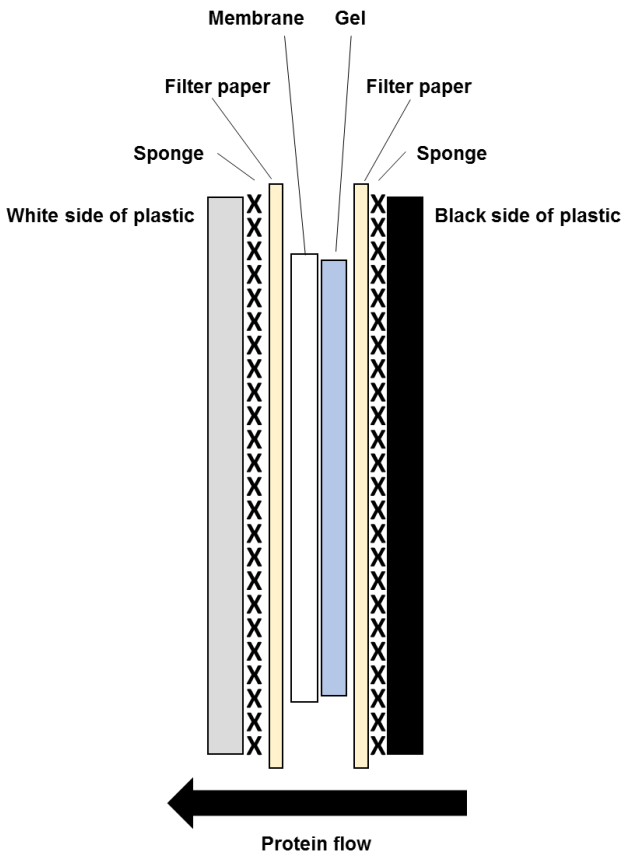

Figure 2.1. The diagram above shows how the western blot transfer sandwich is assembled. Electrical current allows for proteins to migrate from the black side of the sandwich to the white (clear) side, allowing proteins to migrate out of the polyacrylamide gel and onto the nitrocellulose membrane.

Once the two hours had elapsed, the rig was turned off, disassembled, and the membrane was stained with ponceau S solution (Sigma Aldrich, St. Louis, MO, USA) to confirm successful transfer. The membrane was subsequently washed 5 x 5 minutes in PBS (Sigma Aldrich, St. Louis, MO, USA) supplemented with 0.1 % Tween-20 (Sigma Aldrich, St. Louis, MO, USA) (PBS-t). The membranes were then incubated (blocked) in either 5 % Milk (W/V) (Sigma Aldrich, St. Louis, MO, USA) or 5% Bovine Serum Albumin (BSA) (W/V) (Sigma Aldrich, St. Louis, MO, USA) in PBS-t, based on the instructions provided from the antibody supplier, for 1 hour at room temperature with gentle agitation. Next, the membranes were incubated with

the primary antibody of choice overnight at 4°C with gentle agitation in 5% Milk-PBS-t or 5% BSA-PBS-t based on instructions from antibody provider.

2.5.6 Secondary antibody and detection of protein bands

Once the overnight incubation in primary antibody had elapsed, the membranes were washed 5 x 5 minutes PBS-t, followed by incubation with the Horseradish-Peroxidase (HRP) conjugated secondary antibody (Dako, Agilent Technologies, Santa Clara, CA, USA) in either 5% milk-PBS-t or 5% BSA-PBS-t based on what incubation agent was used for the primary antibody. This was performed for 1 hour at room temperature with gentle agitation. Following this, the membranes were washed 5 x 5 minutes in PBS-t, followed by incubation with ECL-chemiluminescent substrate (Thermo Fisher Scientific, Waltham, MA, USA) as per manufacturer's instructions.

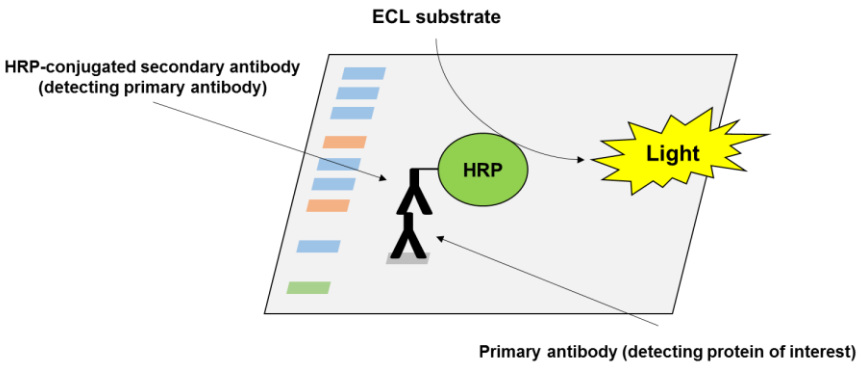

Figure 2.2. Diagram showing the principle of chemiluminescent signal generation during western blot analysis.

As shown in figure 2.2 above, the chemiluminescent ECL substrate reacts with the HRP conjugated to the secondary antibody to produce light, which was detected using an Amersham imager (GE Healthcare, Wauwatsoa, WI, USA).

2.5.7 Stripping and re-probing of nitrocellulose membrane

Following detection of protein bands, the membrane was washed 3 x 5 minutes in PBS-t and immersed in Restore western-blot stripping buffer (Thermo Fisher Scientific, Waltham, MA, USA) for 15 minutes. The membranes were subsequently washed for a further 3 x 5 minutes in PBS-t, followed by re-blocking in either 5% milk-PBS-t or 5% BSA-PBS-t for 1 hour. Finally, the membranes were incubated with the primary antibody, and the western blot protocol was carried out as described previously.

2.6 RNA isolation and qRT-PCR analysis

2.6.1 RNA extraction and quantification

Cells were lysed using 500 ul TriSure (Bioline, London, UK) per well in a 6-well plate. Cells were left in TriSure for 5 minutes at room temperature and transferred to a sterile 1.5 ml eppendorf tube. One hundred and twenty-five µl of chloroform (Sigma Aldrich, St. Louis, MO, USA) was added to each tube and the tubes were vortexed briefly, followed by standing at room temperature for 3 minutes and centrifuged at 18,000 x g for 30 minutes.

Following centrifugation, the top aqueous layer was removed from the tube and placed into a fresh 1.5 ml eppendorf tube (Greiner Bio-One, Kremsmunster, Austria). Care was taken to ensure the interphase was not disrupted at this point, as this can lead to contamination of RNA samples. Isopropanol (Sigma Aldrich, St. Louis, MO, USA) was added at a volume of 250 µl, inverted vigorously for 15 seconds and left to incubate at room temperature for 15 minutes. The samples were then subject to centrifugation at 18,000 x g for 20 minutes and the supernatant was removed. The RNA pellet was washed in 1 ml 70 % ethanol (Sigma Aldrich, St. Louis, MO, USA) and centrifuged at 18,000 x g for 10 minutes. The supernatant was discarded, and samples were centrifuged a final time at 18,000 x g for 1 minute to collect all residual ethanol at the bottom of the tube, which was discarded via micropipette. The samples were left to air-dry for 20 minutes in the fume hood,

and afterwards, the RNA pellet was resuspended in 20 µl nuclease-free H_2O (Promega, Madison, WI, USA).

A nanodrop was used to quantify RNA and check the quality of RNA extracted. The nanodrop was blanked using nuclease-free H_2O and 1 µl of sample was loaded on the nanodrop pedestal. RNA quantification was provided as X ng per 1 µl, and RNA quality was determined based on the 260/280 value (samples should be over 1.8) and the 260/230 value (samples should be close to/exceed 2.0).

2.6.2 cDNA synthesis

One µg of total RNA was used per cDNA synthesis reaction. The final reaction volume for each sample was brought to 7 µl using nuclease-free H_2O. Samples were made up in thin-wall PCR strip tubes (Sigma Aldrich, St. Louis, MO, USA). 1 µl of DNAse 1 amplification grade (Invitrogen, Thermo Fisher Scientific, Waltham, MA, USA) and 1 µl 10X reaction buffer (Invitrogen, Thermo Fisher Scientific, Waltham, MA, USA) was added to each tube and samples were incubated at room temperature for 15 minutes. Following incubation, 1 µl of EDTA (Invitrogen, Thermo Fisher Scientific, Waltham, MA, USA) was added to each tube and samples were incubated at 65°C for 10 minutes. Samples were then placed on ice, and 1 µl of random primers (Invitrogen) and 1 µl of dNTPs (Bioline, London, UK) were added to each tube once the samples had chilled. Next, 4 µl 5X first strand buffer (Invitrogen, Thermo Fisher Scientific, Waltham, MA, USA), 2 µl DTT (Invitrogen, Thermo Fisher Scientific, Waltham, MA, USA) and 1 µl RNAse-OUT (Invitrogen, Thermo Fisher Scientific, Waltham, MA, USA) was added to each tube and samples were incubated on ice for 5 minutes, at which point 1 µl of SuperScript 3 reverse transcriptase (Invitrogen, Thermo Fisher Scientific, Waltham, MA, USA) was added to each tube, and samples were placed into a T100 thermal cycler (Bio-Rad Laboratories, Hercules, CA, USA) using the cDNA synthesis protocol detailed below.

Table 2.3. Times and temperatures used for cDNA synthesis.

Step 1	Step 2	Step 3
42 ºC for 90 minutes	70 ºC for 15 minutes	4 ºC infinite hold

2.6.3 Quantitative Reverse Transcriptase-PCR (qRT-PCR)

To quantify the level of gene expression from RNA samples, qRT-PCR was used. First, an RT-PCR master-mix was made (13.2 µl nuclease-free H_2O, 2.4 µl 5 nM forward primer, 2.4 µl 5 nM reverse primer, 20 µl SYBR-Green (Promega, Madison, WI, USA)) per sample for technical duplicates. 19 µl of RT-PCR master-mix was pipetted into each well of a 96 well plate (Thermo Fisher Scientific, Waltham, MA, USA) followed by 1 µl of cDNA per well. A plate seal (Thermo Fisher Scientific, Waltham, MA, USA) was placed onto the 96 well plate and plate was centrifuged at 3,000 x g for 3 minutes at 4ºC. The plate was then loaded into a 7500 Real Time PCR system machine (Thermo Fisher Scientific, Waltham, MA, USA) and qRT-PCR was carried out using the protocol listed below.

Table 2.4 Times and temperatures for qRT-PCR.

Step 1	Step 2	Step 3 (repeat for 40 cycles)	
50 ºC for 2 minutes	95 ºC for 10 minutes	95 ºC for 10 seconds	60 ºC for 1 minute

For analysis, the average cycle-threshold (CT) value between technical replicates for each test gene was calculated. Next, the average CT value between technical replicates for the endogenous control (18S rRNA unless stated otherwise) was calculated, and this was deducted from the average CT value of the test gene to give the delta CT (DCT) value. To calculate the delta-delta CT value (DDCT), the DCT value of the test sample was deducted from the DCT value of the experimental control (vehicle control in most cases). The DDCT was finally converted to the relative quantification (RQ) value by the

following equation; **POWER(2,-(DDCT sample))**. All analysis was performed on Microsoft Excel.

2.7 Endogenous protein immunoprecipitation

2.7.1 Antibody-bead crosslinking

20 µl protein A sepharose beads (Sigma Aldrich, St. Louis, MO, USA) were used per immunoprecipitation. Beads were washed 5 times in PBS-t. After the last wash, the antibody was incubated with the beads overnight with gentle agitation at 4°C in 1 ml PBS-t. The concentration of the antibody against the bait protein was always used at the same concentration as the isotype negative control antibody.

The next day, beads were washed twice in 0.2 M sodium tetraborate (Sigma Aldrich, St. Louis, MO, USA), pH 9.0. To crosslink beads to the antibody, the antibody-bead conjugate was incubated in 1 ml 0.2 M Sodium Tetraborate, supplemented with 0.02 M dimethylpirimophosphate (DMP) (Sigma Aldrich, St. Louis, MO, USA) for 30 minutes at room temperature with gentle agitation. The pH of the DMP solution was checked prior to incubation with beads, as crosslinking must be performed at a pH above 8.3. Following this, beads were washed once in 0.2 M ethanolamine pH 8.0 (Sigma Aldrich, St. Louis, MO, USA), followed by a two-hour wash in 0.2 M ethanolamine at room temperature with gentle agitation in order to quench the crosslinking step. Once complete, the beads were washed once in PBS, and re-suspended in 1 ml PBS. Beads were stored at 4°C until they were required (used within 1 week).

2.7.2 Immunoprecipitation

Briefly, antibodies and beads were crosslinked as described in section 2.7.1. Extra beads were prepared and crosslinked with the IgG negative control antibody for pre-clearing steps mentioned below. When needed, beads were spun down at 3000 x g for 1 minute, the supernatant was discarded and beads

were washed in 1 ml low-stringency lysis buffer (recipe can be found under appendices, section A) for 4 hours. For immunoprecipitation, 1 ml low-stringency lysis buffer was pipetted onto cells, and cells were scraped into fresh eppendorf tubes. These were left on ice for 10 minutes, with vortexing every 2 minutes. Lysates were spun at 18,000 x g for 10 minutes and the supernatant was retained. Lysates were then incubated with “pre-clear beads” (coupled to IgG negative control antibody) for 1 hour at 4°C. Next, the supernatant was removed from the “pre-clear beads” and the BCA assay was used to determine total protein concentration. Equal concentrations of protein per condition were made up to 1 ml in low-stringency lysis buffer, transferred to immunoprecipitation beads, and the immunoprecipitation was performed overnight at 4°C with gentle agitation. The next day, beads were spun down at 3000 x g for 1 minute at 4°C and the supernatant was discarded. Beads were washed 3 times in 1 ml low-stringency lysis buffer, and after the final wash the beads were resuspended in LDS loading buffer for Western blot analysis.

2.8 Bacterial techniques

2.8.1 Growing bacteria from glycerol stocks

Prior to thawing bacteria stocks, broth and plates were prepared as follows; Luria-Bertani (LB) broth was made using 20 g LB (Sigma Aldrich, St. Louis, MO, USA) in 1 L H_2O. LB/agar plates were made using 20 g LB & 15 g agar (Sigma Aldrich, St. Louis, MO, USA) in 1 L H_2O. Both LB broth and LB/agar solutions were autoclaved and allowed to cool below 55°C prior to the addition of ampicillin (Sigma Aldrich, St. Louis, MO, USA) to a final concentration of 50 ng/ml. Plates were poured beside a Bunsen burner to ensure a sterile work environment. Once plates had set, the bacteria stocks were thawed on ice and a sterile pipette tip was used to stab the stock and streak it gently onto the LB-agar plate. Plates were incubated at 37°C overnight to allow for bacteria growth. The next day, individual colonies were selected from the plate and inoculated in 5 ml LB-broth (containing ampicillin). Inoculation was left for roughly 8 hours, or until the culture was sufficiently cloudy.

2.8.2 DNA extraction from bacteria cultures

Bacteria grown previously were pelleted by centrifugation at 3000 x g for 5 minutes. Supernatant was removed and pellets were used for DNA extractions. The mini-prep kit (Qiagen, Hilden, Germany) was used to extract plasmid DNA from bacteria as per manufacturer's instructions. Once extracted, DNA was quantified using a Nanodrop, and stored at -20°C.

2.8.3 Bacteria cell transformation

For transformations, XL10-Gold ultracompetent bacteria cells (Agilent Technologies, Santa Clara, CA, USA) were used in all instances. Briefly, 2 µl DNA and 1 µl β-mercaptoethanol (Agilent Technologies, Santa Clara, CA, USA) was added to 45 µl XL10-Gold ultracompetent cells, followed by a 30-minute incubation on ice. Samples were then heat-pulsed at 42°C for 30 seconds, followed by a 2-minute incubation on ice. Pre-warmed LB-broth was added to each sample at a volume of 500 µl, followed by a 1 hour incubation at 37°C with gentle agitation. The sample was plated equally over 2 LB-Agar plates containing ampicillin, and incubated for greater than 16 hours at 37°C before colonies were picked and extracted using methods described previously.

2.9 Site-directed Mutagenesis

Primers used to create LXD-mutants were generated manually while adhering to the strict manufacturers guidelines for creating mutant-primers. Kit used to generate LXD mutants was the QuikChange XL Site Directed Mutagenesis Kit (Agilent Technologies, Santa Clara, CA, USA). The template plasmid used was the pCMV6-XL5-CART plasmid. Briefly, a PCR mix was made for each desired mutation as per manufacturer's instructions, and the mutant strand was generated using a Mastercycler Gradient (Eppendorf Scientific) using the cycle parameters shown below.

Table 2.5. PCR settings for site-directed mutagenesis protocol

Stage	Cycles	Temperature (ºC)	Time
1	1	95	1 minute
2	18	95	50 seconds
		60	50 seconds
		68	4 minutes 30 seconds
3	1	68	7 minutes

Following PCR cycles, the template plasmid was digested using the DPN1 restriction enzyme (Agilent Technologies, Santa Clara, CA, USA). As this plasmid was purified from E. *coli,* the methyl-groups on this plasmid make it susceptible to digestion from the DPN1 enzyme, whereas the mutant plasmid will not contain these methyl-groups. 2 µl of the digestion product was used to transform the XL-Gold ultracompetent cells as described previously. Positive control for mutagenesis was performed using the pWhitescript plasmid and mutant primers supplied as per manufacturers guidelines. DNA was extracted as described previously, and the DNA product was verified by MWG Eurofins using the T7 primer to confirm successful amplification of mutant plasmid.

2.10 Estrogen Responsive Element (ERE)-Dual luciferase reporter assay

2.10.1 Principle of ERE-dual luciferase reporter assay

An ERE-dual luciferase reporter assay uses an ERE-Luciferase plasmid to assess whether the experimental conditions in question can affect estrogen receptor activity. The ERE-luciferase plasmid contains the luciferase enzyme under the control of a promotor containing tandem repeats of an estrogen responsive element. Activation of the estrogen receptor results in the binding of the receptor to the promotor region of the plasmid, allowing for the transcription and ultimately translation of the luciferase enzyme. The luciferase

enzyme catalyses the conversion of luciferin to oxyluciferin, and in the process, emits light. To control for transfection efficiency and cell number variation, a CMV-Renilla is co-transfected with the ERE-luciferase plasmid. Reinilla luciferase converts coelenterazine to coelentaramide, which also produces light. Below are the reactions which take place within this experiment.

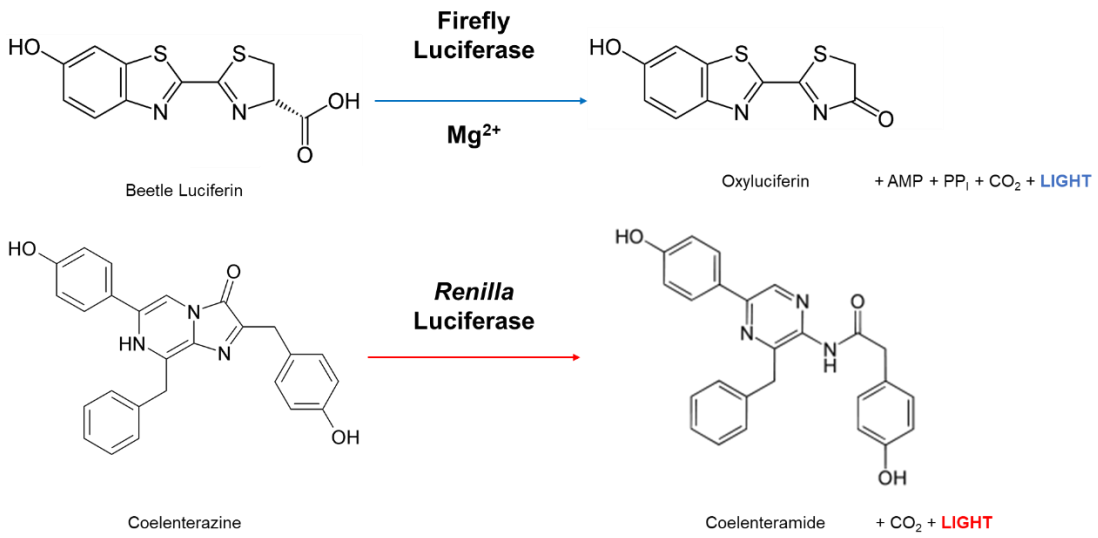

Figure 2.3. Reactions carried out during the dual luciferase reporter assay.

2.10.2 Dual transient transfection of ERE-luc and Renilla reporter plasmids

The Dual-Luciferase reporter assay kit (Promega, Madison, WI, USA) was used for all experiments detailed. All Dual-Luciferase reporter assays were carried out in 24 well plates. Cells were seeded at a density to allow for 70 – 80% confluency 24 hours post seeding (roughly 50,000 cells per well achieved this). Once the 24 hours had elapsed, cells were transfected using dharmafect (Dharmacon, Lafayette, CO, USA) as per manufacturer's instructions. The concentrations of each plasmid transfected were as follows; 250 ng ERE-Luc plasmid, 50 ng CMV-Renilla plasmid. The next day, the medium was removed and cells were washed with PBS. The medium was replaced with hormone-

stripped medium for a further 72 hours. For estradiol treatments within this experiment, 1 nm 17-beta estradiol (Sigma Aldrich, St. Louis, MO, USA) was added to the cells after the 72 hour period had elapsed, and these cells were left for a further 24 hours. For LXD-mutant studies, 1 µg of pCMV-CART / pCMV-CART-mutant plasmids were co-transfected with the ERE-luc & CMV-Renillla plasmids. The remainder of the experiment was completed as per manufacturer's instructions. Light was detected using a Fluroskan Ascent FL luminometer (Thermo Fisher Scientific, Waltham, MA, USA), and firefly luciferase activity was normalised to the renilla luciferase reading prior to data analysis.

2.11 RNA sequencing

2.11.1 Experimental design and sample preparation

Cells were seeded in 6 well plates at a seeding density of 300,000 cells per well. The next day, the medium was removed, cells were washed in PBS, and medium was replaced for hormone-stripped medium. Cells were further incubated for 24 hours, followed by the addition of doxycycline at a concentration of 1 µg/ml or suitable vehicle control (H_2O). Following 72 hours in these treatment conditions, medium was removed, cells were washed in PBS and trypsinized using phenol red-free trypsin (Gibco, Thermo Fisher Scientific, Waltham, MA, USA). Cells were centrifuged at 300 x g, and the pellet was split in two, one half for RNA extraction and one half for protein extraction to confirm cells were expressing CART. Both protein and RNA were extracted from cell pellets as described in section 2.5.1. This was performed 3 times to generate 3 independent experiments for each treatment condition prior to library preparation.

2.11.2 Library preparation and RNA sequencing

A nanodrop was used to quantify the extracted RNA, and samples were diluted in nuclease-free H_2O (Promega, Madison, WI, USA). The RNA integrity and quality was first checked using a Bioanalyzer, whereby an RNA integrity number (RIN) above 8 was deemed as acceptable. The total quantity of RNA used for the library preparation was 100 nG for all samples, and the libraries were prepared using the NeoPrep system (Illumina, San Diego, CA, USA) as per manufacturers guidelines. All libraries were normalised within this protocol.

Following library preparation, samples sequenced using a 2 x 75 base pair, paired-end, sequencing kit (Illumina, San Diego, CA, USA) on a NextSeq 500 (Illumina, San Diego, CA, USA)

For RNA sequencing, bioinformatic support was provided by Dr. Bruce Moran of University College Dublin using the pipeline detailed in section 2.11.3 – 2.11.5.

2.11.3 Data preparation

Fastq files from the paired-end data were downloaded from Illumina's BaseSpace suite. Quality of data was checked following FastQC. If multiple fastq files were generated for single samples, they were concatenated in Unix shell using the "cat" command. Next, the data was trimmed in order to remove bass calls of poor quality (Phred score < 20). Sequencing adaptors were further removed using the BBDuk tool in the BBMap package.

2.11.4 Alignment and processing of trimmed data

The trimmed data was aligned to the human hg19/GRCh37 reference genome using STAR (version 2.5.2a) (Dobin et al., 2012). The BAM file generated was sorted by coordinate, and duplicate reads were marked within the BAM file using the Picard-Tools "MarkDuplicates" call. The featureCounts tool from the SubRead package (Liao et al., 2014) was used to produce read counts, which

were then combined for all samples and used as the input for differential gene expression analysis.

2.11.5 Differential expression

The DESeq2 package (Love et al., 2014) was used to perform differential expression (DE) analysis in the statistical package R. Genes were removed if the data.frame of counts identified a gene with a sum of 0 across all samples. Samples names, their group (i.e., VEH or DOX) and the appropriate biological replicate number were used to generate a “conditions” data.frame, and this (as well as the counts) were loaded into a DESeq2DataSet class object using the DESeqDataSetFromMatrix call. The design variable was set as “~group”. The DESeq call produced results comparing cells treated with vehicle or doxycycline. The text file generated contained each gene expressed (Ensembl gene ID as well as Entrez gene ID), the FDR adjusted p-value, and the Log2foldchange. Principal component analysis (PCA) was performed in order to determine the similarity of all biological replicates across both treatment groups following standard protocols from the DESeq2 guide. Finally, the edgeR package call was used to generate Fragments-per-kilobase per million reads (FPKMs) (McCarthy et al., 2010, Robinson et al., 2012).

2.11.6 Gene ontology (GO) analysis of differentially expressed genes

Gene Ontology (GO) analysis was performed through the website DAVID. Ensembl gene IDs for significantly upregulated/downregulated genes were inputted to the database and the gene list was used to examine whether any of the identified genes were associated with certain biological processes. Due to the large amount of comparisons made, terms were only considered significant if the Benjamini-adjusted p value was below 0.05, rather than the non-adjusted p value.

2.11.7 Heatmap generation

Heatmaps for graphical representation of significantly differentially expressed genes were generated using Z-scores of each gene. Z scores were generated from FPKM values using the following formula: ((FPKM sample - population mean)/population standard deviation). Z scores were imported to Perseus, where hierarchial clustering of the dataset was performed to generate heapmaps (default parameters were used).

2.11.8 Gene Set Enrichment Analysis (GSEA)

GSEA was performed through the Broad Institute's online GSEA portal (software.broadinstitute.org/GSEA). Ensembl gene IDs for significantly upregulated or downregulated genes generated from the bioinformatic pipeline mentioned previously were uploaded to the software, all overlaps were checked, and the FDR q-value threshold was set to 0.05.

2.12 Mining of publicly-available ERα ChIP-seq datasets

RNA-sequencing is an extremely powerful "omic" technology for understanding the effect specific experimental conditions can have on the transcriptomic landscape of given samples. However, it is difficult to know what transcription factors are driving the expression/repression of these genes. Understanding whether ERα had previously been shown to bind the promotor region of these genes was of particular interest to this study, and so an in-*silico*, data mining excursion was carried out. To achieve this, the cistrome database was employed (cistrome.org), and the cistrome data browser portal was accessed. ESR1 was imputed as the "factor", and only T47D biological sources were considered (since the T47D cell lines were used for RNA-sequencing). The "putative targets" file was downloaded to the R statistical environment, where the target genes from our RNA-sequencing data could be searched against the downloaded dataset. A table containing the Gene name, the coordinate of given gene, and score from the ChIP-seq database, was generated.

2.13 Mass spectrometry analysis of Immunoprecipitated ERα-protein complexes

2.13.1 Experimental design

For mass-spectrometry analysis, 15 individual 150 mm plates were used per immunoprecipitation condition. Briefly, 2,000,000 Tet-ON T47D cells were seeded into each plate, and medium was changed to hormone-stripped RPMI 24 hours later. Following a 24 hour incubation in this medium, the cells were supplemented with the given treatment conditions for a further 72 hours, at which point the individual plates (per condition) were pooled and collected.

2.13.2 Mass spectrometry immunoprecipitation

2.13.2.1 General notes

All buffers and reagents were sterile filtered through a 0.22 µm filter (Merck, Kenilworth, NJ, USA) to minimise contamination, and all work was carried out in a clean fume hood to minimise keratin contamination. The final wash of beads was performed in PBS with no NP-40, as detergents are known to cause issues with the mass-spectrometer. At this point, a small volume of beads were aliquoted for western-blot analysis prior to in-solution digest to ensure the achieved immunoprecipitation had been specific. The beads used for mass-spectrometry analysis were subject to in-solution digest as soon as possible

2.13.2.2 Antibody-bead crosslinking

20 µl protein A sepharose beads (Sigma Aldrich, St. Louis, MO, USA) were used per immunoprecipitation. Beads were washed 5 times in PBS-t. After the last wash, the antibody was incubated with the beads overnight with gentle agitation at 4ºC in 1 ml PBS-t. The concentration of the antibody against the

bait protein was always used at the same concentration as the isotype negative control antibody (10 µg per IP in this experiment).

The next day, beads were washed twice in 0.2 M sodium tetraborate (Sigma Aldrich, St. Louis, MO, USA), pH 9.0. To crosslink beads to the antibody, the antibody-bead conjugate was incubated in 1 ml 0.2 M sodium tetraborate, supplemented with 0.02 M dimethylpirimophosphate (DMP) (Sigma Aldrich, St. Louis, MO, USA) for 30 minutes at room temperature with gentle agitation. The pH of the DMP solution was checked prior to incubation with beads, as crosslinking must be performed at a pH above 8.3. Following this, beads were washed once in 0.2 M ethanolamine pH 8.0 (Sigma Aldrich, St. Louis, MO, USA), followed by a two-hour wash in 0.2 M ethanolamine at room temperature with gentle agitation in order to quench the crosslinking step. Once complete, the beads were washed once in PBS, and re-suspended in 1 ml PBS. Beads were stored at 4°C until they were required (used within 1 week).

2.13.2.3 Preparation of cell lysates for immunoprecipitation

Cells were collected in 50 ml round-bottom tubes and washed twice in 10 ml PBS (Sigma Aldrich, St. Louis, MO, USA). Cells were then lysed using 1.2 ml buffer C (recipe can be found under appendices, section A) per immunoprecipitation. Buffers with ionic detergents were not used for extraction due to their denaturing capabilities. Samples were sonicated using a Branson digital sonifier (15 seconds on, 15 seconds off, 30% intensity). Followed by homogenisation using a tight-fitting dounce homogenizer, 20 strokes were applied per sample. The samples were then left to rotate for 20 minutes at 4°C, followed by centrifugation at 18,000 x g. The supernatant was collected and subsequently dialysed, using 15 kDa SnakeSkin dialysis tubing (Thermo Fisher Scientific, Waltham, MA, USA), against 50 volumes buffer C100 (recipe can be found under appendices, section A). This was left at 4°C overnight, or for a minimum time of 5 hours. Dialysed samples were subsequently subject to centrifugation at 18,000 x g for 20 minutes at 4°C. The supernatant was retained, and samples were quantified using the BCA assay (detailed above). An input sample was kept at this point for each sample.

2.13.3.4 Immunoprecipitation

Antibody-bound beads were blocked/equilibrated for 1 hour at 4ºC with gentle agitation in 1 ml buffer C100 containing 0.1 mg/ml insulin (Sigma Aldrich, St. Louis, MO, USA), 0.2 mg/ml chicken egg albumin (Sigma Aldrich, St. Louis, MO, USA), and 1% fish skin gelatine (Sigma Aldrich, St. Louis, MO, USA). Beads were then transferred to Protein LoBind-eppendorfs (Sigma Aldrich, St. Louis, MO, USA), washed in 1 ml Buffer C100, and incubated with desired quantity of protein for 3 hours at 4ºC with gentle agitation. The immunoprecipitation was performed in the presence of 225 units benzonase (Sigma Aldrich, St. Louis, MO, USA) to prevent detection of false-positive interactions based on proximity of proteins on DNA. Beads were then washed 5 times in Buffer C100 + 0.02 % NP-40 (Sigma Aldrich, St. Louis, MO, USA). After the final wash, the beads were resuspended in loading buffer (LDS + 10% Beta-Mercaptoethanol) and incubated at 100ºC on a ThermoMixer (Eppendorf, Hamburg, Germany) at 1200 RPM for 8 minutes. Samples were centrifuged briefly at 5,000 x g and the loading buffer was loaded into the gel for western blotting.

2.13.3.5 In-solution digestion of proteins

Beads were washed twice in 500 µl LS buffer (150 mM NaCl, 50 mM Tris pH 8.0, 5 mM EDTA, 1 M DTT (Sigma Aldrich, St. Louis, MO, USA), 10 mM PMSF (Sigma Aldrich, St. Louis, MO, USA), aprotinin (Sigma Aldrich, St. Louis, MO, USA) & leupeptin (Sigma Aldrich, St. Louis, MO, USA) 1:1000 (v/v), sterile filter through 0.45 nm filter (Merck, Kenilworth, NJ, USA)). Each wash involves a 5 minute incubation with gentle agitation at 4ºC, followed by centrifugation at 1,500 x g for 1 minute. Once completed, the supernatant was discarded and 8 M urea (Sigma Aldrich, St. Louis, MO, USA) (made up in HPLC-grade H_2O (Thermo Fisher Scientific, Waltham, MA, USA)) was added at the same volume as the beads within the tube (20 ul for this experiment), followed by 40 µl 100 mM ammonium bicarbonate (Sigma Aldrich, St. Louis, MO, USA) (made up in HPLC-grade H_2O). Next, calcium chloride ($CaCl_2$) (Sigma Aldrich, St. Louis, MO, USA) (made up in HPLC-grade H_2O) was added to a final

concentration of 5 mM, followed by the addition of DTT (made up in 100 mM ammonium bicarbonate) to a final concentration of 1 mM. Samples were mixed gently and left at room temperature for 15 minutes. Idoacetamide (Sigma Aldrich, St. Louis, MO, USA) was prepared in ammonium bicarbonate and added to the samples to a final concentration of 5 mM.

These steps aid in the denaturing and linearization of proteins bound to the antibodies. The idoacetimide prevents disulphide bridges from re-forming, thus keeping the proteins denatured and linear, allowing tryspin to cleave most of the available arginine/lysine residues within the proteins. This was left at room temperature for a further 15 minutes in the dark, at which point the pH of each sample was checked using pH paper (Sigma Aldrich, St. Louis, MO, USA). Samples must be within the neutral pH range, as trypsin will not optimally work outside this. Once samples were checked, 1 µg proteomic grade Trypsin (Sigma Aldrich, St. Louis, MO, USA) was added to each sample. Samples were incubated in a Thermomixer (Thermo Fisher Scientific, Waltham, MA, USA) at 37°C and 300 RPM overnight.

2.13.3.6 Acidification of digested peptides

Once the overnight incubation in tryspin was complete, the beads were spun down at 3000 x g for 2 minutes and the supernatant was transferred to fresh, Protein Lo-Bind Eppendorf tubes (Sigma Aldrich, St. Louis, MO, USA). Bead wash solution was prepared (0.1% trifluroacetic acid (TFA) (Sigma Aldrich, St. Louis, MO, USA) in HPLC grade H_2O) and 20 µl was used to wash the beads. It is critically important to add the TFA to the water, rather than add TFA to the tube and add H_2O on top of the TFA. Failure to do so may result in poly-ethylene glycol (PEG) contamination. Beads were spun down at 3000 x g for 5 minutes and the supernatant was combined with the supernatant collected previously. 100 % TFA was added to the samples at a volume which resulted in the final TFA concentration being 1 %. At this point, pH of all samples was checked on pH paper, as samples must be ~pH 2.0 prior to zip-tip equilibration. Finally, samples were vacuum centrifuged for 1 hour at 55°C.

2.13.3.7 C18 zip-tip equilibration

Methods such as SILAC (stable isotope-labelling of amino acids in cell culture) allow for quantitative data acquisition from mass spectrometry experiments, however, these methods can be expensive and time-consuming to optimise and carry out. Recent advances in the field of proteomics have allowed for the development of algorithms capable of performing label-free quantification (LFQ) of peptides from mass spectrometry experiments. A critical pre-requisite to performing LFQ of peptides is to ensure all samples are normalised prior to mass spectrometry analysis. To do this, C18 zip-tips (Merck, Kenilworth, NJ, USA) can be used as they bind exactly 5 µg of peptides, thus normalising all samples to a known quantity of peptides. C18 zip-tip equilibration is further advantageous as this single process desalts, concentrates and purifies the peptides for analysis. The method for zip-tipping was carried out as per manufacturer's instructions with the following deviations; The samples were not diluted in equilibration solution (0.1% TFA in HPLC-grade H_2O) to begin, as TFA has already been introduced to the samples during the acidification steps. Wetting solution (100% HPLC-grade acetonitrile (ACN) (Thermo Fisher Scientific, Waltham, MA, USA) was used once, rather than the stated three times in the manufacturers protocol. Equilibration solution used was 0.1% TFA in HPLC-grade H_2O, and washing was performed once rather than the stated three times as described in the manufacturers protocol. Binding of peptides was performed by pipetting up and down 20 times, rather than the manufacturers recommended 5-10 times. This was to ensure the C18 resin was completely saturated with 5 µg peptides. The elution buffer was made up as follows; 60:40 ACN:HPLC-grade H_2O + 0.1% TFA. This process was repeated 3 times per sample to ensure enough peptides were eluted for 3 technical replicates.

Once complete, samples were dried under vacuum centrifuge until ~ 2 µl was left in each tube. The peptides were re-suspended in 20 µl buffer K (97% HPLC-grade H_2O, 2.5% ACN, 0.5% acetic acid (Sigma Aldrich, St. Louis, MO, USA), centrifuged at 10,000 x g for 10 minutes, and 18 µl was transferred to mass spectrometry-compatible tubes (Sigma Aldrich, St. Louis, MO, USA). Samples were stored at -20°C until they were collected by the UCD proteomics

core for liquid-chromatography tandem mass spectrometry (LC-MS/MS) analysis on a Q-Exactive Orbitrap (Thermo Fisher Scientific, Waltham, MA, USA).

2.13.3.8 MaxQuant search parameters

In order to convert the mass spectra to identified proteins, the MaxQuant software was used. Most parameters on MaxQuant were kept as default. Trypsin was selected as the enzyme within the study, the false discovery rate (FDR) was set to 5%, the label free quantification (LFQ) option was checked, and “match between runs” was set to on.

2.13.3.9 Statistical analysis using Perseus

The protein groups text file generated from MaxQuant was imported to Perseus for data analysis. Figure 2.4 below shows the workflow used to generate the working data matrix, matrix 7. Once this was generated, all proteins which had been identified in more than 1 IgG sample per condition were removed, generating a new matrix 8.

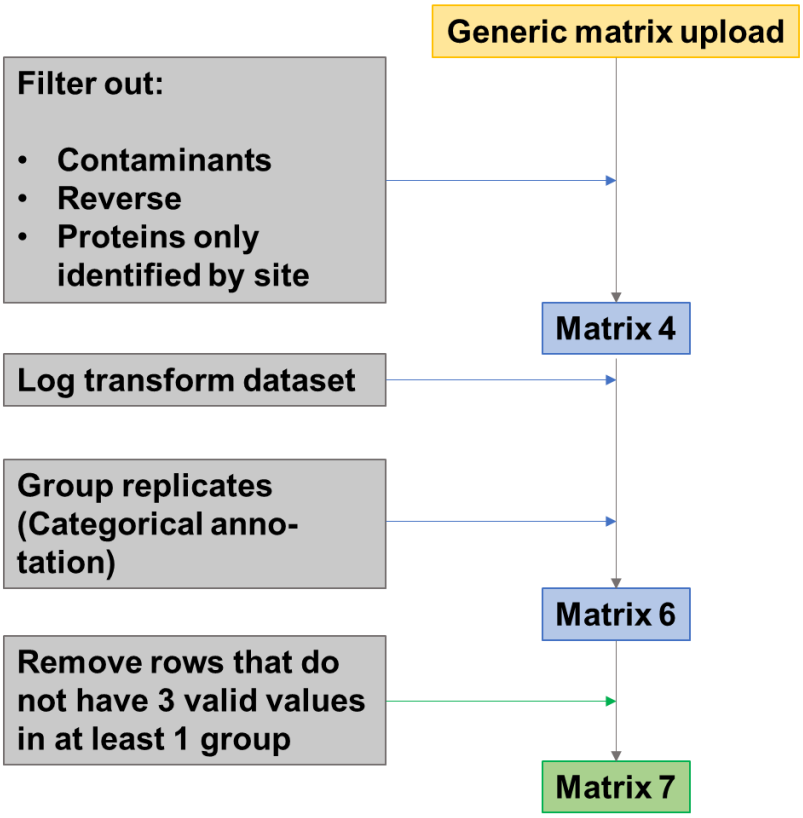

Figure 2.4. Perseus workflow carried out to generate the working matrix, matrix 7.

Once these matrices were generated, missing values were converted to 0 for hierarchical clustering (Euclidean distance, pre-processed with k-means). Principal component Analysis (PCA) was performed from matrix 7 after all missing values had been imputed from a normal distribution (Width: 0.3, down shift: 1.8, mode: total matrix). In matrix 8, missing values in ERα IP samples were also imputed from a normal distribution to allow for volcano plot generation. The FDR was set to 5% for all analysis. Quality of the immunoprecipitation was determined by assessing known interactors of the estrogen receptor and whether these were pulled out in our study.

LFQ values from each experiment can be found under appendices, section E.

2.13.3.10 STRING and PANTHER analysis for identified proteins

The STRING database (string-db.org) was accessed in order to understand if any of the identified proteins had previously been shown to interact with the estrogen receptor before. Importantly, all interaction sources, as well as the confidence threshold, are detailed in each results section pertaining to STRING searches.

The PANTHER database (pantherdb.org) was used to further understand the data generated from Perseus. The molecular function, biological process, and protein class of uploaded proteins could be assigned using this database, which aided in the understanding of what effect CART may be having on the estrogen receptor interactome.

2.14 Small interfering RNA (siRNA) techniques

2.14.1 siRNA transfection optimisation

Investigating the optimal siRNA concentration and transfection reagent volume in our cell lines was achieved using the si-GLO transfection (Dharmacon, Lafayette, CO, USA) control. A “reverse-transfection” was set up as per manufacturers guidelines (Dharmacon, Lafayette, CO, USA). Briefly, cells were seeded at a density to allow for 70 – 80% confluency on the day of transfection (500,000 cells per 6 well plate roughly). Plates were set up as shown below in figure 2.5, covering a wide concentration of siRNA and transfection reagent (Dharmafect transfection reagent 1) (Dharmacon, Lafayette, CO, USA).

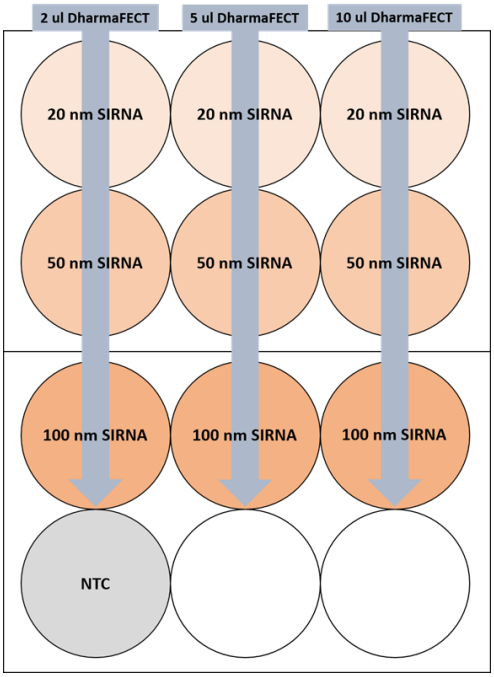

Figure 2.5. Diagram showing how the optimal transfection conditions were determined using the siGLO transfection control.

Cells were left for 72 hours post transfection, at which point they were imaged using a 470 nm filter enabled microscope. After imaging, an MTT assay was used to assess dharmafect toxicity as described previously. Transfection efficiency, as well as viability post transfection, were considered prior to moving forward with the transfection conditions. It was determined that 50 nm siRNA was the optimal concentration of siRNA, and a value between 5 and 10 µl dharmafect transfection reagent 1 was determined as the optimal volume of transfection reagent (7 ul). The reverse transfection was chosen over the standard transfection following imaging cells.

2.14.2 siRNA transfections

4 individual siRNAs were purchased from Dharmacon targeting SMARCD1. The maximum recommended concentration of each siRNA (100 nM) was transfected into cells using 7 µl dharmafect transfection reagent 1. 72 hours

later, RNA was extracted, cDNA synthesis was completed and qRT-PCR was used to determine which siRNA performed best. From this, it was determined that siRNA 1 and 4 achieved the best knockdown of SMARCD1 expression, and so these were chosen for further analysis.

For following experiments, Tet-ON T47D cells were seeded at a density of 300,000 cells per well in 6 well plates on day 1. 50 nM of siRNA (Dharmacon, Lafayette, CO, USA), and 7 µl dharmafect transfection reagent 1 (Dharmacon, Lafayette, CO, USA) was used per transfection. The reverse transfection was carried out as per manufacturers guidelines. On day 3, cells were washed and medium was changed for medium containing 1 µg/ml doxycycline or suitable vehicle control. This was left for a further 72 hours, at which point protein/RNA was extracted for further analysis.

2.14.3 Cellular response to anti-endocrine agents following SMARCD1 knockdown

On day 1, Tet-ON T47D cells were seeded at a density of 400,000 cells per well and reverse transfected as described above. On day 3, cells were trypsinized, counted and re-seeded to 96 well plates at a density of 4,000 cells per well. Cells were also re-seeded to 24 well plates at a density of 50,000 cells per well. Following re-seeding, medium was supplemented with the given concentrations of 4-OH tamoxifen, fulvestrant, or suitable vehicle control (DMSO). Medium was further supplemented with 1 µg/ml doxycycline or suitable vehicle control (H_2O). This was left for 72 hours, at which point the MTT assay was performed as described previously in the 96 well plates. RNA was extracted from the 12 well plates using TriSure as described previously to confirm SMARCD1 knockdown, and to confirm CART expression.

Chapter 3. Investigating the consequence CART has on the transcriptional landscape of ER+ breast cancer

3.1 Introduction

3.1.1 CART and cancer

The role of CART in cancer has been introduced in section 1.2 of this study. While there are many associations between CART and cancer highlighted in section 1.2, there is very little in the way of understanding how CART affects these cancers. This presents an exciting opportunity to build on previous research to understand the role CART may play in breast cancer (Brennan et al., 2012). This previous research, highlighted in figure 3.1, characterized the ability for CART to alter the function of ERα.

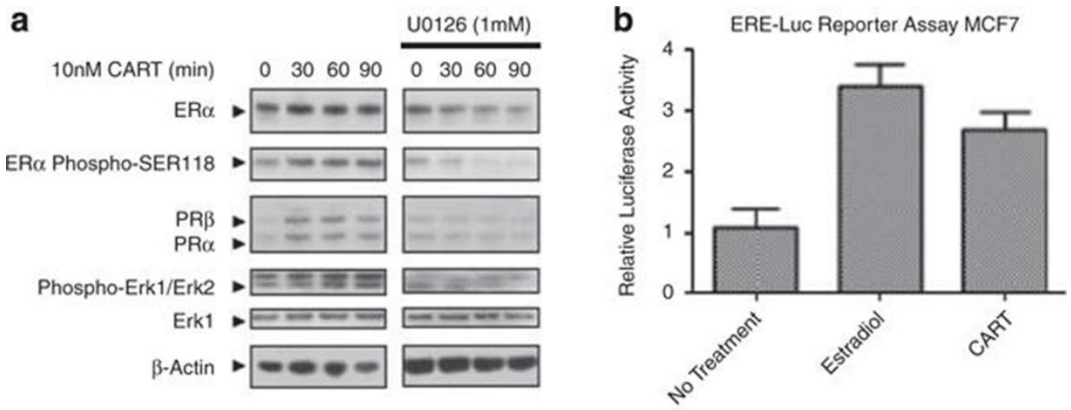

Figure 3.1. CART can alter the function of ERα. A. Treatment with displays increased expression of PGR, as well as increased phosphorylation of ERα at serine-118. **B.** CART treatment results in increased ERα activity as demonstrated by an ERE-luc reporter. Brennan et al., 2012.

3.1.2 The role of LxxLL motifs in nuclear receptor function

Nuclear hormone receptors require coregulators for their function (Onate et al., 1995). This study also characterized the first known hormone receptor coregulator, named SRC-1 (Steroid Receptor Coactivator-1). In 1998, it was discovered that a specific motif, known as the LXD motif, mediates critical

interactions between nuclear receptors, and are necessary for co-activator recruitment (McInerney et al., 1998). It is now understood that multiple LXD motifs exist within SRC-1, and they are essential for the interaction with nuclear receptors (Loinder et al., 2004). Indeed, these LXD motifs are neither specific for ERα or SRC1. For example, an LXD motif within the androgen receptor coregulator ARA70 was previously found to be essential for an interaction with the vitamin-D receptor (VDR), and was partially responsible for its transactivation (Ting et al., 2005). The general coregulator p300 is known to contain multiple LXD motifs within its sequence, which are critical for mediating interactions with multiple nuclear hormone receptors (Plevin et al., 2005). Furthermore, the LXD motif is not only used by coactivators of nuclear receptors. LXD motifs are also essential for interactions between nuclear receptors and co-repressor proteins. The nuclear corepressor NCOR is known to mediate interactions with both the retinoic acid receptor alpha, and thyroid hormone receptor beta, in an “LXD” dependent manner (Loinder et al., 2004). Interestingly, the amino acid sequence downstream of the LXD motif is also known to play a critical role in the coregulator-receptor affinity. For example, p300 typically binds receptors at lower affinities to NCOA proteins, and this is thought to be due to flanking polar amino acid residues, disrupting the binding (Plevin et al., 2005).

3.1.3 Transcriptomic profiling

RNA-seq was first brought to the forefront of scientific research in 2008, with a number of studies published in quick succession highlighting transcriptomic profiles in yeast (Nagalakshmi et al., 2008, Wilhelm et al., 2008), mice (Mortazavi et al., 2008), and stem cells (Cloonan et al., 2008). Interestingly, the HeLa ovarian cancer cell line was one of the first cell lines to have its transcriptome profiled via RNA-seq (Morin et al., 2008). RNA-seq has allowed for the detection of novel transcripts as well as sequence variations (Wang et al., 2009), with current methods offering extremely accurate sequencing coverage for relatively low cost. Nowadays, a typical RNA-seq experiment involves the isolation of RNA from samples to be sequenced, which is

converted to cDNA and specific sequencing adaptors are added to allow for sample identification (library). These libraries are sequenced, and the generated “reads” can be aligned to a reference genome.

RNA-seq has already significantly benefited breast cancer research. For example, The Cancer Genome Atlas (TCGA) has performed RNA sequencing of a large cohort of breast cancer patients (Ciriello et al., 2015). The authors have already utilized this data to characterize invasive lobular carcinoma as a clinically, and molecularly, distinct disease (Cirello et al., 2015). Furthermore, the authors have made this data publicly available through the cBioportals suite, allowing cancer researchers around the globe to understand the clinical implications of their research. The future for RNA-seq is also bright, with the implementation of single-cell RNA-seq techniques (Haque et al., 2017). With the increasing knowledge that tumors are typically extremely heterogenous, the implementation of single-cell RNA seq may help in dealing with the complexities of heterogenous samples.

3.1.4 Chromatin immunoprecipitation sequencing (ChIP-seq)

While RNA sequencing identifies the transcriptional landscape of cells, it cannot show, with absolute certainty, what transcription factors are controlling the expression of these genes. For this, research groups typically use a technique known as ChIP-seq. ChIP-seq works by using antibodies that can recognise a transcription factor of interest. The transcription factor is crosslinked to DNA, followed typically by sonication to remove any DNA which the transcription factor is not bound to. The factor is then immunoprecipitated, unlinked from the DNA, and the DNA sequence is sequenced and mapped to the human genome. This provides all putative DNA binding sites for that factor in the condition introduced by the experiment. A workflow for how this works can be seen in figure 3.2.

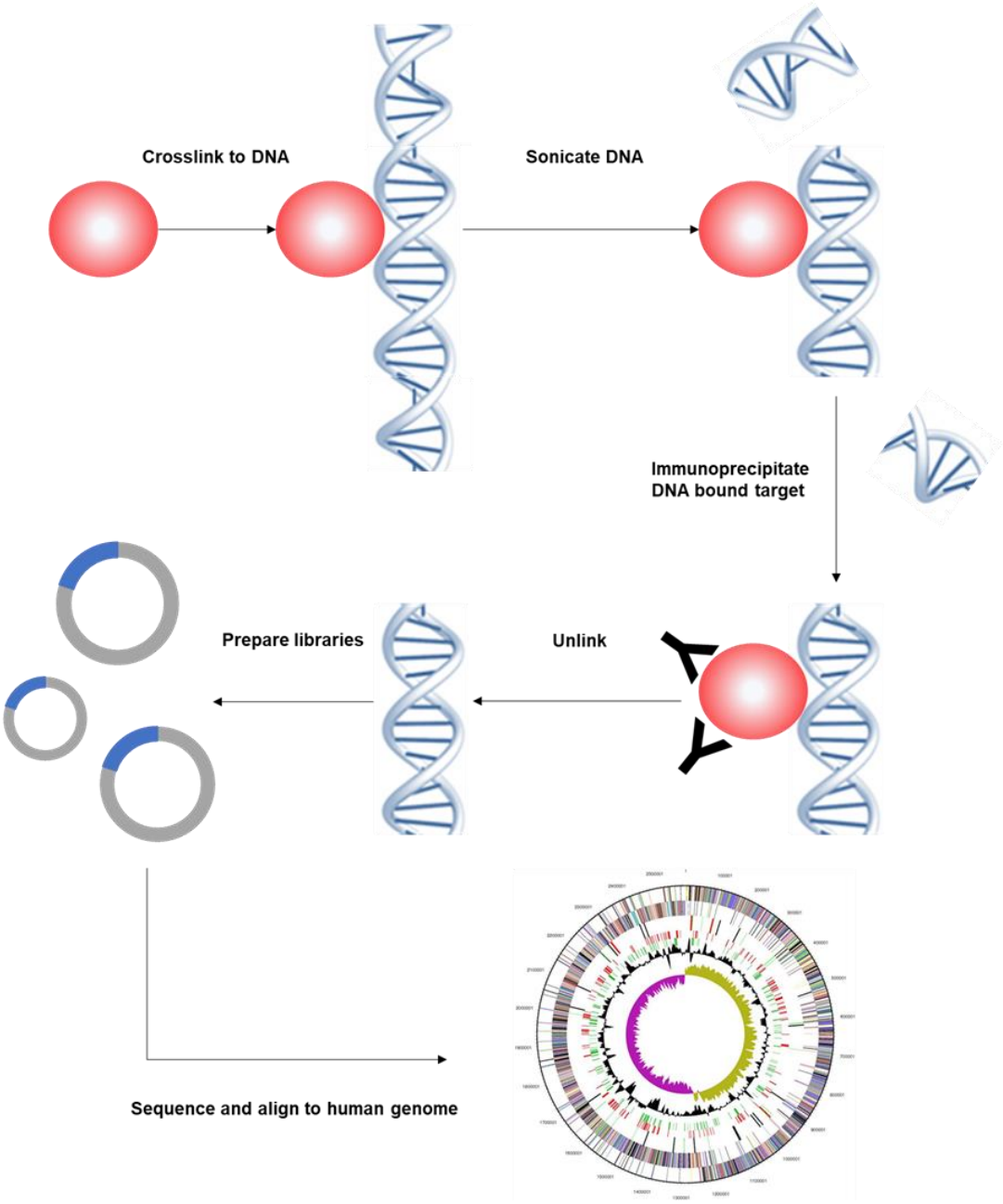

Figure 3.2. Typical workflow of a ChIP-seq experiment.

ChIP-seq can be used in parallel with RNA sequencing, which would highlight not only the binding sites for a given transcription factor, but whether this binding site pertains to increased/decreased expression of the gene. For example, this approach was used to great effect recently to highlight the fascinating relationship between the progesterone receptor (PGR) and ERα

(Mohammed et al., 2015). The authors of this study highlighted that PGR could interact with ERα, and using ChIP-sequencing, they proved that this interaction was capable of redirecting ERα chromatin binding events (Mohammed et al., 2015). RNA sequencing was used to confirm that these binding events were indeed active binding events, and the binding signature was suggested to predict good clinical outcome (Mohammed et al., 2015).

3.1.3 Aims of chapter

There are currently no published studies characterizing the effect CART can have on the transcriptional landscape of cells. Given data published previously (Brennan et al., 2012), we felt CART may play a role in regulating both genes associated with estrogen-induced growth, and genes relating to ERα itself. Our main goals of this chapter are as follows:

- Are LXD motifs within the sequence of CART critical for altering ERα activity?
- Characterize the transcriptome of cells expressing CART via RNA-seq
- Mine publicly-available ERα ChIP-seq datasets in an attempt to characterize if any of the genes regulated by CART have previously reported ERα binding events at their promotor region

3.2 Results

3.2.1 Investigating the effect CART has on common ERα target genes

Data published in 2012 highlighted that CART could signal through the MAP-Kinase pathway, phosphorylate ERα at serine-118, and increase the expression of the Progesterone Receptor (PgR), a common ERα target gene (Brennan et al., 2012) (figure 3.1). In the same year, a study emerged which highlighted that CART could positively influence the growth of small bowel carcinoid cancer cells, and CART could increase the expression of Cyclin-D1 (CCND1). As CCND1 is another ERα target gene, we investigated whether cells treated with CART show an increase in the expression of these targets. In figure 3.3, we report that T47D cells stimulated with CART show a rapid phosphorylation of ERK, and show increased expression of both PgR and Cyclin-D1 on the protein level. As these are both ERα target genes, we next examined whether we could detect an increase in these genes at the mRNA level. Taken together, this data highlights that T47D cells treated with CART show altered expression of gene associated with ERα.

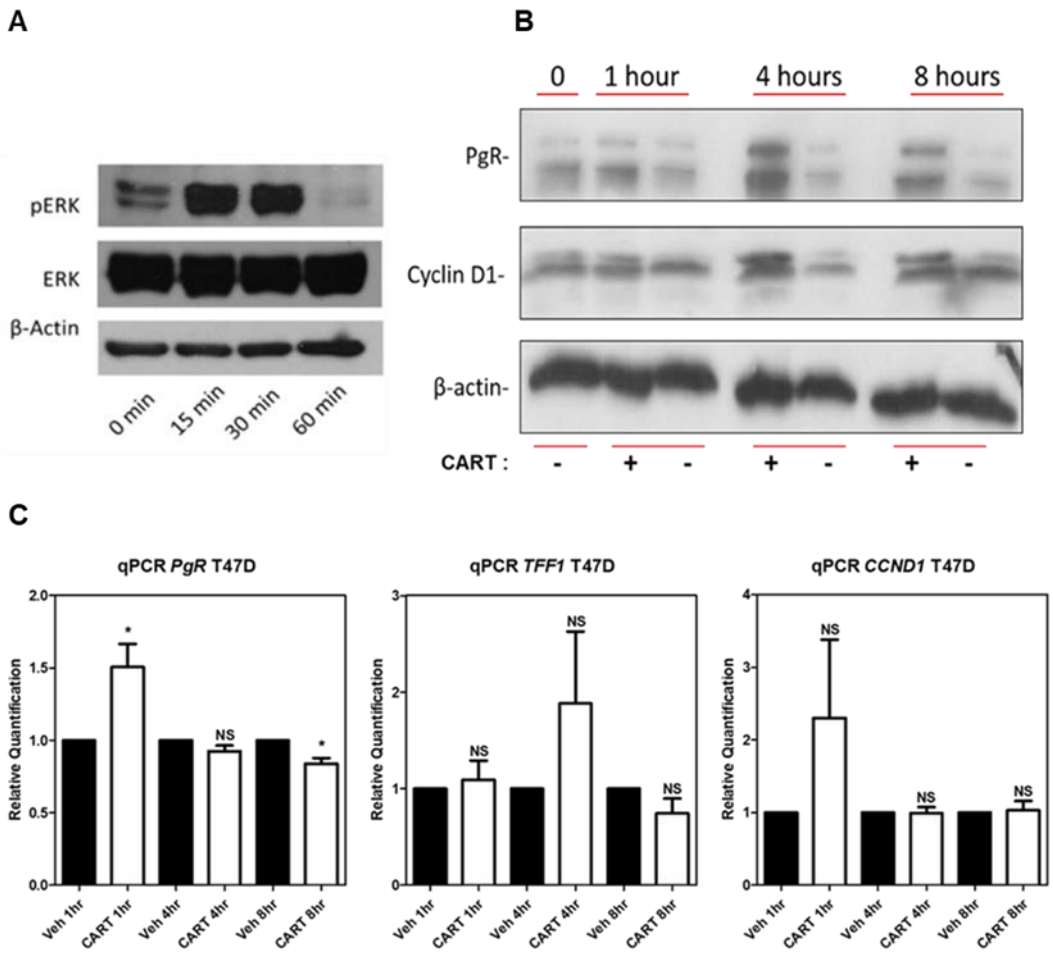

Figure 3.3. CART increases the phosphorylation of ERK, and increases the expression of ERα target genes.

A. Western blot analysis of phosphorylated ERK (pERK) levels following stimulation with 10 nm CART for the mentioned times. Total ERK and actin were used as endogenous and loading controls. **B.** Western blot analysis of PGR and CCND1 expression following stimulation with 10 nm CART for the mentioned times. Actin was used as the loading control. **C.** Expression of *PGR*, *TFF1* and *CCND1* was assessed using qRT-PCR following stimulation with 10 nm CART for the mentioned times. Mean +/- SEM between 3 independent experiments is plotted. All statistical tests were performed against the suitable vehicle control for each time point. A two-tailed students t-test was used to calculate statistical significance. * - $p<0.05$, NS – not significant

Further, we sought to utilize publicly available data from both the TCGA (provisional dataset, most recent citation Ciriello et al., 2015) dataset and the METABRIC (Curtis et al., 2012, Pereira et al., 2015) dataset. Data is publicly accessible through the cBioportals suite (Cerami et al., 2012, Gao et al., 2013). For this investigation, we investigated whether common ERα target genes were significantly higher in patients with high levels of CART. A Z-score cut off score of +/- 1 was applied to both databases prior to searching, and CARTPT was used as the query gene. In figure 3.4, we found that patients with elevated CART levels also have higher levels of common ERα target genes. Both the p value, as well as the Benjamini-Hochberg ajusted q value, for all genes are reported in both tables.

TCGA dataset, mRNA expression (microarray)						
Gene	Mean mRNA expression		Standard deviation		P-value	Q-value
	Altered	Unaltered	Altered	Unaltered		
CARTPT	4.6	0.46	2.62	0.55	**6.08 e-19**	**1.04 e-14**
ESR1	3.37	2.18	2.01	2.8	**5.79 e-5**	**3.91 e-3**
PKIB	1.82	0.65	1.4	1.74	**2.92 e-8**	**5.57 e-5**
PGR	1.26	0.14	2.18	2.45	**2.58 e-4**	**9.09 e-3**
TFF1	-1.15	-2.27	2.3	2.09	**3.91 e-4**	**0.0116**
CCND1	0.28	0.25	1.38	1.37	0.85	0.93
GREB1	-1.17	-1.67	1.42	1.41	**0.0109**	0.08
MYC	-1.51	-1.24	0.83	0.94	**0.017**	0.106

METABRIC dataset, mRNA expression (microarray)						
Gene	Mean mRNA expression		Standard deviation		P-value	Q-value
	Altered	Unaltered	Altered	Unaltered		
CARTPT	11.34	5.61	2.08	0.28	**1.67 e-51**	**3.02 e-47**
ESR1	11.08	9.52	1.25	2.14	**2.34 e-23**	**1.37 e-20**
PKIB	9.99	8.58	1.02	1.29	**1.07 e-26**	**1.21 e-23**
PGR	6.81	6.20	1.11	1.01	**1.98 e-7**	**1.67 e-6**
TFF1	10.83	8.96	2.63	2.70	**7.22 e-11**	**1.38 e-9**
CCND1	12.43	11.91	0.83	1.12	**8.67 e-9**	**1.02 e-7**
GREB1	5.54	5.52	0.15	0.15	0.225	0.361
MYC	8.99	8.87	1.01	1.10	0.232	0.369

Figure 3.4. Patients in both METABRIC and TCGA datasets with high levels of CART have significantly higher levels of many ERα target genes.

3.2.2 An investigation into a potential structure-function relationship between CART and ERα

Thus far, our current and previous work has focused on cells stimulated with CART peptide and what effect this has on ER+ breast cancer cells. Upon analysing the amino-acid sequence of CART, we discovered 3 “LxxLL” or “LxxLL like” (known hereafter as LXD) motifs to exist within CART. These motifs are known multifunctional binding sequences critical for transcriptional regulation of steroid hormone receptors (Plevin et al., 2005). Site-directed mutagenesis was used to exchange the double Leucine amino acids with double Alanine amino acids. The pWhitescript control plasmid (Agilent) contains a stop codon (TAA) in the position where a glutamine codon (CAA) would usually reside in the β-galactosidase gene. Using mutant primers, the stop codon can be switched to a glutamine codon, resulting in active expression of galactosidase. When streaked on a plate containing X-gal, the β-galactosidase can break down X-gal and produce visible blue colonies.

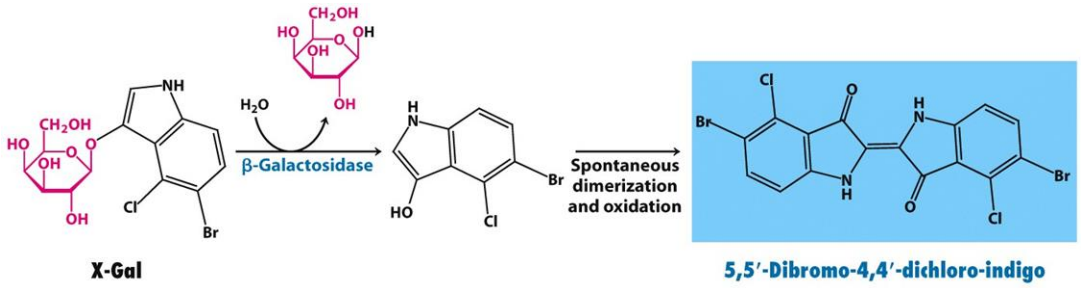

Figure 3.5. X-Gal is broken down by active galactosidase to produce blue bacterial colonies, indicating a successful site-directed mutagenesis protocol.

Image sourced from Biochemistry, Seventh Edition. Berg, Tymoczko, Stryer

Below, figure 3.6A highlights blue colony growth, confirming successful site-directed mutagenesis protocol. In figure 3.6B, the identified LXD motifs are shown, as well as the alanine replacements that were made using site directed mutagenesis.

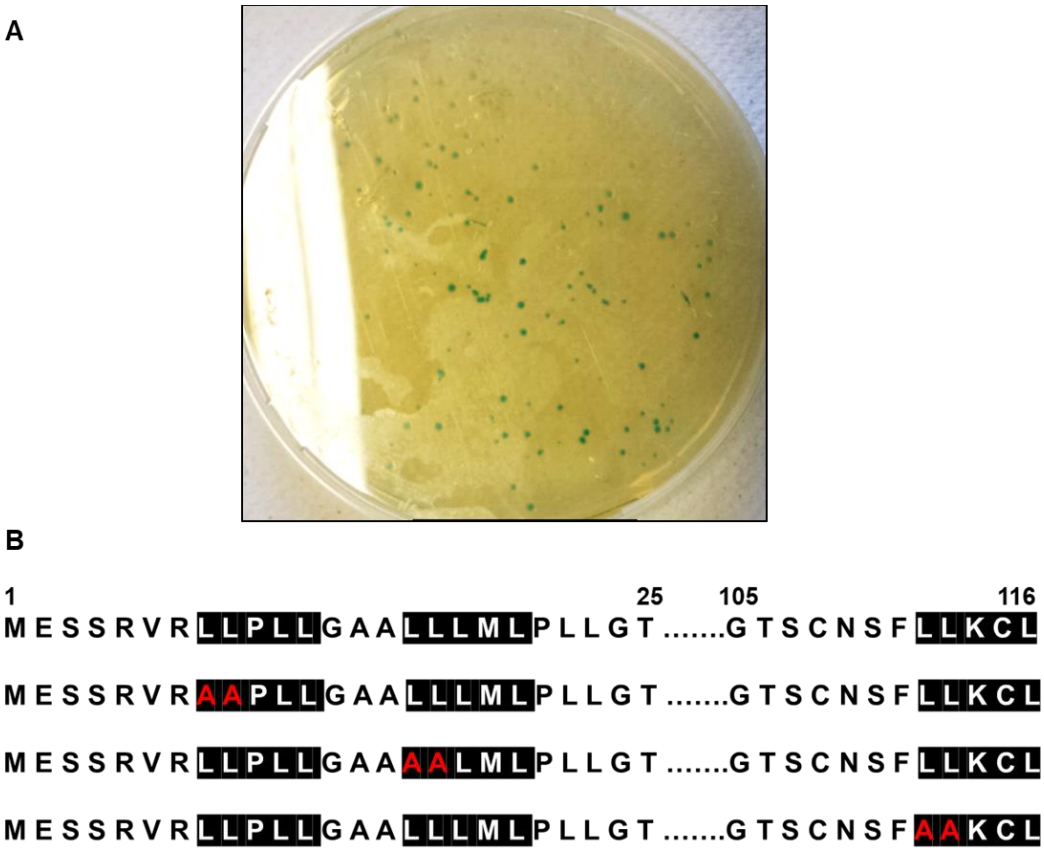

Figure 3.6. Conformation of successful site-directed mutagenesis.

A. Following PCR of pWhitescript plasmid using supplied mutant primers, XL10-Gold ultracompetent bacteria were transformed and streaked on IPTG-containing LB-agar plates overnight. Blue colonies were observed. **B.** Identification of three LXD motifs within CART, and the mutations inserted into each.

Next, each plasmid was ectopically expressed in MCF7 cells to investigate whether the inserted mutations had any effect on the expression of CART. As

demonstrated in figure 3.7, CART is still detected in all mutant-transfected cell lines, confirming the mutations do not affect the expression of CART.

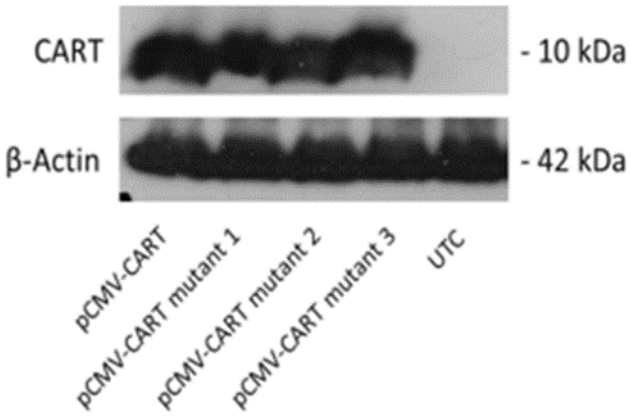

Figure 3.7. Ectopic expression of CMV plasmids in MCF7 cells confirms CART is still expressed following mutating each LXD motif.

MCF7 cells were transfected with 1 µg of each plasmid. Western blot analysis was used to confirm CART expression following transfection. Actin was used as the loading control. UTC – Untransfected control

Next, each plasmid was ectopically expressed in both MCF7 and T47D cells, and an ERE-Dual luciferase reporter assay was used to determine if these mutations had any effect on the ability for CART to alter ERα function. As reported in figure 3.8, we discovered that mutating LXD-motif 1 within CART resulted in a significant decrease in ERα function compared to the parental CART-vector control in T47D cells.

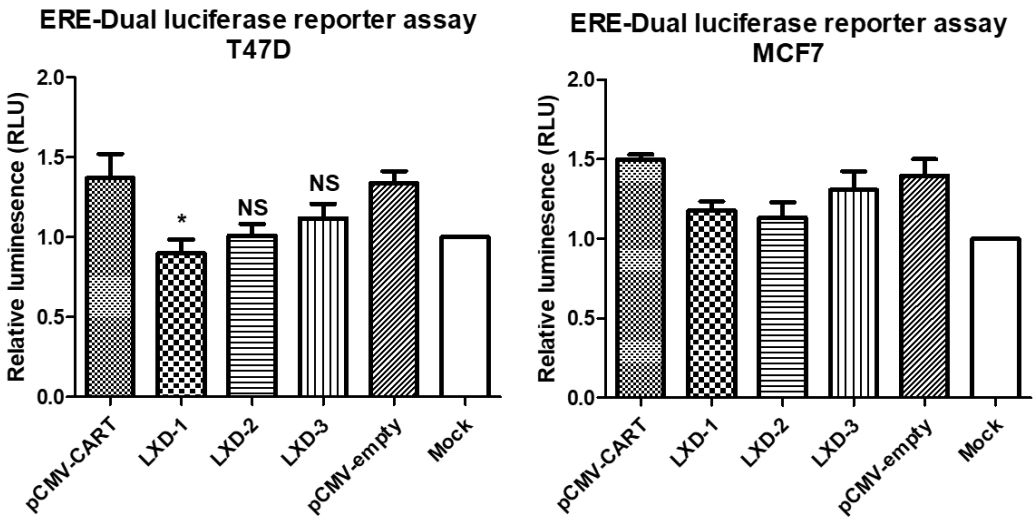

Figure 3.8. Introducing mutations into LXD motifs within CART alters ERα function.

Cells were co-transfected with ERE-luc, CMV-Renilla and CMV-CART vectors, and the ERE dual luciferase reporter assay was carried out three days later. Mean +/- SEM between 3 independent experiments for T47D cells, and 2 independent experiments for MCF7 cells, is plotted. Statistical tests of each LXD mutant were compared against pCMV-CART. A one-way ANOVA was used to calculate statistical significance. Statistical analysis was not performed on MCF7 cells due to the presence of only 2 independent experiments. * $p<0.05$

3.2.3 Generation of stable, inducible, T47D cell lines

Having further established a relationship between CART and ERα, we next sought to examine the effect CART has on the transcriptional landscape of ER+ breast cancer cells. For this, stable-inducible cell lines were produced, allowing us to control the expression of CART prior to RNA sequencing. The principle of this system, as well as the successful expression of CART in response to increasing concentrations of doxycycline, is shown in figure 3.9.

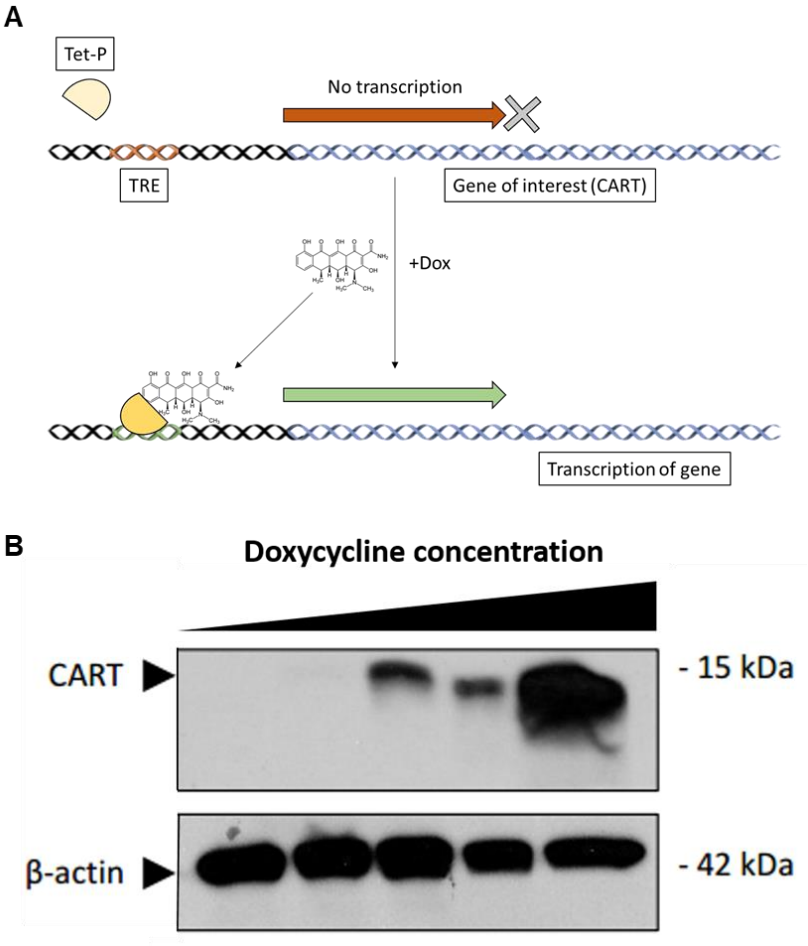

Figure 3.9. Cells show an increased expression of CART following treatment with increasing concentrations of doxycycline.

A. Principle of the Tet-ON system employed to control the expression of CART in T47D cells. **B.** Tet-ON T47D cells were treated with 10 - 0.01 um doxycycline for 72 hours. Western blot analysis was used to detect CART expression, and actin was used as the loading control.

3.2.4 Using the Tet-ON T47D cell line for RNA-sequencing

A handful of studies have shown, in a low-throughput manner, what genes may be controlled by CART (Brennan et al., 2012, Landerholm et al., 2012), but a large-scale study into the global effect CART has on the transcriptional landscape of cells remains incomplete. Therefore, we induced Tet-ON T47D cells to express CART under hormone-stripped conditions, and performed

RNA-sequencing in an effort to address this. In figure 3.10, western blot analysis confirmed cells were expressing CART in 3 independent experiments.

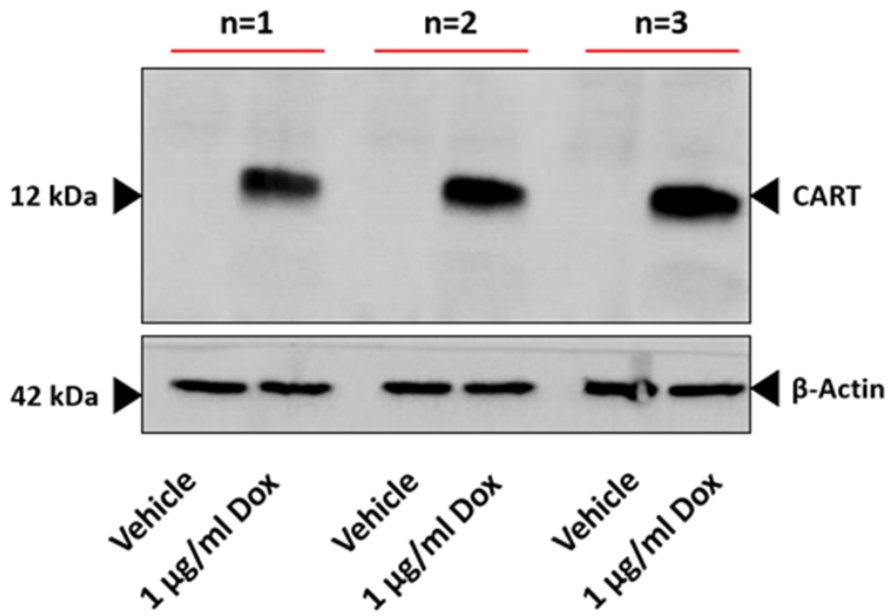

Figure 3.10. Three independent experiments were used for RNA-sequencing analysis.

Cells were hormone starved for 24 hours, then treated with either doxycycline, or vehicle control, for a further 72 hours in hormone-stripped medium. Western blot analysis was used to confirm CART expression. Actin was used as the loading control.

3.2.5 Principal component analysis (PCA) and heatmap generation reveals a number of significantly differentially expressed genes by CART

Following RNA-sequencing, PCA was performed in order to represent how each replicate grouped relative to the suitable vehicle control. In figure 3.11, we see that treatment groups do not overlap with one-another. PCA plot was provided by Dr. Bruce Moran.

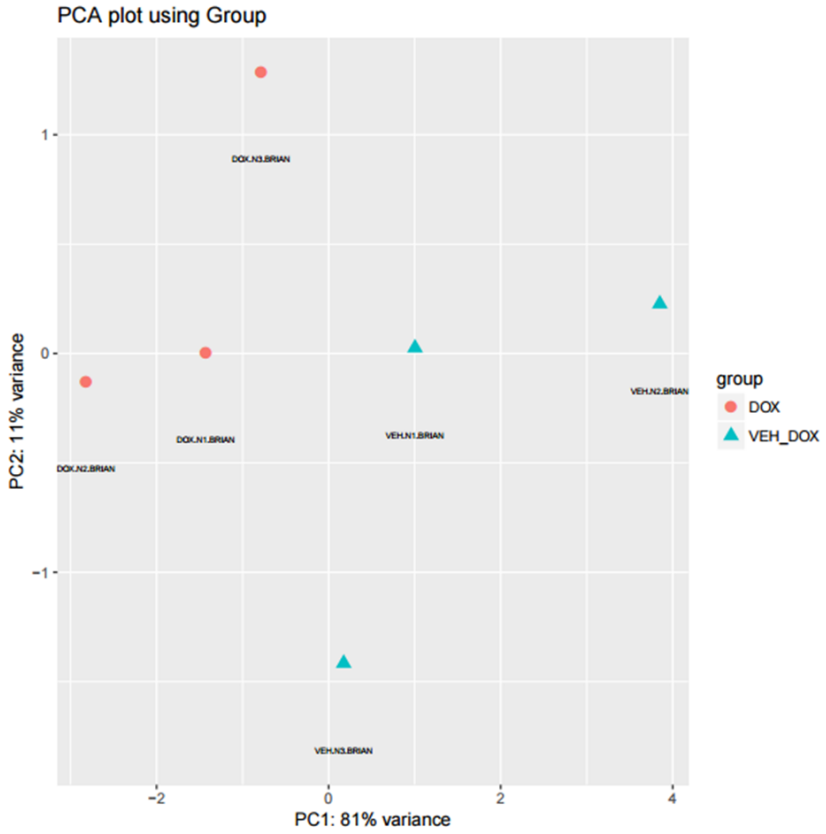

Figure 3.11. PCA highlights the grouping pattern for each individual treatment group, and each biological replicate.

Next, the DEseq package was used to calculate what genes were significantly ($p<0.05$) (absolute fold change < 1) upregulated/downregulated between treatment groups. This revealed 156 genes which were significantly downregulated by CART, and 100 genes which were significantly upregulated by CART. The FPKMS values for these genes were converted to Z-scores in order to generate a heatmap (figure 3.12). This heatmap highlights the 256 significantly differentially expressed genes from our data.

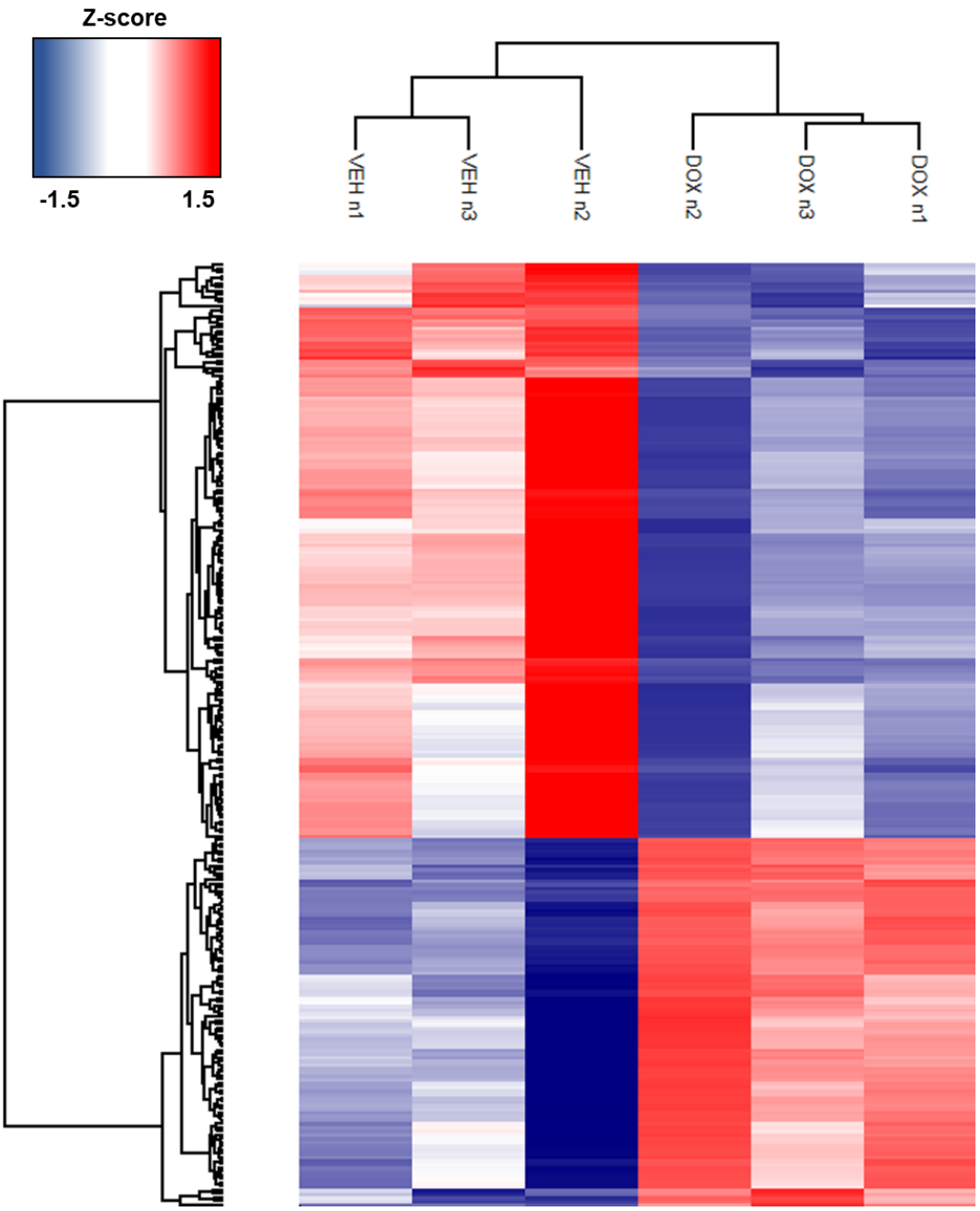

Figure 3.12. Z-score heatmap reveals 2 distinct clusters, highlighting the 100 significantly upregulated, and 156 significantly downregulated genes, following CART expression.

3.2.6 Gene Ontology (GO) analysis of significantly upregulated genes

Having identified that CART expression results in 100 significantly upregulated genes, we next sought to characterize whether any of these genes are associated with biological processes, molecular functions and diseases.

Originally, we had intended to apply a modest Benjamini-adjusted p-value of 0.1 to these lists, however, no gene sets were identified to have a p-value less than this adjusted value. We therefore used the non-adjusted p-value, and applied a cut off value of 0.05. Full tables can be found under the appendices, section D.

First, we examined what biological processes these genes are associated with. In figure 3.13, we see that genes increased by CART are mainly involved in the process of transcription. This suggests that CART increases the expression of genes allowing for altered transcriptional regulation in ER+ breast cancer cells.

GO: Biological process	P-Value	Count	Genes	Bonferroni	Benjamini
Reciprocal meiotic recombination	0.003726	3	ATM, C11ORF80, RAD51B	0.689132	0.689132
Regulation of transcription from RNA polymerase II promoter	0.010642	6	BRWD1, ELF5, HLTF, TCF7L2, ZNF518A, ZSCAN5A	0.964878	0.812592
Transcription, DNA-templated	0.012498	13	ATF7IP2, BDP1, BRWD1, ESR1, TCF7L2, ZKSCAN8, ZNF518A, ZNF573, ZNF680, ZNF69, ZNF736, ZNF91, ZSCAN5A	0.980487	0.73078

Figure 3.13. Genes upregulated by CART are mainly involved in biological processes associated with transcription.

Next, we examined what molecular functions are typically associated with these upregulated genes (figure 3.14). Similar to figure 3.13, we see that genes associated with the process of transcription and DNA binding are upregulated by CART. Again, this adds further evidence that CART increases the expression of genes that normally function to drive transcription.

GO: Molecular function	P-Value	Count	Genes	Bonferroni	Benjamini
RNA polymerase II core promoter proximal region sequence-specific DNA binding	0.004251	6	ESR1, HLTF, NFAT5, TCF7L2, ZNF680, ZNF736	0.382098	0.382098
Nucleic acid binding	0.008893	9	CPSF6, HLTF, TMEM161B, ZKSCAN8, ZNF69, ZNF91, ZNF518A, ZNF573, ZSCAN5A	0.635569	0.396319
Transcription factor activity, sequence-specific DNA binding	0.024629	8	ESR1, NFAT5, TCF7L2, ZKSCAN8, ZNF91, ZNF518A, ZNF573, ZSCAN5A	0.940267	0.609095
DNA binding	0.026281	11	ATM, BDP1, ESR1, HLTF, PHC3, RAD51B, ZNF69, ZNF91, ZNF518A, ZNF573, ZSCAN5A	0.950684	0.528755

Figure 3.14. The molecular function of genes upregulated by CART are mainly involved in function such as DNA binding and transcription.

Lastly, we examined whether any of these genes had previously been implicated in other disease states. Reassuringly, we see genes associated with obesity to be upregulated by CART. The role of CART in feeding and obesity is very well understood (see chapter 1), and so it is not surprising to identify genes upregulated by CART to be associated with obesity. Genes which were upregulated by CART were also seen to be associated with tobacco use disorder. An aspect of CART in cancer that we had not examined previously (figure 3.15).

GAD Disease	P-Value	Count	Genes	Bonferroni	Benjamini
Tobacco Use Disorder	0.02906	17	ANKS1B, ARHGEF38, BDP1, BRWD1, DGKH, ESR1, L3HYPDH, PPP1R12B, RAD51B, SHTN1, TAMM41, TBC1D32, TCF7L2, TTC6, UGGT2, WDR27, ZNF680	0.99	0.99
Obesity	0.033267	5	ALPK1, CARTPT, ESR1, LYPLAL1, TCF7L2	1	0.99974

Figure 3.15. Genes upregulated by CART are associated with tobacco-use disorder and obesity.

3.2.7 Gene set enrichment analysis (GSEA) of genes significantly upregulated by CART

Following GO analysis, we next sought to compare genes upregulated by CART against publicly available datasets in order to understand if any of these genes have been associated with any experimental datasets relevant to cancer. Gene sets below an adjusted p value of 0.05 were considered statistically significant. The full list of significant datasets can be found in the appendices, section D. Interestingly, our search highlighted 3 gene sets that were associated with the cell cycle (figure 3.16). This was an intriguing finding, as preliminary data from our studies also showed that CART could increase the quantity of cells found in the S and G2/M phases of the cell cycle vs the untreated control cells (figure 3.17).

GSEA, Gene Set Name	Description	FDR q-value	Genes
PYEON_CANCER_HEAD_AND_NECK_VS_CERVICAL_UP	Up-regulated genes in head and neck cancer compared to cervical carcinoma samples.	1.15E-05	ENOSF1, ANKRD36, BRWD1, ESR1, CCDC14, C11ORF80, HNRNPU-AS1, HLTF
RODRIGUES_THYROID_CARCINOMA_POORLY_DIFFERENTIATED_DN	Genes down-regulated in poorly differentiated thyroid carcinoma (PDTC) compared to normal thyroid tissue.	4.81E-05	ENOSF1, NKTKR, MALAT1, HOOK3, ANKRD10, EPB41L5, PHC3, ZNF573, ZNF518A, C11ORF61, C6ORD170, NPIPL3
JOHNSTONE_PARVB_TARGETS_3_DN	Genes down-regulated upon overexpression of PARVB in MDA-MB-231 cells (breast cancer) cultured in 3D Matrigel only.	6.92E-03	CCDC14, NKTR, HOOK3, N4BP2L2, SENP7, PACRGL, TCF7L2, CPSF6, IMMP1L, BDP1
WHITFIELD_CELL_CYCLE_S	Genes periodically expressed in synchronized HeLa cells (cervical carcinoma), with peak during the S phase of cell cycle.	1.22E-02	ENOSF1, ANKRD36, CCDC14, SLC25A27, KIAA1598
BENPORATH_CYCLING_GENES	Genes showing cell-cycle stage-specific expression [PMID=12058064].	1.83E-02	ENOSF1, CCDC14, NKTR, ANKRD10, SLC25A27, SLC25A36, KIAA1598, ZSCAN5A
WAMUNYOKOLI_OVARIAN_CANCER_LMP_DN	Genes down-regulated in mucinous ovarian carcinoma tumors of low malignant potential (LMP) compared to normal ovarian surface epithelium tissue.	2.26E-02	C11ORF80, MALAT1, ANKRD10, EPB41L5, S100PBP
RODRIGUES_THYROID_CARCINOMA_ANAPLASTIC_DN	Genes down-regulated in anaplastic thyroid carcinoma (ATC) compared to normal thyroid tissue.	2.98E-02	BRWD1, NKTR, HOOK3, ZNF573, ZNF518A, SLC25A27, UGGT2
LASTOWSKA_NEUROBLASTOMA_COPY_NUMBER_DN	Genes with copy number losses in primary neuroblastoma tumors.	4.38E-02	NKTR, ZNF518A, C11ORF61, ATM PACRGL, S100PBP, FAM149B1, TBC1D12
WHITFIELD_CELL_CYCLE_G1_S	Genes periodically expressed in synchronized HeLa cells (cervical carcinoma), with peak during the G1/S phase of cell cycle.	4.77E-02	NKTR, ANKRD10, SLC25A27, SLC25A36

Figure 3.16. GSEA of genes significantly upregulated by CART.

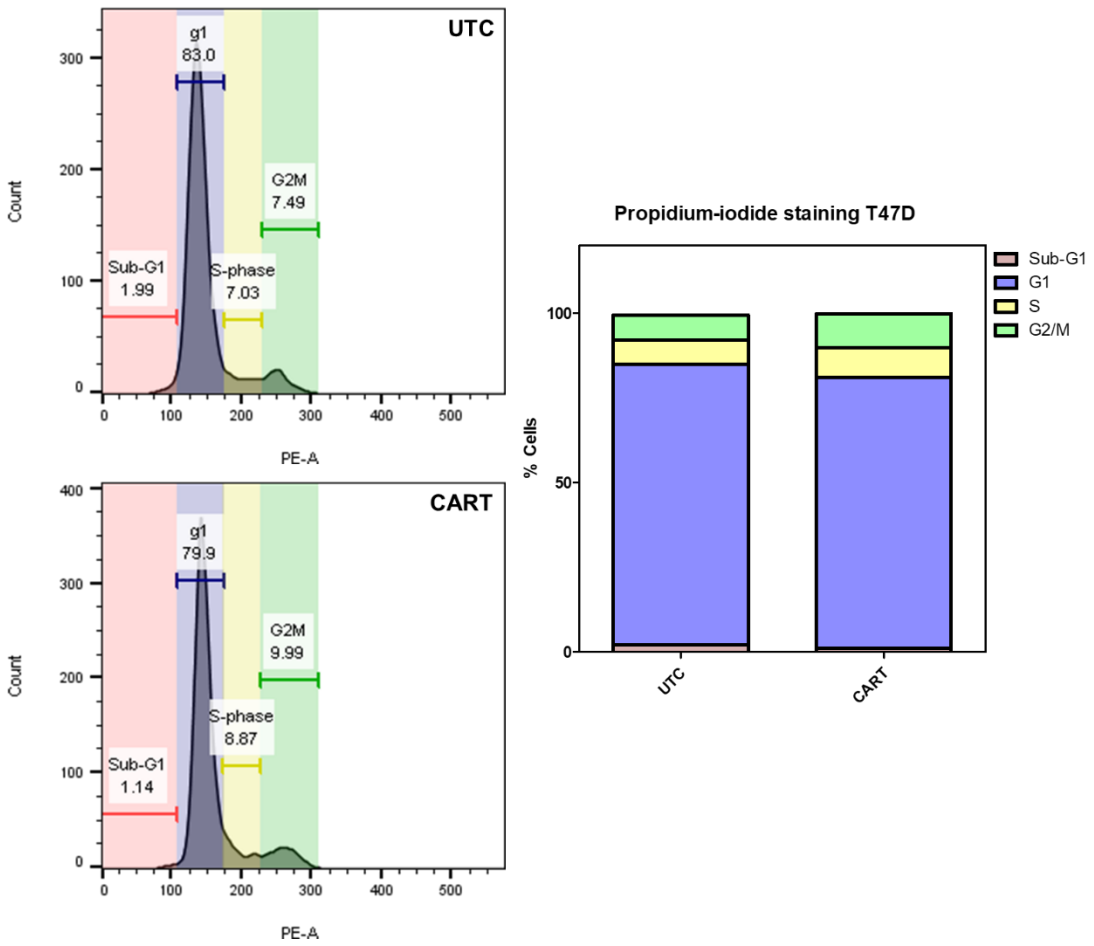

Figure 3.17. CART treatment results in an increase of cells in the S and G2/M phases of the cell cycle.

Parental T47D cells were serum starved for 24 hours, followed by treatment with 10 nm CART peptide for 1 hour. Propidium-iodide staining was used to investigate the effect CART stimulation had on the cell cycle.

3.2.8. GO analysis of genes significantly downregulated by CART

Next, we sought to characterize the processes that are associated with genes downregulated by CART. A Benjamini ajusted p-value of 0.1 was applied as a cut-off, as there were many more biological processes identified in the downregulated gene set when compared to the significantly upregulated gene set. Full lists are provided in the appendices, section D.

GO: Biological process	P-Value	Count	Genes	Bonferroni	Benjamini
Translational initiation	5.80E-22	22	EIF3B, EIF3C, EIF3CL, FAU, RPL13, RPL23, RPL27, RPL34, RPL35, RPL35A, RPL37, RPL37A, RPL38, RPL41, RPL7A, RPS9, RPS15A, RPS20, RPS21, RPS23, RPS27, RPS28	4.50E-19	4.50E-19
Cell-cell adhesion	1.85E-09	16	ALDOA, CORO1B, ENO1, HSPA8, KRT18, LDHA, PRDX1, PUF60, PFN, PKM, RAB11B, RPL7A, RPL34, S100A11, TACSTD2, TRIM29	1.44E-06	2.05E-07
Canonical glycolysis	1.27E-06	6	ALDOA, ENO1, GAPDH, PGK1, PGAM1, PKM	9.88E-04	1.24E-04
Glycolytic process	5.13E-06	6	ALDOA, ENO1, GAPDH, LDHA, PGK1, PGAM1	0.003976	4.43E-04
Gluconeogenesis	1.89E-05	6	ALDOA, ENO1, FBP1, GAPDH, PGK1, PGAM1	0.014536	0.001463
Regulation of mRNA stability	1.25E-04	7	HSPA1B, HSPA8, HSPB1, PSMB4, PSMB5, PSMC3, UBB	0.09245	0.00878
Platelet aggregation	2.47E-04	5	ACTB, ACTG1, FIBP, GNAS, HSPB1	0.174362	0.01584
ATP biosynthetic process	0.001307	4	ALDOA, ATP5E, ATP5L, PKM	0.637563	0.0751
NIK/NF-kappaB signalling	0.001521	5	PPP4C, PSMB4, PSMB5, PSMC3, UBB	0.693055	0.080903
Tumor necrosis factor-mediated signaling pathway	0.001955	6	KRT8, KRT18, PSMB4, PSMB5, PSMC3, UBB	0.780995	0.096288

Figure 3.18. Genes downregulated by CART are associated with a wide range of biological processes, such as cell-cell adhesion, glycolysis and NIK/NF-kappaB signalling.

GAD Disease	P-Value	Count	Genes	Bonferroni	Benjamini
Acquired Immunodeficiency Syndrome / Disease Progression	2.55E-06	21	ATP5E, ATP5L, FASTK, NAXE, NDUFA4, RAB11B, CHCHD1, CHCHD2, CKMT1B, COX4I1, GPX4, IDH2, LDHA, HLAB, MRPS18B, MRPS7, PRDX1, ROMO1, RPL34, RPL35A, UQCRC1	0.001713	0.001713

Figure 3.19. Genes downregulated by CART are associated with acquired immunodeficiency syndrome / disease progression.

3.2.9 Using publicly available ChIP-seq data to characterize if any differentially expressed genes have previously been shown to contain promoter binding sites for ERα

The first aim of this chapter focused on identifying the genes that are differentially expressed following treatment with CART, and what biological processes they are typically associated with. Following this, we aimed to utilize publicly available ChIP-seq databases to identify if any of the significantly differentially expressed genes were potential ERα target genes. Publicly available ChIP-seq data was accessed through the Cistrome data browser suite (cistrome.db.org) (Mei et al., 2017). Significantly differentially expressed genes were compared against 5 experiments (table 3.1). All experiments used the T47D cell line as their biological source.

Table 3.1. Reference experiments used for identifying potential ERα target genes

Number	Reference	Conditions
1	Mohammad et al., 2015	Full medium 3 hours, replicate 1
2	Mohammad et al., 2015	Full medium 3 hours, replicate 2
3	Mohammad et al., 2015	Full medium 3 hours, replicate 3
4	Ross-Innes et al., 2012	Standard growth conditions
5	Gertz et al., 2013	10 nm E2 1 hour

The columns in both figure 3.20 and 3.21 labelled “Score 1- 5” reference the score which was assigned for this ERα binding event in each experiment (Score 1, for example, represents the score from experiment 1 in table 3.1). This exercise identified several genes from our RNA sequencing experiment that have reported ERα binding events in their promotor regions. This suggests that the expression/repression of these genes may be mediated through CART altering the function of ERα.

Gene	Chromosome	Tx START	Tx END	Score 1	Score 2	Score 3	Score 4	Score 5
ARHGEF38	chr4	105552619	105680913	1.093	0.779	0.778	1.45	1.213
		105552619	105631680	1.093	0.779	0.778	1.45	1.213
BRWD1	chr21	39296436	39313786	0.436	0.443	0.439	1.671	1.653
		39185477	39313786	0.436	0.443	0.439	1.671	1.653
C11orf80	chr11	66744735	66843516	0.094	0.094	0	0.614	0.506
CARTPT	chr5	71719162	71719162	0.037	0.037	0.018	1.077	0.916
ELF5	chr11	34478794	34513800	0.155	0.062	0.062	0.216	1.226
		34478794	34511799	0.143	0.057	0.057	0.202	1.202
ESR1	chr6	151807318	152103273	1.206	0.61	0.671	1.219	0.619
		151807678	152103273	1.2	0.605	0.606	1.215	0.614
		151805672	152103273	1.132	0.596	0.597	1.145	0.58
		151805672	152103273	1.132	0.569	0.569	1.145	0.58
		151690495	152103273	0.671	0.569	0.569	2.687	2.22
HOOK3	chr8	42896889	43030539	0.548	0	0.549	1.449	1.447
PPP1R12B	chr1	202462742	202588569	0.421	0.175	0	0.022	0.076
		202462742	202588569	0.421	0.095	0	0.022	0.076
		202540113	202588569	0.226	0.095	0	0.321	0.309
		202348701	202438242	0	0	0	1.158	1.158
SLC25A36	chr3	140941819	140979943	0.603	0.603	0.601	1.363	0.786
ZNF91	chr19	23357695	23395467	0.496	0.496	0.497	1.042	1.012

Figure 3.20. Top 10 genes identified as ERα target genes in the upregulated dataset.

Table displays gene ID, transcription start and end site, and ChIP score.

Gene	Chromosome	Tx START	Tx END	Score 1	Score 2	Score 3	Score 4	Score 5
ANXA9	chr1	150982022	150995638	0.604	0.818	0.816	1.448	1.541
HSPB1	chr7	76302557	76304297	1.053	0.504	0.504	2.932	2.785
ISYNA1	chr19	18434387	18438301	0.425	0.426	0.426	1.708	1.705
		18434387	18438162	0.423	0.424	0.423	1.7	1.697
		18434387	18437309	0.409	0.409	0.409	1.653	1.645
JUP	chr17	41754606	41786712	0.464	0.464	0.464	2.194	1.676
KRT18	chr12	52948870	52952901	1.644	1.645	0.843	2.84	2.707
		52949058	52952901	1.639	1.64	0.84	2.827	2.695
KRT19	chr17	41523616	41528389	1.128	1.13	1.378	2.951	3.037
KRT8	chr12	52897186	52949866	1.62	1.62	0.829	2.775	2.647
		52897186	52926469	0.937	0.936	0.589	2.59	2.269
		52897186	52905084	0.752	0.752	0.554	1.827	2.122
RHOB	chr2	20447073	20449440	0.465	0.529	0.451	2.148	2.93
SPINT1	chr15	40844047	40857655	0.49	0.684	0	1.861	2.799
		40844047	40857655	0.49	0.684	0	1.861	2.799
		40844444	40857655	0.482	0.68	0	1.857	2.787
TMSB4X	chrX	12975106	12977227	1.081	1.149	1.082	1.316	1.744

Figure 3.21. Top 10 genes identified as ERα target genes in the downregulated dataset.

Table displays gene ID, transcription start and end site, and ChIP score.

3.2.10 Validation of genes using qRT-PCR

Conventional qRT-PCR was used to validate our RNA sequencing findings (figure 3.22). The gene *PKIB* was not initially identified as a significantly differentially expressed gene, but we did notice it's expression was higher in cells expressing CART (FPKMS based), and so it was included in our validation efforts. We found that CART could significantly increase the expression of the majority of these genes. Importantly, we saw a strong significant increase in the expression of *ESR1*, the gene corresponding to ERα, in cells expressing CART.

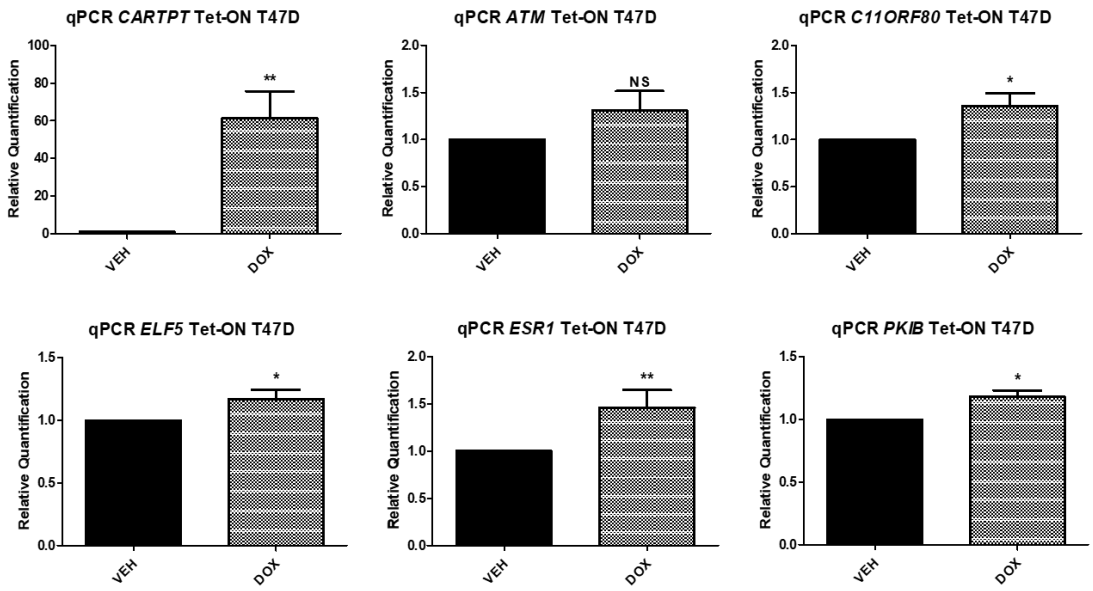

Figure 3.22. CART expression results in the significant increase of many genes identified via RNA sequencing.

Cells were treated with doxycycline, or vehicle control, for 72 hours in hormone stripped medium. Expression of genes identified from RNA-seq were examined using qRT-PCR. Mean +/- SEM between 3 independent experiments is plotted. A 1-tailed students t-test was used to calculate statistical significance. * - $p<0.05$, ** - $p<0.01$, NS – not significant.

3.2.11 Examining the top differentially expressed genes based on FPKMS difference

RNA sequencing thus far aided in identifying 256 significantly differentially expressed genes. Many of these genes were significantly increased following validation, however, it was difficult to ignore the fact that these genes were only seen to be modestly increased. Furthermore, it was clear from figure 3.12 that the level of differential expression for these genes was not uniform between replicates. It appeared that replicate 1, and certainly replicate 2, showed the greatest increase in expression of these genes, whereas the Z-scores in replicate 3 appeared to show the least difference between treatment groups. We therefore took the top 200 genes upregulated by CART based on

FPKMS difference between induced and uninduced samples, and created a heatmap to represent these (figure 3.23).

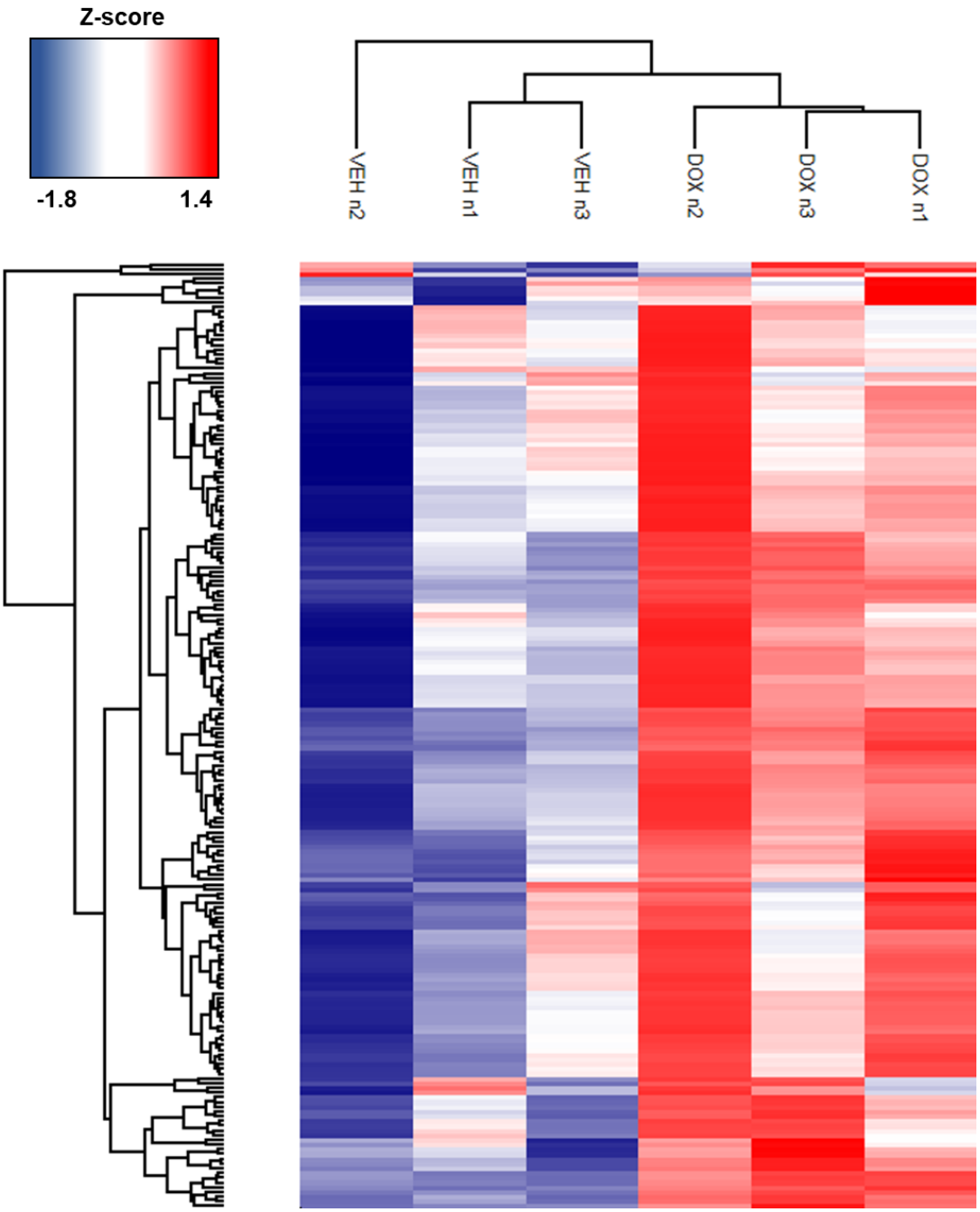

Figure 3.23. Heatmap of Z-scores for the top 200 genes based on FPKMS difference.

Next, we performed GSEA to establish whether these genes are associated with any previously established gene-sets. Specifically, we were interested in identifying whether these genes were associated with breast cancer in any way. To our surprise, a vast number of gene sets associated with anti-endocrine resistance were significantly associated with these genes (figure 3.24). Another interesting finding was a group of genes that were found to be downregulated in cells undergoing apoptosis in response to doxorubicin. Since these genes were increased in response to CART, it is tempting to speculate that the increased expression of these genes may affect the cells ability to undergo apoptosis. Furthermore, a number of these genes were also identified in gene sets as ERα target genes, or genes regulated by estradiol (figure 3.24).

GSEA, Gene Set Name	Description	FDR q-value	Genes
GRAESSMANN_APOPTOSIS_BY_DOXORUBICIN_DN	Genes down-regulated in ME-A cells (breast cancer) undergoing apoptosis in response to doxorubicin [PubChem=31703].	3.70E-03	TRPS1, PNN, ELF5, PARD6B, MYOF, ADK, PTPN11, ARGLU1, RBM39, PDE7A, DDX17, TRIM44, LYPLAL1, CCDC84, C16ORF74
GOZGIT_ESR1_TARGETS_DN	Genes down-regulated in TMX2-28 cells (breast cancer) which do not express ESR1 [GeneID=2099]) compared to the parental MCF7 cells which do.	3.52E-06	ESR1, PRLR, MLPH, TRPS1, INADL, TMEM45B, PGR, SEMA3C, ELF5, SRSF4, MALAT1, CAP2, NCAM2, C9ORF150
MASSARWEH_TAMOXIFEN_RESISTANCE_DN	Genes down-regulated in breast cancer tumors (formed by MCF-7 xenografts) resistant to tamoxifen [PubChem=5376].	1.63E-04	ESR1, PRLR, PGR, CDV3, AP1S2, PARD6B, MYOF, CTPS2
CREIGHTON_ENDOCRINE_THERAPY_RESISTANCE_1	The 'group 1 set' of genes associated with acquired endocrine therapy resistance in breast tumors expressing ESR1 and ERBB2 [GeneID=2099;2064].	5.45E-03	ESR1, PRLR, PGR, CAP2, AP1S2, MYOF, ADK, FAM155A
CREIGHTON_ENDOCRINE_THERAPY_RESISTANCE_5	The 'group 5 set' of genes associated with acquired endocrine therapy resistance in breast tumors expressing ESR1 but not ERBB2 [GeneID=2099;2064].	1.67E-02	SYCP2, ICA1, TMEM45B, PLEKHF2, NCAM2, FNBP1, SAMD4A
CREIGHTON_ENDOCRINE_THERAPY_RESISTANCE_4	The 'group 4 set' of genes associated with acquired endocrine therapy resistance in breast tumors expressing ESR1 but not ERBB2 [GeneID=2099;2064].	1.27E-02	PGR, CDV3, PARD6B, SFPQ, MED13L, LYPLAL1
RIGGINS_TAMOXIFEN_RESISTANCE_DN	Genes down-regulated SUM44/LCCTam cells (breast cancer) resistant to 4-hydroxytamoxifen [PubChem=63062] relative to the parental SUM44 cells sensitive to the drug.	1.98E-02	ESR1, KIAA1598, SEMA3C, MYOF, PTPN11
DOANE_BREAST_CANCER_ESR1_UP+B17:C17	Genes up-regulated in breast cancer samples positive for ESR1 [GeneID=2099] compared to the ESR1 negative tumors.	1.82E-02	ESR1, MLPH, SEMA3C, PGR
MASSARWEH_RESPONSE_TO_ESTRADIOL	Genes rapidly up-regulated in breast cancer cell cultures by estradiol [PubChem=5757].	4.13E-02	PGR, CDV3, MYOF
HUANG_DASATINIB_RESISTANCE_DN	Genes whose expression negatively correlated with resistance of breast cancer cell lines to dasatinib [PubChem=3062316].	4.85E-02	PRLR, TRPS1, ICA1

Figure 3.24. GSEA reveals genes which are associated with anti-endocrine resistance, as well as genes which have been characterized as ERα target genes.

Next, we aimed to validate these genes via qRT-PCR. In figure 3.25, we report that while many of these genes were increased in cells expressing CART, this was not seen to be a significant correlation. The main issue most certainly lies with the variation of expression between the 3 independent experiments. For many of the genes, an increase was seen in 2 replicates, whereas 1 replicate typically did not show an increase. This is in line with the RNA sequencing data, whereby we saw the expression of these genes was typically only increased in 2 out of 3 of the replicates. Taken together, we feel that these genes are certainly worthy of further investigation, but caution must be exercised when analysing the expression of these genes across samples going forward.

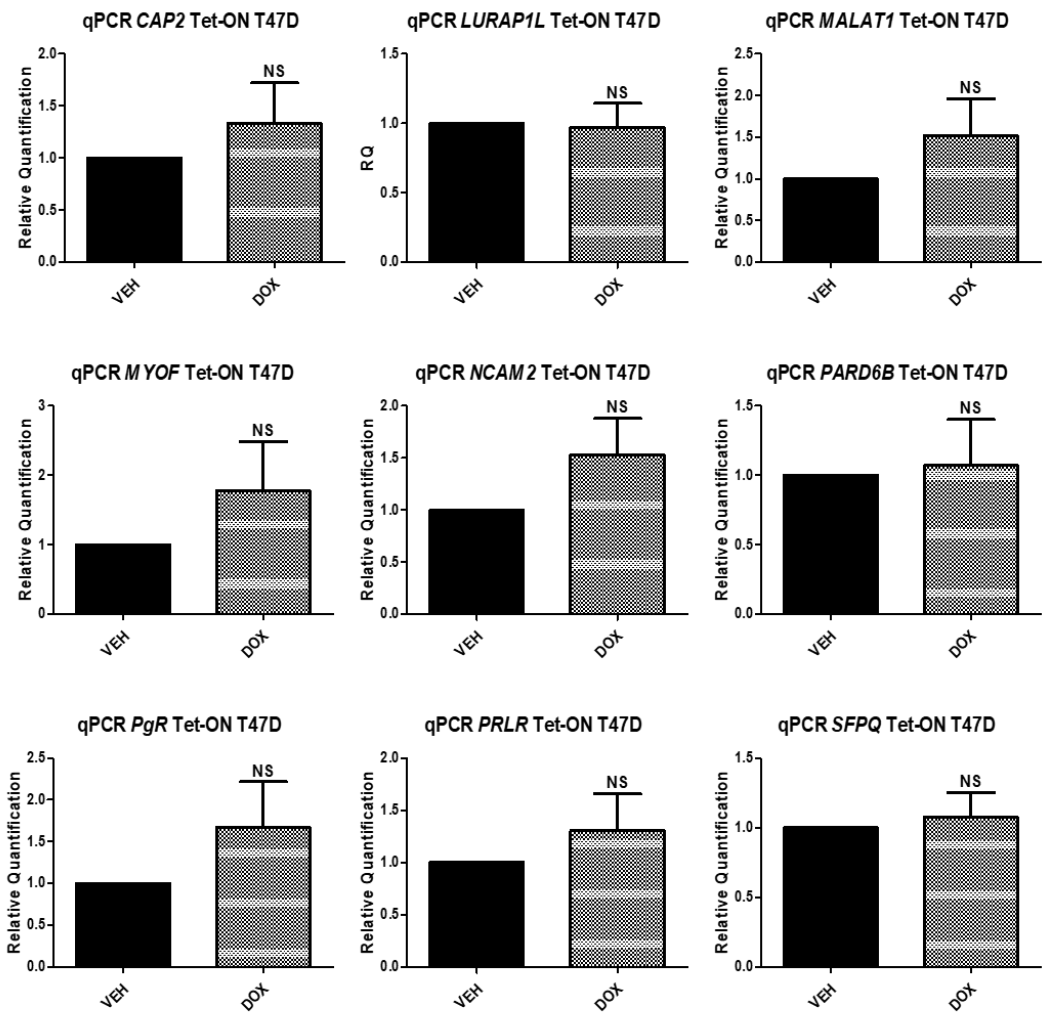

Figure 3.25. Attempted validation of putative ESR1 target genes, as well as genes associated with anti-endocrine resistance.

Cells were treated with doxycycline, or vehicle control, for 72 hours in hormone stripped medium. Expression of genes identified from RNA-seq were examined using qRT-PCR. Mean +/- SEM between 3 independent experiments is plotted. A 2-tailed students t-test was used to calculate statistical significance. NS – not significant.

3.2.12 Cellular response to anti-endocrine agents

Finally, having identified that CART may be responsible for an increase in genes associated with anti-endocrine resistance, we aimed to examine whether cells expressing CART respond worse/better to 2 common anti-

endocrine agents, fulvestrant and tamoxifen. The action of fulvestrant and tamoxifen have been discussed in further detail in section 1.2 of this study. In figure 3.26, we report that cells expressing CART show a modest, but significant, increase in tolerability to high-dose tamoxifen (p=0.042). Interestingly, cellular response to fulvestrant is completely unaltered in cells expressing CART, suggesting that CART expression drives a modestly-resistant phenotype to tamoxifen, but not fulvestrant.

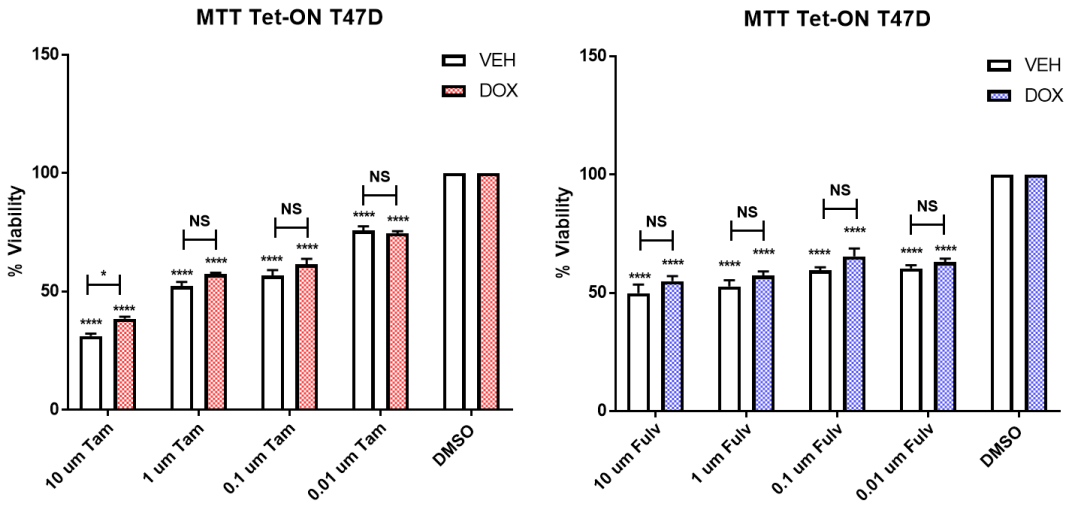

Figure 3.26. Cellular response to tamoxifen, but not fulvestrant, is altered in cells expressing CART.

Cells were treated with doxycycline, or vehicle control, as well as the anti-endocrine agents at the respective concentrations mentioned above, for 72 hours. For both anti-endocrine agents, VEH and DOX treated cells were normalised to their respective DMSO treated counterparts. Mean +/- SEM between 3 independent experiments is plotted. A two-way ANOVA with Tukey's multiple comparison post-test was used to calculate statistical significance. * - p<0.05, **** - p<0.0001, NS – not significant.

3.3 Discussion

3.3.1 CART can alter the expression of ERα target genes

Consistent with previously published data, CART treatment resulted in the increased phosphorylation of ERK (Lakatos et al., 2005, Brennan et al., 2012, Sathanoori et al., 2013). Longer time points highlighted that CART could increase the expression of both the progesterone receptor and cyclin D1, again consistent with previously published data (Brennan et al., 2012, Landerholm et al., 2012). We confirmed that this increase in expression was due to the transcripts for each gene increasing, rather than through other mechanisms such as reduced protein turnover, using qRT-PCR. We also included the gene Trefoil factor-1 (TFF1), as this is another common ERα target gene. Using qRT-PCR, we see that CART significantly, and rapidly, increases the expression of *PGR*. The expression of *CCND1* was increased across all three independent experiments at one hour, however due to the variation between replicates, this was not deemed statistically significant. Expression of *TFF1* was not increased in all independent experiments at any time, and so was not considered a gene regulated by CART.

Having shown that CART can alter the expression of ERα target genes, we next sought to examine if patients with high levels of CART also present with elevated levels of common ERα target genes. Consistent with the previous data, it was clear that many ERα target genes were elevated in patients with corresponding high expression of CART. This was seen across two independent cohorts of patients (and indeed had been reported previously by Brennan et al., 2012), strengthening our hypothesis that CART may alter the function of ERα.

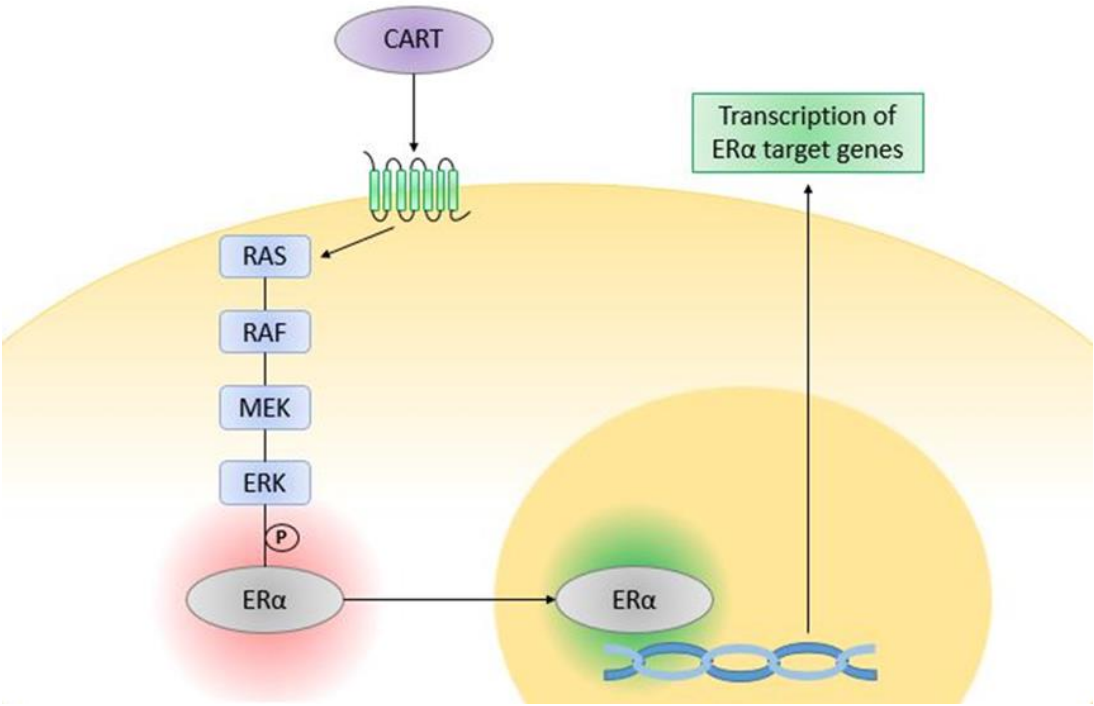

Figure 3.27. Graphical representation of CART signalling in ER+ breast cancer.

3.3.2 The role of LxxLL motifs in CART mediated ERα activity

As mentioned in section 3.2.2, CART contains three LXD motifs within its sequence. LXD motifs are known to mediate critical interactions between nuclear receptors, and are necessary for co-activator recruitment (McInerney et al., 1998). For example, LXD motifs within NCoA1/SRC1 are required for the functional interaction with CBP/p300 (McInerney et al., 1998). The fact that 3 of these exist within the sequence of CART was certainly worthy of further investigation. First, the leucine residues were replaced with alanine residues via site-directed mutagenesis, an amino acid substitution which has been used in many past studies (Schaufele et al., 2000, Dong et al., 2006). Following mutation of each of these motifs, we found a general trend of decreased ERα activity when both motifs 1 and 2 were mutated, compared to pCMV-CART, and the decrease seen from mutating LXD motif 1 in T47D cells was statistically significant. This suggests that LXD motifs within CART may indeed be important in mediating ERα function.

3.3.3 Genes significantly upregulated by CART

To our knowledge, this is the first and only investigation into the consequence CART can have on the transcriptional landscape of cells. While this offers a unique opportunity to discover truly novel findings, it makes the data somewhat difficult to interpret. For example, our analysis only characterized 100 genes which were significantly upregulated by CART, which may seem like a relatively small number for an RNA sequencing experiment. However, it is entirely possible that since breast cancer cells do not express CART under normal conditions (Brennan et al., 2012), the changes made by expressing CART may be subtle, but significant.

An increase in the expression of *ESR1* was arguably the most interesting result from the list of significantly upregulated genes. This increase had been noticed previously at the protein level (Brennan et al., 2012), but this confirmed CART was transcriptionally altering the expression of ERα. Furthermore, CART could increase the expression of the transcription factor E74-linked factor 5 (ELF5). ELF5 has previously been implemented as a suppressor of estrogen sensitivity in breast cancer, which may indicate acquired resistance to tamoxifen (Kalyuga et al., 2012). Further, a more recent study characterized ELF5 to be overexpressed in cell-line models of tamoxifen resistance, and ELF5 promotor methylation was typically higher in primary tumours when compared to secondary tumours in patients receiving anti-endocrine therapy (Fitzgerald et al., 2016).

The finding that genes upregulated by CART are associated with tobacco use disorder was also an intriguing finding. We had never previously associated CART expression in breast cancer with tobacco use. The only tentative link associating CART with tobacco use is a study published in 2016 (Kaya et al., 2016). This study reported that nicotine could regulate the expression of CART mRNA levels in the mesocorticolimbic system *in vivo*, and the authors suggest that CART may play a role in the nicotine reward system. It would be extremely interesting to examine whether CART expression correlates with patients smoking history, an association we have never before considered.

Using GSEA, a number of genes were identified to show cell cycle-specific expression in a number of datasets. For example, ENOSF1 and CCDC14 were shown in one study to show peak expression during S-phase of the cell cycle (Whitfield et al., 2002). ANKRD10 and NKTR, both upregulated in cells expressing CART, were also shown to show peak expression during the G1/2 phase of the cell cycle (Whitfield et al., 2002). Reassuringly, these same genes were characterized in another, independent gene set to display cell cycle stage-specific expression (Ben-Porath et al., 2008). This is relevant to this study for a number of reasons. First, previously published data characterized the protein expression of Cyclin D1 to be increased by CART in colon cancer cells (Landerholm et al., 2012). Work from this current study highlighted that this increase in Cyclin D1 expression could also be noticed in breast cancer cells (figure 3.3). As Cyclin D1 is required for the progression of cells through the G1 phase of the cell cycle (Baldin et al., 1993), it was interesting to see these genes associated with the G1/S and S phases of the cell cycle to be increased. Next, we have shown in preliminary studies that CART can increase the number of cells found in the S and G2/M phases of the cell cycle, suggesting CART can promote cell cycle progression. It would be interesting to examine this phenomenon further in multiple cell lines, as well as in further time-points.

3.3.4 Genes significantly downregulated by CART

While 100 genes were found to be significantly upregulated by CART, 156 genes were found to be significantly downregulated by CART. While examining the biological processes associated with these genes, two processes stood out as cancer-relevant processes. First, we saw that CART decreases the expression of genes associated with cell to cell adhesion. One of the most important hallmarks of Invasive Lobular Carcinoma is the loss of E-cadherin expression. Loss of E-Cadherin occurs in the vast majority of Invasive Lobular Carcinoma cases, and typically allows for the progression of a more invasive disease (Singhai et al., 2011). While E-Cadherin itself was not seen to be among the genes downregulated by CART, it is an important

example of how decreased expression of genes associated with cell adhesion can result in a more invasive disease, and is certainly an aspect worthy of further investigation.

We see a decrease in the expression of enzymes involved in glycolysis and glycolytic pathways. This is important, as altered cellular metabolism is one of the key hallmarks of cancer (Hanahan et al., 2011). This was first reported by Otto Warburg, who made the landmark discovery termed “the Warburg effect” (Warburg et al., 1927) in 1927. This central dogma suggests cancer cells typically produce ATP through the less efficient process of glycolysis, rather than oxidative phosphorylations (Warburg et al., 1927). This results in increased glycolysis in cells, which is the opposite of what we see in terms of gene expression. This may suggest CART drives a “Reverse Warburg” phenotype, which is thought to be closely related to cancer cell metastasis (Pavlides et al., 2010). While it is difficult to associate decreased gene expression of glycolytic enzymes with decreased levels of glycolysis, this would first be something important to investigate prior to carrying out a large investigation into the effect CART expression has on the metabolic potential of cancer cells. Importantly, many studies have highlighted that CART does indeed play a role in biological processes involving glucose. In 2005, it was reported that altered beta cell morphology and glucose intolerance were phenotypes exhibited in CART knock-out mouse models (Wierup et al.,2005). In 2013, CART was shown to protect beta cells against glucotoxicity, as well as increase cellular proliferation (Sathanoori et al., 2013). In terms of altering mitochondrial enzyme function, CART has previously been reported to activate succinate dehydrogenase 2, a key enzyme in the citric acid cycle (Mao et al., 2007). These studies highlight that CART has been implicated previously to play a role in glucose homeostasis, and alter mitochondrial enzyme function. Therefore, it would be intriguing to examine the precise effect CART has on the metabolic potential of breast cancer cells.

3.3.5 ERα can bind promotor regions of genes identified in RNA sequencing post treatment with CART

The commendable increase in accessibility of publicly available data allows smaller experiments such as this, to benefit from large studies carried out by other groups. Cistrome is a database which compiles publicly available ChIP-seq data from many transcription factors in multiple sources (Mei et al., 2017). We wished to examine whether any differentially expressed genes have previously been shown to contain ERα binding sites within the transcription initiation site. For this, we compared our list of differentially expressed genes to five experiments from three studies. The first study (Mohammad et al., 2015) came from an elegant study published 2 years ago in which Mohammad and colleagues investigated the structural and molecular relationship between PGR and ERα. The conditions for this experiment were T47D cells treated with normal growth medium treatment for 3 hours, and we accessed all three biological replicates for this condition. The next study was from the same group, but a different experiment (Ross-Innes et al., 2012). The treatment conditions for this study were T47D cells under normal growth conditions. Finally, the last experiment was from a different group (Gertz et al., 2013). The treatment conditions for this were T47D cells treated with 10 nm estradiol for 1 hour.

In comparing our genes to these datasets, we identified that many of our genes have previously been reported as containing ERα binding sites. More importantly, we found that genes both upregulated and downregulated by CART may be classified as potential ERα target genes. This highlights that CART may not only function to increase the transcriptional regulation of ERα, but also repress its transcriptional ability. We hypothesized that CART may alter the binding partners of ERα at this point, which gave rise to the investigation into the effect CART has on the ERα interactome presented in our next chapter.

However, there is one point which should be taken into consideration prior to making definitive conclusions. Without completing an ERα ChIP-seq experiment in our own model of CART expression, it is impossible to

definitively conclude that CART regulates the expression of these genes by altering the function of ERα. Transcription is an extremely complicated process which is often over-simplified. Many transcription factors are known to bind multiple different gene promotors (MYC is a classic example of this) (Loven et al., 2013). On the other hand, a single transcription factor (such as the Glucocorticoid Receptor) can act to both promote and repress transcription (Latchman. 2001). This becomes further complicated when one considers the effect various transcription complexes can have on the same transcription factor (Latchman. 2001). Performing an ERα ChIP-seq experiment would confirm the presence of ERα at promotor regions attaining to these genes, which could then be validated by low-throughput ChIP qRT-PCR. At the very least, the hypothesized binding sites provided by Cistrome could be used to design primers for use in a low-throughput experiment to confirm the presence of ERα at these sites in the presence of CART.

3.3.6 CART increases the expression of a subset of genes associated with tamoxifen resistance

Finally, we examined what gene sets were associated with the top 200 upregulated genes by CART. We identified that a number of these genes were classified as genes either regulated by estradiol, or putative ERα target genes. Reassuringly, *ELF5* appeared in one data set as a potential ERα target gene (Gozgit et al., 2007). *ELF5* was also seen to contain possible ER binding sites from our ERα ChIP-seq publicly available data, and was validated by conventional qRT-PCR. *ELF5* was not detected in another dataset as a gene upregulated by estrogen (Massarweh et al., 2008). Perhaps *ELF5* is regulated by ERα, but not in response to estradiol. This would be in line with published data, suggesting that ELF5 suppresses estrogen sensitivity and may confer resistance to tamoxifen (Kalyuga et al., 2012).

A number of gene sets associated with tamoxifen resistance were linked with the top 200 genes from RNA-seq (figure 3.24). For example, genes falling under “gene set 1” and “gene set 4” (Creighton et al., 2008) are genes which were found to be higher in cells that were estrogen sensitive compared to cells

with acquired endocrine resistance (Creighton et al., 2008). In contrast, genes falling into “group 5” were found to be at higher levels in cells with acquired endocrine-resistance compared to estrogen sensitive cells (Creighton et al., 2008). This data is moderately conflicting, given that increased expression of these genes would infer both a sensitive and resistant phenotype to anti-endocrine therapy. We examined whether cells expressing CART responded differently to two common anti-endocrine agents, fulvestrant and tamoxifen. Cells expressing CART responded equally as well to fulvestrant as cells not expressing CART, however, cells expressing CART appeared to tolerate tamoxifen modestly better (figure 3.26). Examining the expression of genes from all three gene “groups” mentioned above in response to CART and anti-endocrine therapy would represent the clearest way to understand how CART seemingly increases gene sets associated with both anti-endocrine sensitivity and resistance. Perhaps it is possible that the decreased sensitivity to tamoxifen is partly due to an increase in the expression of genes which are usually suppressed in breast cancer cells undergoing doxorubin-induced apoptosis (Graessmann et al., 2007). This may indicate that CART increases the expression of genes which are usually suppressed in cells undergoing apoptosis, and so perhaps CART affects the ability for cells to undergo apoptosis.

Chapter 4. Proteomic investigation into the effect of CART on the Estrogen Receptor interactome

4.1 Introduction

4.1.1 Analysis of protein complexes

Proteins rarely work alone in human cells. Oftentimes, it is the proteins physically interacting (termed the interactome) with the target protein of interest that dictates its function. The nuclear hormone receptor ERα, is a classic example of a protein whose function is significantly dictated by its interacting partners. Cytoplasmic ERα can interact with molecular chaperone proteins (such as HSP90) which can facilitate its transport from the cytoplasm to the nuclear region of the cell (Pratt et al., 1997). Once in the nucleus, ERα can interact with a host of factors that may dictate whether transcription is activated or repressed (Onate et al., 1995, Lamb et al., 2000, Wu et al., 2003). Understanding the consequence a given treatment condition has on the interactome of a protein presents the opportunity to gather a huge amount of information pertaining to this relationship.

One of the earliest methods for testing whether proteins interacted involved the use of a technique known as the yeast two-hybrid screen, first proposed nearly 30 years ago (Fields et al., 1989). In this technique, an interaction between a protein of interest (bait) and the protein being tested (prey) would result in the expression of reporter genes enabling the growth of yeast (Fields et al., 1989). High-throughput variations of this screen were developed, and were separated into either the matrix/array approach, or the library approach (Bruckner et al., 2009). However, these screening methods are not without their flaws, with false-negative interactions being an issue for the array approach, and false-positive interactions being an issue for the library approach (Bruckner et al., 2009).

The technological advances made in mass spectrometry, as well as the increase in dedicated computational platforms capable of handling data from these experiments, has resulted in mass spectrometry quickly becoming the gold standard for deconstructing and understanding complicated protein complexes. Careful immunoprecipitation of a protein of interest (target/bait) will result in many interacting partners also being immunoprecipitated. Due to the

non-specific nature of antibodies, an “isotype-matched” non-specific antibody is typically used in tandem with the immunoprecipitation of the target protein. Proteins identified in the negative control antibody are considered false-positive/non-specific interactors, and are typically removed from analysis. This step is crucial, as the contribution of non-specific interactors can be substantial (Mohammed et al., 2016).

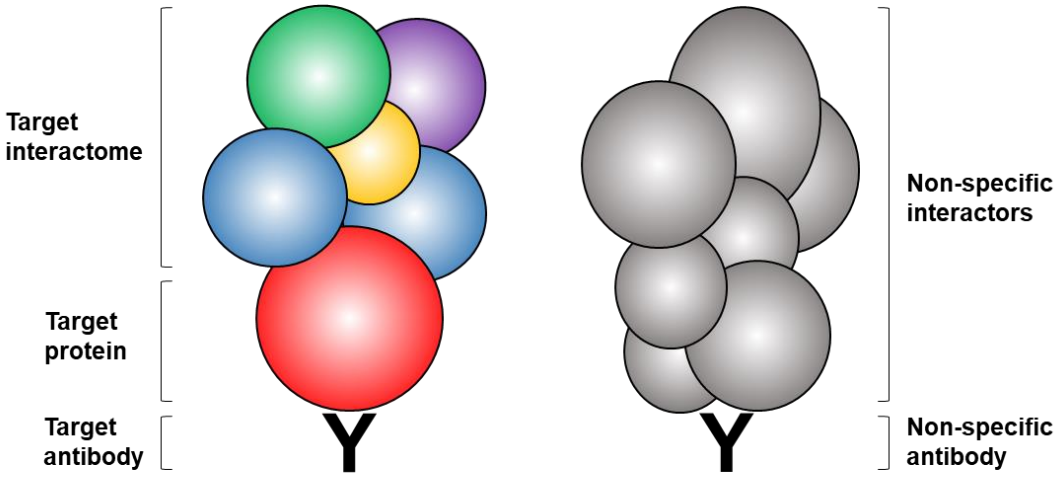

Figure 4.1. Immunoprecipitating a target protein results in interacting partners also becoming purified.

Following immunoprecipitation, the protein complexes are enzymatically digested, purified and “peptide sequenced” on a mass spectrometer. The resulting mass spectra generated refer to the peptides which were identified by the mass spectrometer. These spectra can be processed and mapped to the human proteome using computational software such as MaxQuant (Tyanova et al., 2016). The resulting files can be statistically processed using software such as Perseus (Tyanova et al., 2016), which allows for the discovery of the interacting partners of a protein of interest for the given experimental condition.

4.1.2 ERα interaction networks

It is now widely accepted that ER+ breast cancers rely on estrogen (E_2) and ERα for their growth. This fundamental understanding resulted in the development of the first anti-endocrine agent used to treat this subtype of breast cancer, tamoxifen. Tamoxifen proved (and indeed still proves) to be an effective treatment strategy for ER+ breast cancer. The knowledge that E2 mediates ERα activity through the recruitment of coregulators (Onate et al., Science 1995) has resulted in an impressive level of work in this field, with many groups identifying complexes which aid in ERα function, and may also confer sensitivity to tamoxifen. Below are a handful of significant examples of these interaction networks.

Fascinatingly, the first identified coregulator of ERα was initially identified by a yeast two-hybrid screen of the progesterone receptor (Onate et al., 1995). The identified protein was found to stimulate activation of all steroid receptors tested within their study, and was subsequently named Steroid Receptor Coactivator-1 (SRC-1). While necessary for the function of ERα, recent studied have implicated SRC-1 as a key driver of tamoxifen resistance in multiple studies of anti-endocrine resistance (Redmond et al., Res. 2009, Qin et al., 2009).

Cyclin D1 has also previously been reported as a coregulator of ERα (Lamb et al., 2000). Cyclin D1 is thought to antagonize the BRCA1 mediated repression of ERα activity (Wang et al., 2005), and more recent work highlights the importance for cyclin D1 in mediating estrogen signalling *in vivo* (Casimiro et al., 2013).

Work from Professor Jason Carroll of Cambridge University has significantly contributed to the field of deciphering the ERα interactome. In 2011, a study published by Carroll and colleagues highlighted that FOXA1, a pioneer factor, was critical for mediating the normal function of ERα, and was necessary for the function of tamoxifen (Hurtado et al., 2011). A number of years later, the same group utilised ERα -immunoprecipitation followed by mass spectrometry to characterize GREB1 as an ERα cofactor (Mohammed et al., 2013). The study went on to characterize GREB1 as a necessary cofactor for ERα activity,

and showed that high expression of GREB1 resulted in good clinical outcome (Mohammed et al., 2013). Finally, a landmark study published in 2015 characterized an interaction between ERα and the progesterone receptor (PGR) using ERα immunoprecipitation mass spectrometry (Mohammed et al., 2015). This study articulately demonstrated that PGR could interact with ERα to direct ERα chromatin binding. The unique expression signature characterized by these binding events was shown to be associated with good clinical outcome (Mohammed et al., 2015).

The above examples are only a small fraction of the identified coregulators which can aid in the function of ERα. The given examples were intended to highlight not only the requirement of these coregulators for ERα function, but also that their expression may help in predicting response to anti-endocrine therapy. Furthermore, the studies shown in which GREB1 (Mohammed et al., 2013) and PGR (Mohammed et al., 2015) were identified as ERα binding partners highlights the sheer power immunoprecipitation mass spectrometry experiments can have in terms of understanding nuclear receptor functions.

4.1.3 Aims of chapter

It is clear that coregulator recruitment is a necessary step for nuclear receptor function. In chapter 3 of this study, we characterized that CART may have a functional relationship with ERα. We therefore hypothesized that utilizing ERα immunoprecipitation-mass spectrometry may help us identify differentially recruited ERα interactors in cells expressing CART. The main aims of this chapter are as follows:

- Attempt to identify whether CART has any effect on the ERα interactome

- Attempt to prove that there are common interactors to ERα in the presence of CART using two independent ERα antibodies

- Characterize if any proteins recruited to ERα may be suitable targets for disrupting ERα binding events

4.2 Results

4.2.1 Investigating if CART is a physical interactor of ERα

As reported in figure 3.6, mutating LXD-motif 1 within CART resulted in a significant decrease in ERα activity. This lead us to hypothesize that CART may be a physical interactor of ERα. As demonstrated in figure 4.2, immunoprecipitation of ERα does not result in CART co-immunoprecipitating, and immunoprecipitation of CART does not result in ERα co-immunoprecipitating. This suggests that CART does not physically interact with ERα.

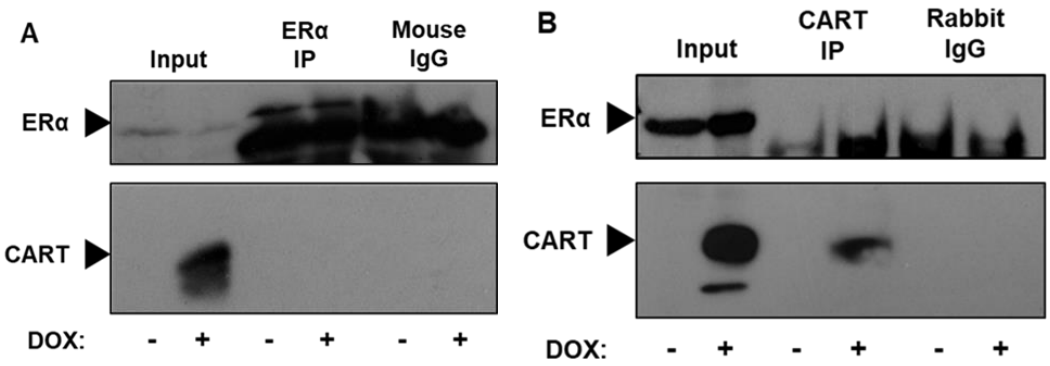

Figure 4.2. CART is not a physical interactor of ERα.

A. Following immunoprecipitation of ER, western blot analysis was used to confirm ERα pull-down, and test whether CART was co-immunoprecipitated with ERα. **B.** Following immunoprecipitation of CART, western blot analysis was used to confirm CART pull-down, and test whether ERα was co-immunoprecipitated with ERα. Both experiments were performed in Tet-ON T47D cells.

4.2.2 Mass spectrometry workflow and ERα immunoprecipitation

Having established that CART is not a physical interactor of ERα, we hypothesized that CART may influence the interacting partners of ERα. A workflow (figure 4.3) for performing ERα immunoprecipitation, followed by in-solution tandem mass spectrometry was established in collaboration with Dr. Adrian Bracken of Trinity College Dublin, and Dr. Gerard Cagney of University College Dublin (UCD).

Cells were treated with 1 µg/ml doxycycline or water as the suitable vehicle control for 72 hours. Additional samples were treated with 1 nM E2 or EtOH vehicle control for the same duration as cells mentioned above. This was performed in order to understand if any novel ERα interactors identified following CART expression were also detected in cells treated with estrogen for the same duration of time.

All raw label-free quantification (LFQ) values for subsequent results can be found under appendices, section E.

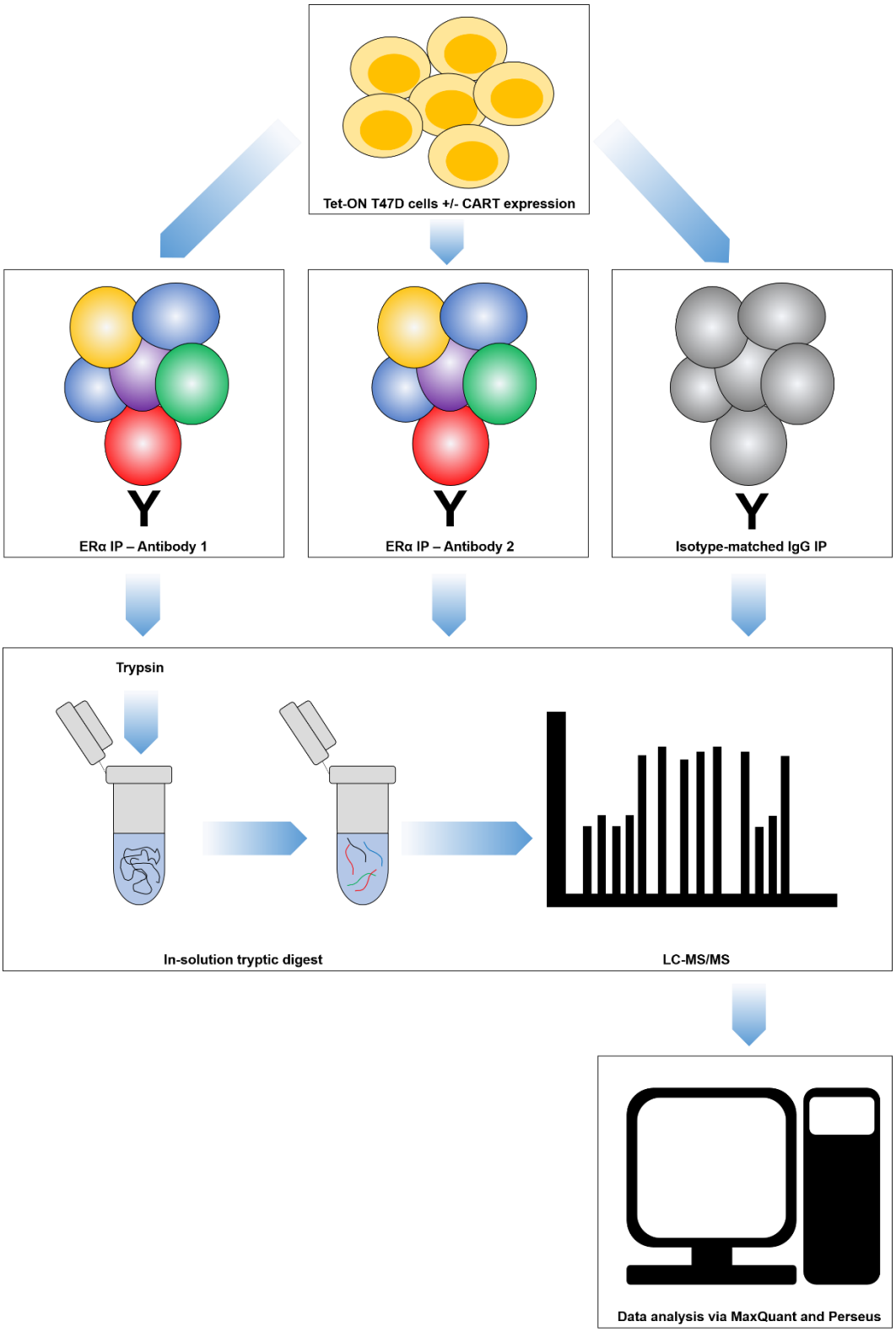

Figure 4.3. Established workflow for mass spectrometry analysis following ERα immunoprecipitation.

For this study, it was decided that the use of 2 individual antibodies (SC-8005 (D12) and SC-8002 (F10)) raised against ERα for immunoprecipitation may help in handling of the large amounts of data typically generated from studies such as these. This technique has been implemented by our collaborators previously (Streubel et al., 2017). The idea was to perform ERα IP mass spectrometry using both antibodies, remove any non-specific interactors as detected in the isotype-matched IgG control, and look at interactors common to both antibodies.

As shown in figure 4.4 A, no non-specific binding was detected in the IgG negative control lanes, and ERα was indeed immunoprecipitated following the IP protocol. The immunoprecipitation of ERα appeared more specific using the D-12 antibody when compared against the F-10 antibody. As seen from figure 4.4 B, cells which had received 1 μg/ml doxycycline were expressing CART, and this was not detected in any other samples.

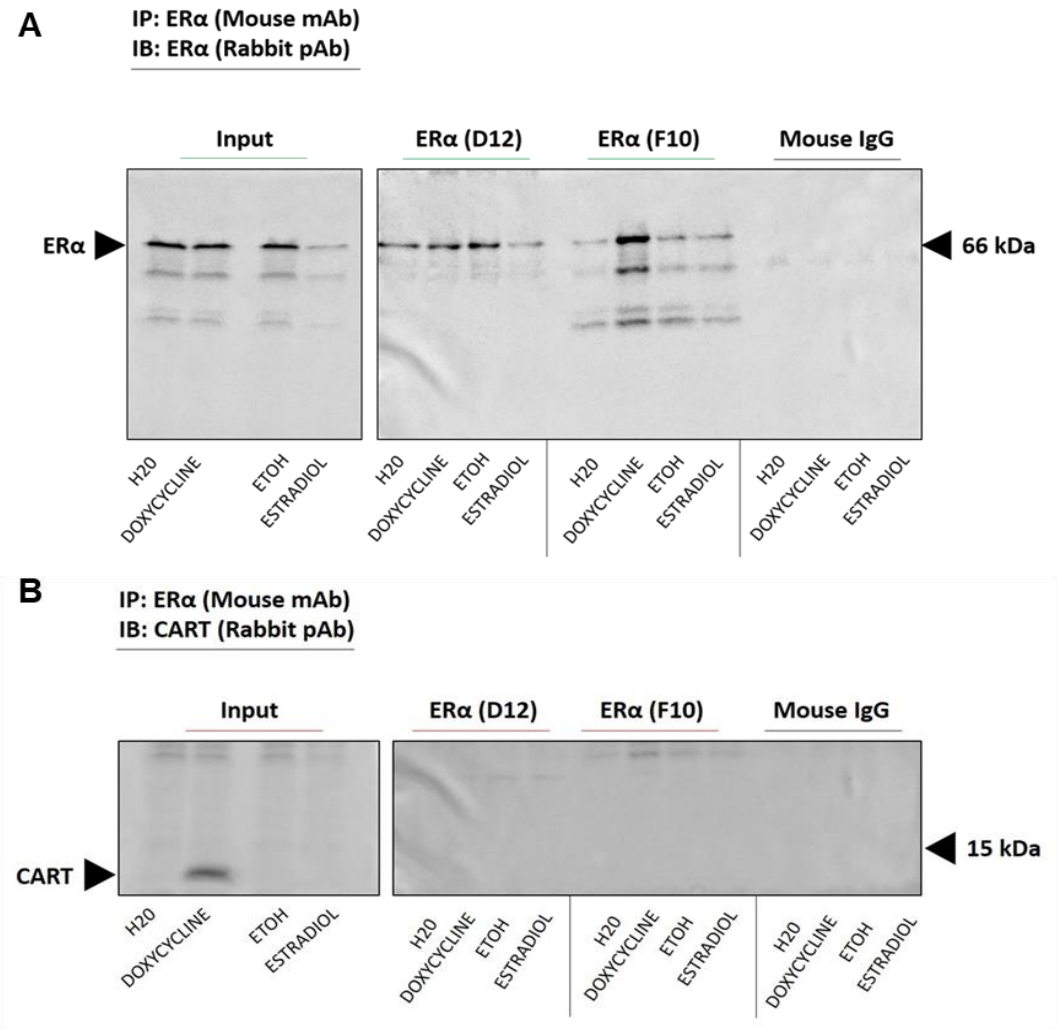

Figure 4.4. Western blot analysis of immunoprecipitation samples used for mass spectrometry analysis.

A. Western blot analysis of beads used for mass spectrometry analysis confirmed a positive immunoprecipitation of ERα **B.** Membranes were stripped and re-probed for CART to confirm samples that received doxycycline were expressing CART.

4.2.2 Hierarchical clustering, principal component analysis (PCA) and volcano plot generation of data from ERα D-12 immunoprecipitation

Principal component analysis (PCA) was carried out on all samples in order to assess if there was an overlap between ERα IP samples and IgG IP samples. Next, hierarchical clustering was performed on samples following the removal of proteins which were detected in more than one IgG sample per condition.

This generated a heatmap that allowed for a simplistic visualisation of how the treatment conditions clustered relative to the vehicle controls, as well as what proteins were identified in each sample. Following this, missing values in the ERα IP samples were imputed from a normal distribution (Hein et al., Cell 2015), which allowed for a 2-sided t-test and subsequent volcano plot generation. The volcano plots rank the log2 label free quantification (LFQ) difference between the 2 treatment groups on the X-axis, and the -log p-value on the Y axis, allowing for the visualisation of whether proteins are significantly associated with ERα in the presence/absence of CART. The Blue-Red colour scheme was used to represent LFQ values, where Blue = low LFQ values, and Red = high LFQ values. For volcano plots, proteins significant in the vehicle treated cells were highlighted blue, and proteins significant in the treated cells (DOX or E2) were highlighted red. Proteins that did not reach statistical significance were highlighted grey.

First, we show PCA and the generated LFQ heatmap for ERα IP samples +/- DOX (D-12 antibody). As demonstrated in figure 4.5, replicates for each sample group together, and importantly, each treatment group clusters together.

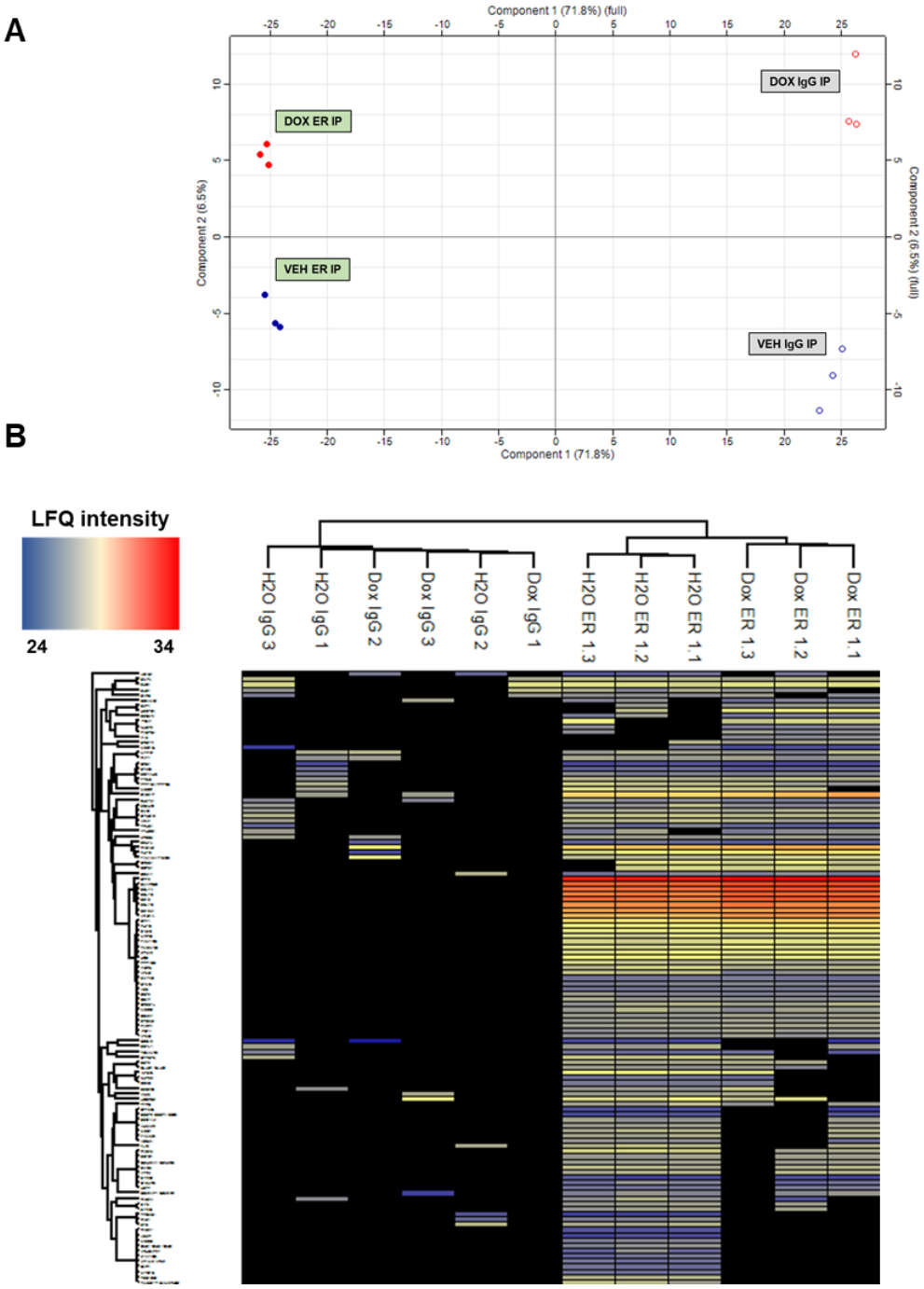

Figure 4.5. Principal component analysis and hierarchical clustering of samples +/- CART expression (D-12 antibody)

A. PCA plot demonstrates treatment groups cluster separately from one-another. **B.** Hierarchical clustering further demonstrates that treatment groups form distinct clusters. Label free quantification (LFQ) intensities ranging from 24 (modestly detected) to 34 (abundantly detected) for each identified protein is represented on this heatmap. Black area of the plot represents proteins not identified.

As can be seen from figure 4.6, there were 14 proteins significantly associated with ERα in the presence of CART, and 21 proteins significantly associated with ERα in the absence of CART. The majority of the proteins found to be recruited to ERα in the presence of CART were known members of the BAF-chromatin remodelling complex (ARID1A, SMARCD1, SS18), however, 2 proteins (HECTD4 & WIZ) had not previously been identified as ERα interactors.

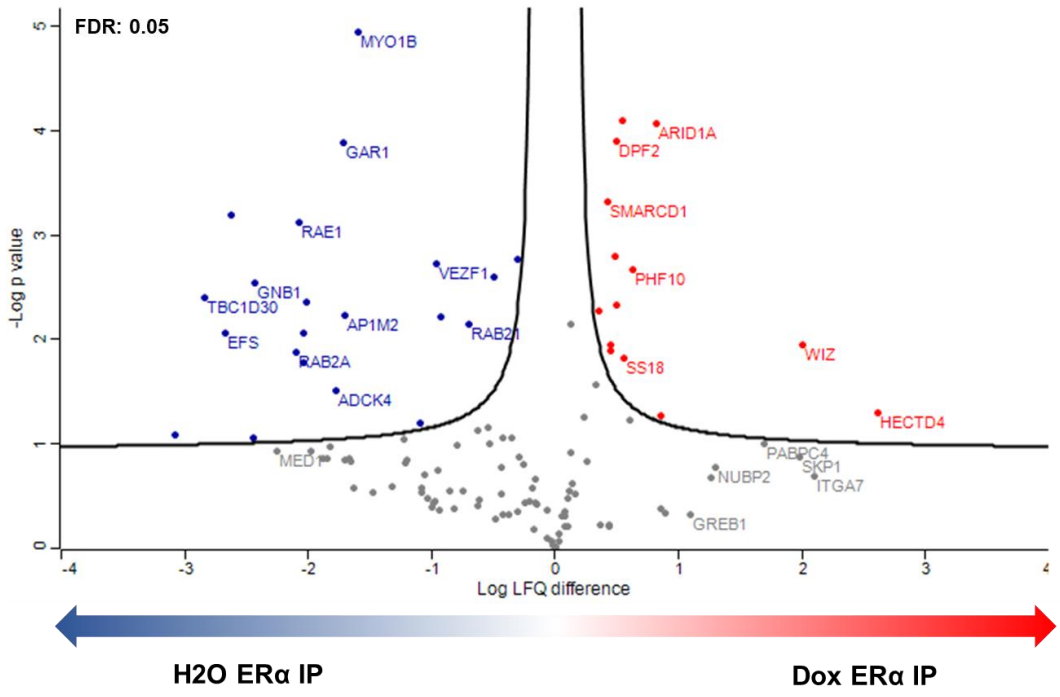

Figure 4.6. Volcano plot of identified proteins in ERα immunoprecipitation samples +/- CART expression (D-12 antibody).

A two-sided t-test was used to represent proteins significantly associated with ERα in the presence/absence of CART. A false-discovery-rate (FDR) of 5% was applied to this test, and the log fold change was kept at the default value of 0.1.

Next, we show PCA and the generated LFQ heatmap for ERα IP samples +/- E2 (D-12 antibody). As demonstrated in figure 4.7, replicates for each sample group together, and each treatment group clusters together.

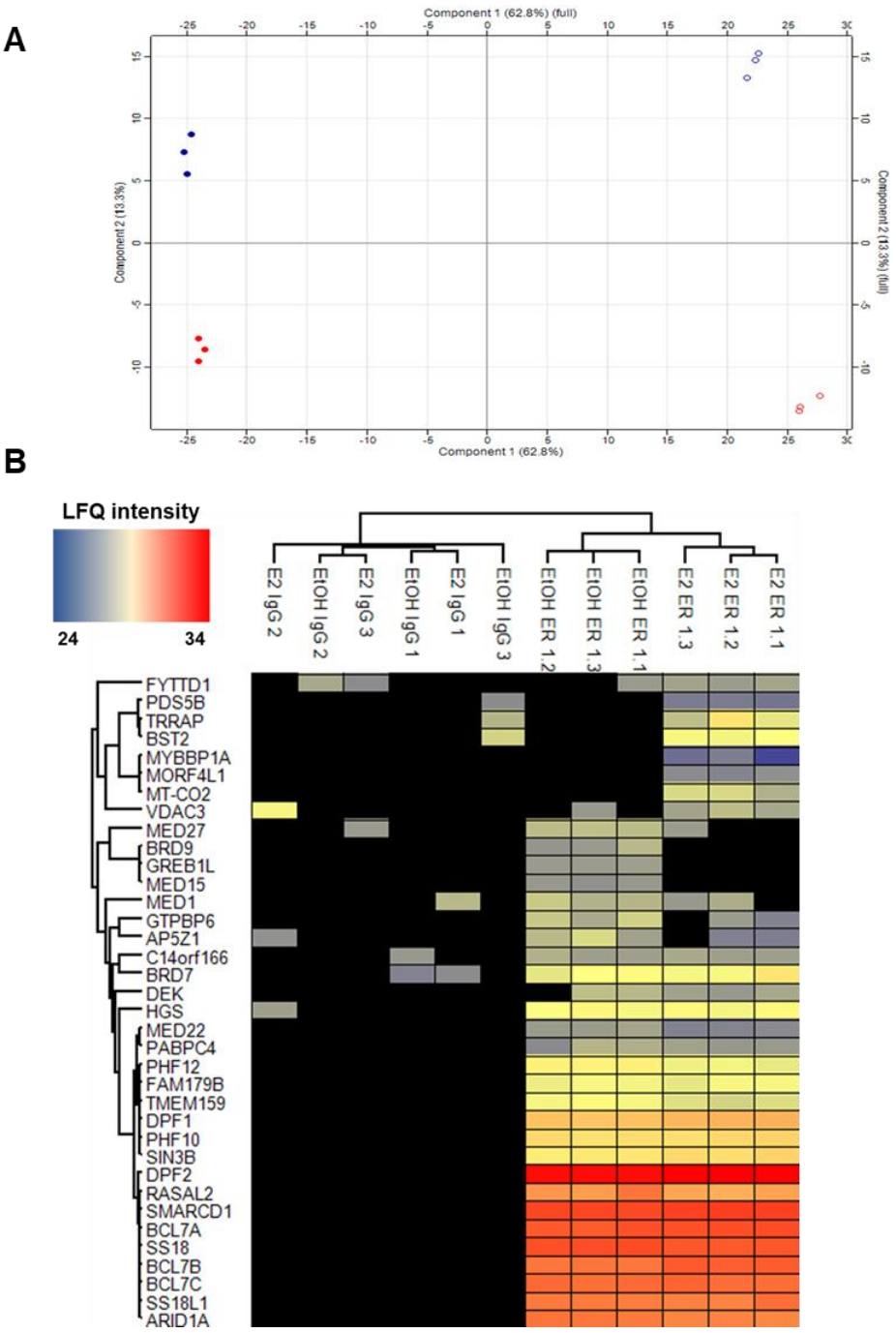

Figure 4.7. Principal component analysis and hierarchical clustering of samples +/- 1 nm E2 treatment (D-12 antibody).

A. PCA plot demonstrates treatment groups cluster separately from one-another. **B.** Hierarchical clustering further demonstrates that treatment groups form distinct clusters. Label free quantification (LFQ) intensities ranging from 24 (modestly detected) to 34 (abundantly detected) for each identified protein is represented on this heatmap. Black area of the plot represents proteins not identified.

In the E2 treated positive control samples (figure 4.8), there were 10 proteins significantly associated with ERα in the presence of E2, and 10 proteins significantly associated with ERα in the absence of E2. Neither HECTD4 or WIZ were found in the ER IP samples.

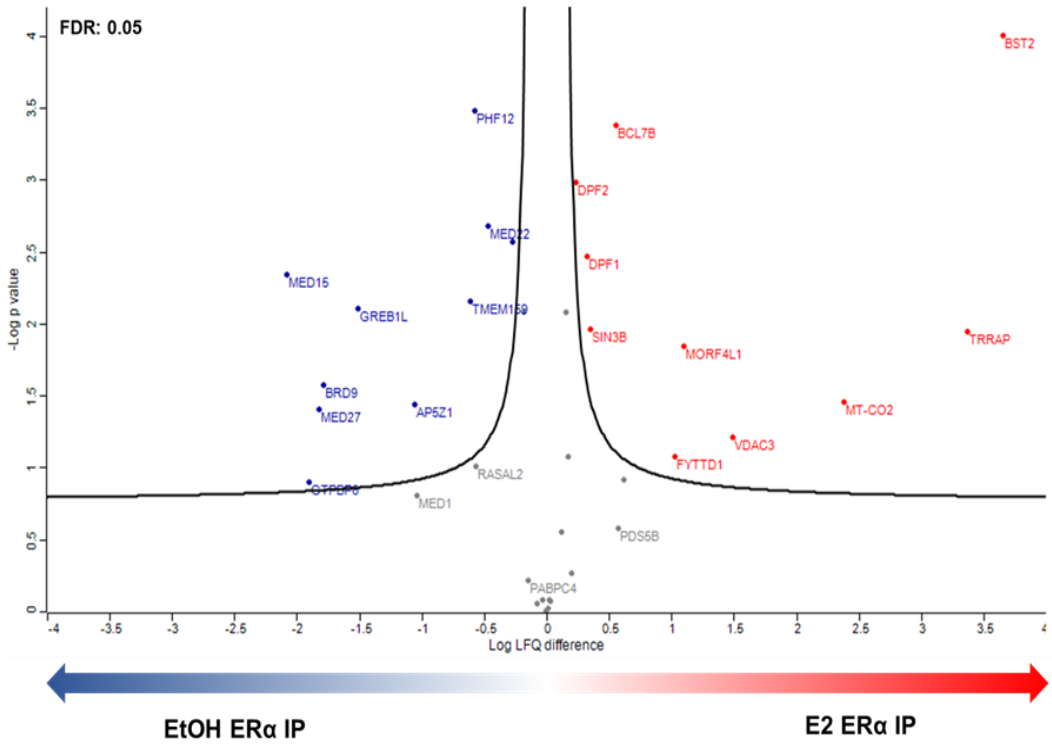

Figure 4.8. Volcano plot of identified proteins in ERα immunoprecipitation samples +/- 1 nm E2 treatment (D-12 antibody).

A two-sided t-test was used to represent proteins significantly associated with ER in the presence/absence of E2. A false-discovery-rate (FDR) of 5% was applied to this test, and the log fold change was kept at the default value of 0.1

4.2.3 Hierarchical clustering, principal component analysis (PCA) and volcano plot generation of data from ERα F-10 immunoprecipitation

The next aspect of this study involved the use of a second, independent antibody raised against ERα. Antibody concentration, as well as protein quantity, was kept consistent between antibodies. Data generated for this antibody was treated the same as explained in section 4.2.2. Different colours are used to represent the different antibody (Purple = low LFQ score, Orange = high LFQ score). For volcano plots, proteins significant in the vehicle treated cells were highlighted purple, and proteins significant in the treated cells (DOX or E2) were highlighted orange. Proteins that did not reach statistical significance were highlighted grey.

First, PCA and hierarchical clustering was performed on cells expressing CART vs not expressing CART. As demonstrated in figure 4.9, replicates for each sample group together, and importantly, each treatment group clusters together.

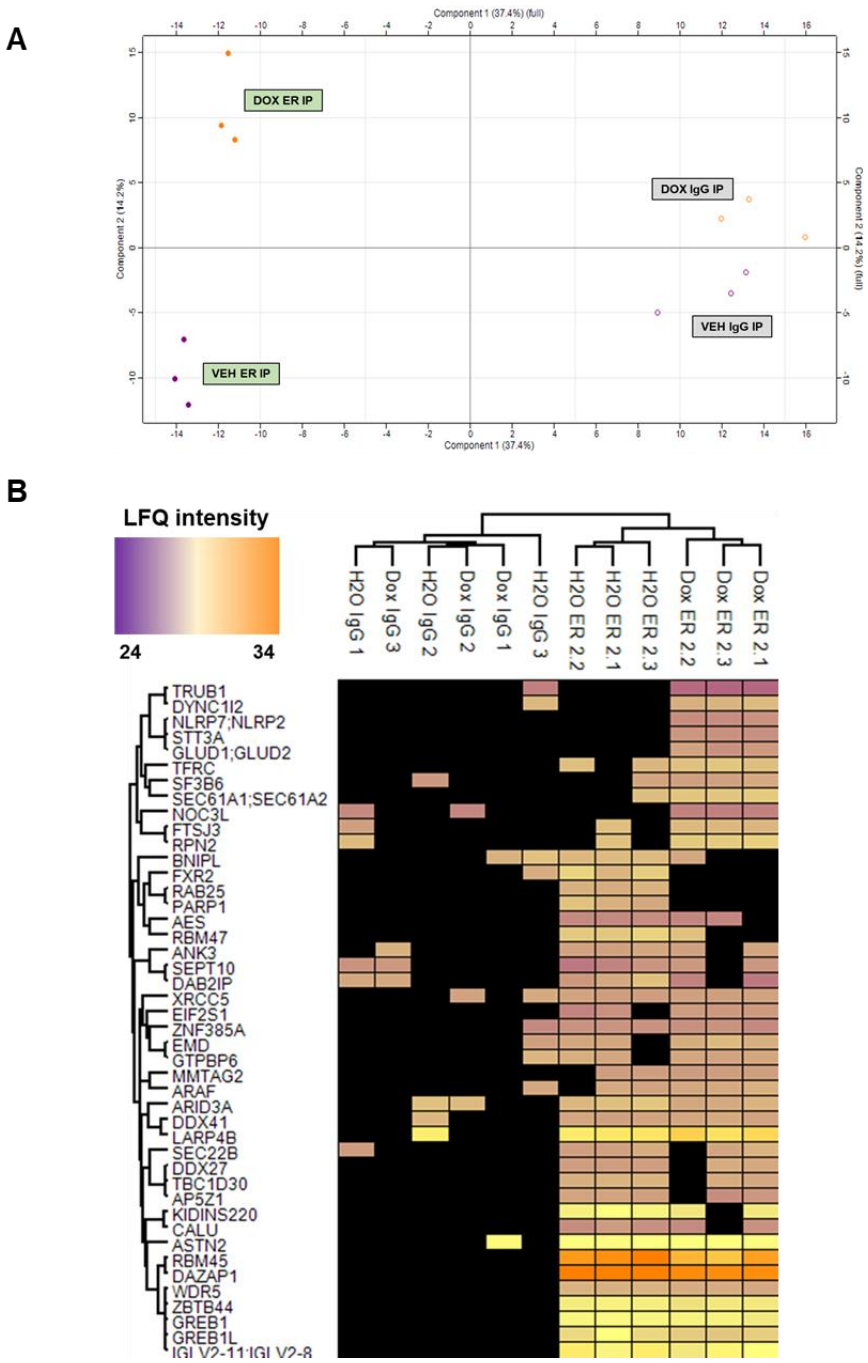

Figure 4.9. Principal component analysis and hierarchical clustering of samples +/- CART expression (F-10 antibody)

A. PCA plot demonstrates treatment groups cluster separately from one-another. **B.** Hierarchical clustering further demonstrates that treatment groups form distinct clusters. Label free quantification (LFQ) intensities ranging from 24 (modestly detected) to 34 (abundantly detected) for each identified protein is represented on this heatmap. Black area of the plot represents proteins not identified.

In figure 4.10, we identified 9 proteins significantly associated with ERα in the presence of CART (such as NLRP7 and NOC3L), and 9 proteins significantly associated with ERα in the absence of CART (such as PARP1 and RAB25).

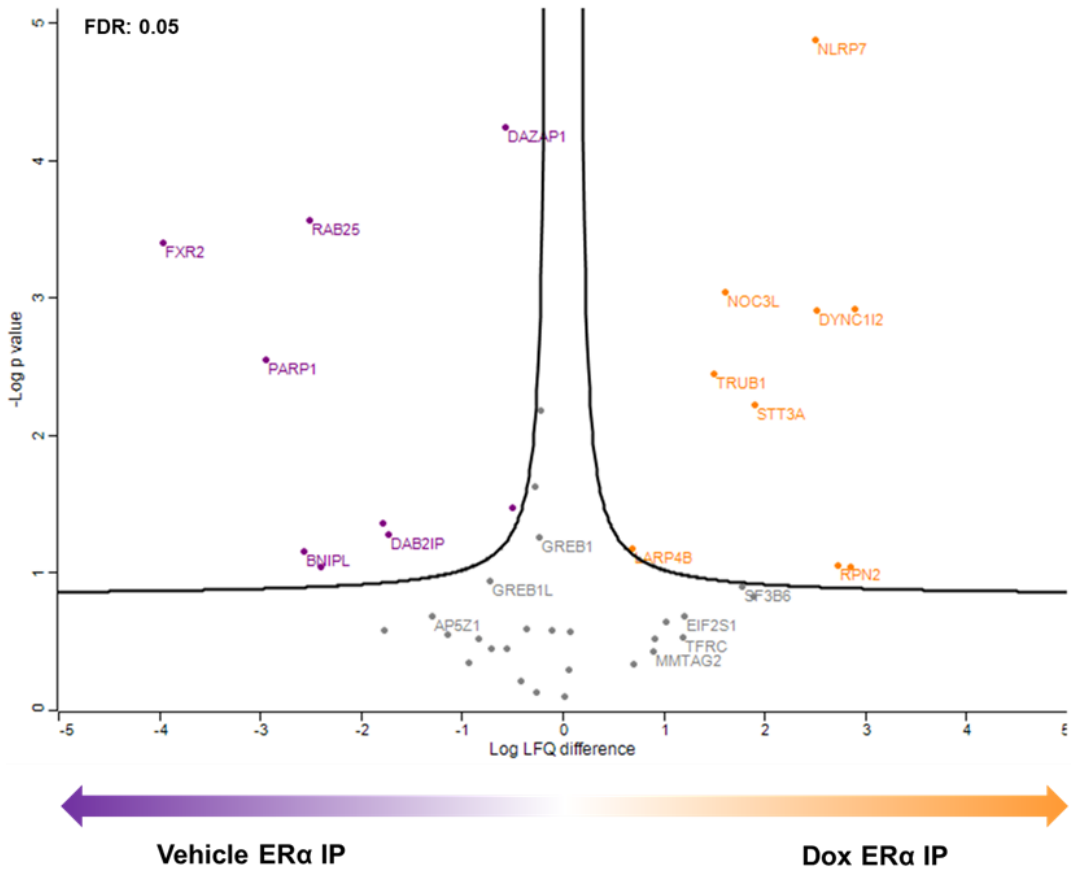

Figure 4.10. Volcano plot of identified proteins in ERα immunoprecipitation samples +/- CART expression (F-10 antibody).

A two-sided t-test was used to represent proteins significantly associated with ER in the presence/absence of CART. A false-discovery-rate (FDR) of 5% was applied to this test, and the log fold change was kept at the default value of 0.1.

Next, we show PCA and the generated LFQ heatmap for ERα IP samples +/- E2 (F-10 antibody). As demonstrated in figure 4.11, replicates for each sample group together, and each treatment groups clusters together.

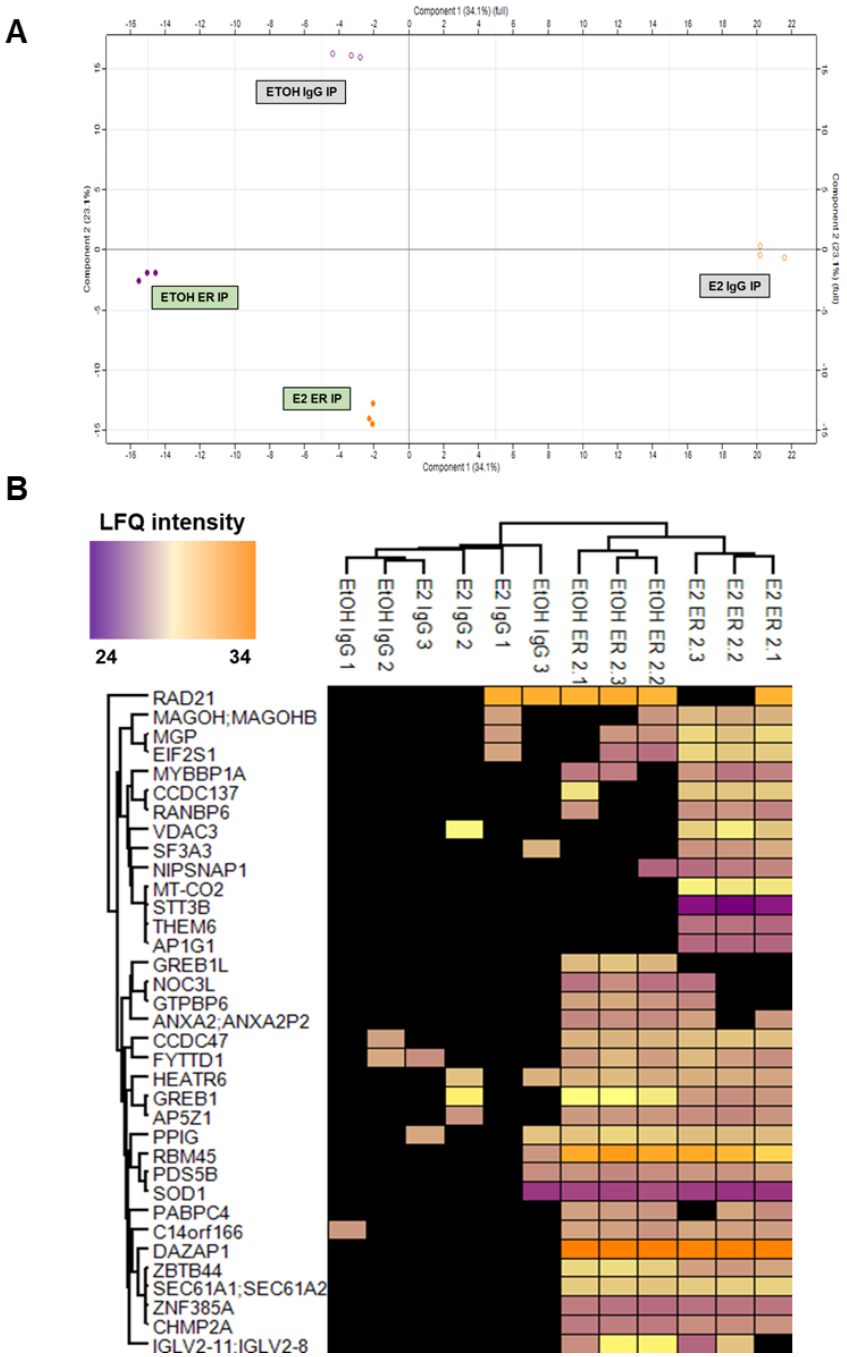

Figure 4.11. Principal component analysis and hierarchical clustering of samples +/- 1 nm E2 treatment (F-10 antibody).

A. PCA plot demonstrates treatment groups cluster separately from one-another. **B.** Hierarchical clustering further demonstrates that treatment groups form distinct clusters. Label free quantification (LFQ) intensities ranging from 24 (modestly detected) to 34 (abundantly detected) for each identified protein is represented on this heatmap. Black area of the plot represents proteins not identified.

As demonstrated in figure 4.12, we identified 10 proteins significantly associated with ERα in the presence and absence of estradiol.

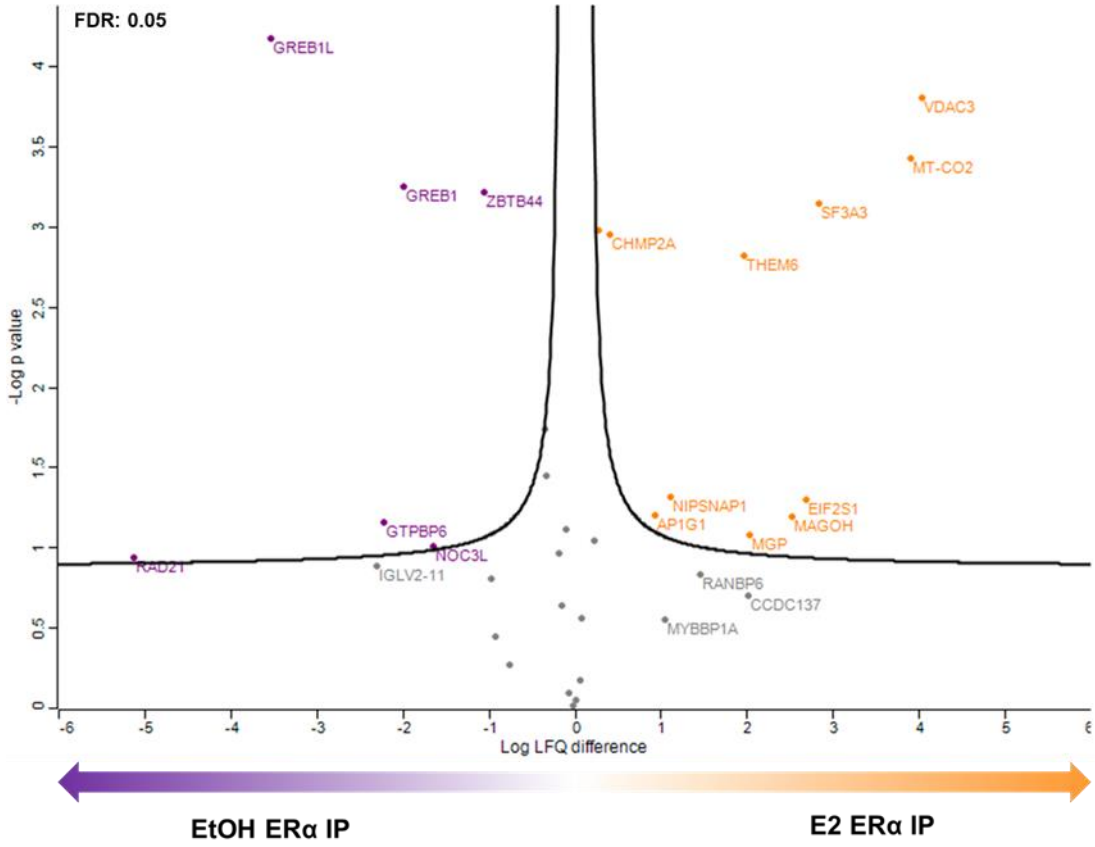

Figure 4.12. Volcano plot of identified proteins in ERα immunoprecipitation samples +/- 1 nm E2 treatment (F-10 antibody).

Eleven proteins were significantly associated with ER in the presence of E2, and six in the absence. A false-discovery-rate (FDR) of 5% was applied to this test, and the log fold change was kept at the default value of 0.1.

4.2.4 Comparing common interactors between ERα IP samples using both D-12 and F-10 antibodies

As mentioned previously, a goal of this study was to use two independent antibodies raised against ERα to investigate what proteins are common to both antibodies. The main goal of this approach was to identify robust interactors, whose interaction with ERα is modulated by CART. The D-12 antibody (sc-8005) is raised against the N-terminus of ERα, and the F-10 antibody (sc-8002) is raised against the C-terminus of ERα. Both antibodies had previously been used in an impressive landmark study of the human endogenous coregulator complexome (Malovannaya et al., 2011).

First, all interactors in the ERα D-12 antibody (117 in total) were compared to the interactor list from the ERα F-10 antibody (44 in total). In total, 22 proteins were found to be common to both antibodies. We identified several well-characterized ERα interactors common to both antibodies, including GREB1 (Mohammed et al., 2013), GREB1L (Mohammed et al., 2013) and PARP1 (Zhang et al., 2013). A plot was created in which the LFQ difference of each protein from the D-12 antibody was plotted against the LFQ difference identified in the F-10 antibody (figure 4.13). Only 5 proteins were found to follow the same trend across both antibodies (ANK3, AP5Z1, RAB25, SEC22B and TBC1D30), and these were only found to be associated with ERα in the absence of CART.

None of these proteins were determined to be significant in either volcano plot generated in figure 4.6 and 4.10. For example, AP5Z1 and TBC1D30 were identified as significantly enriched in the H_2O ERα IP samples from the D-12 antibody (figure 4.6), but not in the H_2O ERα IP samples from the F-10 antibody (figure 4.10).

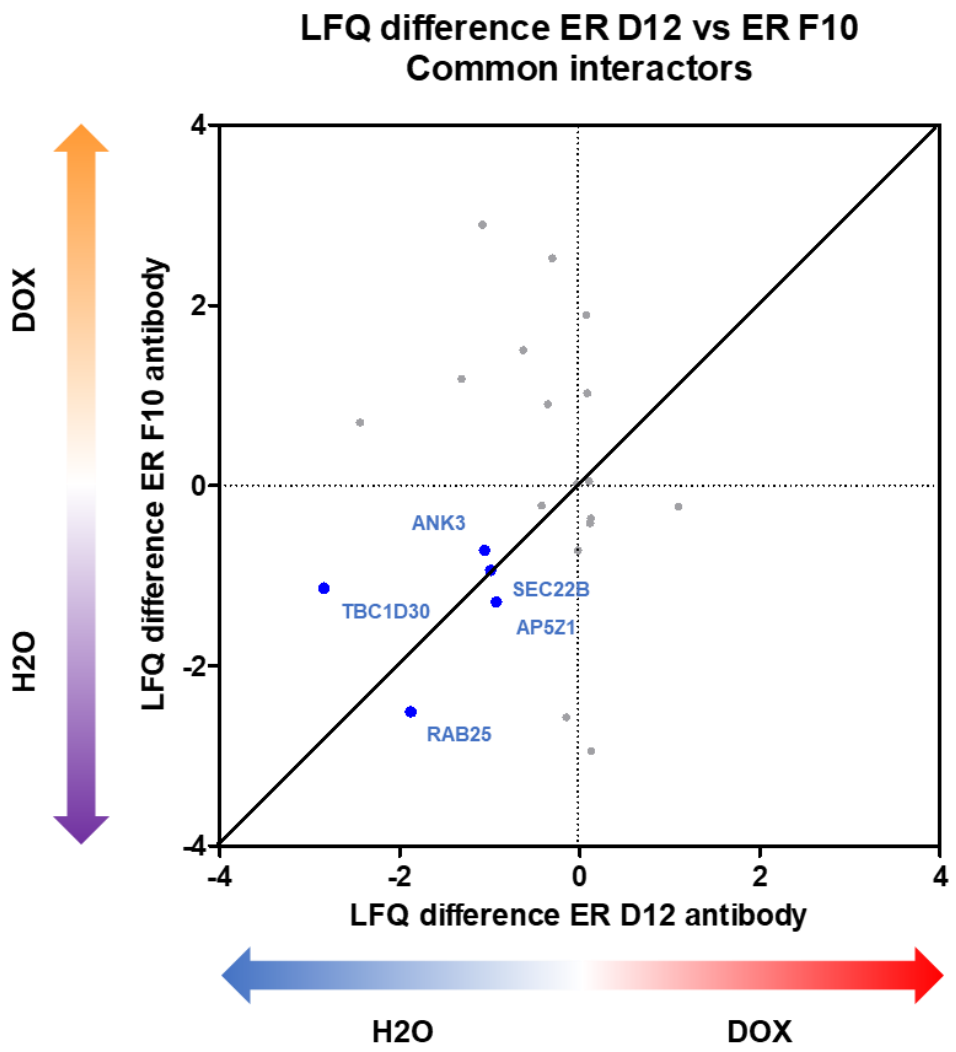

Figure 4.13. There are no common interactors recruited to ERα by CART. Label-free quantification (LFQ) difference for proteins common to each antibody were plotted. In total, there were 22 proteins common to both antibodies following removal of the IgG samples.

Since no robust trends were identified when comparing the D-12 and F-10 antibodies, we decided to focus our efforts on interacting proteins from one of the antibodies rather than both. Concern was initially raised following western blot analysis of beads sent for mass spectrometry analysis (figure 4.4), as lanes which had been immunoprecipitated using the ERα F-10 antibody appeared to have significantly more non-specific binding compared to the lanes of the ERα D-12 antibody.

To understand this, we performed PCA on all samples which were sent for mass spectrometry analysis (figure 4.14). On this plot, it was clear that the F-10 antibody grouped much closer to the non-specific mouse IgG antibody across all samples.

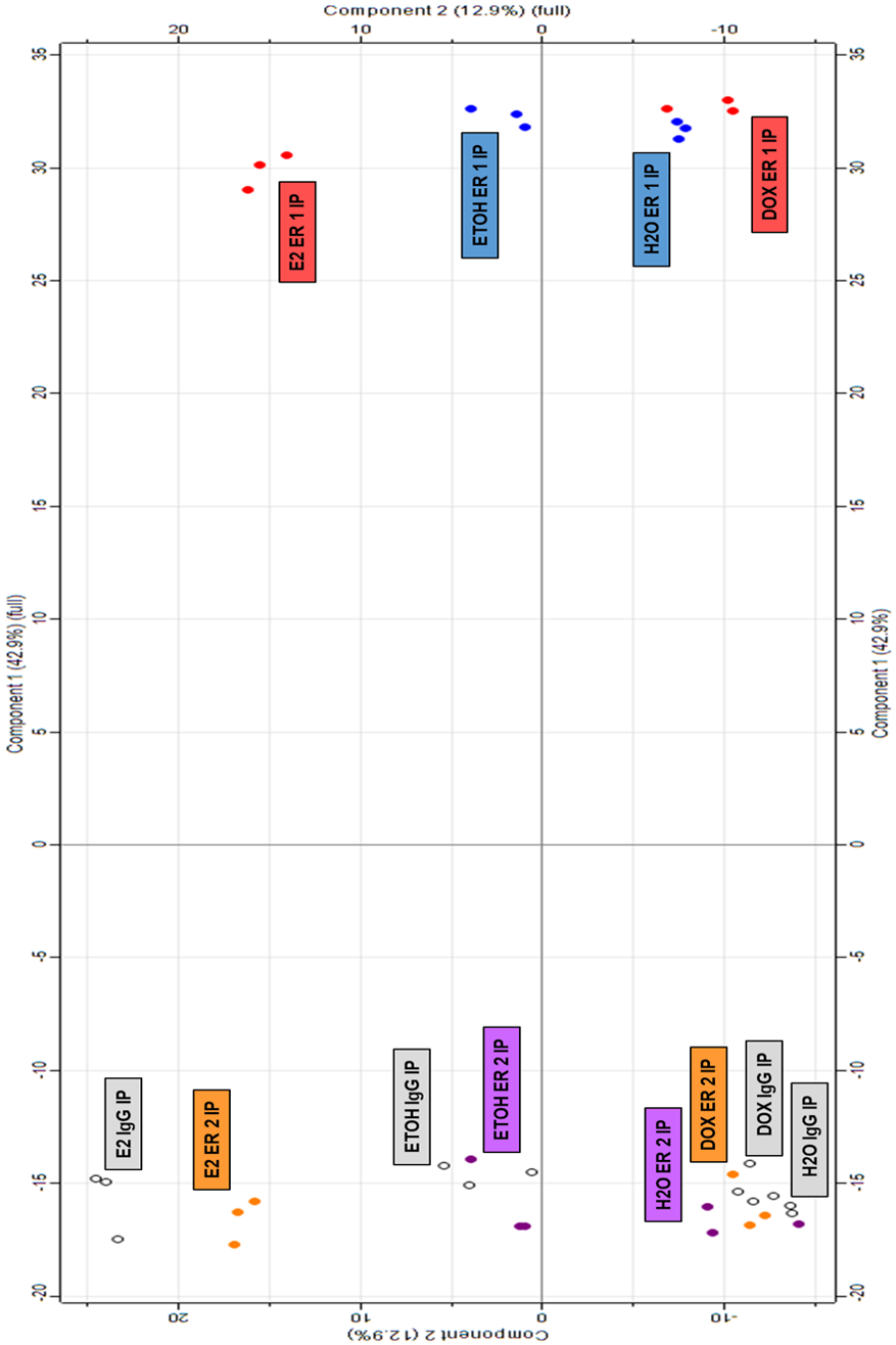

Figure 4.14. Principal component analysis (PCA) shows samples from F-10 antibody group closer with the IgG negative control samples than the D-12 antibody.

In addition to this, all interactors identified from both antibodies were uploaded to the STRING database (string.db.org) to test whether any of these had previously been shown to interact with ERα. Only interactions with supporting experimental data were considered. ERα was found to interact with 11 proteins from the D12 antibody list (ARID1A, CCNC, GREB1, GNB1, MED1, PARP1, RAF1, SKP1, SMARCD1, WDR5 and XRCC5), but only 4 proteins (GREB1, PARP1, WDR5 and XRCC5) from the F-10 antibody list.

Based on the aforementioned observations, we chose to focus solely on the data generated from the ERα D-12 antibody.

4.2.5 Using PANTHER to assign protein class to identified interactors in the presence/absence of CART

As shown in figure 4.6, we identified 14 proteins significantly associated with ERα in the presence of CART, and 21 proteins significantly associated with ERα in the absence of CART.

In the presence of CART (figure 4.15), it was determined that most of the identified proteins fall into the “nucleic acid binding” or “transcription factor” protein classes, while in the absence of CART (figure 4.16), many more protein classes, such as “Transporters”, “Transfer/carrier protein” and “enzyme modulator” were found. Taken together, these data may suggest that, in the presence of CART, ERα interacts with proteins linked to transcriptional regulation, whereas in the absence of CART, many of the interacting proteins are involved in processes independent of transcriptional regulation.

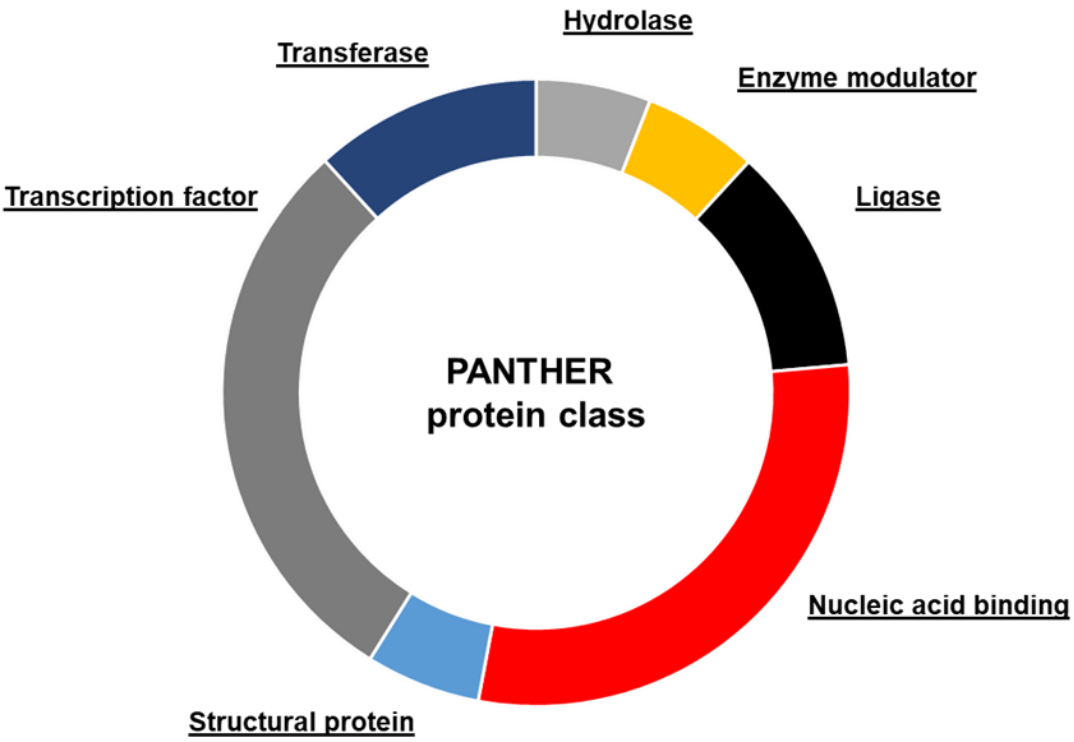

Protein class	Protein ID
Enzyme modulator	RASAL2
Hydrolase	SIN3B
Ligase	HECTD4, PHF12
Nucleic acid binding	DPF2, PHF10, SIN3B, SS18, SMARCD1
Structural protein	FAM179B
Transcription factor	DPF2, PHF10, PHF12, SIN3B, WIZ
Transferase	DPF2, PHF10

Figure 4.15. Proteins significantly recruited to ERα in the presence of CART are members of the "nucleic-acid binding" and "transcription factor" protein classes.

The list of proteins identified from mass spectrometry analysis were uploaded to PANTHER in order to assign a protein class to each target.

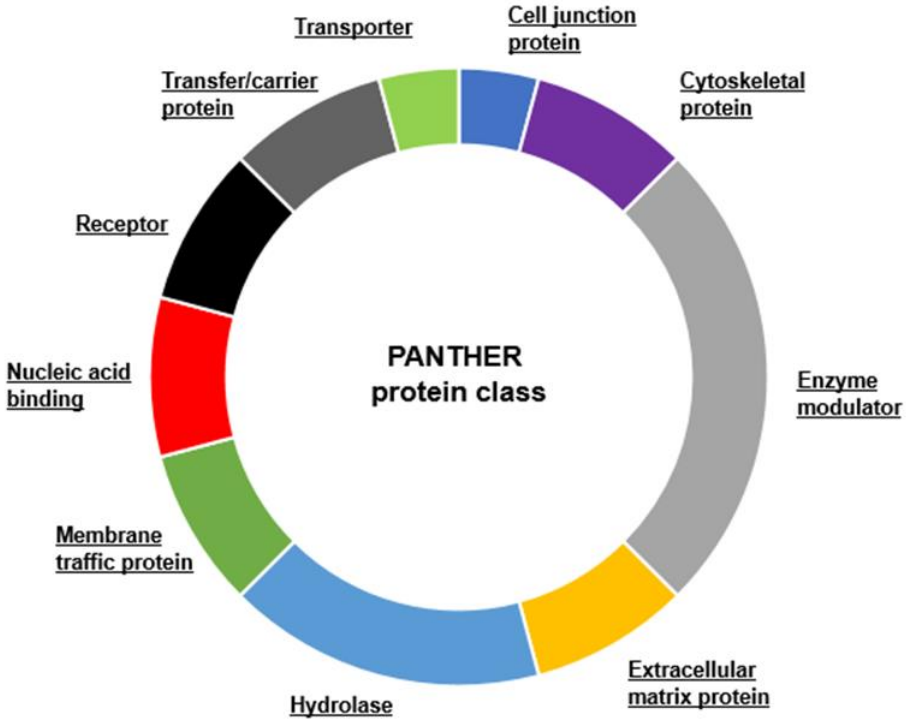

Protein class	Protein ID
Cell junction protein	**MYO1B**
Cytoskeletal protein	**MYO1B, DYNC1/2**
Enzyme modulator	**ARHGAP27, GNB1, GNB2, GNB4, MYO1B, TBC1D30**
Extracellular matrix protein	**AP1M1/AP1M2**
Hydrolase	**GNB1, GNB2, GNB4, TBC1D30**
Membrane traffic protein	**TMED7/TMED7-TICAM2**
Nucleic acid binding	**GAR1, RAE1**
Receptor	**AP1M1/AP1M2**
Transfer/carrier protein	**TMED7/TMED7-TICAM2**
Transporter	**NUP88**

Figure 4.16. Proteins significantly recruited to ERα in the absence of CART are associated with protein transport/trafficking.

The list of proteins identified from mass spectrometry analysis were uploaded to PANTHER in order to assign a protein class to each target.

4.2.6 The STRING interaction database shows previously reported interactions between ERα and proteins identified via mass spectrometry.

Understanding whether any proteins identified from the mass spectrometry experiment had previously been shown to interact with ERα was a key objective within this study. Proteins that were deemed significant from the volcano plots, as well as any proteins which were > 1.5 LFQ values to the opposing treatment condition were uploaded to STRING. The confidence threshold for all experiments was set to low (0.150), as maps showing the strength of the evidence to support the interaction were also generated and added to each figure (for example, figure 4.17). Co-expression, databases, experiments and textmining were selected as active interaction sources. Table 4.1 details what colour is used to represent each interaction source.

Table 4.1. Selectable interaction sources, and the representative colour for each source.

Known interactions	
From curated databases	**Experimentally determined**
Light blue	Pink

Predicted interactors		
Gene neighbourhood	**Gene fusions**	**Gene co-occurrence**
Green	Red	Blue

Others		
Text mining	**Co-expression**	**Homology**
Yellow	Black	Purple

This search highlighted 4 proteins which had previously been experimentally proven as an interactor of ERα (figure 4.17). SMARCD1 & ARID1A, both members of the BAF chromatin remodelling complex, were identified as

experimentally proven interactors of ERα (Hsiao et al., 2003) (Flajollet et al., 2007). Moreover, ERα had also been shown to interact with SKP1 (Zhou et al., Oncogene 2014), a protein which makes up part of the SCF ubiquitin ligase complex, and SIN3B (Zhu et al., 2006), a chromatin binding protein involved in transcriptional repression. As shown in figure 4.17 B, the strength of the data supporting the interaction between ERα and ARID1A, SMARCD1 and SKP1 is noticeably stronger than the data supporting the interaction between ERα and SIN3B.

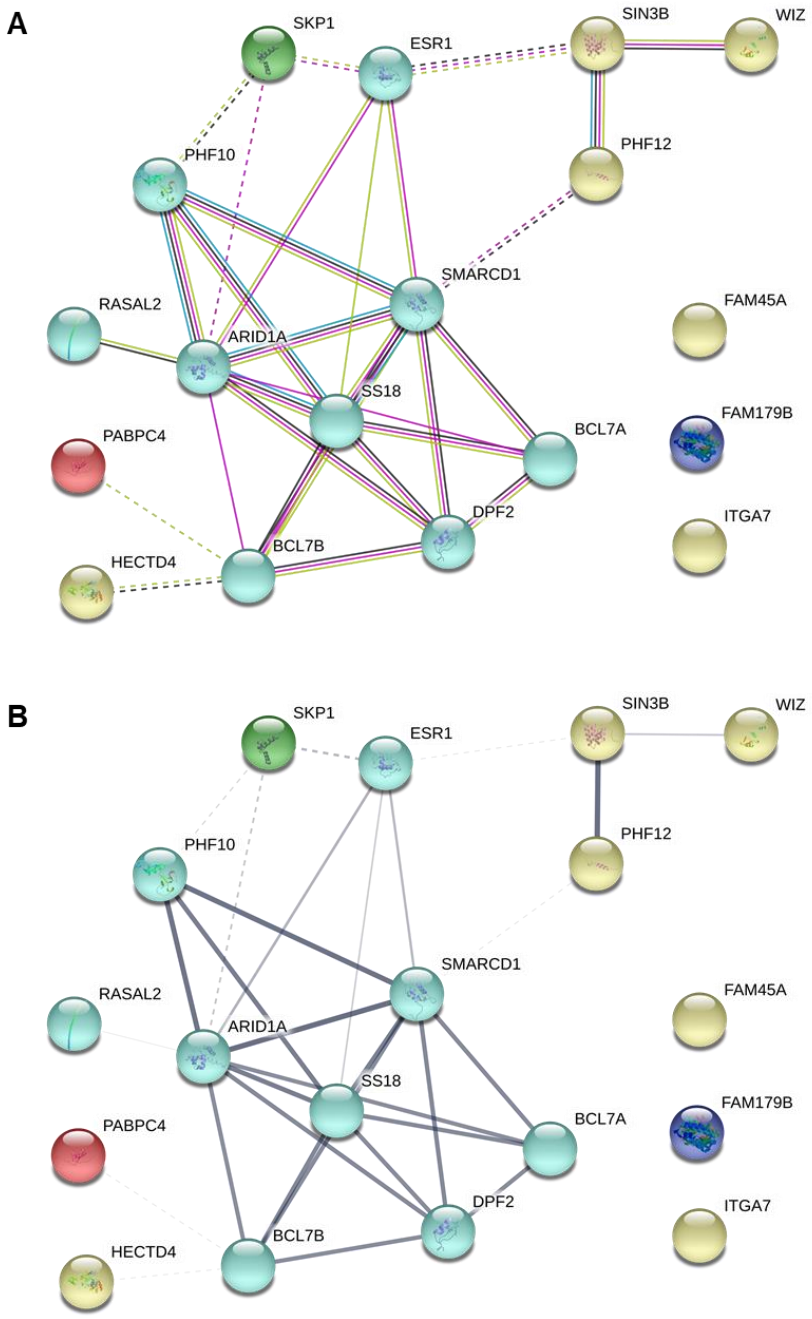

Figure 4.17. STRING diagram shows a previously reported interaction between ERα, ARID1A, SIN3B, SKP1 and SMARCD1.

A. Four proteins associated with ERα in the presence of CART have previously been shown to interact with ERα. Network lines within A indicate the type of interaction evidence. **B.** Network line thickness represents the strength of the data supporting the identified interaction. PPI enrichment p-value = 9.97 e-11

4.2.7 Using STRING to understand whether WIZ and HECTD4 are direct interactors of ERα

As mentioned in section 4.2.6, most of the proteins significantly associated with ERα in the presence of CART are known members of the BAF-chromatin remodelling complex (ARID1A, SMARCD1, SS18 for example). There were two proteins which had not previously been shown to interact with ERα, HECTD4, a poorly understood E3-ligase, and WIZ (Widely Interspaced Zinc-finger motifs), a protein understood to bind DNA and mediate protein-protein interactions with the G9a histone methyltransferase complex (Isbel et al., 2016). In order to try understand whether these proteins were true-novel ERα interactors or not, the STRING search was first expanded to allow "no-more than 10 additional interactors through from the database (figures 4.18 and 4.19).

As demonstrated from figure 4.18, existing experimental evidence supports an interaction between HECTD4 and SMARCC2 (Dilworth et al., 2005), a member of the BAF chromatin remodelling complex, as well as CUL1 (Mathew et al., 2012), a core subunit of the SCF ubiquitin ligase complex. In figure 4.19, we highlight that the strength of the data supporting HECTD4's interaction with CUL1 and SMARCC2 is poor. Intriguingly, however, there is strong experimental data in agreeance with an interaction with ESR1, SKP1 and CUL1. This suggests that HECTD4 may interact with ERα through the SCF ubiquitin ligase complex, but it is also entirely possibly that HECTD4 is a novel, CART driven, ERα interactor.

Figure 4.18 highlights that WIZ may interact with SIN3B (Bantscheff et al., 2011). As demonstrated in figure 4.19, the confidence of the data supporting the interaction between WIZ and SIN3B is reasonably strong. Furthermore, as demonstrated in figure 4.17 and 4.18, there is evidence supporting an interaction between SIN3B and SMARCA4 (Pal et al., 2003) as well as between SIN3B and ERα (Zhu et al., 2006). Taken together, we hypothesize that CART plausibly drives cooperation between WIZ and ERα, which is mediated through SIN3B and members of the BAF chromatin remodelling complex.

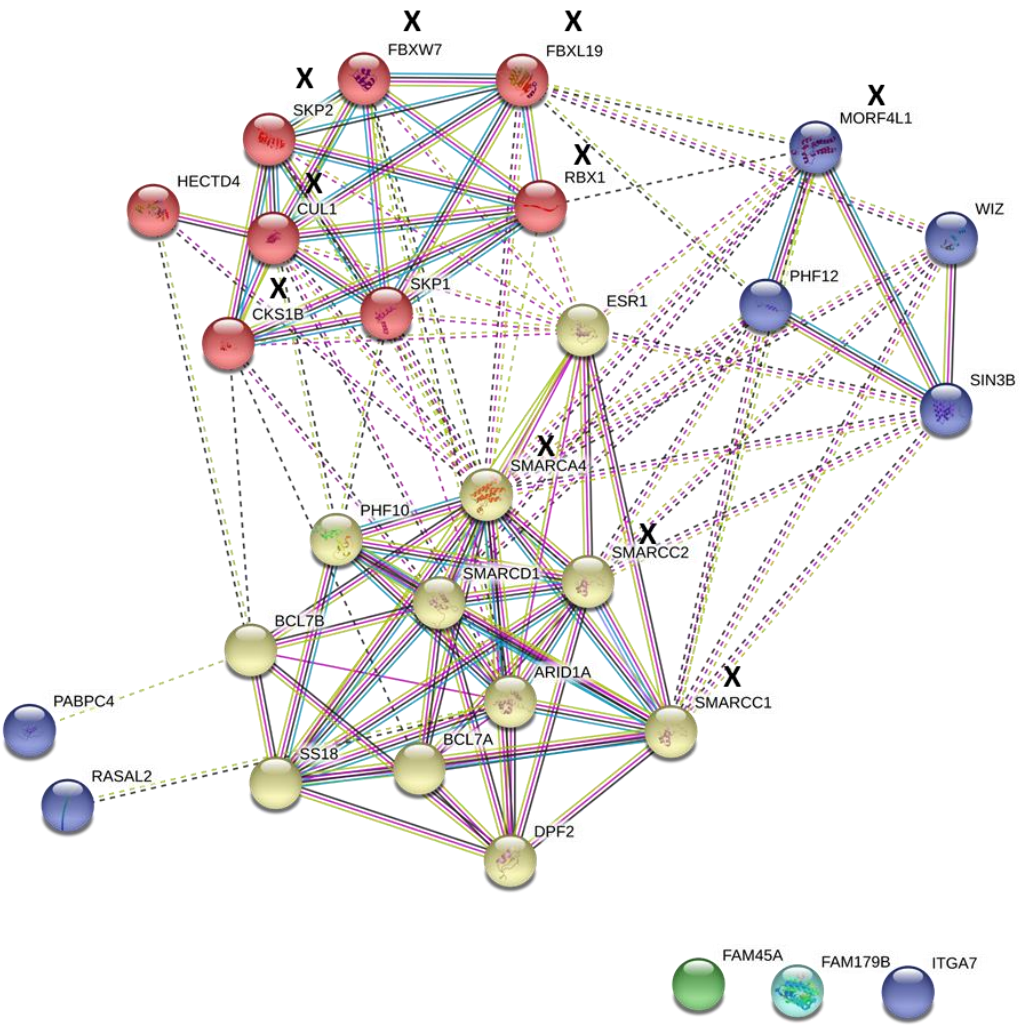

Figure 4.18. HECTD4 and WIZ may be indirect interactors of ERα.

Using STRING, it is suggested that HECTD4 may interact with ERα through the SCF ubiquitin ligase complex, and WIZ may interact with ERα through SIN3B. Clusters were defined by K-means processing of 5 possible clusters. Proteins marked with X are targets which STRING added to the search.

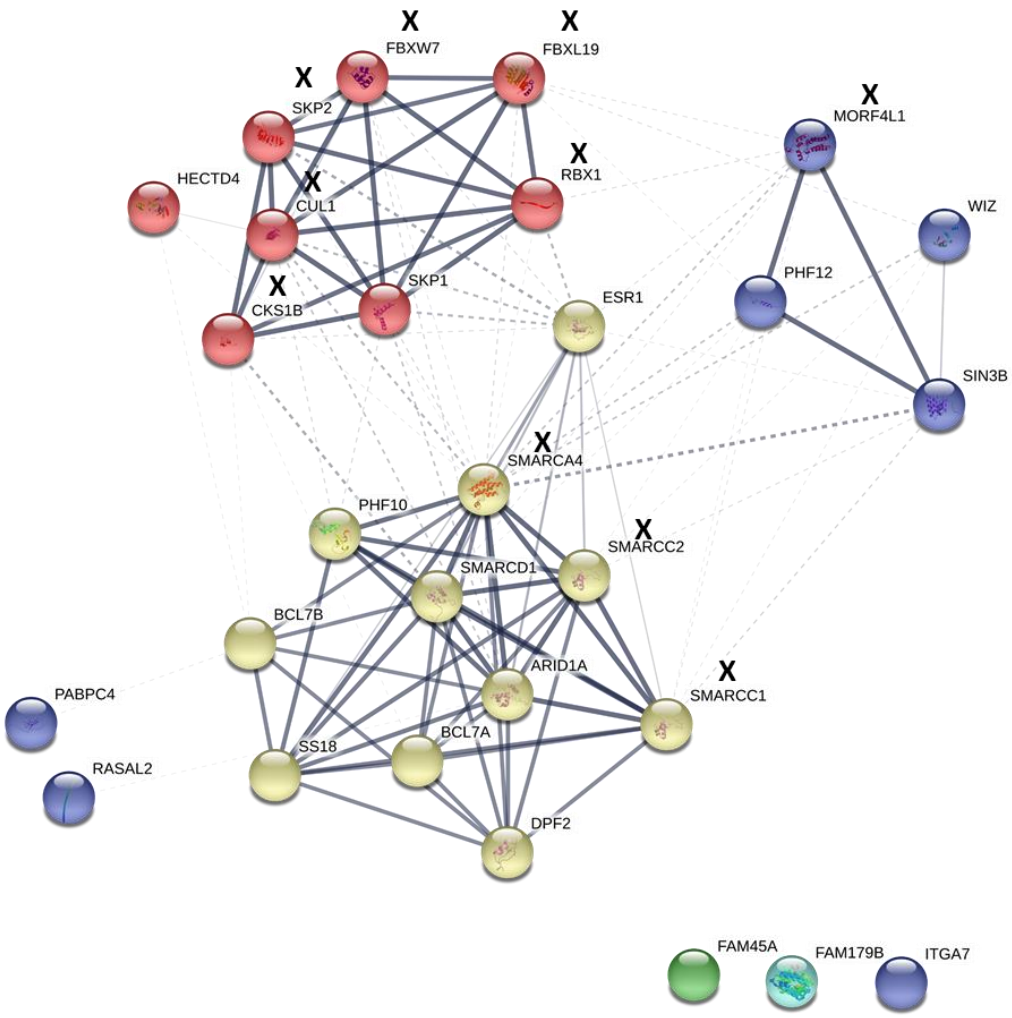

Figure 4.19. Confidence of the supporting data from figure 4.18.

Based on data confidence, it is possible CART drives an interaction between ERα and WIZ, mediated through SIN3B and members of the BAF complex. The data supporting an indirect interaction between HECTD4 and ERα through the SCF ubiquitin ligase complex is poor, suggesting this interaction between HECTD4 and ERα may be a novel interaction driven by CART. Clusters were defined by K-means processing of 5 possible clusters. Proteins marked with X are targets which STRING added to the search.

4.2.8 Attempted validation of interaction between ERα, HECTD4 and WIZ

Both HECTD4 and WIZ were the top differentially recruited ERα interactors in the presence of CART. In order to confirm whether these proteins were indeed

interactors of ERα following CART expression, Co-Immunoprecipitation assays were performed, in which ERα was immunoprecipitated, and western blot analysis was used to investigate whether HECTD4 or WIZ was co-immunoprecipitated with ERα. In figure 4.20, we show that while a band for WIZ is indeed detected following ER IP in the presence of CART, a similar band is seen in the non-specific IgG control. This result makes it impossible to definitively conclude whether WIZ is indeed an ERα interactor or not. Further, as shown in figure 4.20, HECTD4 was not detected in the input lanes (predicted molecular weight: 440 kDa), or the ERα IP lanes, again hindering our abilities in concluding whether HECTD4 interacts with ERα or not.

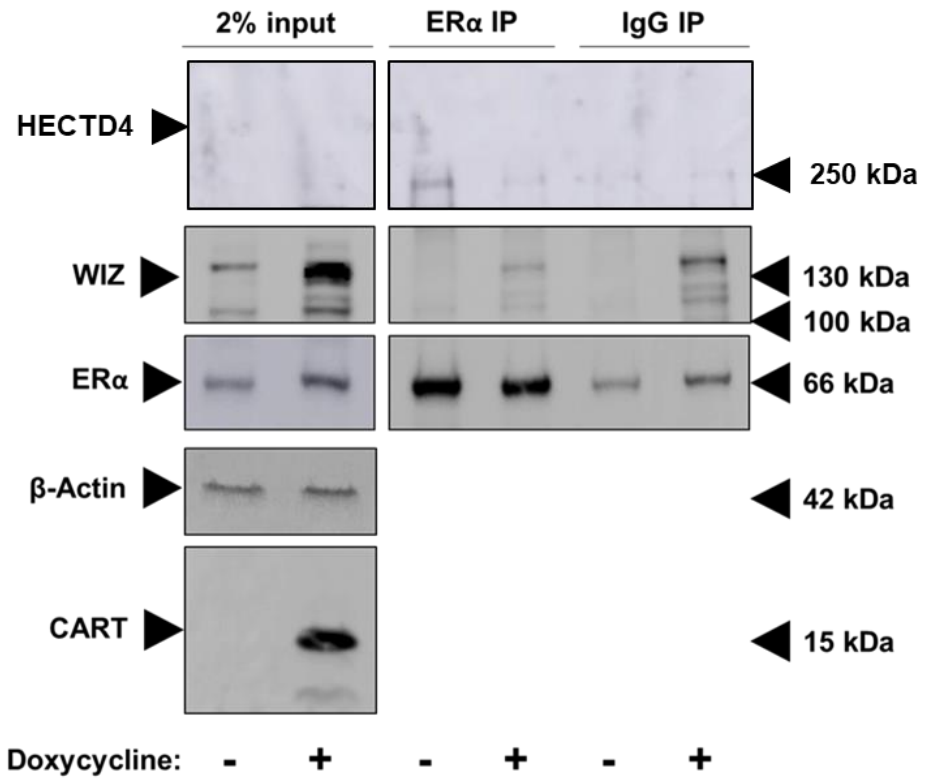

Figure 4.20. Unsuccessful validation of an interaction between ERα, HECTD4 and WIZ.

Following immunoprecipitation of ERα, western blot was used to confirm if either HECTD4, or WIZ, was co-immunoprecipitated with ERα. Western blot analysis was also used to highlight cells that received dox were expressing CART. Actin was used as a loading control.

4.2.9 Investigating the impact CART has on the turnover of ERα

While much of our work has concentrated on the effect CART has on the activity of ERα, the possibility of CART affecting the turnover of ERα remains to be explored further. It is difficult to infer a potential reason why WIZ may interact with ERα, however, the presence of HECTD4 in our mass spectrometry experiments was the first indicator that CART expression may result in altered turnover of ERα. HECTD4 is an E3 ligase, meaning that is possess the ability to transfer ubiquitin moieties from E2 ligases to target proteins (Dwane et al., 2017). This ubiquitin transfer (be it mono or polyubiquitin chains) can have significant functional consequences on the target protein, ranging from proteolysis to transcriptional regulation (Dwane et al., 2017).

To investigate whether CART altered the turnover of ERα, an experiment was established in which cells were treated with the eukaryotic transcriptional inhibitor cycloheximide (CHX). The experiment was performed under 4 conditions, -CART/-E2, -CART/+E2, +CART/-E2 and +CART/+E2. No difference was noticed in the presence of E2, however, as demonstrated in figure 4.22, the expression of CART resulted in the increased stability of ERα in the absence of E2. We noticed that levels of ERα were maintained at higher levels even in the absence of CHX (figure 4.21). This made it difficult to conclusively determine if CART expression increases the stability of ERα. To account for this increased expression of ERα, the levels of ERα in the CHX treated cells were normalised to the levels of ERα in the CHX vehicle (DMSO) treated cells. Surprisingly, we noticed that levels of ERα were maintained longer in cells expressing CART vs cells not expressing CART (figure 4.23). These data would suggest that CART expression potentially results in the decreased turnover of ERα.

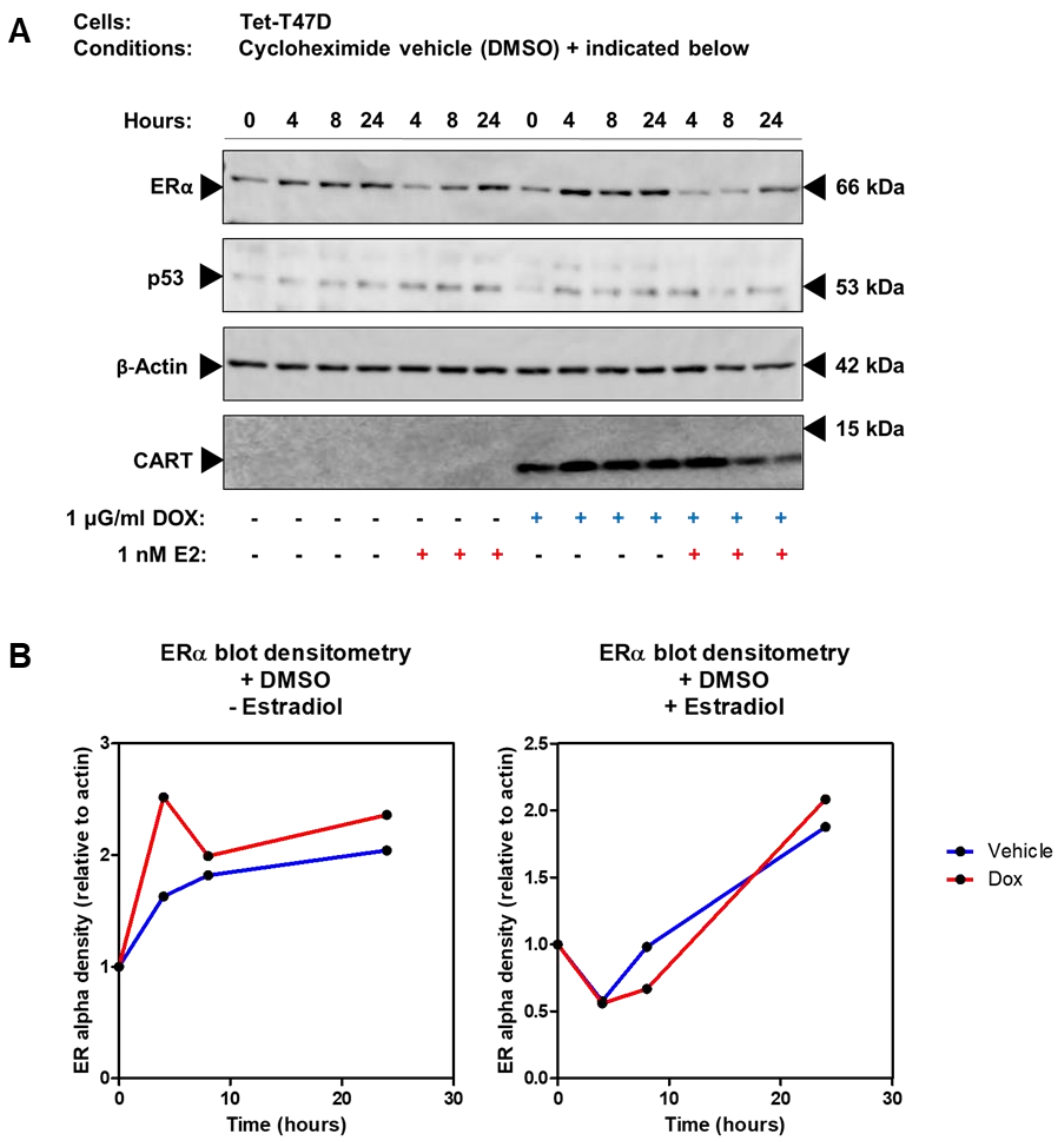

Figure 4.21. ERα alpha levels are maintained at higher levels when cells are expressing CART.

A. Western blot analysis of ERα levels over 24-hour treatment time with cycloheximide vehicle (DMSO). The tumour suppressor protein p53 was used as a positive control for CHX treatment due to the short half-life of this protein. **B.** Densitometry analysis of ERα levels relative to actin.

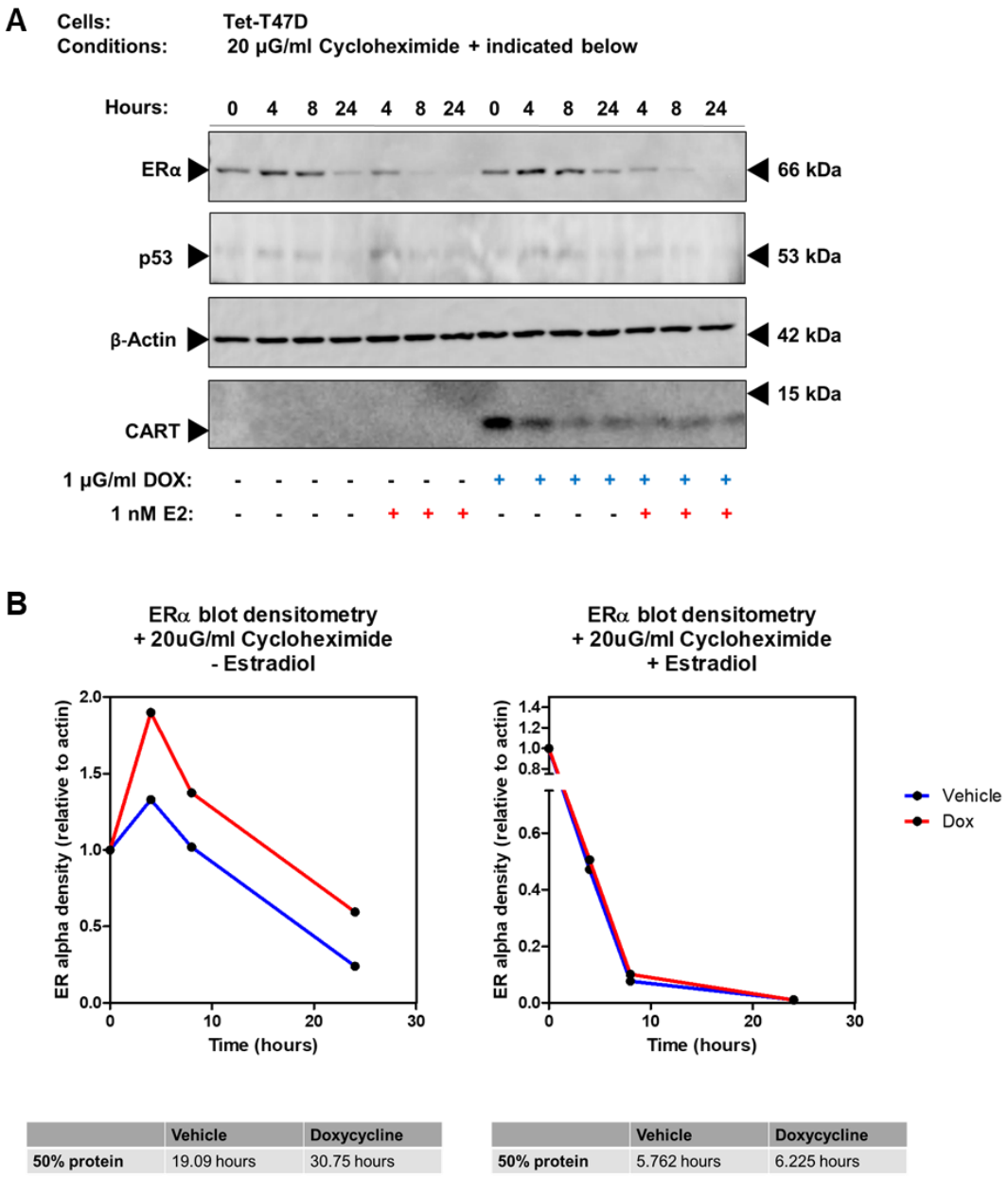

Figure 4.22. CART expression results in the decreased turnover of ERα.

A. Western blot analysis demonstrates higher levels of ERα when cells are expressing CART vs when cells are not expressing CART in the presence of CHX. **B.** Densitometry analysis of ERα levels relative to actin.

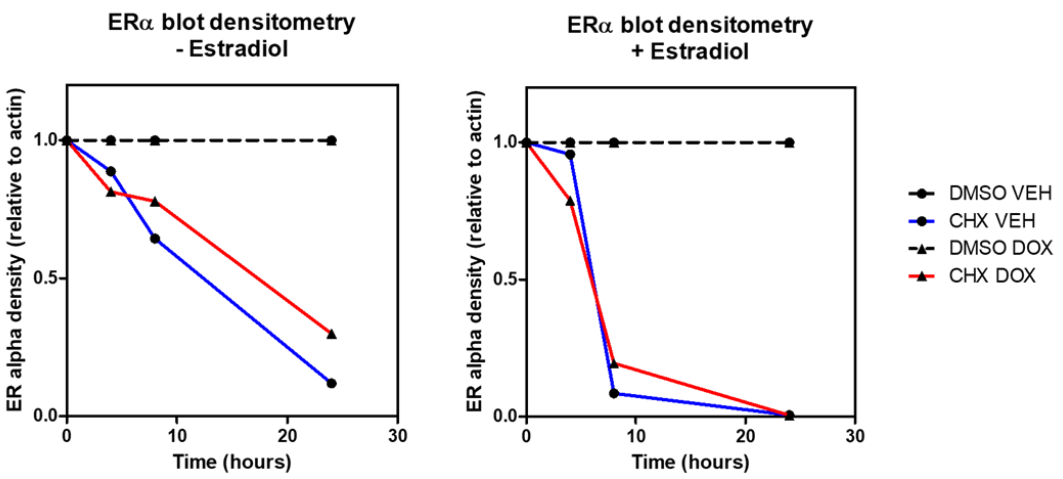

	Vehicle	Doxycycline
50% protein	13.395 hours	16.914 hours

	Vehicle	Doxycycline
50% protein	9.288 hours	8.928 hours

Figure 4.23. ERα levels in CHX treated cells were normalised to ERα levels in DMSO treated cells, and an increase in stability of ERα was still observed in the absence of estradiol.

ERα levels in the CHX treated experiment were normalised to the DMSO vehicle experiment, and relative density was plotted.

4.2.9 Validation of the interaction between SMARCD1 and ERα

We initially identified multiple members of the BAF-chromatin remodelling complex to be recruited to ERα following CART expression. Our PANTHER analysis identified SMARCD1 to be involved in nucleic acid binding (figure 4.15), and data generated from the STRING database (Figure 4.17) confirmed a previously reported interaction between ERα and SMARCD1 (Hsiao et al., 2003). This study suggested that SMARCD1 was a critical mediator of nuclear receptor function, and so we hypothesized that CART may be driving an interaction between SMARCD1 and ERα to facilitate transcriptional regulation. One of the major goals of this study was to identify proteins that may be controlling ERα function, and whether we could modulate the expression of these proteins to prevent this. We therefore validated the interaction between SMARCD1 and ERα (figure 4.24). Importantly, densitometry analysis did not highlight an increased immunoprecipitation of ERα, which proved that SMARCD1 was an interactor of ERα, and the expression of CART results in a recruitment of SMARCD1 to ERα.

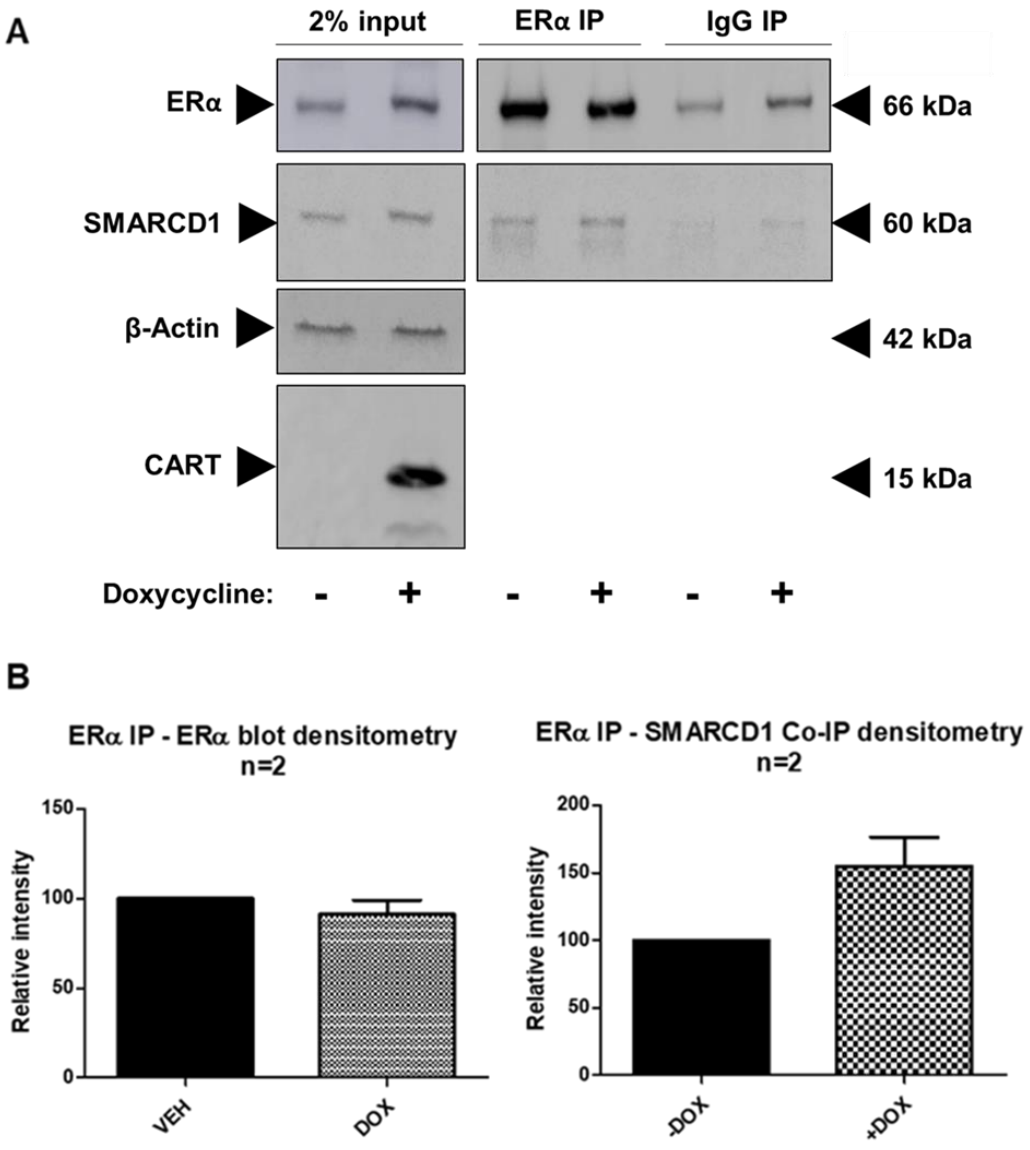

Figure 4.24. Co-immunoprecipitation validation of interaction between SMARCD1 and ERα.

A. Following ERα immunoprecipitation, western blot was used to confirm successful ERα immunoprecipitation, as well as successful SMARCD1 co-immunoprecipitation. Western blot analysis was also used to highlight cells that received dox were expressing CART. Actin was used as a loading control. **B.** Densitometry was performed on imageJ to assess the levels of SMARCD1 and ER in cells expressing CART (+DOX) and cells not expressing CART (-DOX). Mean +/- S.E.M. between 2 independent experiments is plotted. Figure A is representative of 2 independent experiments.

4.3 Discussion

4.3.1 LXD motifs within CART do not allow for an interaction between ERα and CART

As discussed in section 3.3, we found a significant decrease in CART-driven ERα activity following ectopic expression of a CART plasmid with LXD-motif 1 mutated. This suggested that LXD motifs within CART may indeed be important in mediating ERα function, and as LXD motifs usually mediate interactions between nuclear hormone receptors and coregulators, we hypothesized that CART may be a physical interactor of ERα. However, as shown in figure 3.2, CART was not determined as a physical interactor. The possible reason for the aforementioned decrease in ERα activity following LXD-motif mutation may lie with where these LXD motifs are situated within CART. The first two LXD motifs identified in CART lie within the signal peptide, and not the active 42-89 CART peptide. It is possible that, through introducing mutations within the signal peptide of CART, the transport and secretion of CART is altered. Testing if these mutations do indeed affect the secretion of CART may help further understand these experiments.

Molecule processing

Feature key	Position(s)	Description	Actions	Graphical view	Length
Signal peptide	1 – 27	1 Publication	Add BLAST		27
Chain (PRO_0000004433)	28 – 116	Cocaine- and amphetamine-regulated transcript protein	Add BLAST		89
Peptide (PRO_0000004434)	28 – 66	CART(1-39)	Add BLAST		39
Peptide (PRO_0000004435)	69 – 116	CART(42-89)	Add BLAST		48

Figure 4.25. UNIPROT database highlights the presence of a signal peptide at the beginning of the CART protein.

Perhaps if these mutations did affect the secretion of CART, and this was the reason why a modest decrease in ERα activity was observed, it could be suggested that it is not intracellular CART which alters the function of ERα. Instead, it is the secreted active peptide causing these alterations. Taken

together, these results highlight an interesting relationship between CART and ERα, which we aimed to elucidate further by understanding the effect CART has on the interacting partners of ERα.

4.3.2 Detection of ERα interaction networks using two independent antibodies

The use of one antibody to investigate the effect a given treatment condition can have on interacting partners of a target protein is common to most studies. However, given the large amounts of data typically generated from mass spectrometry experiments, we felt it would be advantageous to use two independent antibodies for ERα, and examine the common interactors. This is a technique used by our collaborators, and has resulted in an impressive publication investigating interacting partners of the chromatin binding protein SIN3A (Streubel et al., 2017). Western blot results presented in figure 4.4 suggested that the F-10 antibody resulted in more non-specific binding. Further, figure 4.14 suggested the F-10 antibody grouped very close with the negative control IgG, suggesting that this antibody may not have been an appropriate choice for our established workflow.

Our study did indeed show common interactors for both antibodies (GREB1 for example), but no common interactors were found to be recruited to ERα in the presence of CART (figure 4.13). In fact, there were only common interactors found between both antibodies in the absence of CART. One possible explanation for this is, in the presence of CART, the D-12 antibody does not have high affinity for the complex detected using the F-10 antibody, and vice versa. Using the F-10 antibody, glutamate dehydrogenase 1/2 (GLUD1, GLUD2) was found to interact with ERα. When searching the Human Protein Atlas (proteinatlas.org), these proteins were found to only exist within the mitochondria (figure 4.26).

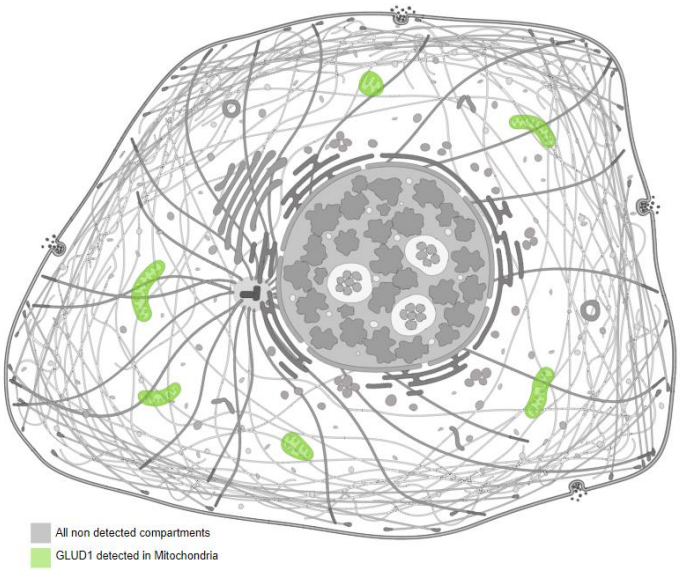

Figure 4.26. The human protein atlas suggests GLUD1 is only expressed in the mitochondria of cells.

Image was taken directly from the human protein atlas page after using GLUD1 as the query gene.

This raises the intriguing possibility that the F-10 antibody detected part of a non-genomic ERα complex driven by CART. ERα is known to not only exist in the nucleus, with studies showing that ERα can also exist on the cell membrane (Levin et al., 2009). ERα has previously been shown, through interacting with Gαi in the calveolae of endothelial cells, to control the activity of nitric oxide synthase (Chambliss KL et al., 2002). Furthermore, ERα has been shown to exist within the mitochondria of cells, and can affect mitochondrial function (Klinge et al., 2008).

To investigate this further, an exciting experiment to perform would to first perform cellular fractionation prior to immunoprecipitating ERα. Enriching for cellular fractions such as the nucleus, cytoplasm and mitochondria, prior to performing ERα IP-mass spec would certainly address the question of whether CART affects both the genomic, and non-genomic, functions of ERα.

4.3.3 CART putatively promotes an interaction between ERα and the zinc-finger protein WIZ

WIZ was not detected in any replicates as an ERα interactor in uninduced cells, but was detected in all replicates in cells expressing CART. In 2015, WIZ was characterised as a core subunit of the G9a/GLP complex, which typically functions as a mediator of histone methylation in specific genomic regions to promote transcriptional repression (Bian et al., 2015). A few months later, another study was published reinforcing WIZ as a key component of the G9a/GLP complex (Simon et al., 2015). Impressively, only a year later, another study emerged to provide evidence that WIZ may act as a transcriptional activator, as well as a transcriptional repressor (Isbel et al., 2016). This study characterized that haplosufficiency of WIZ resulted in a decrease in the expression of genes (via RNA sequencing) that have WIZ binding sites within their promotors (ChIP-seq).

While the above studies certainly highlight WIZ as a fascinating protein, its role as an ERα interactor remains extremely unclear. Indeed, an interaction between WIZ and ERα has not been reported previously. We show that there have been previous studies linking WIZ with other ERα interactors identified in our mass spectrometry study (figure 4.18). This may suggest that CART expression results in ERα interacting with a complex containing WIZ. To try understand a potential reason for this interaction, publicly available WIZ ChIP-seq data was accessed from one of the studies mentioned above (Bian et al., 2015). The top putative target for WIZ was the microRNA MIR6723. This was an interesting finding, as RNA sequencing performed in chapter 3 of this study identified *MIR6723* to be significantly (p=0.002) downregulated in cells expressing CART. Furthermore, *MIR6723* was identified as a potential ERα target gene in multiple publicly available ERα ChIP-seq datasets (Gertz et al., 2013, Mohammed et al., 2015). This may suggest that, through mediating an interaction between WIZ and ERα, CART can function to repress specific genes, an aspect we had not previously anticipated, but certainly one that may be worthy of further investigation.

The interaction between WIZ and ERα would first need to be stringently validated before drawing any definitive conclusions. Perhaps performing ERα IP exclusively on nuclear extracts may help in removing non-specific IgG binding which was evident from our results. Further, the use of immunofluorescence to detect co-localisation of ERα and WIZ may also assist in understanding whether WIZ and ERα interact in the presence of CART, or perhaps another assay, such as the proximity ligation assay (Fredriksson et al., 2002), could be implemented. Next, the ERα ChIP-seq experimental plan highlighted in section 3.3 of this study would aid in understanding what promotor regions are occupied by ERα, and ChIP-re-ChIP could be utilized to prove the presence of WIZ on these promotors.

4.3.4 CART putatively promotes an interaction between ERα and the E3 ligase HECTD4

Along with WIZ, HECTD4 was another protein which was significantly associated with ERα in the presence of CART. HECTD4 is a poorly understood E3 ligase, and very little is understood about this protein and its involvement in disease. Whole genome sequencing of lung adenocarcinoma patients in China identified HECTD4 to be a gene which may be involved in cancer (Wang et al., 2017). A computational study in 2017 identified HECTD4 to be a potential driver gene involved in breast cancer, but was not characterized any further (Rajendran et al., 2017).

Many E3-ligases are known to interact with ERα. Arguably the most well understood E3 ligase which can interact with ERα is BRCA1. This interaction was first characterized in 2002, in a study which demonstrated the interaction between BRCA1 and ERα results in the regulation of vascular endothelial growth factor (VEGF) transcription (Kawai et al., 2002). E3 ligases are typically involved in the turnover of the target protein, but can function as coactivators also (Zhou et al., 2014). Clearly, these are an extremely important class of proteins for the normal function of ERα.

First, we aimed to characterize the potential reason why we found HECTD4 to be an interactor of ERα. We found a modest association between ERα, SKP1

and HECTD4 (figure 4.18). SKP1 is a key component of the SCF ubiquitin ligase complex. This complex works through interchangeable F-box proteins, to recognize a substrate and target it for proteasomal degradation (Skaar et al., 2014). SKP1 has been shown to interact with ERα previously, an interaction which was mediated through the F-box protein SKP2 (Zhou et al., 2014). This study further demonstrated that the interaction between ERα and SKP2 was necessary for driving ER late-gene expression, and G1 cell cycle progression (Zhou et al., 2014). While this does not directly relate to an interaction between SKP1 and HECTD4, it is important to note that this complex can have implications in progression of the cell cycle. Indeed, it may be interesting to examine whether cell-cycle specific genes identified in chapter 3 of this study are still increased if the expression of HECTD4 or SKP1 is compromised. The evidence of the interaction between HECTD4 and CUL1 was poor, and so caution must be exercised before making any definitive conclusions. It is just as likely that HECTD4 is a novel interactor of ERα, driven by CART, independent of the SCF ubiquitin ligase complex.

Validation of a CART-driven interaction between HECTD4 and ERα was unfortunately unsuccessful (figure 4.20). No band corresponding to the predicted molecular weight of HECTD4 (440 kDa) was detected in any immunoprecipitation lanes, or the input lanes. Perhaps the size of HECTD4 compromised our abilities to prove this interaction, and a modified Western blot protocol may need to be established before moving forward with this putative interaction. Despite not achieving a successful validation result, we hypothesized that if the CART-driven interaction between HECTD4 and ERα was real, this may indicate altered turn-over of ERα in the presence of CART. We tested this hypothesis by examining ERα levels in the presence/absence of CART following treatment with cycloheximide (CHX), a broad protein synthesis inhibitor. To our surprise, ERα levels were maintained at higher levels throughout the experiment in the presence of cycloheximide. This would suggest that, if HECTD4 were to be identified as an ERα interactor, it may not be involved in the proteasomal degradation of ERα, and so may be involved in another process. For example, if HECTD4 was to promote K63-linked

ubiquitination of ERα, this may be an indicator of transcriptional regulation (Dwane et al., 2017).

Much work is still necessary in order to fully characterize this interaction. Proving the interaction between HECTD4 and ERα using methods described for interrogating the interaction between WIZ and ERα mentioned in section 4.3.2 would certainly represent the first step forward in proving this interaction, as well as the altered Western blot protocol mentioned above. Following this, the expression of HECD4 could be modulated to examine the effect this has on the function of ERα.

4.3.5 CART expression results in the recruitment of chromatin remodelling complexes to ERα

The overwhelming majority of identified proteins were known members of the BAF chromatin remodelling complex. A full description of the role BAF chromatin-remodelling complexes play in transcriptional regulation can be found in section 5.1.1 of this study. When these were identified, we first performed searches to understand what protein(s) may represent the best option for targeting in the final chapter of this study. ARID1A was one of the most significant proteins identified in this study, and showed the largest difference between cells expressing CART and cells not. We initially did not feel targeting ARID1A would be a viable option due to its well understood role as a tumour suppressor (Wu et al., 2013). ARID1A is one of the most frequently mutated genes in cancer, with some cancers such as breast, ovarian and pancreatic reporting a mutation rate of over 30% (Wu et al., 2013). Newly published data, however, suggests that ARID1A may not be a simple tumour-suppressor, and may exhibit context-dependent oncogenic phenotypes (Sun et al., 2017). This may be something to consider when examining this data in the future.

SMARCD1 stood out to us as a potentially important target. First, it had previously been shown to mediate critical interactions with nuclear hormone receptors (Hsiao et al., 2003). Mounting evidence is also propelling SMARCD1 into the spotlight as an important regulator of growth in multiple types of cancer

such as breast (Deng et al., 2014) and gastric cancers (Shen et al., 2015). Given that SMARCD1 is also involved in nucleic acid binding, we felt that bringing this target forward to our final aspect of the study would be a reasonable choice to make. We confirmed that SMARCD1 was indeed recruited to ERα in the presence of CART, and hypothesized that modulating the expression of SMARCD1 may compromise the function of ERα. In figure 4.26, we suggest that the recruitment of these complexes allows ERα to access genomic loci, which may be important in the transcription of ERα target genes. We aim to elucidate this further in the final chapter of this study.

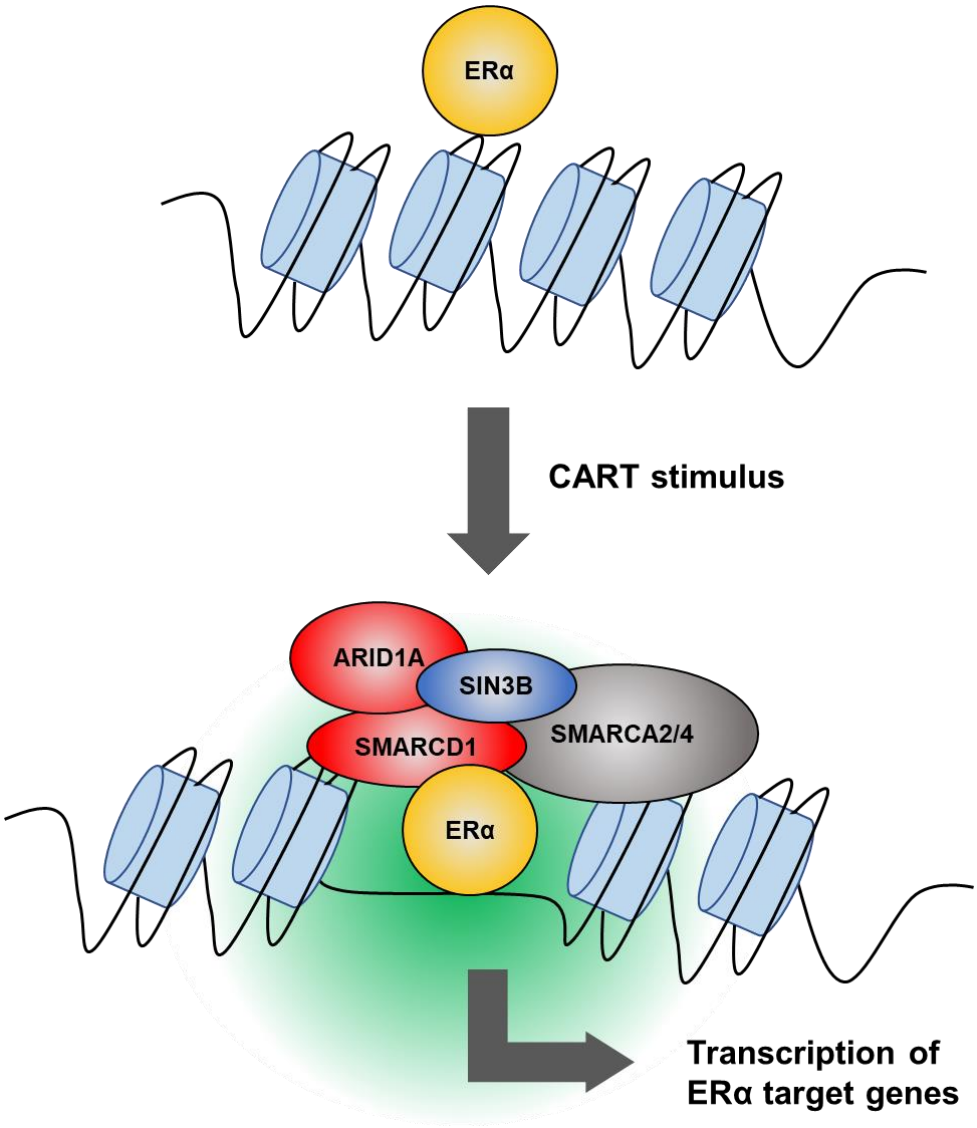

Figure 4.27. The recruitment of chromatin remodelling complexes to ERα may allow for the unwinding of chromatin structures and facilitate DNA binding.

Chapter 5. Investigating the therapeutic potential of SMARCD1 in ER+ breast cancer

5.1 Introduction

5.1.1 The BAF-chromatin remodelling complex

Complexities in biological research are often overlooked and taken for granted. A cell in the human body needs to pack over a meter of genetic material into the nucleus, which is typically no larger than 10 microns in diameter. To achieve this, the DNA is wrapped around histones to create the nucleosome, which is tightly packed with other nucleosomes to create the chromatin structures. These are further looped and condensed to produce the chromosome (Quenet et al., 2012). While this is a truly a remarkable feat, the DNA must still be accessed in order for transcription factors to mediate transcription of genetic material. One of best understood complexes that aids in the unwinding of these structures is known as the BAF chromatin remodelling complex.

The BAF, or SWI/SNF, complex was originally identified in yeast, through a mutant screen for defects in mating type SWItching and sucrose metabolism (Sucrose NonFermentable) (Abrams et al., 1986). This screen identified genes SNF2 and SNF5, which are now understood to correspond to BRG1/SMARCA4 and BAF47/SMARCB1 respectively (Abrams et al., 1986). Below is a table highlighting each subunit identified in yeast, its corresponding human homologues, and what type of subunits these are (table 5.1).

Table 5.1. Subunits of the human BAF complex are either "ATP-ase", "Core" or "Accessory" subunits.

Name in yeast	Name in human	Type of subunit in human
SWI2	BRM (SMARCA2)	**ATPase**
SNF2	BRG1 (SMARCA4)	
SNF5	BAF47 (SMARCB1)	**Core**
SWI3	BAF155 (SMARCC1) BAF170 (SMARCC2)	
SWI1	BAF250A (ARID1A) BAF250B (ARID1B)	**Accessory**
Arp7, Arp9	BAF53A (ACTL6A) BAF53B (ACTL6B)	
SWP73	BAF60A (SMARCD1) BAF60B (SMARCD2) BAF60C (SMARCD3)	
N/A	Actin (β-Actin) BAF57 (SMARCE1) BAF180 (PBRM1) BAF200 (ARID2) BCL7A-C, BCL11 BRD7, BRD9 DPF1-3 (BAF45B-D) GLTSCR1 PHF10 (BAF45A) SS18	
SWP82 SNF6, SNF11 TAF14	N/A	

Table adapted from Sarnowska et al., 2016, and Weissman et al., 2009.

In humans, one ATPase subunit, as well as the listed “core” subunits are required for a functional BAF complex (Sarnowska el al. 2016). It is thought that this complex disrupts DNA-histone binding in an ATP-dependent manner, which results in nucleotide sliding (Sarnowska el al. 2016). Ultimately, this results in the opening of the chromatin, and allows transcription factors to bind genomic loci.

Interestingly, the BAF-complex is known to associate with a huge amount of transcription factors (Weissman et al., 2009), however, the interaction appears to be subunit specific. For example, p53 has previously been characterized to interact with the BAF-complex, an interaction which is thought to be mediated through SMARCD1 (Oh et al., 2008). ERα on the other hand, has been shown to interact with subunits such as SMARCD1 and SMARCE1 (Hsiao et al., 2003, Garcia-Pedrero et al., 2006), with both studies highlighting the importance of the BAF-complex to the normal function of ERα. Contrastingly, neither the vitamin D receptor (VDR) or retinoid-x receptor alpha (RXRA) mediate interactions with the BAF complex through SMARCD1 (Hsiao et al., 2003). Clearly, this complex is extremely important to the normal process of transcription. However, given that different transcription factors appear to mediate interactions with BAF through various subunits, could understanding the exact subunit-transcription factor interaction offer a potential intervention point for inhibiting transcription?

5.1.2 Implications of the BAF-chromatin remodelling complex in cancer

The BAF-complex has long been understood to play a crucial role to both cancer initiation, as well as development. As mentioned previously, this appears to be subtype specific. Both SMARCA2 (BRM) and SMARCA4 (BRG1), the ATPase subunits of the BAF complex, are widely regarded as specialized tumour suppressors. Loss of SMARCA2 expression has previously been reported to cause cells to undergo abnormal growth patterns through an altered cell cycle (Coisy-Quivy et al., 2006). In mouse models of SMARCA2 knockout, mice exposed to the carcinogen ethyl carbamate had an increase in the development of lung adenomas (Glaros et al., 2007). Loss of SMARCA2

expression has also been reported to be associated with prostate cancer (Sun et al., 2007). In addition to SMARCA2, SMARCA4 loss has also been associated with lung cancer (Reisman et al., 2003, Fukuoka et al., 2004) and is a frequently mutated gene in multiple cancers (Hodges et al., 2016).

Another classic example of a BAF complex subunit playing a key role in cancer is that of SMARCB1 in rhabdoid tumours. Biegel and colleagues identified that a chromosomal band which was frequently deleted or translocated was associated with the initiation of malignant-rhabdoid tumours, and that this gene loci corresponded to SMARCB1 (Biegel et al., 1999). SMARCB1 germline alterations have been attributed to a predisposal to a number of cancers (Roberts et al., 2009). Further, loss of SMARCB1 has been attributed to increased CCND1 expression, increased cellular migration, and impaired differentiation (Roberts et al., 2009).

Many studies have identified ARID1A as a tumour suppressor, which is frequently lost/mutated in breast cancer (Mamo et al., 2012, Zhang et al., 2012, Cho et al., 2015). It is also clear from figure 5.1 below that ARID1A is one of the most frequently mutated genes across multiple cancer types (Hodges et al., 2016). However, there is now mounting evidence coming to the forefront of the scientific community stating that this complex is not simply a tumour suppressor complex.

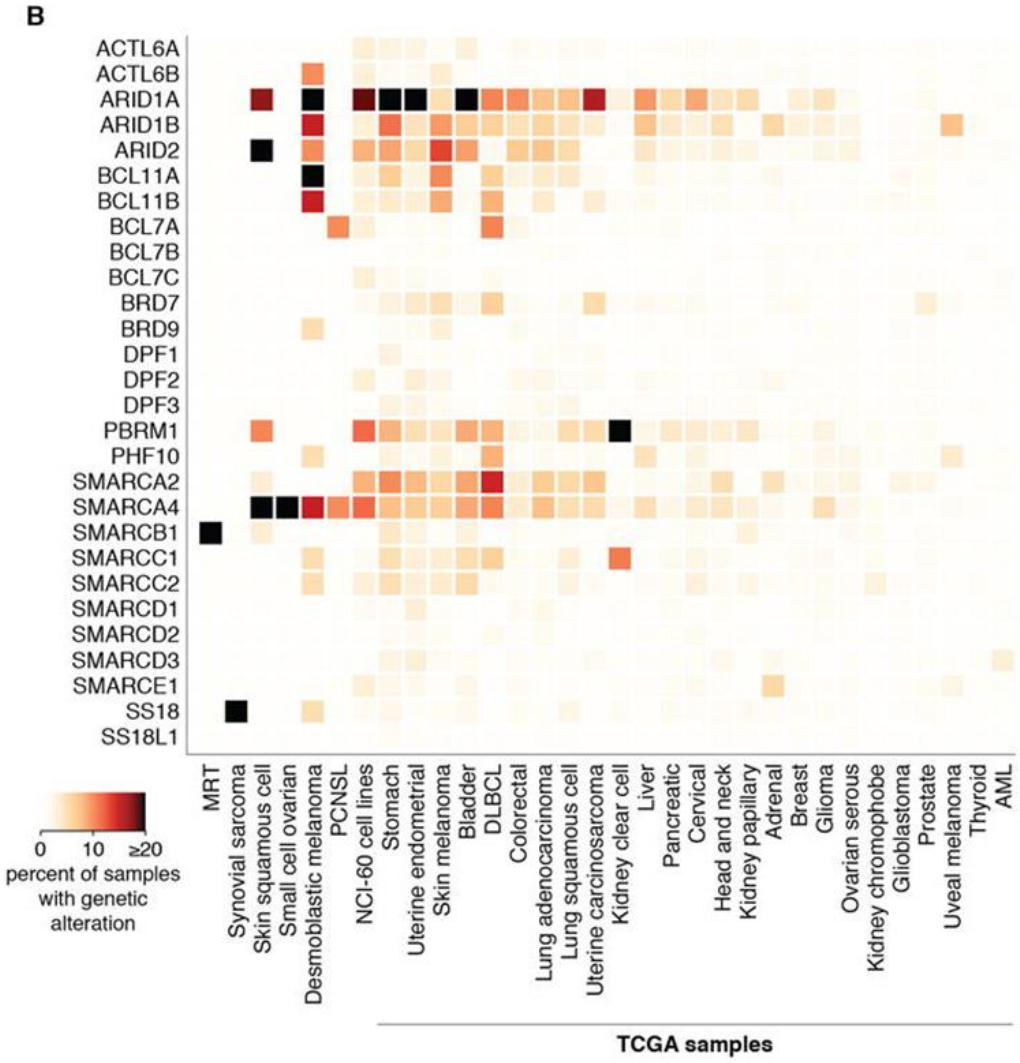

Figure 5.1. BAF complex subunits are mutated in a subunit, and cancer, specific manner.

Image sourced from Hodges et al., 2016.

This year, a study published in Cancer Cell demonstrated that ARID1A is a “two-faced mSWI/SNF subunit” (Sun et al., 2017). The authors eloquently demonstrate that the tumour suppressor function of ARID1A is context dependent, and may also act in an oncogenic manner in liver cancer (Sun et al., 2017). High expression of SMARCC1 has previously been associated with better overall survival in patients with early-stage cervical intraepithelial neoplasia (Shadeo et al., 2008) (indicating a potential tumour suppressor role), but has also correlated with tumour recurrence and de-differentiation in

prostate cancer (Heeboll et al., 2008) (indicating a more oncogenic role). A similar story exists for the subunit SMARCD1. Initially, SMARCD1 was hypothesized to function as a tumour suppressor through mediating the activity of p53 (Oh et al., 2008). A recent study, while not proving a direct interaction with SMARCD1, highlighted that mutant p53 can still access the BAF-complex to mediate transcriptional activity (Pfister et al., 2015). A compelling amount of data has also emerged in recent years, suggesting SMARCD1 is frequently upregulated and correlates with poor survival in both breast and gastric cancer (Deng et al., 2014) (Shen et al., 2015). It is fair to conclude then, that the action of the BAF-complex is more than likely both cancer, and subtype, specific.

5.1.3 Aims of chapter

In chapter 4 of this study, we discovered that SMARCD1 is recruited to ERα by CART. Based on studies discussed in section 5.1.1 and 5.1.2, we hypothesize that SMARCD1 may represent a key regulator of breast cancer growth and ER function. To investigate this, we aimed to answer the following questions:

- Does SMARCD1 expression correlate with survival in cohorts of breast cancer patients?

- What effect does SMARCD1 knockdown have on the growth and morphology of ER+ cells?

- Does modulating SMARCD1 expression prevent CART from increasing the expression of ERα target genes?

5.2 Results

5.2.1 *In silico* analysis of SMARCD1 expression

As discussed in section 5.1.2, the BAF-chromatin remodelling complex plays a significant role in cancer, but the exact role each individual subunit plays still remains unclear. Our first objective was to examine the expression of *SMARCD1* in a dataset of breast cancer patients *in silico*. For this, we chose to examine *SMARCD1* expression in the Gene expression-based Outcome for Breast cancer Online (GOBO) database (Ringner et al., 2011).

In patients, the expression of *SMARCD1* was significantly different across breast cancer molecular subtypes based on the HU classification ($p<0.00001$), but this trend was not seen across molecular subtypes based on the PAM50 classification ($p=0.40933$) (figure 5.2). The expression of *SMARCD1* appeared marginally higher in ER+ breast cancer patients compared to ER- breast cancer patients, but this trend was not statistically significant ($p=0.49584$) (figure 5.2). Finally, *SMARCD1* expression was significantly higher in patients with low grade tumours vs patients with high grade tumours ($p=0.00588$) (figure 5.2).

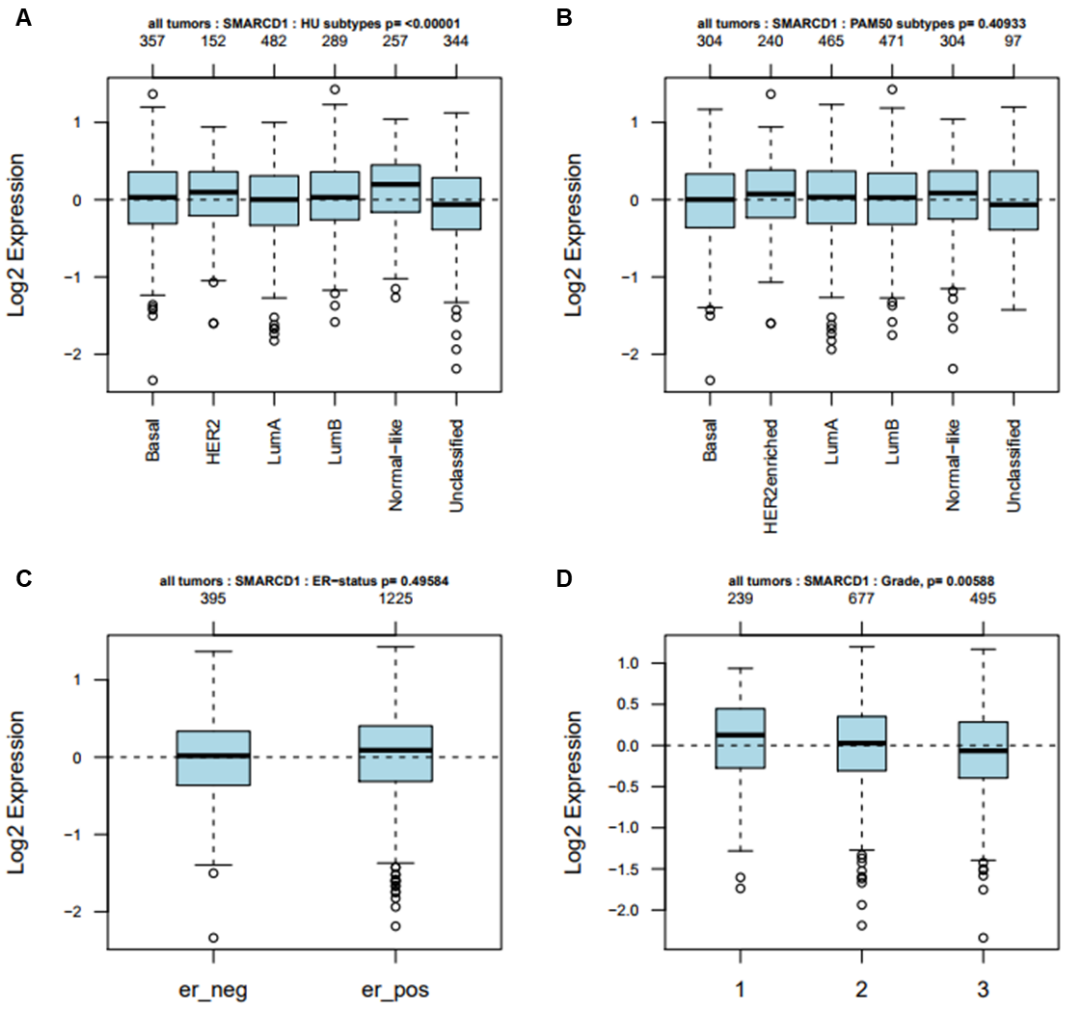

Figure 5.2. *In silico* analysis of *SMARCD1* expression in a cohort of breast cancer patients.

Expression of *SMARCD1* in breast cancer patients of different molecular subtypes based on the **A.** HU (p<0.00001) and **B.** PAM50 (p=0.40933) classification. **C.** *SMARCD1* expression in ER+ and ER- breast cancer patients (p=0.49584). **D.** *SMARCD1* expression in patients of different breast cancer stage (p=0.00588).

Having established that *SMARCD1* expression does not appear to be significantly different across breast cancer subtypes, we next examined whether the expression of *SMARCD1* was associated with poor survival in unstratified breast cancer patients.

Expression of *SMARCD1* across four quartiles was used to investigate whether high expression of SMARCD1 correlated with poor survival. For figures 5.3 and 5.4, each quartile is represented as a different colour line; **Grey – Low expression, Red – Low/Mid expression, Blue – Mid/High expression, Green – High expression.**

High *SMARCD1* expression was significantly associated with poor overall survival (OS) (p=0.00013) (figure 5.3) and poor distant metastasis free survival (DMFS) (p=0.04786) (figure 5.3) in unstratified breast cancer patients. SMARCD1 expression was not seen to be associated with poor relapse free survival (RFS) in unstratified breast cancer patients (figure 5.3).

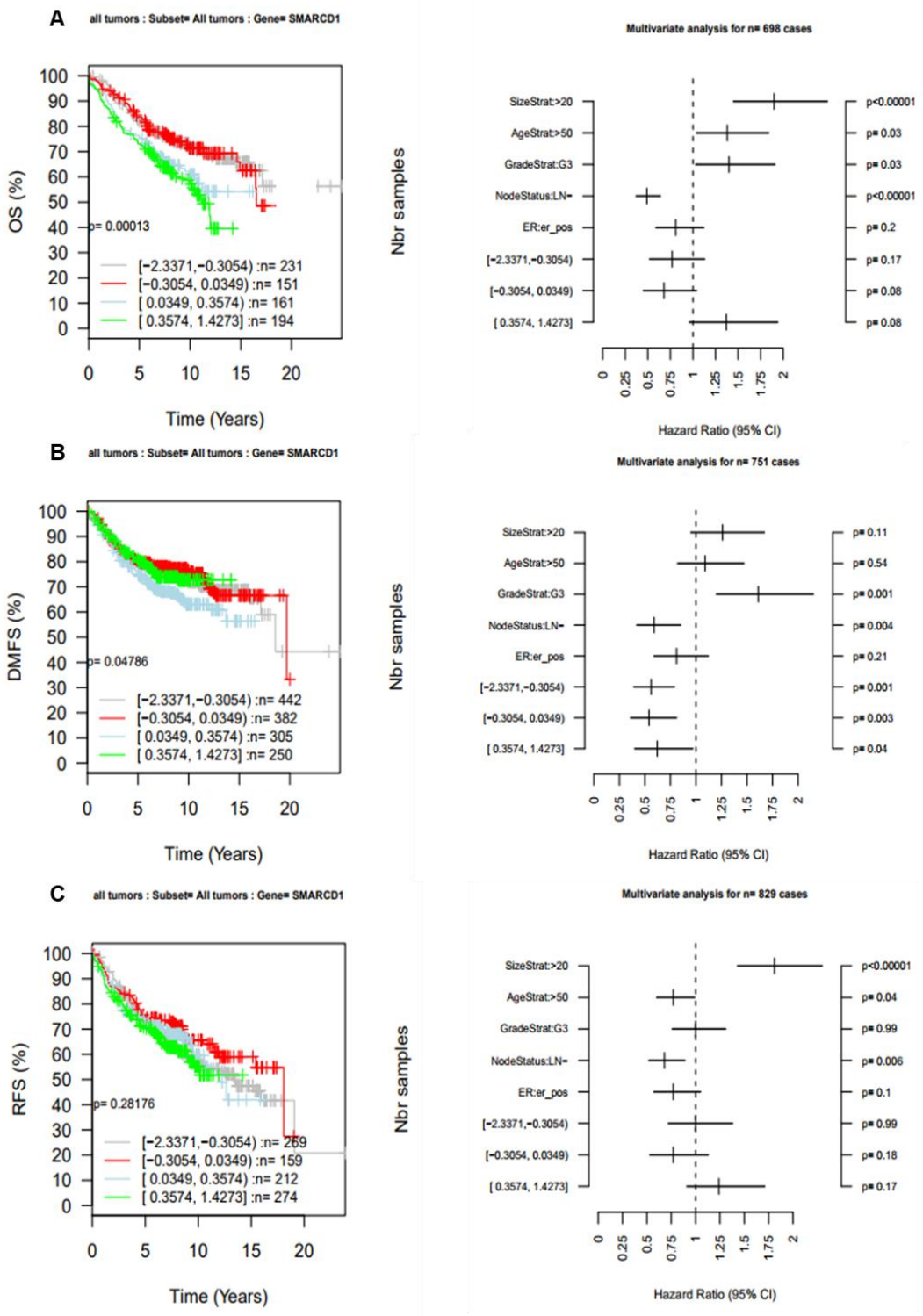

Figure 5.3. High expression of *SMARCD1* expression is significantly associated with poor overall survival (OS), and distant metastasis-free survival (DMFS) in breast cancer patients.

Having identified that high *SMARCD1* expression was significantly associated with poor OS and DMFS in unstratified breast cancer patients, we next sought to investigate whether the expression of *SMARCD1* is associated with the same poor survival rates in patients stratified based on ERα status. To this end, we found that high expression of *SMARCD1* was significantly associated with poor OS ($p<0.00001$) and DMFS ($p=0.01253$) in ER+ breast cancer patients, but not in ER- breast cancer patients (figure 5.4 A and B). High *SMARCD1* expression did not correlate with poor RFS in ER+ or ER- breast cancer patients (figure 5.4 C), similar to our findings in unstratified breast cancer patients (figure 5.3).

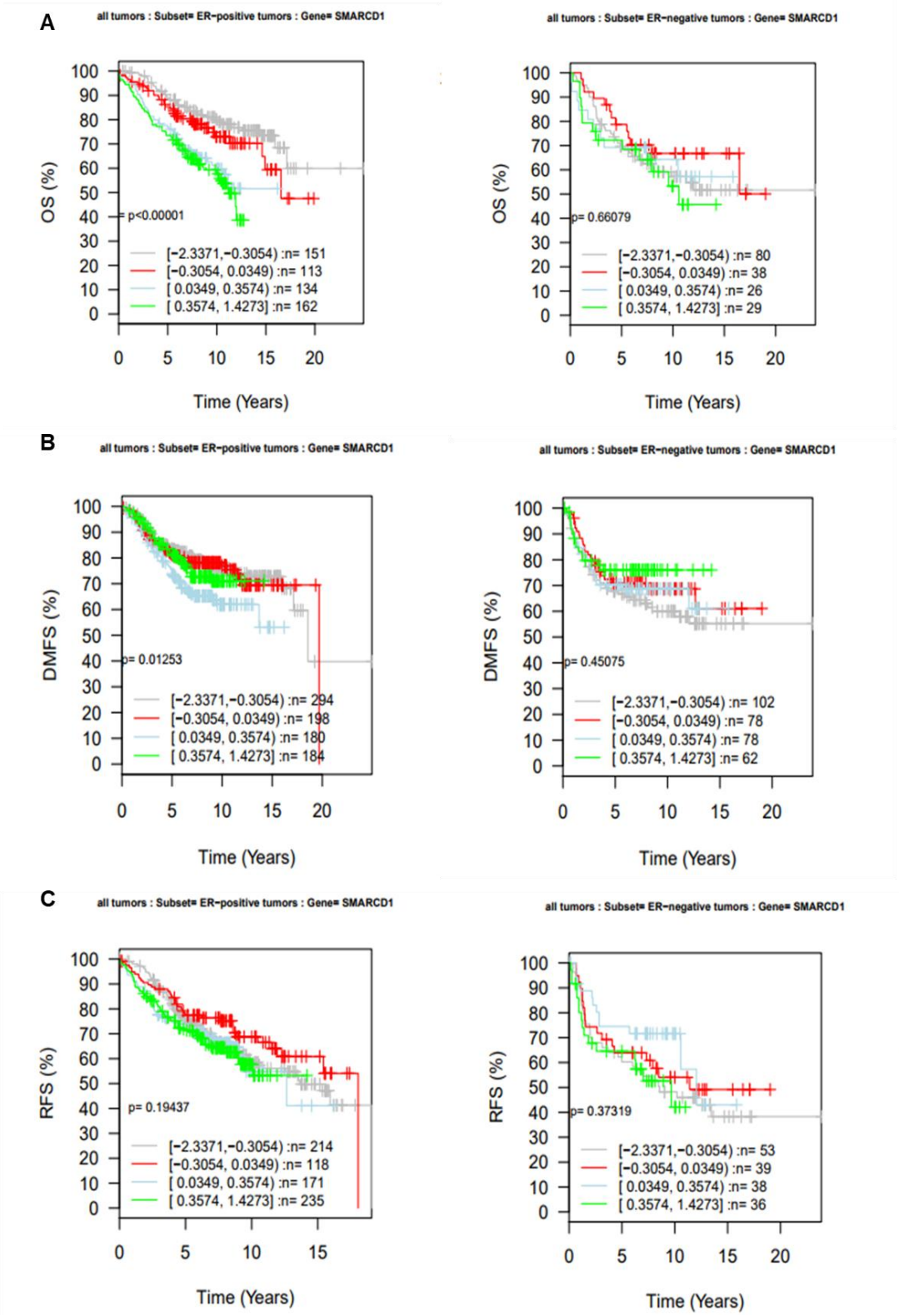

Figure 5.4. High expression of *SMARCD1* is significantly associated with worse OS (A) and DMFS (B) in ER+, but not ER-, breast cancer patients.

5.2.2 Analysis of SMARCD1 expression in a second, independent cohort of breast cancer patients (TCGA dataset)

Having established that high expression of *SMARCD1* is significantly associated with worse survival in an *in silico* database, we next sought to examine whether the expression of SMARCD1 was associated with poor survival in another, independent cohort of patients. We chose to analyse the TCGA dataset, whose data is publicly available through the cBioportals suite (Cerami et al., 2012, Gao et al., 2013). Analysis within this dataset allowed us to correlate not only *SMARCD1* mRNA expression, but also *SMARCD1* copy-number status, and SMARCD1 protein expression, with survival, across a large cohort of breast cancer patients.

First, we examined whether *SMARCD1* copy number status correlated with survival. Data reported in figure 5.5 indicates that *SMARCD1* copy number status is significantly associated with worse overall survival.

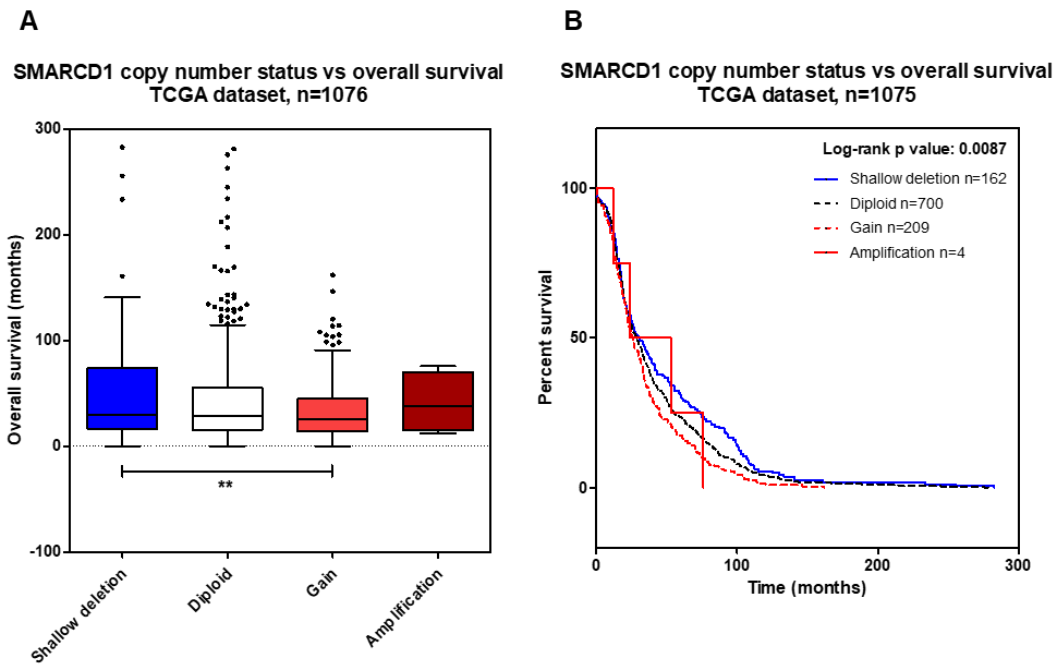

Figure 5.5. *SMARCD1* copy number status is significantly correlated with worse OS in the TCGA dataset of 1076 breast cancer patients.

A. Tukey box-plots plotting overall survival (months) for each copy number status of *CARTPT*. One-way ANOVA p=0.0094. Bonferroni's multiple comparisons test deemed the shallow deletion and gain groups as statistically significant (p<0.01). **B.** Kaplan-Meier curve plotting survival proportions for each copy-number status of *SMARCD1*. Log-rank p value = 0.0087.

Having discovered that *SMARCD1* copy number status was significantly associated with poor survival in the TCGA dataset, we next sought to examine whether *SMARCD1* mRNA expression was also correlated with survival. Data was accessed through the breast cancer survival portal tumorsurvival.org (Shaying Zhao Lab, University of Georgia). Expression of *SMARCD1* was based on upper and lower quartiles, and we analysed *SMARCD1* expression in unstratified breast cancer patients, as well as breast cancer patients stratified based on molecular subtype (figure 5.6). In this figure, we report that high expression of *SMARCD1* is significantly associated with poor survival in unstratified breast cancer patients only (p=0.0097). High expression of SMARCD1 appeared to moderately indicate worse survival in both Basal and

Luminal A breast cancer patients, but this trend was not statistically significant (p=0.096 and 0.16 respectively). Cohort size is indicated below:

Basal:	**High:**	**35**
	Low:	**35**
Luminal A:	**High:**	**105**
	Low:	**105**
Luminal B:	**High:**	**44**
	Low:	**43**
HER2+:	**High:**	**17**
	Low:	**16**
Normal-like:	**High:**	**7**
	Low:	**6**
Unstratified:	**High:**	**276**
	Low:	**275**

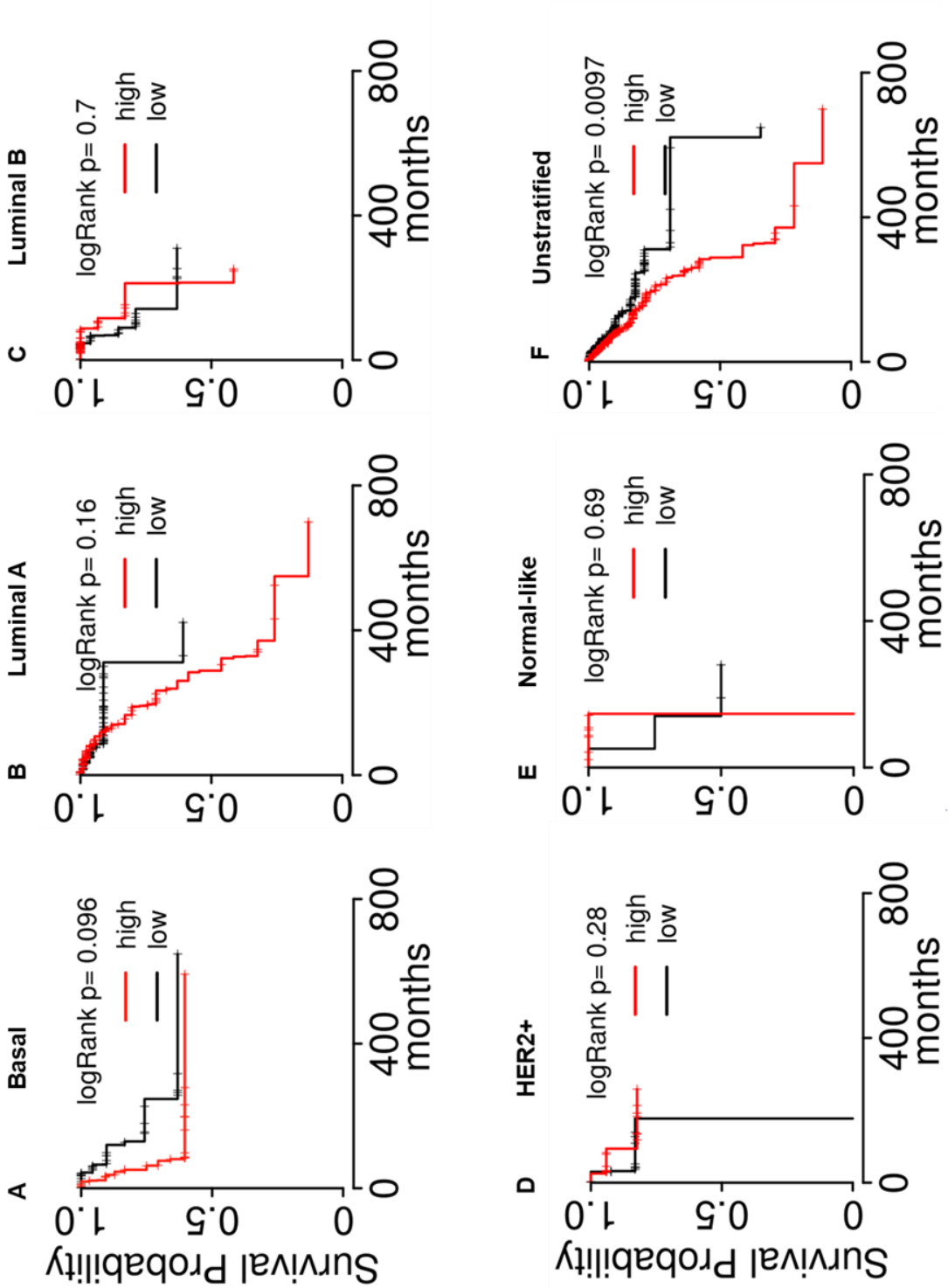

Figure 5.6. *SMARCD1* expression significantly correlates with poor survival in unstratified breast cancer patients within the TCGA dataset. Expression was based on upper and lower quartiles.

Finally, we could examine the protein expression of SMARCD1 in a small number of patients within this dataset. In figure 5.7, we report that high expression of SMARCD1 was also associated with worse OS. Average survival (months) for each quartile was as follows; Low: 37.49, Low-Mid: 54.25, Mid-High: 42.84, High: 29.51

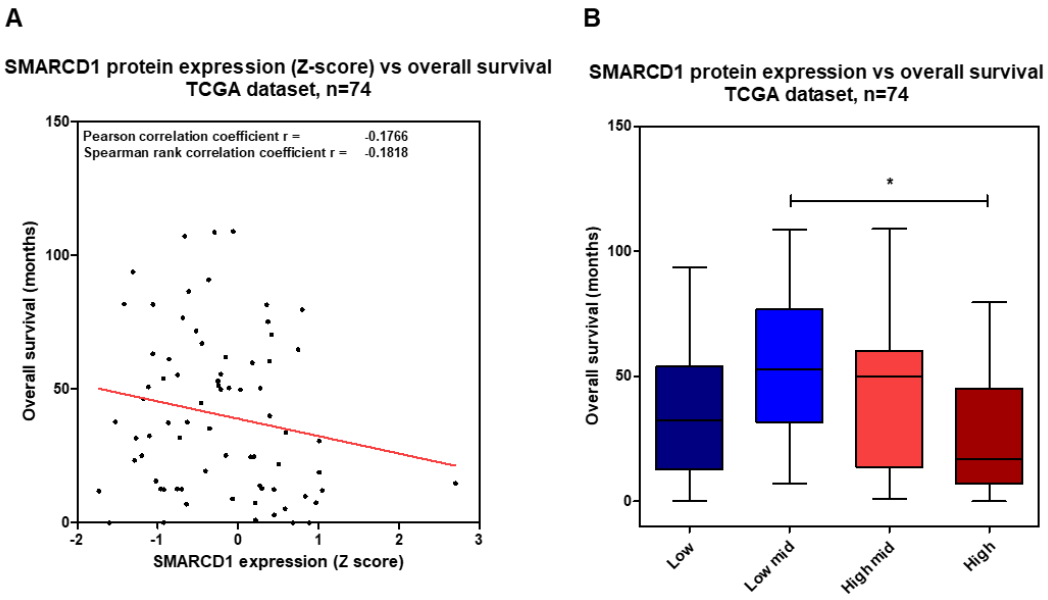

Figure 5.7. High protein expression of SMARCD1 indicates worse OS in the TCGA dataset.

A. OS was plotted against SMARCD1 protein expression. Both Spearman and Pearson rank coefficients are reported. **B.** SMARCD1 protein expression (Z score) was split into quartiles and Tukey box-plots were generated, plotting overall survival of each quartile. One-way ANOVA p = 0.0409. Bonferroni's multiple comparisons test deemed the low-mid and high groups as significantly different ($p<0.05$).

Higher protein expression of SMARCD1 indicating worse OS is in direct contradiction to some studies in the literature, which suggests SMARCD1 is a critical mediator of p53 function (Oh et al., 2008, Hong et al., 2016). As p53 is a widely understood, and vastly important, tumour suppressor, it may be puzzling to understand that expression of SMARCD1 is associated with poor

survival. However, given that p53 is one of the most frequently mutated genes in breast cancer, we thought it necessary to test whether high SMARCD1 protein expression was associated with worse survival in both p53 wild-type (WT) and p53 mutant (MUT) breast cancer patients. In figure 5.8, we report that SMARCD1 expression did not indicate worse OS in p53 WT breast cancer patients. In fact, a marginal increase in survival was seen in patients with WT-p53. In p53-MUT breast cancer patients, however, high expression of SMARCD1 strongly indicated worse overall survival. This may suggest that in patients with defective p53, the expression of SMARCD1 may drive an oncogenic phenotype. This trend was, however, not statistically significant, and so further research is required before drawing definitive conclusions.

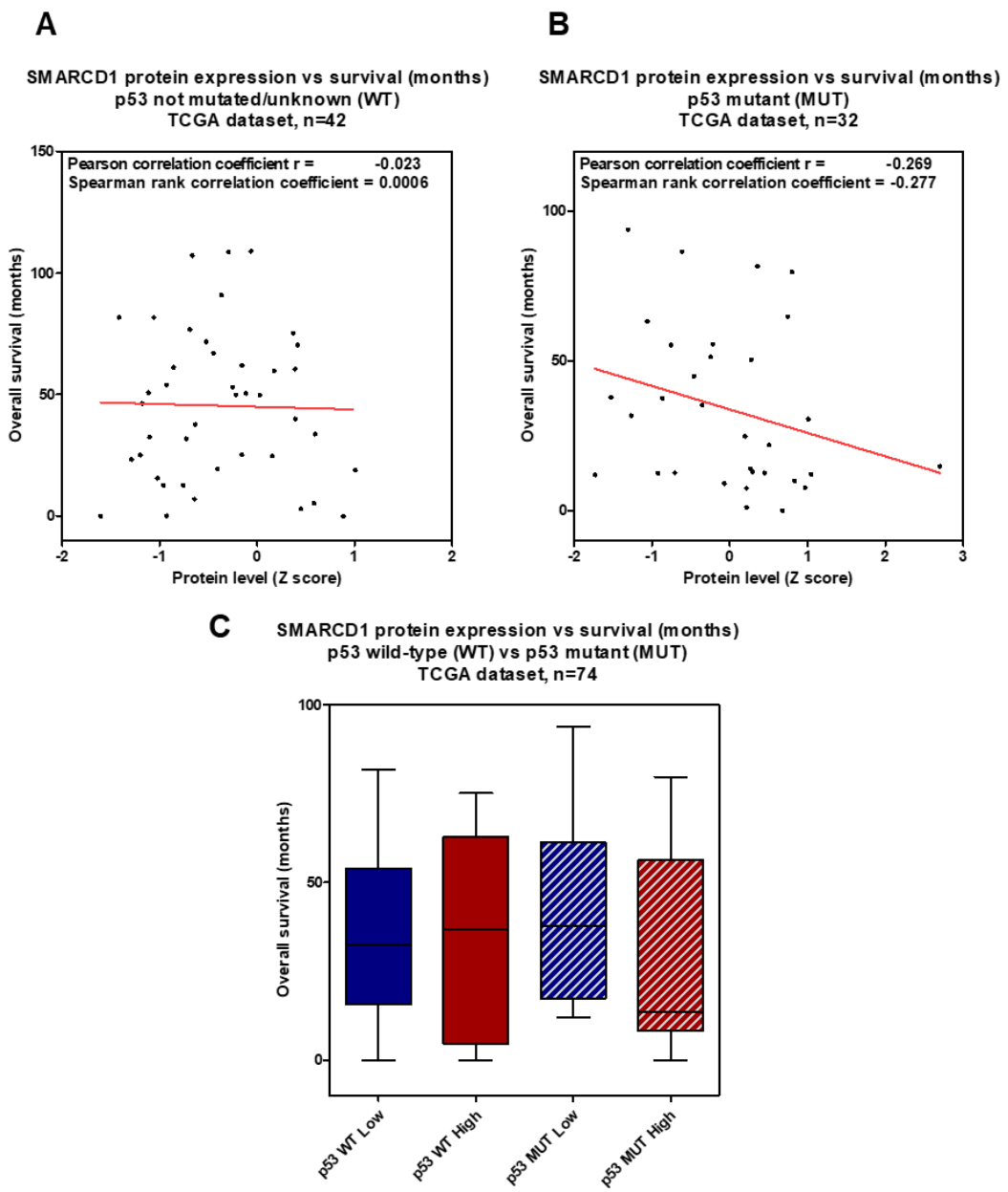

Figure 5.8. High protein expression of SMARCD1 indicates worse OS in p53 mutant breast cancer patients.

TCGA dataset was split into p53 wild-type (WT) (n=42) and p53 mutant groups (MUT) (n=32) **A.** SMARCD1 expression versus OS was plotted for p53 WT breast cancer patients. **B.** SMARCD1 expression versus OS was plotted for p53 MUT breast cancer patients. **C.** Expression was split by median into high and low. Average survival (months) for each group was as follows; p53 WT low: 42.71, p53 WT high: 48.07, p53 MUT low: 41.47, p53 MUT high: 26.33

5.2.3 Optimisation of siRNA transfection conditions prior to modulation of SMARCD1 expression

Data generated in chapter 4 suggests that CART recruits SMARCD1 to ERα, and previous studies have reported SMARCD1 as a critical mediator of nuclear receptor function (Hsiao et al., 2003). Taking this with the data generated in section 5.2.1 and 5.2.2, we hypothesized that modulating the expression of SMARCD1 may have a significant impact on ER+ breast cancer cells.

First, the transfection conditions for the Tet-ON T47D cell line were optimized using siGLO. We found 50 nM of siRNA to be the optimal transfection concentration, and found that 5 – 10 µl Dharmafect transfection reagent 1 was the optimal transfection reagent volume (figure 5.9). Next, we used the MTT assay to determine the cytotoxicity of the varying volumes of Dharmafect, and found the cells to tolerate all volumes of Dharmafect well (figure 5.10). We chose 50 nM as the optimal concentration of siRNA, and 7 µl as the optimal concentration of Dharmafect.

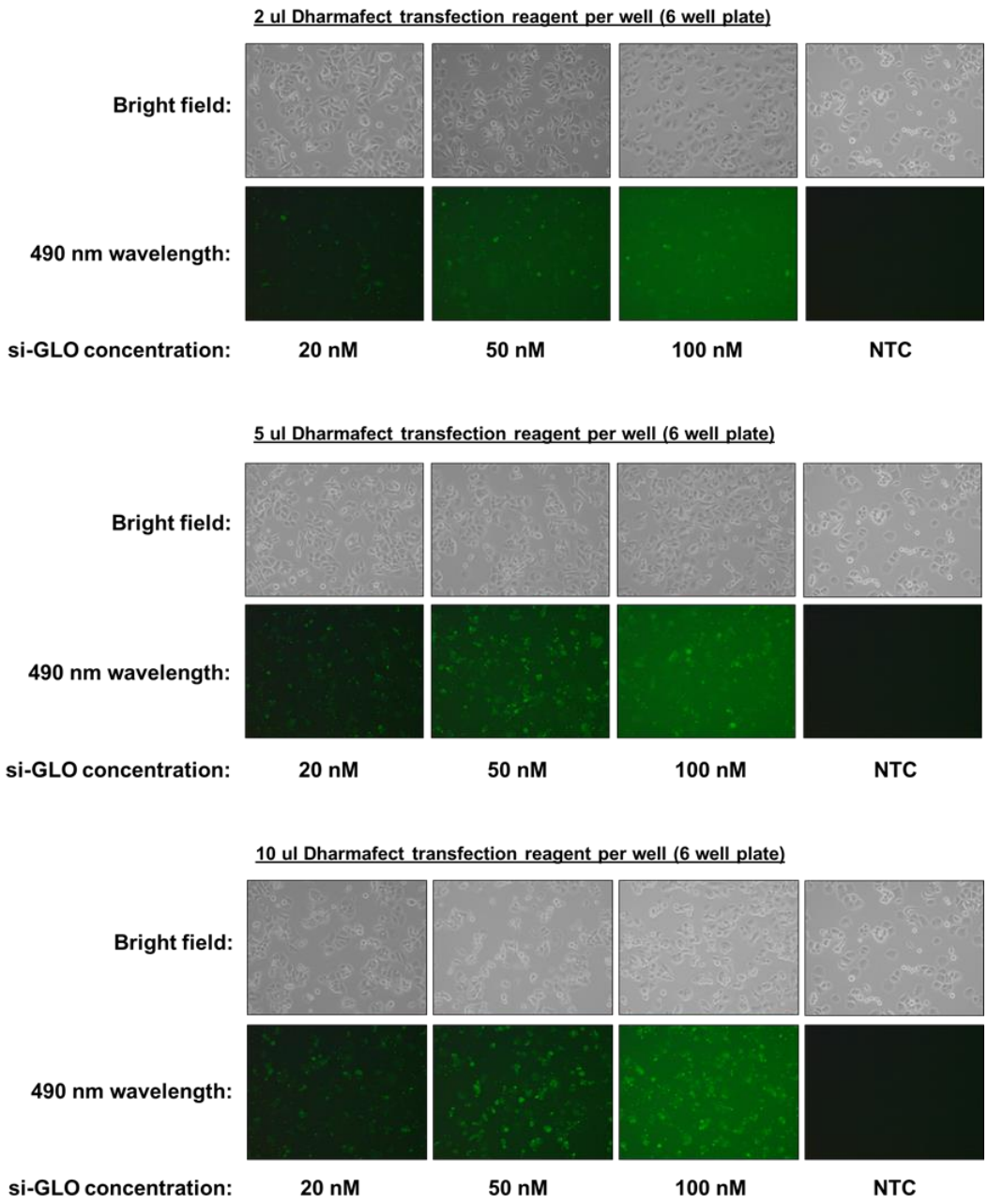

Figure 5.9. Optimisation of siRNA transfection conditions using the reverse transfection protocol.

Cells were transfected using various concentrations of DharmaFECT transfection reagent and si-GLO. Cells were imaged 72 hours post transfection.

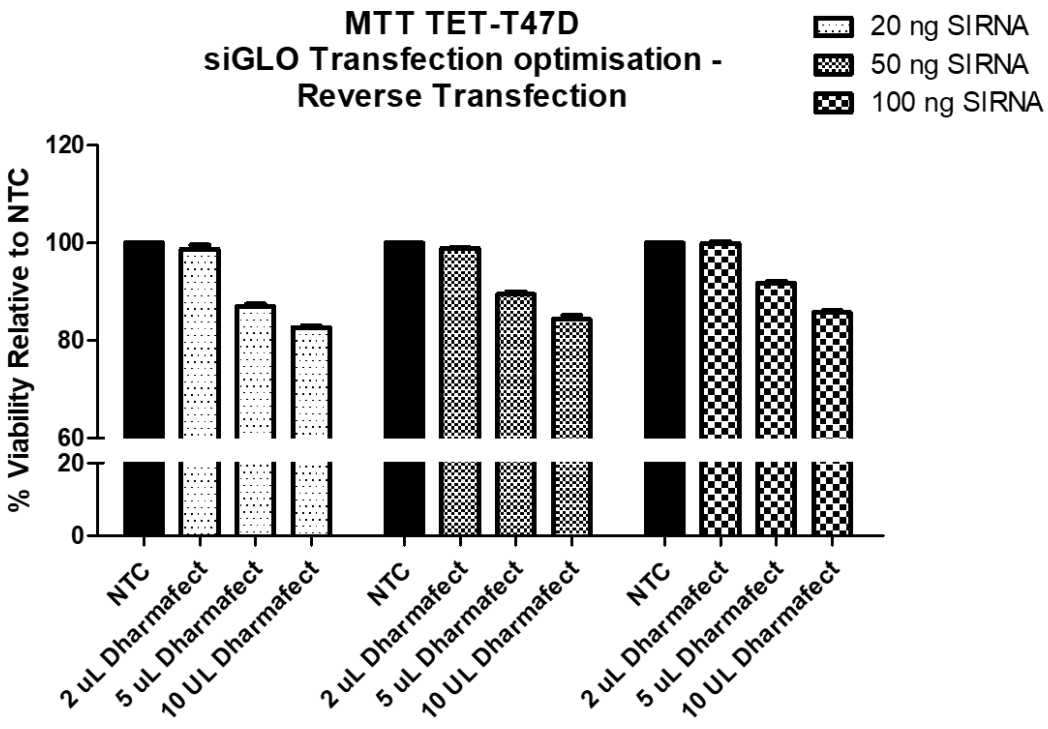

Figure 5.10. The DharmaFECT transfection reagent was well tolerated across all concentrations.

The MTT assay was used to measure viability 72 hours after a reverse transfection with 3 different volumes of DharmaFECT transfection reagent 1. Error bars represent SEM between 3 technical replicates.

5.2.4 Modulating the expression of SMARCD1 using siRNA

Having performed transfection optimisation, we next sought to knock-down the expression of SMARCD1. Four individual, non-overlapping siRNAs were transfected into Tet-ON T47D cells at the maximum concentration recommended by the manufacturer. Western blot, and qRT-PCR analysis (figure 5.11) demonstrated that both si-1 and si-4 achieved the most efficient knockdown of SMARCD1, and so these were brought forward for further analysis.

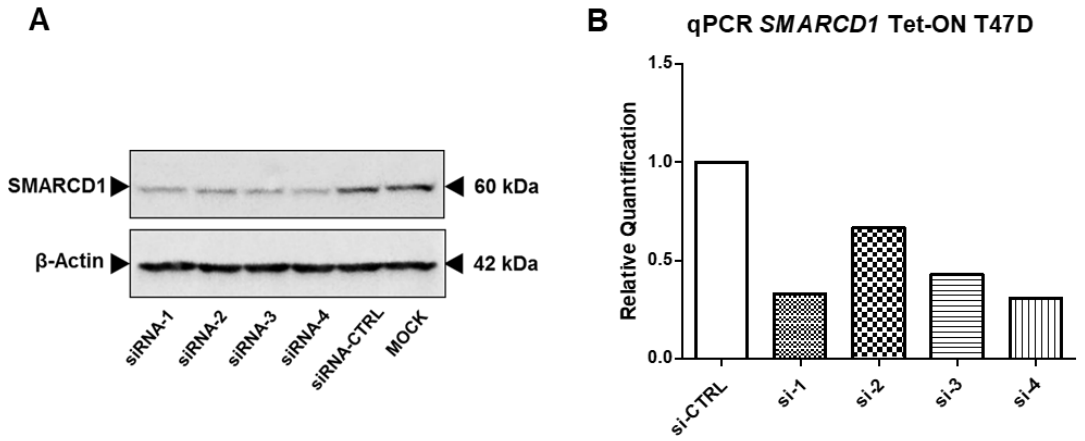

Figure 5.11. SMARCD1 expression is decreased upon transfecting 4 individual, non-overlapping, siRNAs targeting SMARCD1.

A. SMARCD1 expression was assessed 72 hours post knockdown via Western blot. Actin was used as the loading control. **B.** *SMARCD1* expression was assessed 72 hours post knockdown via qRT-PCR.

Next, we validated the siRNA knock-downs in 4 independent experiments, monitoring the morphology of the cells within each experiment (figure 5.12). We noticed modulating the expression of SMARCD1 using si-1 (but not si-4) resulted in altered morphology of the cells. The cells became longer and narrower, rather than the cobble-stone morphology the Tet-ON T47D cells typically exhibit.

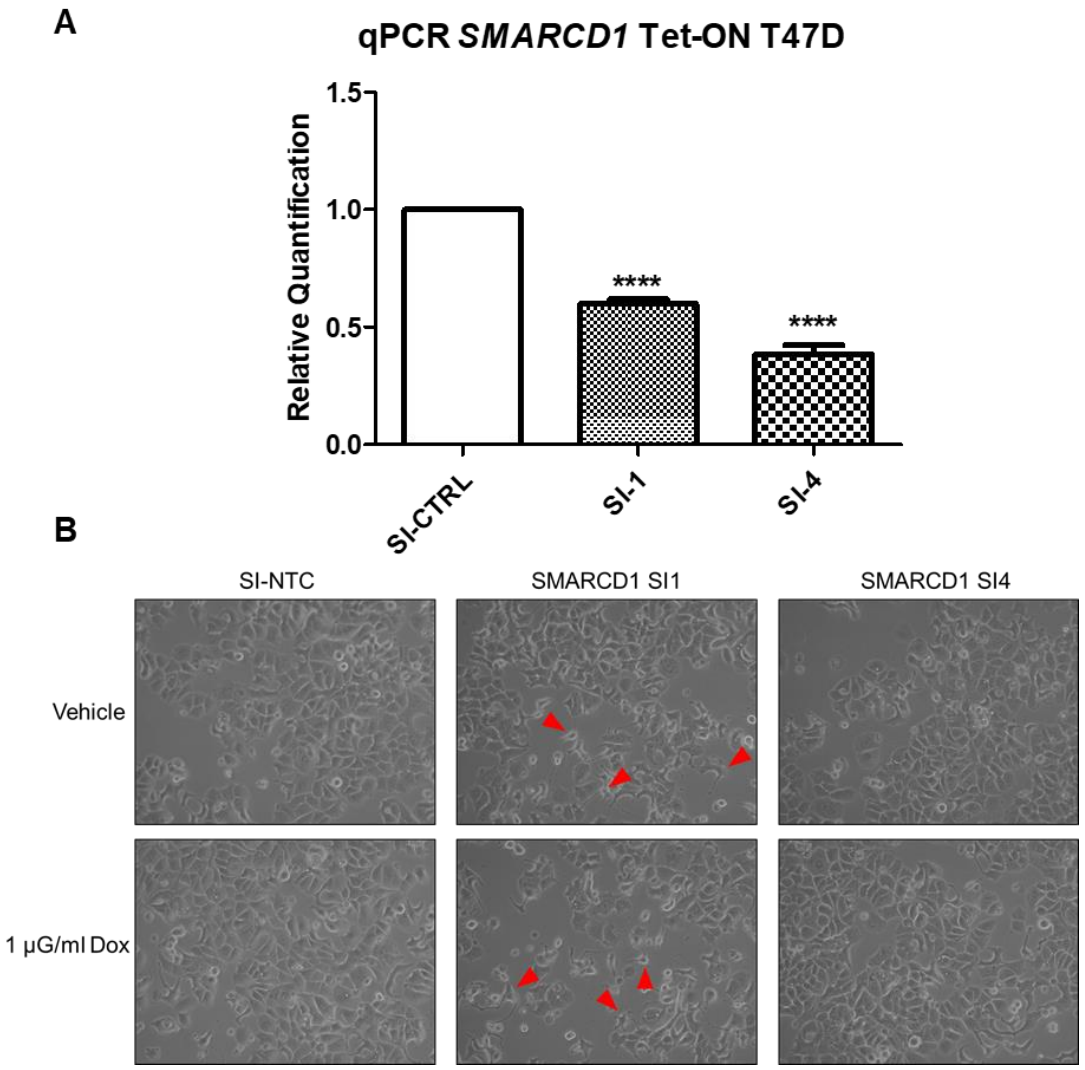

Figure 5.12. Modulating the expression of *SMARCD1* alters the morphology of Tet-ON T47D cells.

A. The expression of *SMARCD1* was assessed six days post knockdown using qRT-PCR. Mean +/- SEM between 3 independent experiments is plotted. One way ANOVA was used to calculate statistical significance **** $p<0.0001$. **B.** Cells appear morphologically different in SMARCD1 si-1 wells compared to si-CTRL/NTC wells (marked with red arrows). This phenotype was not noticed in SMARCD1 si-4 wells.

5.2.5 Investigating the consequence SMARCD1 knockdown has on the growth of ER+ breast cancer cells

Several studies have associated SMARCD1 expression with altered growth patterns in cancer (Deng et al., 2014, Shen et al., 2015). Combined with data generated in 5.2.1 & 5.2.2, we hypothesized that modulating SMARCD1 expression may affect the growth of the Tet-ON T47D cell line. In figure 5.13, we report that knockdown of SMARCD1 using si-1 decreased the growth of cells under all experimental conditions, however, only cells treated with E2 reported a statistically significant decrease in growth compared to si-CTRL cells. This trend was not seen in cells transfected with si-4.

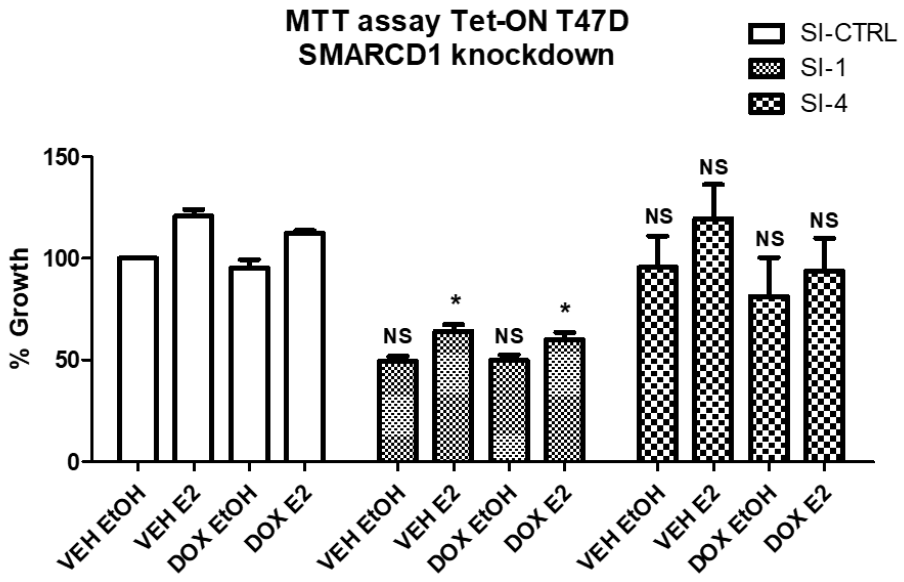

Figure 5.13. SMARCD1 knockdown significantly alters the growth pattern of Tet-ON T47D cells.

Cells were transfected with SMARCD1 si-1, si-4 or si-NTC. Two days later, cells were either induced to express CART (DOX) or not (VEH), as well as treated with 1 nM estradiol (E2) or EtOH as vehicle control for a further 72 hours. Error bars +/- SEM between 3 independent experiments is plotted. A two-way ANOVA with Tukey's multiple comparisons post-test was used to calculate statistical significance. * $p<0.05$, ** $p<0.01$, NS – not significant

5.2.6 Does SMARCD1-knockdown prevent CART from driving the expression of ERα target genes?

Mass-spectrometry analysis of the ERα interactome performed in chapter 4 identified SMARCD1 as a differentially recruited interactor in the presence of CART. Data presented in section 5.2.5 raised the intriguing possibility that SMARCD1 may be an important mediator of ERα-dependent growth. We therefore sought to investigate whether SMARCD1 knockdown had any consequence on the ability of CART to drive the expression of 2 ERα target genes previously been shown to be upregulated by CART (chapter 3), Cyclin-D1 (*CCND1*) and cAMP-Dependent Protein Kinase Inhibitor Beta (*PKIB*).

In figure 5.14, we demonstrate that inducing cells to express CART results in a significant increase in *CART* expression, and SMARCD1 knockdown resulted in a significant decrease in *SMARCD1* expression. Cells expressing CART had higher levels of both *CCND1* and *PKIB* in the si-CTRL group, but this trend was not determined as statistically significant. Levels of *CCND1* were not significantly altered following SMARCD1 knockdown in the presence, or absence, of CART. Cells transfected with si-1 showed a decrease in expression of *PKIB* compared to the si-CTRL group, but this trend was only statistically significant when the expression of *PKIB* was compared against si-CTRL cells expressing CART.

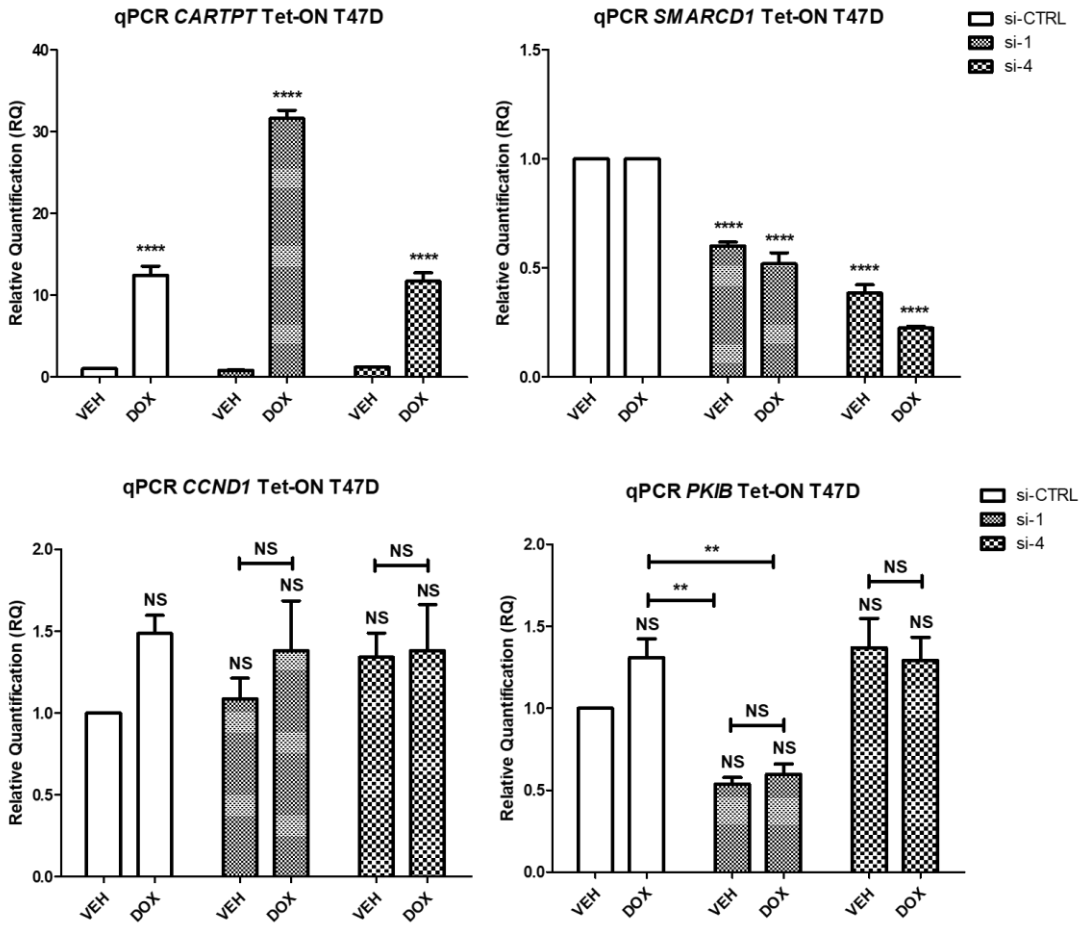

Figure 5.14. *SMARCD1* knockdown results in altered expression of *PKIB*, but not *CCND1*.

Cells were transfected with SMARCD1 si-1, si-4 or si-NTC. Two days later, cells were either induced to express CART (DOX) or not (VEH), for a further 72 hours. QRT-PCR was used to examine the consequence SMARCD1 knockdown had on expression of ERα target genes. Mean +/- SEM between 3 independent experiments is plotted. All statistical tests were performed against un-induced, si-CTRL cells, unless stated otherwise with a bar. A two-way ANOVA with Tukey's multiple comparisons post-test was used to calculate statistical significance. * $p<0.05$, ** $p<0.01$, *** $p<0.001$, **** $p<0.0001$, NS – not significant.

5.2.7 Does SMARCD1-knockdown prevent CART from increasing the expression of potential ERα target genes identified from RNA-sequencing?

Work completed in chapter 3 of this study highlighted genes which may be regulated by CART, and may be driven through activation of ERα. We therefore hypothesized that modulation of SMARCD1 expression may reduce the ability of CART to drive the expression of these genes. Two genes (C11ORF80 and ESR1) were chosen from the list of significantly increased genes, and two genes (CAP2 and MYOF) were chosen from the list of genes whose difference was substantial (but not statistically significant) over the vehicle control.

In figure 5.15, we report that none of the selected genes were significantly increased upon CART induction. However, rather than repress the expression of these genes, we found that SMARCD1 knockdown enhanced the expression of two of these genes. Following SMARCD1 knockdown, the expression of *CAP2* was significantly increased in CART expressing cells. Further, *MYOF* expression was significantly increased in both cells expressing CART and not expressing CART. Both results were only noticed in cells transfected with si-1, not si-4.

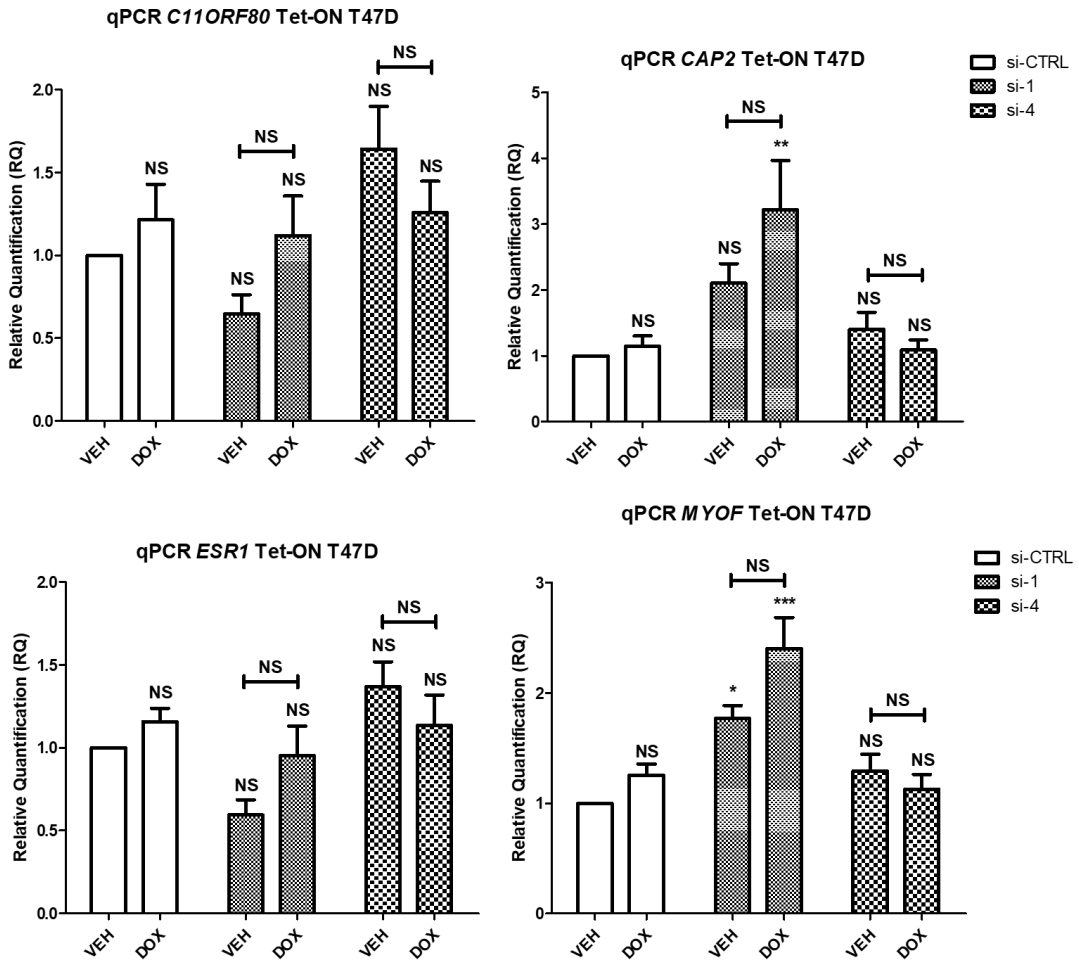

Figure 5.15. SMARCD1 knockdown results in enhanced expression of certain genes identified via RNA-sequencing.

Cells were transfected with SMARCD1 si-1, si-4 or si-NTC. Two days later, cells were either induced to express CART (DOX) or not (VEH), for a further 72 hours. QRT-PCR was used to examine the consequence SMARCD1 knockdown had on expression of genes identified from RNA-seq. Mean +/- SEM between 3 independent experiments is plotted. All statistical tests were performed against un-induced, si-CTRL cells, unless stated otherwise with a bar. A two-way ANOVA with Tukey's multiple comparisons post-test was used to calculate statistical significance. * $p<0.05$, ** $p<0.01$, *** $p<0.001$, **** $p<0.0001$, NS – not significant.

5.2.8 Does SMARCD1-knockdown sensitize breast cancer cells to anti-endocrine therapy?

A previous study highlighted that over-expression of the micro-RNA miR-100 sensitized breast cancer stem cells to anti-endocrine therapy (Petrelli et al., 2015). This study suggested that sensitization to anti-endocrine therapy was potentially due to miR-100 promoting cellular differentiation, and further identified SMARCD1 as a direct target of miR-100. We therefore hypothesized that modulating the expression of SMARCD1 may further sensitize cells to anti-endocrine therapy.

In figure 5.16, we report that knockdown of SMARCD1 does not further sensitize cells to anti-endocrine agents. Indeed, cells transfected with si-1 and treated with 10 μM tamoxifen show a significant decrease in viability compared to si-1 transfected cells treated with DMSO. However, the difference in viability between si-CTRL and si-1 transfected cells, both treated with 10 μM tamoxifen, is not statistically significant. Further, cells transfected with SMARCD1 si-1 show a significant decrease in viability compared to si-CTRL cells treated with either 1 μM tamoxifen or 1 μM fulvestrant. However, the viability of si-1 transfected cells in these treatment conditions is not significantly different to si-1 transfected cells treated with DMSO, again demonstrating SMARCD1 knockdown does not sensitize cells to anti-endocrine agents. No significant differences between si-CTRL and si-4 transfected cells were noted.

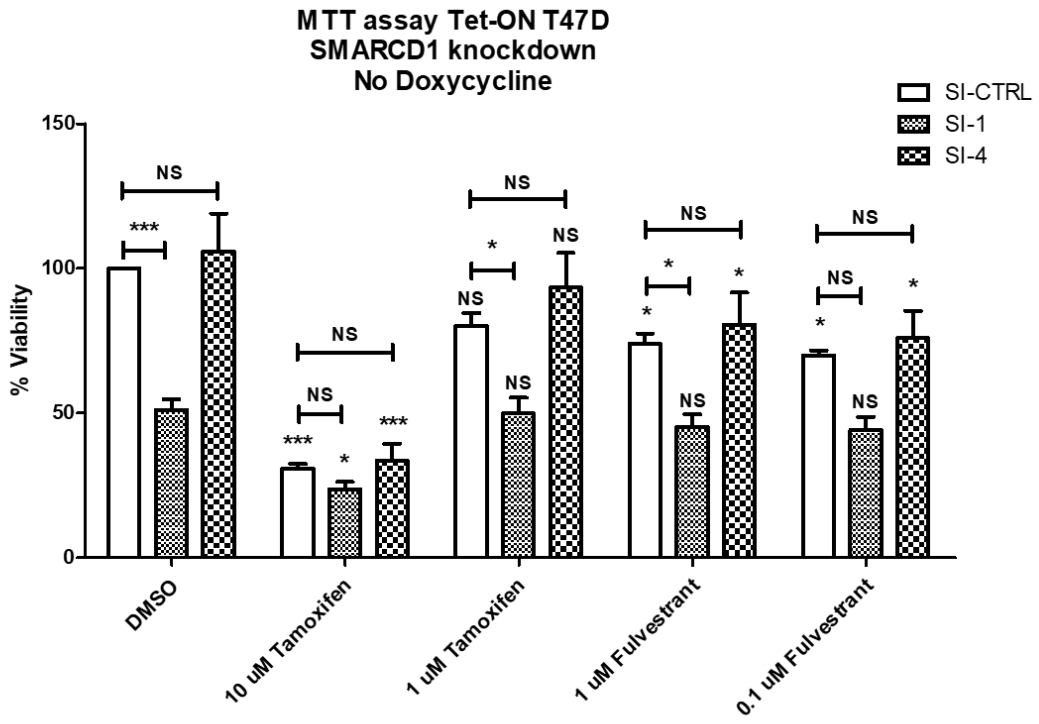

Figure 5.16. Modulation of SMARCD1 expression in un-induced cells does not sensitize cells to anti-endocrine therapy.

Cells were transfected with SMARCD1 si-1, si-4 or si-NTC. Two days later, cells were treated with anti-endocrine agents at the concentrations mentioned above for a further 72 hours. The MTT assay was used to examine cell viability. Mean +/- SEM between 3 independent experiments is plotted. Statistical tests for each siRNA were performed against DMSO treated cells transfected with the corresponding siRNA, unless stated otherwise with a bar. A two-way ANOVA with Bonferroni's multiple comparisons post-test was used to calculate statistical significance. * $p<0.05$, *** $p<0.001$, NS – not significant.

A similar trend to that reported in figure 5.16 is seen in figure 5.17. We could not demonstrate increased cellular sensitivity to either anti-endocrine agents following SMARCD1 knockdown in cells expressing CART, again suggesting that SMARCD1 knockdown does not further sensitize breast cancer cells to anti-endocrine agents.

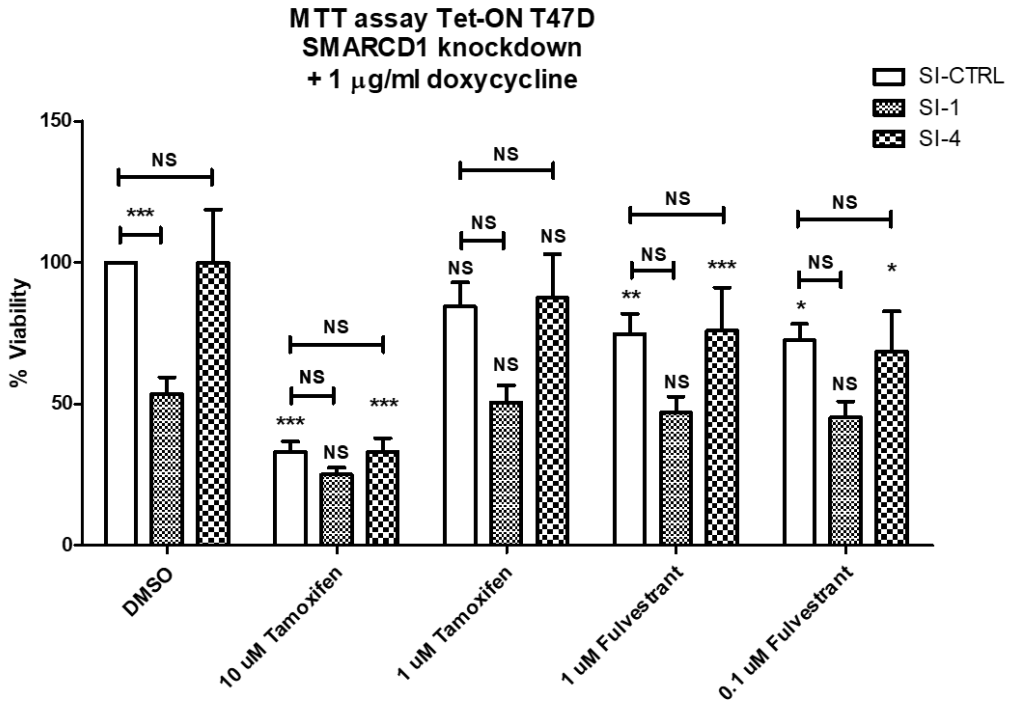

Figure 5.17. Modulation of SMARCD1 expression in DOX-induced cells does not sensitize cells to anti-endocrine therapy.

Cells were transfected with SMARCD1 si-1, si-4 or si-NTC. Two days later, cells were treated with 1ug/ml dox, and treated with anti-endocrine agents at the concentrations mentioned above, for a further 72 hours. The MTT assay was used to examine cell viability. Mean +/- SEM between 3 independent experiments is plotted. Statistical tests for each siRNA were performed against DMSO treated cells transfected with the corresponding siRNA, unless stated otherwise with a bar. A two-way ANOVA with Bonferroni's multiple comparisons post-test was used to calculate statistical significance. * $p<0.05$, ** $p<0.01$, *** $p<0.001$, NS – not significant.

5.2.9 Investigating whether other BAF-complex proteins may play a role in anti-endocrine resistance

Having shown that modulation of SMARCD1 does not further sensitize cells to anti-endocrine therapy, we sought to perform a final investigation into whether any other BAF-complex proteins may play a role in anti-endocrine resistance. The reference samples used were T47D cells from our RNA-sequencing experiment highlighted in chapter 3 (not induced). We compared these values to RNA-sequencing data generated by Ms. Lisa Dwane, who kindly provided raw FPKM values for these genes in the LCC1 and LCC9 cell lines.

The LCC1 cell line was originally derived following passaging of the MCF/MIII cell line through ovariectomized nude mice (Brunner et al., 1993). This cell line is estrogen-independent, but still displays sensitivity to anti-endocrine therapy (Brunner et al., 1993). Following stepwise selection against increasing doses of fulvestrant, the LCC1 cell line gave rise to the LCC9 cell line, which is not only estrogen independent, but also exhibits a resistant phenotype to both fulvestrant and tamoxifen (Brunner et al., 1997). The T47D cell line is considered estrogen sensitive, and anti-endocrine sensitive. This approach identified 2 members of the BAF complex (SMARCB1 & SMARCD2) whose expression is significantly increased in the LCC9 cell line when compared against both the LCC1 and T47D cell line (figure 5.18).

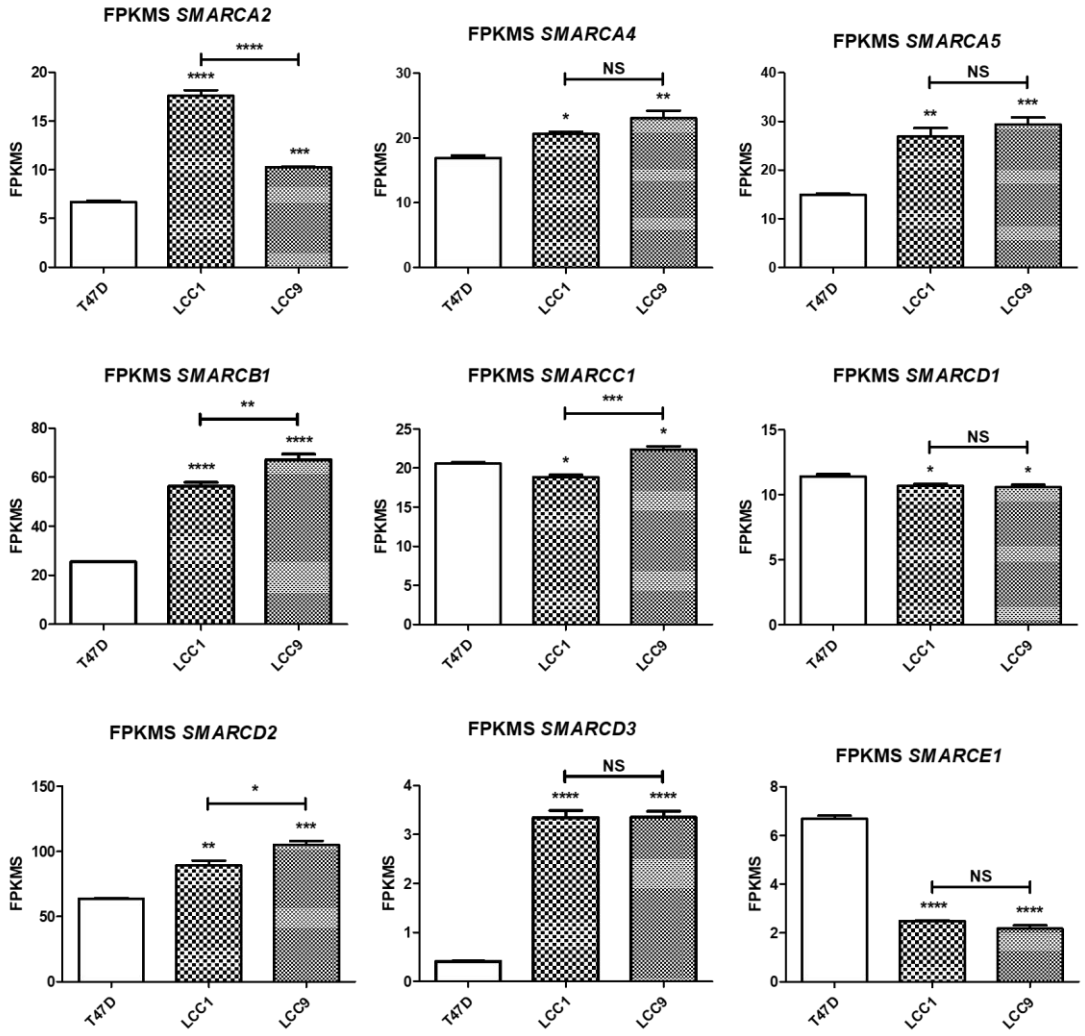

Figure 5.18. Members of the BAF-chromatin remodelling complex are upregulated in anti-endocrine resistant cell-line models.

Raw FPKMS values from RNA-seq data was used to examine the expression of various BAF-chromatin remodelling complex subunits across three cell lines. Mean +/- SEM between 3 independent experiments is plotted. All statistical tests were performed against T47D cells unless stated otherwise with a bar. A one-way ANOVA with Tukey's multiple comparisons post-test was used to calculate statistical significance. * $p<0.05$, ** $p<0.01$, *** $p<0.001$, **** $p<0.0001$, NS – not significant.

5.3 Discussion

5.3.1 SMARCD1 as a marker of poor prognosis in breast cancer

SMARCD1 expression has been associated with poor prognosis in a number of studies, both within breast cancer as well as in a number of different cancers. An impressive study in 2011 brought attention to the fact that SMARCD1 is frequently amplified in lung cancer (Malovannaya et al., 2011). In 2014, SMARCD1 was characterized as a target for miR100 (Deng et al., 2014). The authors reported that modulating the expression of SMARCD1 altered the growth of breast cancer cells both in vitro and in vivo, and further characterized that high expression of SMARCD1 was significantly associated with shorter survival times of patients (Deng et al., 2014). In 2015, a study demonstrated that SMARCD1 expression was markedly upregulated in gastric cancer, and high expression of SMARCD1 was associated with shortened patient survival (Shen et al., 2015). This study further characterized that forced expression of SMARCD1 promoted oncogenic phenotypes of gastric cancer cells both *in vitro* and *in vivo,* and notably, the opposite was seen when SMARCD1 expression was reduced via knockdown (Shen et al., 2015).

Analysis of SMARCD1 expression in our study was consistently in line with these aforementioned studies. We report that *SMARCD1* mRNA expression was significantly associated with worse overall survival in two independent cohorts of breast cancer patients. We also highlight that *SMARCD1* copy number status is significantly associated with worse survival in one of our cohorts of patients. A clear trend was demonstrated in which SMARCD1 protein expression was also associated with worse survival. Finally, we felt it to be of importance to examine the expression of SMARCD1 in both p53 wild-type and p53-mutant breast cancer patients. This was performed as a number of studies have previously characterized SMARCD1 to be a critical mediator of p53 function (Oh et al., 2008, Hong et al., 2016). Surprisingly, high expression of SMARCD1 strongly indicates worse survival in p53-mutant breast cancer patients. Because p53 mutations can result in both p53 redundancy, as well as drive oncogenic p53 signalling, it would be interesting

to examine whether high expression of SMARCD1 facilitates in the oncogenic signalling of p53. Indeed, a study published in 2015 has demonstrated mutant p53 can cooperate with the BAF-chromatin remodelling complex to regulate its transcriptional activity (Prives et al., 2015). It would be fascinating to interrogate the expression of SMARCD1 in mutant p53 cell line models. Further, characterizing whether SMARCD1 cooperated with mutant p53 for transcriptional activity may identify a key mechanism by which SMARCD1 acts in an oncogenic manner in p53 mutant breast cancer, and is certainly an aspect to be considered for future investigation.

The data presented thus far is in strong agreeance with other studies, indicating that SMARCD1 drives oncogenic phenotypes in multiple models of cancer. We feel our data strongly implicates SMARCD1 as a prognostic biomarker in breast cancer, and would certainly warrant a future investigation into the expression of SMARCD1 in multiple cohorts of breast cancer patients. It would be fascinating to examine the expression of SMARCD1 across multiple models of breast cancer (pre-menopausal vs post-menopausal patients for example), investigate whether SMARCD1 is implicated in other subtypes of breast cancer, or whether the expression of SMARCD1 indicates poor response to multiple therapeutic regimes (such as chemotherapy, or additional anti-endocrine therapeutics).

5.3.2 SMARCD1 as a mediator of breast cancer growth, and ERα function

Members of the BAF chromatin remodelling complex have long been understood to mediate critical interactions with nuclear hormone receptors such as ERα. One of the first examples of this was highlighted in a study published in 1994. This early study highlighted that transcriptional activity of ERα was increased following co-expression of hSNF2α (SMARCA2) and hSNF2β (SMARCA4) (Chiba et al., 1994). In 2002, proof of a physical interaction between ERα and SMARCD1 emerged (Hsiao et al., 2003). Given our clinical data generated in 5.2.1 and 5.2.2, and the aforementioned studies suggesting SMARCD1 may mediate oncogenic phenotypes in various

cancers, we hypothesized that modulating the expression of SMARCD1 would have a significant impact on breast cancer cells.

We first noticed that the morphology of cells was altered upon knockdown of SMARCD1 (figure 5.13). However, this was only seen in one of the si-knockdown cell lines. The altered morphology of cells was in agreeance with data from the literature, suggesting that modulating SMARCD1 leads to smaller, narrower cells with shrunken cytoplasmic regions (Alajem et al., 2015). This would suggest that SMARCD1 si-4 knockdown, despite achieving a more efficient knockdown, is not representative of what the literature suggests. This is a common issue for all preceding experiments, and represents a key factor that will need to be addressed before any conclusions can be definitively drawn from our data. Next, we found that knockdown of SMARCD1 could impact the growth of the Tet-ON T47D cell line (figures 5.14). Again, this was only reported in si-1, and not si-4, transfected cells. The significant impact on cell growth in si-1 transfected cells was only seen in cells treated with estrogen, perhaps suggesting SMARCD1 is an important mediator of estrogen-dependent growth. However, while the growth of untreated cells was not significantly decreased, they followed a very similar trend to the estrogen treated cells. Taken together, we feel SMARCD1 is an important factor for the growth of ER+ breast cancer cells, and our data is certainly in agreeance with data from studies in both breast (Deng et al., 2014) and gastric (Shen et al., 2015) cancer, both of which characterized SMARCD1 as an important factor in cancer growth.

As mention in section 5.3, we found SMARCD1 to be recruited to ERα in cells expressing CART (chapter 4). Previously published data suggests SMARCD1 is a critical mediator of ERα function (Hsiao et al., 2003), and our data (figure 5.14) suggests SMARCD1 may be an important mediator of estrogen-dependent growth. Taking this together, we hypothesized that SMARCD1 knockdown may impact the ability for CART to increase the expression of ERα target genes. To test this hypothesis, we examined the effect SMARCD1 knockdown had on the ability for CART to increase the expression of *CCND1* and *PKIB*. Both *CCND1* (Cicatiello et al., 2004) and *PKIB* (Dahlman-Wright et al., 2012) are ERα target genes, and were previously shown to be increased

in cells expressing CART (chapter 3). Data presented in figure 5.15 suggests that levels of CCND1 were increased in cells expressing CART, however, there was no difference in the expression of CCND1 following SMARCD1 knockdown. Contrastingly, levels of PKIB were diminished following SMARCD1 si-1 knockdown (again, this trend was not noticed in the si-4 group). Following SMARCD1 knockdown (si-1), levels of PKIB were significantly reduced in the presence, and absence, of CART when compared to si-CTRL cells expressing CART. This trend was not noticed when levels of PKIB were compared against si-CTRL cells not expressing CART, possibly suggesting that SMARCD1 is indeed an important factor in the ability for CART to alter the function of ERα.

To further our understanding of the relationship between CART, ERα and SMARCD1, we examined whether modulating the expression of SMARCD1 had any impact on the ability for CART to increase the expression of genes identified from RNA sequencing in chapter 3. We chose to examine the expression of *C11ORF80* and *ESR1* from our list of significantly differentially expressed genes, and *CAP2* and *MYOF* from our list of top 200 different genes based on FPKMS difference. Disappointingly, none of these genes were significantly increased in cells expressing CART. This is in direct contradiction to chapter 3, which showed these genes should be increased in cells expressing CART. However, while the RNA sequencing was performed under hormone-stripped conditions, these experiments were completed in full growth medium. The estrogen present in the medium may be impacting CARTs ability to increase the transcription of these genes, and so repeating these experiments under hormone-stripped conditions would certainly represent the clearest path forward from this. Despite CART not increasing the expression of these genes in the si-CTRL wells, a fascinating observation was made, whereby SMARCD1 knockdown enhanced the expression of both *CAP2* and *MYOF*. It is interesting to point this out, as the BAF chromatin remodelling complex is known to mediate both transcriptional activation, as well as repression, in a gene specific manner (Trotter et al., 2008). It is entirely possible, then, that SMARCD1 may act to repress the expression of certain genes under normal growth medium conditions. This makes further sense

when these data are taken into consideration when viewing the effect SMARCD1 knockdown had on the expression of *CCND1* and *PKIB* (figure 5.15). SMARCD1 knockdown had no effect on *CCND1* expression, but did alter *PKIB* expression. It would appear, then, that SMARCD1 may mediate the expression or repression of genes in a gene-specific manner, and may highlight a fascinating interplay between CART and ERα in the balance of transcriptional activation and repression.

Repeating these experiments under hormone-stripped conditions would certainly be the first aspect of further investigation. Next, if the ERα ChIP-seq experiment recommended in section 3.3 was to be completed, it would be fascinating to perform ChIP to prove ERα occupancy at these promotor regions, and ChIP-re-ChIP to test whether SMARCD1 is present at these sites or not. Further, a SMARCD1 ChIP-seq may also be beneficial, and could be combined with data from the ERα ChIP-seq experiment to determine genes which may be controlled by both factors. These data could further be compared with our RNA-seq data (chapter 3) to understand what genes may be actively transcribed/repressed. Taken together, this data implements SMARCD1 as a mediator of breast cancer growth, and an important factor for the function of ERα.

5.3.3 Aberrant expression of BAF-chromatin remodelling complexes in cell-line models of anti-endocrine resistance

The roles BAF-chromatin remodelling complexes, and specifically SMARCD1, plays in anti-endocrine resistance is a poorly understood mechanism. One of the first studies to highlight a potential link between BAF protein complex expression with anti-endocrine resistance was published only 4 years ago (Giessrigl et al., 2013). In this study, the authors highlighted increased expression of five subunits of the BAF complex in a fulvestrant resistant cell line model derived from MCF7 cells (BRG1 (SMARCA4), BAF250A (ARID1A), BAF170 (SMARCC2), BAF155 (SMARCC1) and BAF47 (SMARCB1)). The authors of the study eloquently suggest that increased expression of these complexes may alter nucleosome positioning and redistribute histone

octamers, ultimately resulting in aberrant gene expression and may be a mechanism of fulvestrant resistance (Giessrigl et al., 2013). Shortly after this study, another group highlighted that miR-100 sensitized basal-like breast cancer stem cells to hormone therapy (Petrelli et al., 2015). This was of particular interest to us, as this study characterized SMARCD1 as a target of miR-100. Consequently, we hypothesized that modulating the expression of SMARCD1 may further sensitize cells to anti-endocrine therapy.

While we did notice cells responding better to certain treatment conditions (such as 1 μM tamoxifen) following SMARCD1 si-1 knockdown, the difference in viability between the treatment cells and the cells that received DMSO vehicle control did not significantly differ. This would suggest that modulating SMARCD1 expression does not sensitize these cells to anti-endocrine therapy. There are, however, a number of additional studies which could be used to address this further. For example, rather than using cell lines transiently overexpressing an siRNA targeting SMARCD1, stable knockdown (shRNA) or stable knockout (CRISPR) cell lines could be created to allow for longer-term assays. Preceding this, cells could be exposed to low doses of hormonal therapy over long periods of time to see if this further sensitizes cells to anti-endocrine therapy.

Importantly, these cell lines are ultimately anti-endocrine sensitive. The study which highlighted miR-100 sensitizing cells to anti-endocrine therapy was performed in basal-like breast cancer stem cells, which are not typically responsive to anti-endocrine therapy (Petrelli et al., 2015). Because of this, we analysed the expression of SMARCD1, as well as eight other members of the BAF-chromatin remodelling complex across the LCC1 and LCC9 cell lines. The expression was compared to T47D cells, which is certainly a modest flaw of this study, as these cell lines were not derived from T47D cells. Indeed, they were derived from MCF7 cells (Brunner et al., 1994, 1997), however, transcriptomic data was unavailable for these cells, and so the T47D cell line was used instead. To account for this minor flaw, it was agreed that for a gene to be considered an appealing future target, it’s expression must differ between all three cell lines.

Remarkable similarities were noticed with the expression of these proteins, and a study mentioned previously which linked BAF proteins with anti-endocrine resistance (Giessrigl et al., 2013). The aforementioned study found SMARCA4, SMARCB1, SMARCC1 and SMARCC2 to be increased in a cell line model of fulvestrant resistance. In our data, SMARCA4 was found to be significantly upregulated in both the LCC1 and LCC9 cell lines when compared to T47D cells, and a similar trend was seen for an increased expression between the LCC1 and LCC9 cell lines. SMARCB1 and SMARCC1 were both found to be significantly higher in the LCC9 cell line compared to the LCC1 cell line, but only SMARCB1 was found to be significantly increased across all three cell lines. This is an important finding, as SMARCB1 was found to be recruited to ERα by CART. Ultimately, it was excluded from our final list of interactors due to a weak signal for SMARCB1 in the IgG negative control samples. This is discussed further in chapter 6 of this study, but we feel that proteins such as SMARCB1 may still worthy of further investigation due to the huge difference between ERα IP lanes and IgG IP lanes. It would be intriguing to examine if, through mediating interactions between ERα and SMARCB1, CART drives a resistant phenotype. The interaction between these proteins and ERα would first need to be validated by conventional Co-IP assays. Repeating the above experiments using SMARCB1 as the target for siRNA would certainly be the first step forward. Additionally, it would be exciting to perform these knockdowns in the LCC9 cell line, as it already exhibits a robustly resistant phenotype to tamoxifen. While this would more than likely not involve CART, it is certainly a future study which should be considered.

In terms of SMARCD1 expression in these cell lines, we did not notice any distinguishable difference between the LCC1 and LCC9 cell lines. While this does not rule out a potential role for SMARCD1 in anti-endocrine resistance, it does make it less likely given the differential expression of other subunits such as SMARCB1. However, given the impressively positive data generated thus far for SMARCD1, we feel it would be extremely interesting to examine the effect SMARCD1 knockdown has on either the LCC1 and LCC9 cell lines.

Chapter 6. General Discussion

6.1 Key findings

While the survival rates for breast cancer are most certainly on the rise, it is still unfortunate to know that a significant proportion of patients will regrettably succumb to their disease. Molecular and pathological classification of breast cancer certainly aids in the identification of appropriate treatment regimens for patients, but research into why certain patients do not respond well to their therapy is still of vital importance to cancer research.

Initially, CART was identified as a marker of poor prognosis in ER+, lymph node-negative breast cancer (Brennan et al., Oncogene 2012). We found that CART treatment could increase the expression of common ERα target genes, and this increase in ERα gene targets was clinically validated in both the TCGA and METABRIC dataset.

Owing to the identified relationship between CART and ERα, and the fact that no research has currently mapped the transcriptional landscape of CART expressing cells, we used RNA sequencing to address this. We also utilized publicly available ERα ChIP-seq data to identify whether ERα binding events had previously been reported for these genes. Crucially, this data highlighted that genes upregulated by CART have previously been classified as potential ERα target genes, and indeed, both genes upregulated and downregulated by CART were found to have ERα binding events at transcription factor binding sites associated with these genes. These data suggested to us that CART may impact the interactome of ERα, and targeting these binding partners may present with an exciting opportunity for identifying targets capable of diminishing ERα activity.

Our mass spectrometry analysis identified members of the BAF chromatin remodelling complex to be associated with ERα in the presence of CART. We suggest that CART expression may result in the recruitment of chromatin remodelling complexes to ERα in order to facilitate ERα chromatin binding events. Our review of available literature suggested that SMARCD1 had been implemented as a marker of worse survival in multiple cancers, and was a critical mediator of nuclear receptor function. Consequently, we hypothesized

that modulating the expression of SMARCD1 may be a rational strategy for impeding ERα function.

Interestingly, high SMARCD1 expression was found to be significantly associated with worse survival in two independent cohorts of breast cancer patients. Modulation of SMARCD1 expression resulted in both altered growth, and morphology, of breast cancer cells. Furthermore, SMARCD1 knockdown highlighted that SMARCD1 may act in a gene-specific manner to enhance, or repress, transcription. Finally, while modulating the expression of SMARCD1 did not further sensitize our cells to anti-endocrine therapy, subsequent analysis of the expression of chromatin remodelling complexes in cell line models of anti-endocrine resistance identified 2 BAF complex subunits which are certainly worthy of further investigation.

Though the above passage represents the “key findings” of our study, we also identified a number of exciting paths worthy of further investigation which may aid in understanding the role of CART in breast cancer. These are appropriately discussed further in section 6.2.

To conclude our key findings, we suggest that CART recruits members of the BAF chromatin remodelling complex to ERα in order to facilitate transcriptional activity, and SMARCD1 represents a powerful prognostic factor which appears to be key factor for the normal function of ERα in ER+ breast cancer.

6.2 Future directions

When discussing the future directions of this study, it is hard to deny that the most fruitful experiment to perform would be a chromatin immunoprecipitation sequencing (ChIP-seq) experiment. ChIP-seq has been discussed in section 4.1.2 of this study, however, elaborating on the benefit this technique could have on this study is worthy of further discussion. First, an ERα ChIP-seq experiment would be invaluable for the data generated from our RNA-seq studies. We utilized publicly available ERα ChIP-seq data to highlight ERα binding events pertaining to many of the differentially expressed genes identified in response to CART. However, given that an investigation into the

precise effect CART can have on the chromatin binding events of ERα has never been completed, it is impossible to say with absolute certainty that ERα is controlling the expression of these genes. Even though ERα binding events were identified in regions pertaining to these genes in response to estrogen, it is entirely possible that CART may direct other transcription factors to these genes. Likewise, just because ERα binding events were not identified in other differentially expressed genes, this does not mean that these are not controlled by ERα in response to CART. Overlapping an ERα ChIP-seq experiment with our RNA-sequencing data would allow us to identify the precise genes which are regulated by ERα in response to CART, and this would undoubtedly provide us with invaluable insight into the complex relationship between CART and ERα.

If a ChIP-seq experiment was to be undertaken, I feel it would also be extremely beneficial to perform a SMARCD1 ChIP-seq experiment. The ability to overlap an ER ChIP-seq experiment with a SMARCD1 ChIP-seq experiment would identify key binding sites shared by both factors in the presence of CART. These targets could be compared to our generated RNA-seq data to examine what genes are actively transcribed or repressed by this complex, and would aid in understanding the balance between transcriptional activation/repression governed by this complex. It would be further intriguing to investigate the overlap of binding events between SMARCD1 and ERα, given that SMARCD1 knockdown does not appear to sensitize breast cancer cells to anti-endocrine therapy. It is possible that SMARCD1 may not represent the best target when investigating the potential role BAF complex proteins play in anti-endocrine resistance. Indeed, a number of other chromatin remodelling complex subunits were identified within this study to be upregulated in a cell line model of anti-endocrine resistance. Two of these (SMARCB1 and SMARCC1) were also highlighted in a previous study to be upregulated in a model of fulvestrant resistance. Interestingly, there is overlap between ERα and SMARCB1 & SMARCC1 binding events in the TCGA dataset (figure 6.1). Unfortunately, SMARCD1 was not a selectable target in this dataset, and so the overlap between SMARCD1 and ERα binding events remains elusive.

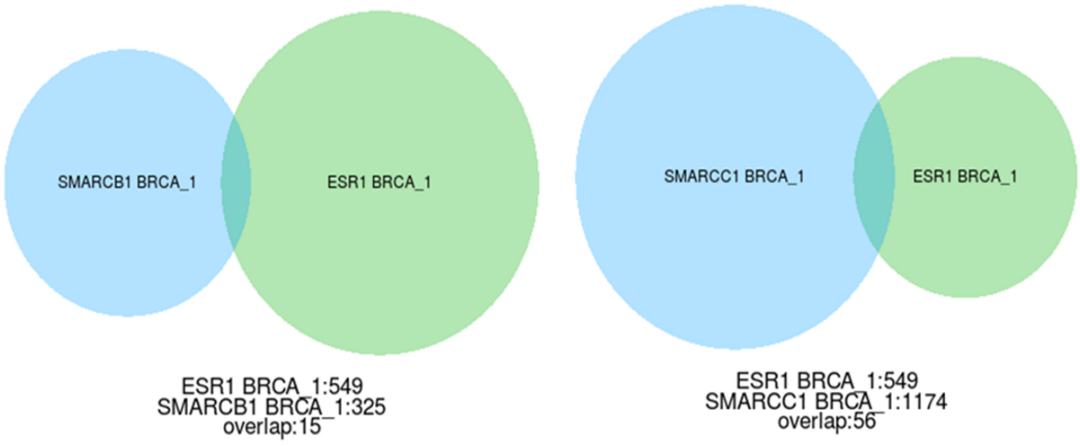

Figure 6.1. An overlap in transcription factor binding events is seen between ERα and SMARCB1, as well as between ERα and SMARCC1. Data was obtained through the Cistrome cancer browser (cistrome.org/CistromeCancer).

It would be exciting to confirm whether SMARCB1 and SMARCC1 are recruited to ERα in response to CART. Interestingly, both SMARCB1 and SMARCC1 were found to be enriched in cells expression CART in our ERα IP-mass spec experiment, however, they were initially filtered out of the final list due to a signal present for these proteins in the IgG control (and therefore, were not validated). The signals pertaining to these proteins in the IgG control are substantially lower than the signals detected in the ERα IP samples, and so perhaps the most logical way forward with this is to test, via low-throughput Co-IP assays, if these are indeed recruited to ERα in response to CART. Furthermore, modulating the expression of SMARCD1, as well as both SMARCB1 and SMARCC1, in a cell line model of anti-endocrine resistance (LCC9 for example) and testing whether this re-sensitized cells to anti-endocrine therapy may also be of benefit.

The discovery that high SMARCD1 expression indicated worse survival in p53 mutant, but not p53 wild-type, breast cancer patients was fascinating. As described in section 6.1.2, the role BAF-complexes play in cancer is complicated, and is often context dependent. A recent study highlighted that mutant p53 can still cooperate with the BAF complex to mediate transcriptional

activity (Pfister et al., 2015). These key pieces of information infer the possibility that SMARCD1 may act as an oncogene in p53-mutant breast cancer, but not in p53 wild-type breast cancer. Our data suggests that high expression of SMARCD1 indicates worse survival in these patients, and so may represent a prognostic tool for characterizing high-risk p53-mutant breast cancer patients. Indeed, a significant body of work is still necessary to prove this. For our future directions, we aim to characterize whether SMARCD1 interacts with p53 of varying mutational backgrounds. Further, we aim to understand the exact consequence that arises from this potential interaction by modulating the expression of SMARCD1 in these cell lines. Finally, we aim to further our understanding of SMARCD1 expression in these patients by staining large tissue microarrays (TMA) for both p53 wild-type and p53-mutant breast cancer patients. With these experiments, we hope to understand whether SMARCD1 acts in an oncogenic fashion in p53 mutant breast cancer, and whether targeting SMARCD1 is a rational therapeutic strategy for this type of cancer.

In cells expressing CART, ERα IP-mass spec also identified two novel ERα interactors. Both HECTD4 and WIZ have, to our knowledge, never been reported as ERα interactors. This was an extremely exciting finding, however, issues were encountered when validation of these interactions was attempted. A band corresponding to WIZ was detected in ERα IP samples expressing CART, and no band was detected in cells not expressing CART. However, the presence of a band in the IgG control made this impossible to classify WIZ as a specific interactor. HECTD4 has a reported molecular weight of 440 kDa, and so perhaps a modified western blot protocol would need to be considered to allow for successful transfer of HECTD4. An immunocytochemical co-localisation study could also be used to see, in the presence of CART, whether HECTD4 and WIZ co-localize with ERα. If WIZ and ERα were to co-localise, this would more than likely occur in the nucleus given WIZ's role as a zinc-finger protein. Following validation, perhaps a WIZ ChIP-seq experiment could be used to elucidate whether WIZ interacts with ERα to redirect chromatin binding events. Further, given that WIZ is a known transcription factor itself, it

is possible that CART may re-direct WIZ-chromatin binding events through an interaction with ERα, as well as re-directing ERα chromatin binding events through an interaction with WIZ. This has been summarised in figure 6.2.

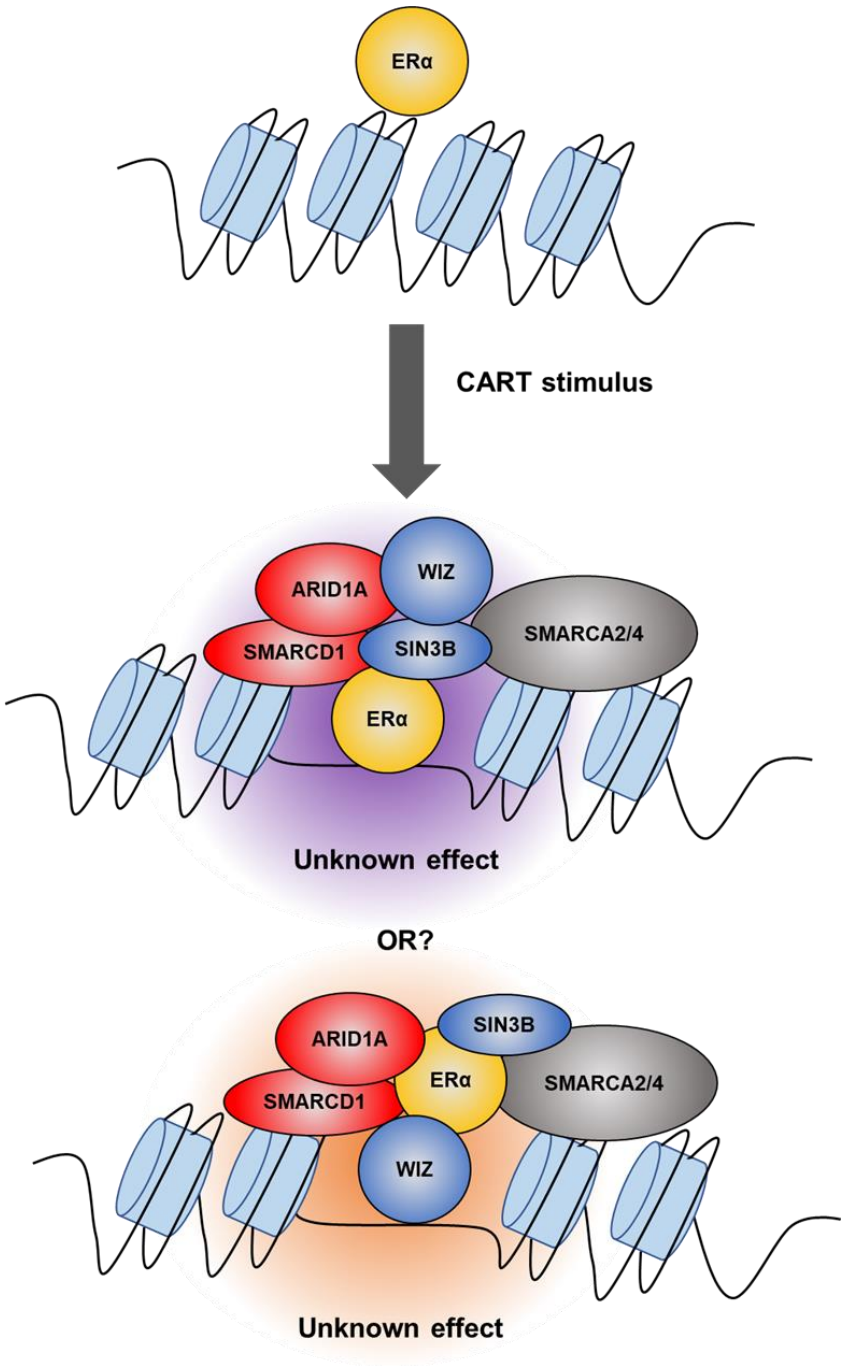

Figure 6.2. Possible models for how ERα interacts with WIZ

Initially, we suspected that an interaction between ERα and HECTD4 may result in the increased turnover of ERα. Surprisingly, however, we found that levels of ERα appeared to be maintained longer in the presence of CART.

While this does not prove HECTD4 increases the stability of ERα, it may be an area worthy of further investigation. However, another angle that may prove fruitful is the possibility that HECTD4 acts as a CART-driven coactivator of ERα. While HECTD4 itself is quite understudied, another member of the same family, HECTD1, has been characterized as an activator of ERα at enhancer regions (Li et al., 2015). Within this study, the authors highlighted that condensins recruit HECTD1 to active enhancer regions to modulate the binding of enhancer-associated coactivators/corepressors to facilitate coding gene activation (Li et al., 2015). Furthermore, both P300 and RIP140 were identified as targets capable of being ubiquinated by HECTD1, and HECTD1 ChIP-seq revealed the presence of HECTD1 binding events at genomic loci pertaining to ERα gene targets, such as *GREB1*, *TFF1* and *PGR*. HECTD1 was also characterized as an ERα interactor. It is tempting to speculate then, that CART may promote an interaction between ERα and HECTD4 to act in a similar manner to HECTD1. If this were to be true, HECTD4 would certainly represent a very attractive therapeutic target moving forward, especially given that *HECTD4* expression is significantly higher in ER+ breast cancer, and correlates with poor overall survival (figure 6.3).

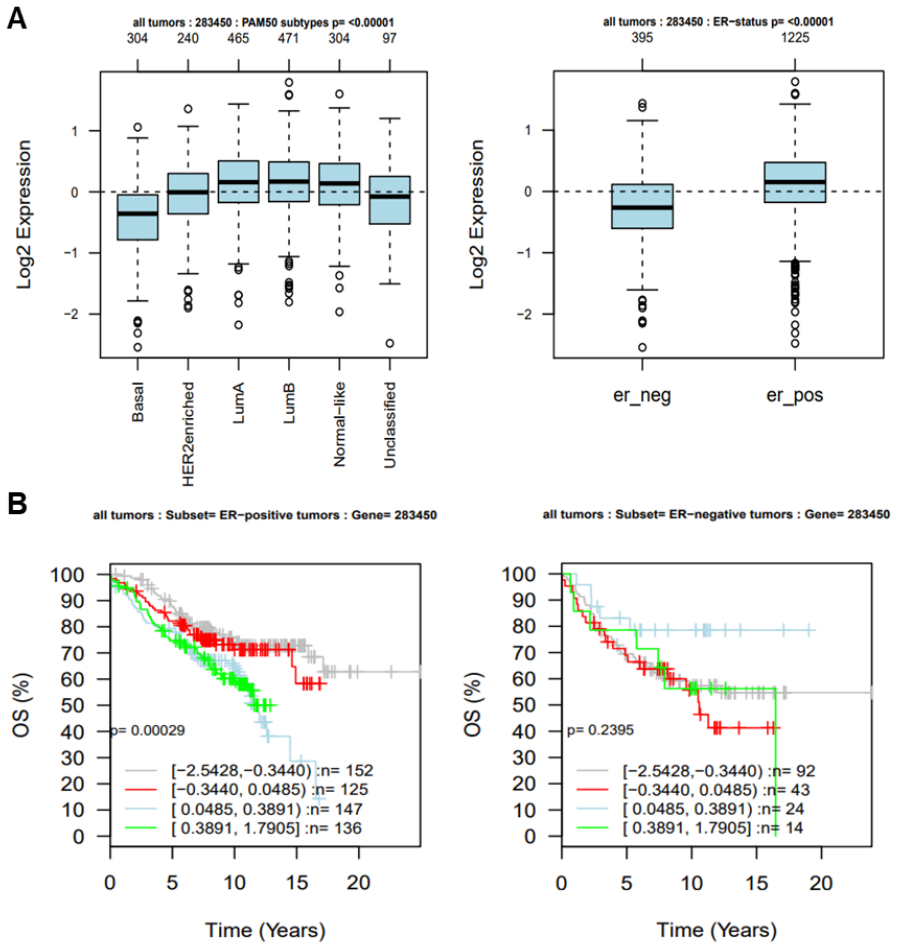

Figure 6.3. *HECTD4* expression is significantly higher in ER+ breast cancer, and correlates with poor survival.

A. Expression of *HECTD4* in PAM50 molecular subtypes of breast cancer, and in ER+/ER- breast cancer patients **B.** Survival data for HECTD4 expression in ER+ and ER- breast cancer patients. **Gene = 283450 refers to the entrez gene ID for *HECTD4*.**

We demonstrated in chapter 4 of this study that we could successfully immunoprecipitate CART in our inducible-cell line model. There is currently no evidence in the literature of a large-scale investigation into the CART interactome. Indeed, one study has highlighted that CART can interact with, and enhance the function of, Succinate Dehydrogenase 2 (SDH2) (Mao et al., 2007). This was identified through a yeast two-hybrid screen a decade ago, yet no more information pertaining to the interacting partners of CART has

been uncovered. We demonstrated the power of IP-mass spec in chapter 4 of this study, and so perhaps this presents an exciting opportunity for identifying the interactome of CART. Understanding the protein networks that CART can influence would undoubtedly provide us with extensive insight into the role of CART in breast cancer, and may even benefit the broader community of scientific researchers dedicated to studying CART in other diseases.

While all cancers are distinctly different to one-another, a certain collection of shared traits are known to exist between them. These have been termed the defining “Hallmarks of Cancer” (Hanahan et al., 2011). One of these hallmarks is the ability for the cancer cell to “activate invasion and metastasis”. RNA sequencing data generated in chapter 3 of this study suggested that CART may indeed contribute to this hallmark of cancer for a number of reasons. First, a proportion of downregulated genes were found to be significantly associated with cell to cell adhesion. As discussed in section 3.3, a loss of the cell adhesion molecule E-cadherin is one of the defining molecular hallmarks of invasive lobular carcinoma. While E-cadherin was not among the genes downregulated by CART, it is important to highlight E-cadherin loss as this demonstrates loss of cell adhesion molecules can contribute to a more invasive cancer. Interestingly, CART has previously been shown to enhance the migratory abilities of subventricular zone cells from the contralateral subventricular zone to the ischemic cortex in a model of Stroke in rats (Luo et al., 2013). Furthermore, the long non-coding RNA *MALAT1* was seen to be upregulated by CART. *MALAT1* (Metastasis Associated Lung Adenocarcinoma Transcript 1) has been demonstrated, in numerous studies, to contribute to cancer metastasis (Gutschner et al., 2013, Zhou et al., 2015). Therefore, it may be of benefit to examine whether CART can contribute to invasion/metastasis using MatriGel invasion assays, and whether a change in the invasive capabilities could be attributed to CART increasing the expression of *MALAT1*, or decreasing the expression of genes associated with cell-cell adhesion.

The ability for tumours to form new blood vessels in order to facilitate growth and enhance nutrient availability is another defining hallmark of cancer, termed Angiogenesis. Our current research did not suggest CART may play a role in angiogenesis, however, evidence within the literature suggests that CART does indeed promote angiogenesis (although this has not yet been proven within the field of cancer). A study published in 2016 recognised that, following introduction of an artificial stroke to adult rats, post-treatment of CART significantly induced angiogenesis as a mechanism of vascular repair (Liu et al., 2016). Given the sheer importance of angiogenesis in cancer, I feel that this is certainly an aspect worthy of further investigation. The use of an angiogenesis-marker ELISA array, combined with a tube-formation assay may represent an appropriate manner for measuring the angiogenic potential of CART *in vitro*. An *in vivo* angiogenesis study would certainly represent the gold-standard for investigating this hypothesis, but significant *in vitro* data would be vital before this could be considered.

One aspect of CART which was not investigated in this study is whether CART confers sensitivity/resistance to aromatase inhibitors (AIs). AIs were introduced in chapter 1 of this study. Briefly, AIs (eg. letrozole) function by blocking the conversion of pre-estrogen hormones to estrogen, by blocking the action of the aromatase enzyme. CART may have a significant impact on sensitivity to aromatase inhibitors, given the link between CART and body mass. Obesity is known as a risk factor for breast cancer, potentially related to the increased expression of aromatase in adipose tissues, which would allow for higher levels of estrogen to stimulate breast cancer growth. A systematic review in 2014 suggested that the efficacy of AIs is diminished in obese patients (Ioannides et al., 2014), however, the authors were clear that further clinical studies are needed before drawing definitive conclusions. The role of CART in obesity was discussed in detail in section 1.2.4 of this study, but briefly, while CART can indeed function as an anorectic neuropeptide, it's expression can still remain high in obese subjects. Furthermore, leptin (which is known to be produced by adipose tissue) has previously been shown to increase CART levels in mice (Kristensen et al., 1998), and enhance the

expression of aromatase in MCF7 cells (Catalano et al., 2003). A study in ovarian granulosa cells, published in 2016, agreed that leptin could increase the expression of CART, but disagreed with the idea that leptin increased aromatase expression (Ma et al., Endocrinology 2016). In fact, this study demonstrated that both leptin and CART significantly decreased the expression of aromatase. Furthermore, the authors showed that CART expression positively correlated with body-mass index (BMI) in women (Ma et al., 2016). Indeed, a previous study had already demonstrated that CART diminished aromatase expression in bovine granulosa cells (Sen et al., 2007). A possible reason for the discrepancy in results may be due to groups working in different tissue sources, however, the presented evidence suggests that a link between CART, BMI and aromatase expression may exist. This presents with a fascinating opportunity to examine whether CART confers sensitivity/resistance to this type of therapy. Perhaps examining CART expression in a cohort of AI treated patients, and investigating whether CART expression correlated with survival would address this.

Further, the studies mentioned above may aid in understanding why patients with high levels of CART respond poorly to tamoxifen. The same group that identified CARTs ability to diminish aromatase expression in bovine granulosa cells also suggested that CART administration potently inhibits estradiol production in bovine granulosa cells (Sen et al., 2007, Lv et al., 2009). The authors of these studies suggest that CART negatively regulates the production of estradiol, as well as aromatase, as a mechanism of dominant follicle selection (Lv et al., 2009). This raises the intriguing possibility that, in breast cancer patients with high levels of CART, estradiol production is diminished, resulting in an ER+ breast cancer that adapts to estrogen-independent growth, and so may not respond as well to anti-endocrine therapy. Indeed, our RNA sequencing results suggested that CART could increase the expression of *ELF5*, a transcription factor previously implemented in reduced estrogen sensitivity (Kalyuga et al., 2012), and acquired tamoxifen resistance (Kalyuga et al., 2012, Fitzgerald et al., 2016).

Finally, it is tempting to speculate that a potential role for CART in breast cancer may lie within the tumour microenvironment. CART is known to protect neurons against oxidative stress in neuronal cells deprived of glucose and oxygen (Sha et al., 2013, Sha et al., 2014). Further, CART has been implemented as a potential antioxidant which may play a role in protecting not only mitochondrial DNA, but also cellular macromolecules such as proteins and lipids, against oxidative stress (Mao et al., 2012). Given that tumour microenvironments can be extremely hypoxic, it is tempting to suggest that CART, through protecting cells against oxidative stress, provides the tumour with a competitive advantage for survival. This has been summarised in figure 6.4.

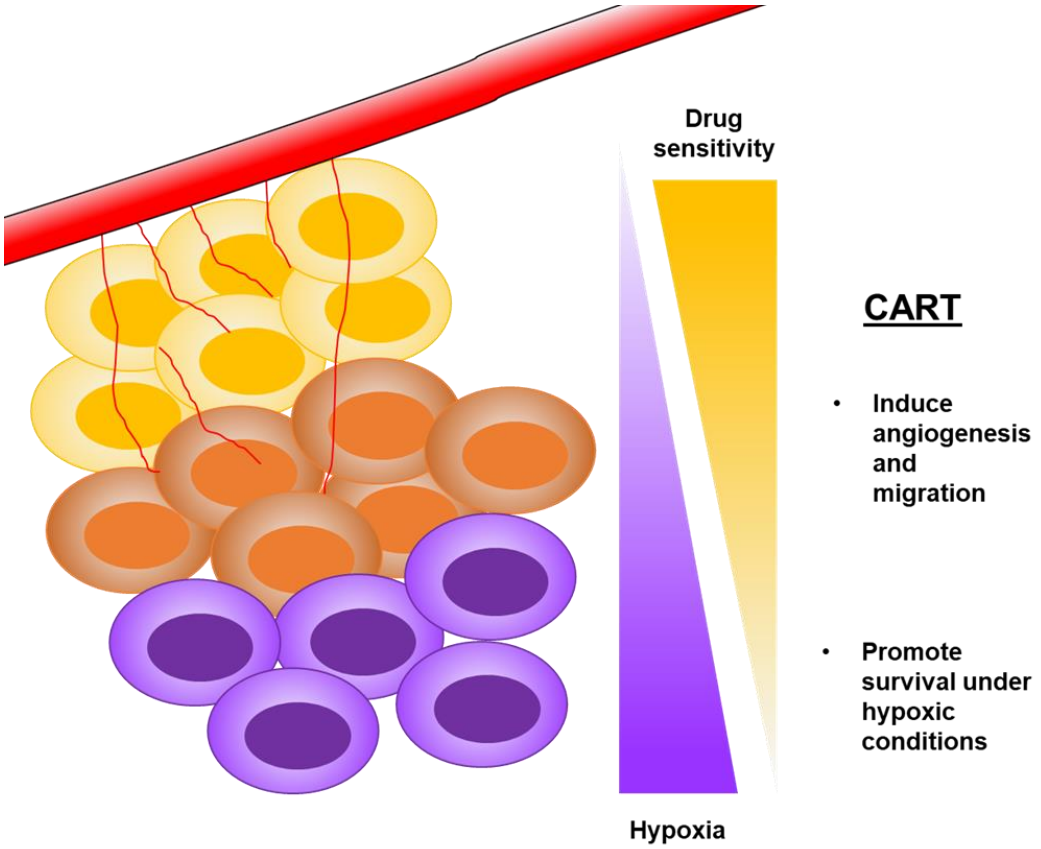

Figure 6.4. Possible mechanisms by which CART can promote survival in the tumour microenvironment.

6.3 Conclusions

The results generated from this study are a culmination of 4 years of dedication to gain a better understanding of why CART may indicate worse survival in breast cancer patients. Our results indicate that a complex relationship between CART and ERα exists within ER+ breast cancer, in which CART can both alter the function of ERα, and alter its binding partners.

CART was shown to promote a cooperation between ERα and the BAF complex. Our work highlighted that SMARCD1 may be a critical mediator of breast cancer growth, and ER function. Further, our research demonstrated that BAF-complex subunits are amplified in models of anti-endocrine resistance, and further research may highlight whether these are actionable targets in the fight against anti-endocrine resistance.

Additionally, our work potentially highlighted two novel ERα interactors driven by CART. While we did not elucidate the mechanisms by which these interactors work through, we feel, through further research, these may be key in understanding the precise effect CART has on ERα in ER+ breast cancer.

Lastly, RNA sequencing data has highlighted potential processes altered by CART in ER+ breast cancer, some of which are associated with response to anti-endocrine therapy. Understanding the exact consequence that results from the CART-driven alteration of these processes may provide invaluable insight into mechanisms by which CART indicates worse survival in patients.

Ultimately, I hope my research has highlighted key areas which may be critical in understanding why CART drives poor prognosis in ER+ breast cancer patients, and I hope I have contributed, even a small amount, to our fight against breast cancer.

Appendices

Section A; Buffers and Solutions

RIPA buffer

50 mM Tris-HCL (adjust pH 8.0)

2 mM EDTA

150 mM NaCl

0.5 % (W/V) Sodium Deoxycholate

0.1 % (W/V) SDS

1.0 % (V/V) NP-40

Low-stringency lysis buffer

50 mM HEPES (adjust pH to 7.5)

1 mM EDTA

100 mM NaCl

10 % (V/V) Glycerol

0.5 % (V/V) NP-40

Buffer C (mass spectrometry immunoprecipitation lysis buffer)

20 mM HEPES (adjust pH to 7.6)

420 mM NaCL

1.5 mM $MgCl_2$

0.2 mM EDTA

20% (V/V) Glycerol

Buffer C-100 (mass spectrometry immunoprecipitation dialysis buffer)

20 mM HEPES (adjust pH to 7.6)

100 mM KCl

1.5 mM $MgCl_2$

0.2 mM EDTA

20% (V/V) Glycerol

Ethanolamine solution

200 mM Ethanolamine Hydrochloride in ddH_2O

Adjust pH to 8.0

Sodium Borate solution

200 mM Sodium Borate in ddH_2O

Adjust pH to 9.0

Dimethyl Pimelimidate (DMP) crosslinking solution

20 mM DMP in Sodium Borate solution (recipe above)

Ensure pH is above 8.3 prior to crosslinking, adjust accordingly

10X Running buffer

25 mM Tris-Base

1.92 M Glycine

1 % (W/V) SDS

Dilute to 1X buffer in ddH_2O fresh on the day

1X Transfer buffer

0.48 mM Tris-Base

0.39 mM Glycine

20% (V/V) MeOH

Section B; Antibodies, Primer and siRNA sequences

Table 1B. Antibodies used during studies.

Target	Supplier	Application	WB dilution	Clonality & Species
Actin (ACTBD11B7)	Santa Cruz	WB	1:1000	Mouse monoclonal
CART (D6L8J)	Cell Signaling	IP	NA	Rabbit monoclonal
CART (D6M2M)	Cell Signaling	WB	1:500	Rabbit monoclonal
Cyclin D1 (HD-11)	Santa Cruz	WB	1:1000	Mouse monoclonal
ERα (D-12)	Santa Cruz	IP/WB	1:1000	Mouse monoclonal
ERα (F-10)	Santa Cruz	IP/WB	1:1000	Mouse monoclonal
ERα (D8H8)	Cell Signaling	WB	1:250	Rabbit monoclonal
ERK (C-16)	Santa Cruz	WB	1:1000	Rabbit polyclonal
HECTD4	Biorbyt	WB	1:250	Rabbit polyclonal
Normal mouse IgG	Millipore	IP	NA	Mouse monoclonal
Normal rabbit IgG	Millipore	IP	NA	Rabbit polyclonal
P53 (9282)	Cell Signaling	WB	1:1000	Rabbit polyclonal
PGR (D8Q2J)	Cell Signaling	WB	1:1000	Rabbit monoclonal
Phos-ERK (E-4)	Santa Cruz	WB	1:1000	Mouse monoclonal
SMARCD1 (23)	Santa Cruz	WB	1:1000	Mouse monoclonal
WIZ	Novus	WB	1:1000	Rabbit polyclonal

IP – Immunoprecipitation, WB – Western blot, NA – Not applicable

Table 2B. Primer sequences used during studies

Gene	Forward sequence	Reverse sequence
18S	GAGGATGAGGTGGAACCTCT	AGAAGTGACGCAGCCCTCTA
ATM	ATCTGCTGCCGTCAACTAGAA	GATCTCGAATCAGGCGCTTAAA
C11ORF80	TACCCTTCGACTGGGCGTT	AGCAATGCTCCCTTTGATACATC
CAP2	CCCTGCCCTTGGATGGATAG	ACGCTGATACTGTGGATGCTA
CART	TGGCCAAGTCCCCATGTG	CGATCCTTGCCCCTTTCC
CCND1	GCTGCGAAGTGGAAACCATC	CCTCCTTCTGCACACATTTGAA
ELF5	TAGGGAACAAGGAATTTTTCGGG	GTACACTAACCTTCGGTCAACC
ESR1	ATCCACCTGATGGCCAAG	GCTCCATGCCTTTGTTACTCA
LURAP1L	TCCTCAGGCAAGAGATGGTTA	TGATGGACTCGATGCTCTCATT
MALAT1	AGGCGTTGTGCGTAGAGGA	GGATTTTTACCAACCACTCGC
MYOF	TAATTGGCACGGCGACTGTAG	GGAGATCAGCTTGTACGGCAG
NCAM2	GGGGTTGCTTGTCAGTAGC	TTCAGGTTCACCAATCGCTGT
PARD6B	TTGGAGCTGAATTTCGTCGGT	AGCCTACCAAAACGTCAACATT
PGR	GACACCTTGCCTGAAGTTTCG	CTGCGTCTTTTCGTCGGAC
PKIB	GGGACAGGAAAGATAGGAGAAAG	CAGACTCCACGTCAGTCATTT
PRLR	TCTCCACCTACCCTGATTGAC	CGAACCTGGACAAGGTATTTCTG
SFPQ	AGCGATGTCGGTTGTTTGTTG	AGCGAACTCGAAGCTGTCTAC
SMARCD1	GAGACCAGGTATGTTGCCAGG	CCAGGTCGGACTGAAGGGT
TFF1	CGCTCCCAGTGTGCAAATAAG	GAACGGTGTCGTCGAAACAC

Table 3B. Primer sequences used to generate LXD-CART mutants

	Forward sequence	Reverse sequence
CART-LXD mutant 1	TGAGGCTGCTGCCCGCGGC GGGCGCCGCCCTGCTG	CAGCAGGGCGGCGCCCGCC GCGGGCAGCAGCCTCA
CART-LXD mutant 2	TGGGCGCCGCCGCGGCGCT GATGCTACC	GGTAGCATCAGCGCCGCGG CGGCGCCCA
CART-LXD mutant 3	GCAATTCCTTCGCGGCGAA GTGCTTATG	AAGCACTTCGCCGCGAAGG AATTGC

Table 4B. SMARCD1 siRNA sequences

siRNA	Sequence
SMARCD1 si-1	GGCAAUAUAUUAAGACACA
SMARCD1 si-2	UAAGUCAGAUGCCGAGGAU
SMARCD1 si-3	UUAAUCAUGUCAUCAGUGU
SMARCD1 si-4	GACAAUGACUGAUGUGGUG

Section C; Vector maps

Figure 1C. ERE-TATA Luciferase plasmid

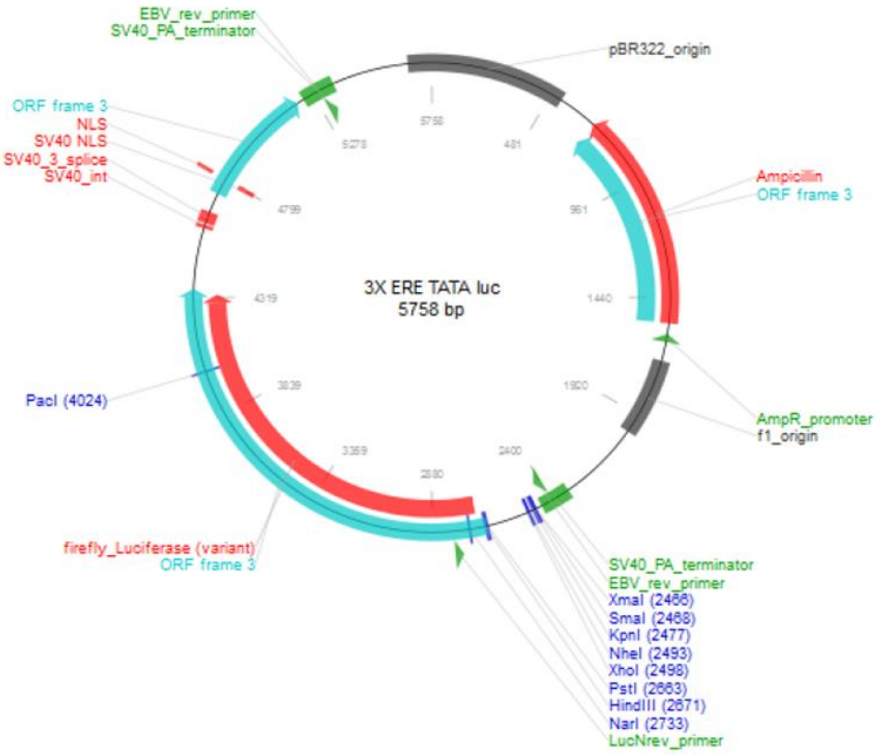

Figure 2C. CMV-Renilla plasmid

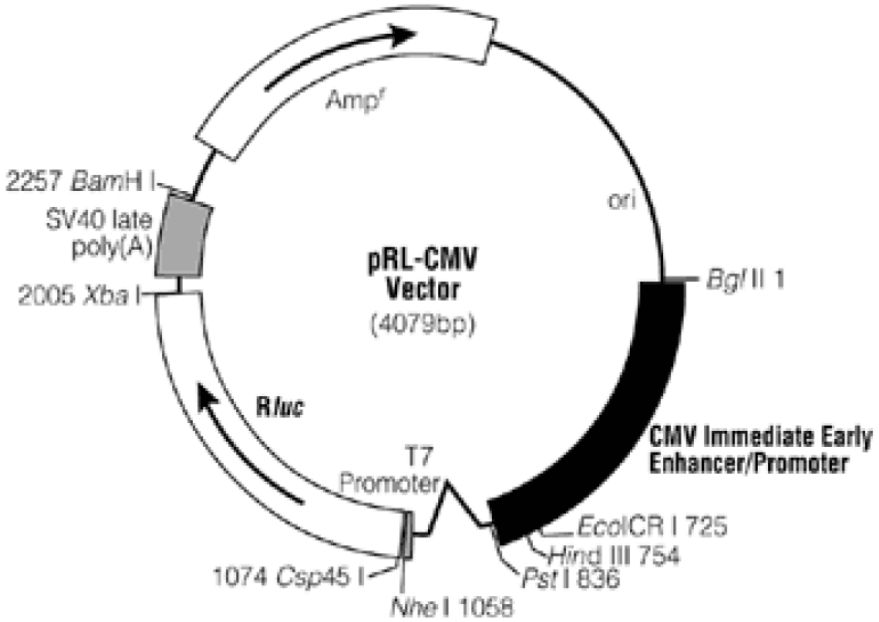

Figure 3C. CMV6-XL5 (CMV-CART) plasmid

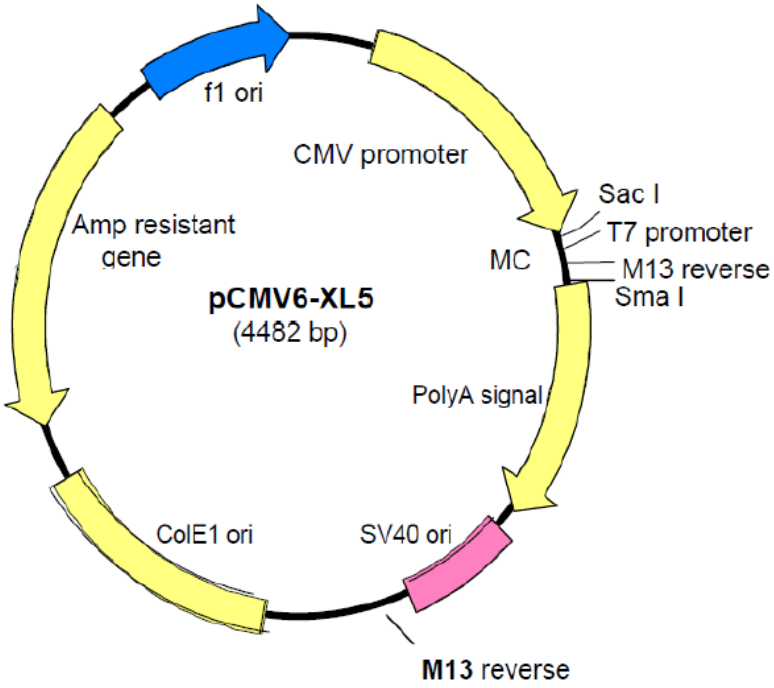

Figure 4C. PLVX-Tet-ON-ADVANCED plasmid

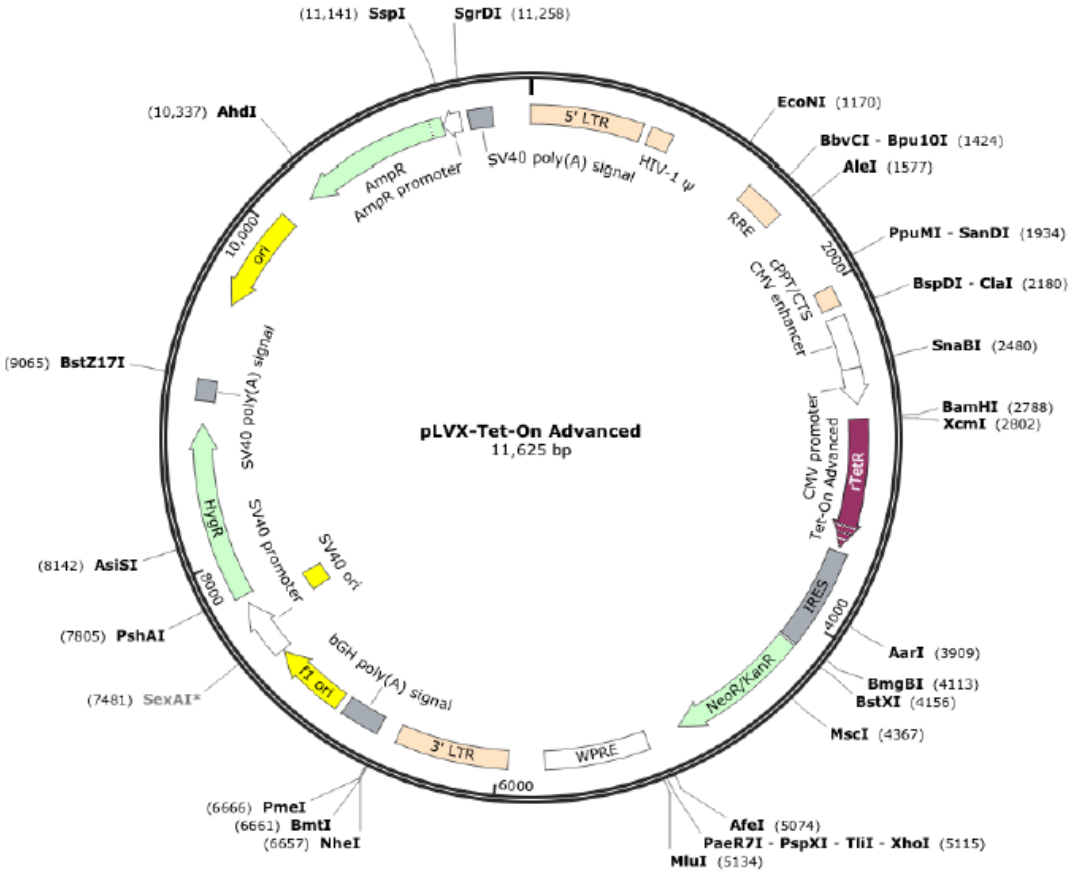

Figure 4E. PLVX-Tight-PURO plasmid

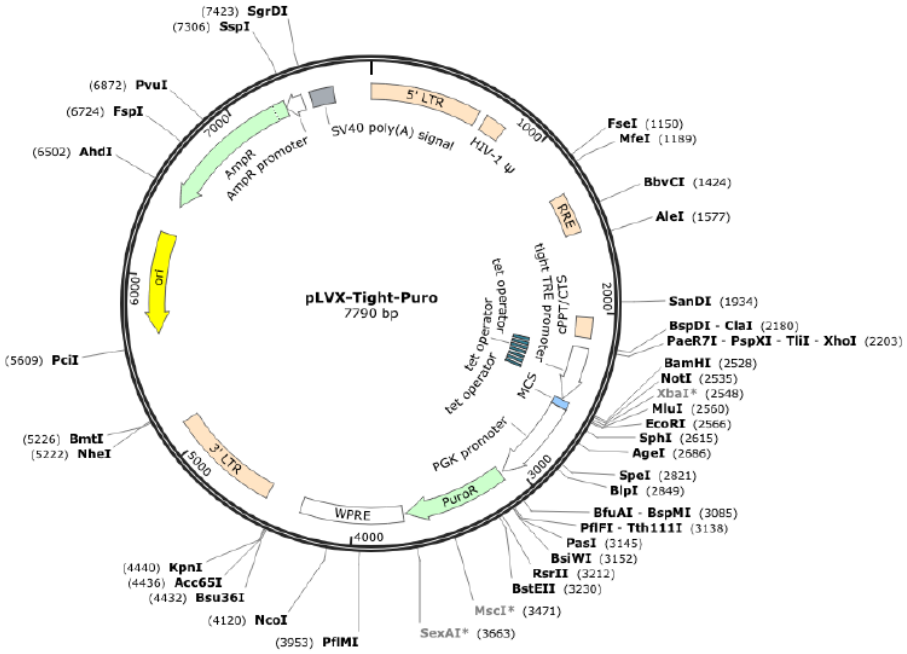

Section D; RNA-seq

For all Gene Ontology (GO) tables, the p value, as well as the Benjamini/Bonferroni corrected p value is displayed. For Gene Set Enrichment Analysis (GSEA) tables, the false discovery rate (FDR) adjusted q value is reported with the non-adjusted p value. The count column refers to how many of the input genes were associated with that term. If more than 20 terms/sets were identified from the input genes, only the top 20 are displayed here (noted in table legends). The only exception to this is table 9D, the GSEA for top 200 upregulated genes based on FPKMS difference, as some gene sets outside the top 20 were discussed in chapter 3.

Table 1D. Gene ontology (molecular function) of genes significantly upregulated by CART

GO term Molecular function	Count	P value	Bonferroni	Benjamini
Polymerase II core promoter proximal region sequence-specific DNA binding	6	0.004251	0.382098	0.382098
Nucleic acid binding	9	0.008893	0.635569	0.396319
Transcription factor activity, sequence-specific DNA binding	8	0.024629	0.940267	0.609095
DNA binding	11	0.026281	0.950684	0.528755
Metal ion binding	11	0.087931	0.99997	0.875082
RNA polymerase II transcription factor activity, sequence-specific DNA binding	3	0.094289	0.999986	0.845128

Table 2D. Gene ontology (biological process) of genes significantly upregulated by CART

GO term Biological process	Count	P value	Bonferroni	Benjamini
Reciprocal meiotic recombination	3	0.003726	0.689132	0.689132
Regulation of transcription from RNA polymerase II promoter	6	0.010642	0.964878	0.812592
Transcription, DNA-templated	13	0.012498	0.980487	0.73078
Protein localization to centrosome	2	0.053306	1	0.986247
Strand displacement	2	0.076094	1	0.992948
Regulation of transcription, DNA-templated	9	0.082162	1	0.988581

Table 3D. Gene ontology (GAD disease) of genes significantly upregulated by CART

Term GAD Disease	Count	P value	Bonferroni	Benjamini
Tobacco Use Disorder	17	0.02906	0.999999	0.999999
Obesity	5	0.033267	1	0.99974
Response to antipsychotic treatment	2	0.054919	1	0.999898
Breast Neoplasms	2	0.07359	1	0.999911
Ovarian cancer	3	0.083267	1	0.999794
Colonic Neoplasms|Microsatellite Instability	2	0.091901	1	0.999607
Diabetes Mellitus	3	0.096334	1	0.999143
Type 2 Diabetes| edema | rosiglitazone	12	0.099347	1	0.99831

Table 4D. Gene Set Enrichment Analysis (GSEA) of genes significantly upregulated by CART

Gene set	Description	Count	P value	FDR Q value
PYEON_CANCER_HEAD_AND_NECK_VS_CERVICAL_UP	Up-regulated genes in head and neck cancer compared to cervical carcinoma samples.	8	1.87E-09	1.15E-05
RODRIGUES_THYROID_CARCINOMA_POORLY_DIFFERENTIATED_DN	Genes down-regulated in poorly differentiated thyroid carcinoma (PDTC) compared to normal thyroid tissue.	12	1.56E-08	4.81E-05
BASAKI_YBX1_TARGETS_DN	Genes down-regulated in SKOC-3 cells (ovarian cancer) after YB-1 (YBX1) [GeneID=4904] knockdown by RNAi.	9	2.49E-08	5.11E-05
JOHNSTONE_PARVB_TARGETS_3_DN	Genes down-regulated upon overexpression of PARVB [GeneID=29780] in MDA-MB-231 cells (breast cancer) cultured in 3D Matrigel only.	10	4.49E-06	6.92E-03
WHITFIELD_CELL_CYCLE_S	Genes periodically expressed in synchronized HeLa cells (cervical carcinoma), with peak during the S phase of cell cycle.	5	9.94E-06	1.22E-02
BENPORATH_CYCLING_GENES	Genes showing cell-cycle stage-specific expression [PMID=12058064].	8	1.78E-05	1.83E-02
WAMUNYOKOLI_OVARIAN_CANCER_LMP_DN	Genes down-regulated in mucinous ovarian carcinoma tumors of low malignant potential (LMP) compared to normal ovarian surface epithelium tissue.	5	2.67E-05	2.26E-02
DING_LUNG_CANCER_EXPRESSION_BY_COPY_NUMBER	The lung adenocarcinoma TSP (tumor sequencing project) genes showing strong correlation between DNA copy number variation and gene expression.	4	2.94E-05	2.26E-02
RODRIGUES_THYROID_CARCINOMA_ANAPLASTIC_DN	Genes down-regulated in anaplastic thyroid carcinoma (ATC) compared to normal thyroid tissue.	7	4.35E-05	2.98E-02
WANG_RESPONSE_TO_GSK3_INHIBITOR_SB216763_UP	Genes up-regulated in RS4;11 cells (MLL, mixed lineage leukemia) in response to SB216763 [PubChem=176158], an inhibitor of GSK3B [GeneID=2932].	6	7.02E-05	4.32E-02
LASTOWSKA_NEUROBLASTOMA_COPY_NUMBER_DN	Genes with copy number losses in primary neuroblastoma tumors.	8	7.83E-05	4.38E-02

Gene set	Description	Count	P value	FDR Q value
BUYTAERT_PHOTODYNAMIC_THERAPY_STRESS_UP	Genes up-regulated in T24 (bladder cancer) cells in response to the photodynamic therapy (PDT) stress.	8	8.60E-05	4.42E-02
NOUZOVA_TRETINOIN_AND_H4_ACETYLATION	Genes whose CpG islands showed greatly increased histone H4 acetylation in NB4 cells (acute promyelocytic leukemia, APL) upon treatment with tretinoin [PubChem=444795].	4	1.18E-04	4.77E-02
NAKAMURA_TUMOR_ZONE_PERIPHERAL_VS_CENTRAL_DN	Down-regulated genes in peripheral zone of human pancreatic cancer growing in the pancreas of nude mice compared to that of the tumor from the central zone.	7	1.22E-04	4.77E-02
HAN_SATB1_TARGETS_DN	Genes down-regulated in MDA-MB-231 cells (breast cancer) after knockdown of SATB1 [GeneID=6304] by RNAi.	6	1.26E-04	4.77E-02
PECE_MAMMARY_STEM_CELL_DN	The '3/3 signature': genes consistently down-regulated in all three pools of normal mammary stem cells (defined by their ability to retain the dye PKH26).	4	1.28E-04	4.77E-02
WHITFIELD_CELL_CYCLE_G1_S	Genes periodically expressed in synchronized HeLa cells (cervical carcinoma), with peak during the G1/S phase of cell cycle.	4	1.32E-04	4.77E-02

Table 5D. Gene ontology (molecular function) of genes significantly downregulated by CART (top 20)

GO term Molecular function	Count	P value	Bonferroni	Benjamini
Structural constituent of ribosome	21	3.25E-16	7.83E-14	7.83E-14
Poly(A) RNA binding	36	3.50E-13	8.22E-11	4.11E-11
Cadherin binding involved in cell-cell adhesion	17	6.32E-10	1.49E-07	4.95E-08
Protein binding	95	5.42E-07	1.27E-04	3.18E-05
GTPase activity	10	7.39E-05	0.017221	0.003468
Structural constituent of cytoskeleton	7	1.90E-04	0.043684	0.007417
Structural molecule activity	9	5.93E-04	0.130125	0.019718
Unfolded protein binding	6	0.001503	0.29769	0.043211
GTP binding	10	0.002627	0.461115	0.066389
RNA binding	12	0.002988	0.505067	0.067917
Glutathione binding	3	0.003	0.506439	0.062175
Identical protein binding	14	0.00451	0.654317	0.084715
Ubiquitin protein ligase binding	8	0.006289	0.772965	0.107787
Proton-transporting ATP synthase activity, rotational mechanism	3	0.007201	0.817032	0.114247
Translation initiation factor binding	3	0.010902	0.923928	0.1578
Glutathione transferase activity	3	0.028836	0.998968	0.349331
NAD binding	3	0.033574	0.999673	0.376297
rRNA binding	3	0.03689	0.999854	0.387816
Heat shock protein binding	3	0.040325	0.999937	0.398961

Table 6D. Gene ontology (biological process) of genes significantly downregulated by CART (top 20)

GO term Biological process	Count	P value	Bonferroni	Benjamini
Translational initiation	22	5.80E-22	4.50E-19	4.50E-19
SRP-dependent cotranslational protein targeting to membrane	19	8.83E-21	6.85E-18	3.43E-18
Nuclear-transcribed mRNA catabolic process, nonsense-mediated decay	20	2.67E-20	2.07E-17	6.90E-18
Viral transcription	19	2.47E-19	1.92E-16	4.80E-17
Translation	21	3.49E-15	2.67E-12	5.34E-13
rRNA processing	19	3.19E-14	2.47E-11	4.12E-12
Cell-cell adhesion	16	1.85E-09	1.44E-06	2.05E-07
Canonical glycolysis	6	1.27E-06	9.88E-04	1.24E-04
Glycolytic process	6	5.13E-06	0.003976	4.43E-04
Gluconeogenesis	6	1.89E-05	0.014536	0.001463
Regulation of mRNA stability	7	1.25E-04	0.09245	0.00878
Platelet aggregation	5	2.47E-04	0.174362	0.01584
ATP biosynthetic process	4	0.001307	0.637563	0.0751
NIK/NF-kappaB signaling	5	0.001521	0.693055	0.080903
Tumor necrosis factor-mediated signaling pathway	6	0.001955	0.780995	0.096288
Microtubule-based process	4	0.002458	0.851908	0.112521
Regulation of translational initiation	4	0.002458	0.851908	0.112521
Retina homeostasis	4	0.003328	0.924757	0.141165
Hepatocyte apoptotic process	3	0.004127	0.959625	0.163316

Table 7D. Gene ontology (GAD disease) of genes significantly downregulated by CART

Term GAD Disease	Count	P value	Bonferroni	Benjamini
Acquired Immunodeficiency Syndrome|Disease Progression	21	2.55E-06	0.001713	0.001713
Liver Cirrhosis, Biliary	4	0.001109	0.525505	0.311164
Pancreatitis	4	0.002214	0.77458	0.391402
Cognitive trait	5	0.008777	0.997327	0.772614
Aging/ Telomere Length	5	0.009036	0.997757	0.704756
Drug-Induced Liver Injury|Liver Failure, Acute	2	0.013676	0.999904	0.786117
Atherosclerosis	7	0.035123	1	0.967693
Leukemia	4	0.047428	1	0.983118
Gastric cancer	3	0.052931	1	0.982761
Autoimmune Diseases|	2	0.053606	1	0.975337
Liver disease, chronic	2	0.053606	1	0.975337
Spondyloarthropathies	2	0.072966	1	0.990231
Alzheimer's Disease	6	0.078719	1	0.989862
Pancreatitis, Alcoholic	2	0.085656	1	0.990235
Esophageal Neoplasms|Oesophageal neoplasm	2	0.091936	1	0.990237
Asthma	7	0.096052	1	0.989155
Autism	6	0.098665	1	0.987259

Table 8D. GSEA of genes significantly downregulated by CART (top 20)

Gene set	Description	Count	P value	FDR Q value
HSIAO_HOUSEKEEPING_GENES	Housekeeping genes identified as expressed across 19 normal tissues.	47	1.13E-61	6.93E-58
MORF_ACTG1	Neighborhood of ACTG1	31	2.42E-49	7.45E-46
MORF_NPM1	Neighborhood of NPM1	32	5.85E-49	1.20E-45
MORF_NME2	Neighborhood of NME2	31	1.05E-47	1.62E-44
MODULE_83	Genes in the cancer module 83.	36	9.58E-46	1.18E-42
MODULE_114	Protein biosynthesis and ribosomes.	36	7.38E-45	7.58E-42
KIM_ALL_DISORDERS_OLIGODENDROCYTE_NUMBER_CORR_UP	Genes whose expression was significantly and positively correlated with the number of perineuronal oligodendrocytes in the layer III of BA9 brain region.	44	2.23E-43	1.96E-40
MODULE_151	Genes in the cancer module 151.	33	1.06E-40	8.19E-38
MORF_TPT1	Neighborhood of TPT1	24	8.30E-39	5.68E-36
KIM_BIPOLAR_DISORDER_OLIGODENDROCYTE_DENSITY_CORR_UP	Genes whose expression significantly and positively correlated with oligodendrocyte density in layer VI of BA9 brain region in patients with bipolar disorder.	39	5.27E-38	3.13E-35
LI_AMPLIFIED_IN_LUNG_CANCER	Genes with increased copy number that correlates with increased expression across six different lung adenocarcinoma cell lines.	27	5.60E-38	3.13E-35
REACTOME_METABOLISM_OF_MRNA	Genes involved in Metabolism of mRNA	30	3.12E-37	1.60E-34
ENK_UV_RESPONSE_KERATINOCYTE_UP	Genes up-regulated in NHEK cells (normal epidermal keratinocytes) after UVB irradiation.	35	3.26E-36	1.54E-33
REACTOME_METABOLISM_OF_RNA	Genes involved in Metabolism of RNA	30	3.17E-35	1.40E-32
KEGG_RIBOSOME	Ribosome	21	3.47E-34	1.42E-31
GRADE_COLON_CANCER_UP	Up-regulated genes in colon carcinoma tumors compared to the matched normal mucosa samples.	38	1.25E-32	4.80E-30
REACTOME_TRANSLATION	Genes involved in Translation	25	8.40E-32	3.04E-29
REACTOME_3_UTR_MEDIATED_TRANSLATIONAL_REGULATION	Genes involved in 3' -UTR-mediated translational regulation	23	7.40E-31	2.53E-28
REACTOME_METABOLISM_OF_PROTEINS	Genes involved in Metabolism of proteins	31	9.76E-31	3.17E-28
REACTOME_PEPTIDE_CHAIN_ELONGATION	Genes involved in Peptide chain elongation	22	1.65E-30	5.08E-28

Table 9D. GSEA of top 200 genes upregulated by CART based on FPKMS difference. Top 50 gene sets are shown

Gene Set	Description	Count	p-value	FDR q-value
CHARAFE_BREAST_CANCER_LUMINAL_VS_MESENCHYMAL_UP	Genes up-regulated in luminal-like breast cancer cell lines compared to the mesenchymal-like ones.	12	3.24E-10	2.00E-06
CHARAFE_BREAST_CANCER_LUMINAL_VS_BASAL_UP	Genes up-regulated in luminal-like breast cancer cell lines compared to the basal-like ones.	11	7.85E-10	2.42E-06
GOZGIT_ESR1_TARGETS_DN	Genes down-regulated in TMX2-28 cells (breast cancer) which do not express ESR1 [GeneID=2099]) compared to the parental MCF7 cells which do.	14	1.72E-09	3.52E-06
MASSARWEH_TAMOXIFEN_RESISTANCE_DN	Genes down-regulated in breast cancer tumors (formed by MCF-7 xenografts) resistant to tamoxifen [PubChem=5376].	8	1.06E-07	1.63E-04
PUJANA_BRCA2_PCC_NETWORK	Genes constituting the BRCA2-PCC network of transcripts whose expression positively correlated (Pearson correlation coefficient, PCC >= 0.4) with that of BRCA2 [GeneID=675] across a compendium of normal tissues.	9	3.96E-07	4.18E-04
KIM_WT1_TARGETS_12HR_DN	Genes down-regulated in UB27 cells (osteosarcoma) at 12 hr after inducing the expression of a mutated form of WT1 [GeneID=7490].	7	4.07E-07	4.18E-04
JOHNSTONE_PARVB_TARGETS_3_DN	Genes down-regulated upon overexpression of PARVB [GeneID=29780] in MDA-MB-231 cells (breast cancer) cultured in 3D Matrigel only.	12	7.90E-07	6.95E-04
SMID_BREAST_CANCER_BASAL_DN	Genes down-regulated in basal subtype of breast cancer samles.	10	3.23E-06	2.49E-03
RODRIGUES_THYROID_CARCINOMA_ANAPLASTIC_UP	Genes up-regulated in anaplastic thyroid carcinoma (ATC) compared to normal thyroid tissue.	10	4.18E-06	2.86E-03
WAMUNYOKOLI_OVARIAN_CANCER_LMP_DN	Genes down-regulated in mucinous ovarian carcinoma tumors of low malignant potential (LMP) compared to normal ovarian surface epithelium tissue.	6	5.20E-06	3.20E-03
GINESTIER_BREAST_CANCER_20Q13_AMPLIFICATION_UP	Genes up-regulated in metastatic breast cancer tumors having type 2 amplification in the 20q13 region; involves MYBL2, STK6 and ZNF217 [GeneID=4605;6790;7764]	5	6.62E-06	3.70E-03

Gene Set	Description	Count	p-value	FDR q-value
GRAESSMAN N_APOPTOSI S_BY_DOXO RUBICIN_DN	Genes down-regulated in ME-A cells (breast cancer) undergoing apoptosis in response to doxorubicin [PubChem=31703].	15	7.20E-06	3.70E-03
TOYOTA_TA RGETS_OF_ MIR34B_AND _MIR34C	Genes down-regulated in HCT116 cells (colon cancer) upon expression of MIR34B or MIR34C [GeneID=407041;407042] microRNAs.	8	8.28E-06	3.73E-03
ONKEN_UVE AL_MELANO MA_UP	Genes up-regulated in uveal melanoma: class 2 vs class 1 tumors.	10	8.48E-06	3.73E-03
CHANDRAN_ METASTASIS _UP	Genes up-regulated in metastatic tumors from the whole panel of patients with prostate cancer.	6	9.45E-06	3.88E-03
NAKAMURA_ TUMOR_ZON E_PERIPHER AL_VS_CENT RAL_DN	Down-regulated genes in peripheral zone of human pancreatic cancer growing in the pancreas of nude mice compared to that of the tumor from the central zone.	9	1.07E-05	3.91E-03
RODRIGUES_ THYROID_CA RCINOMA_P OORLY_DIFF ERENTIATED _DN	Genes down-regulated in poorly differentiated thyroid carcinoma (PDTC) compared to normal thyroid tissue.	10	1.08E-05	3.91E-03
BENPORATH _CYCLING_G ENES	Genes showing cell-cycle stage-specific expression [PMID=12058064].	9	1.27E-05	4.27E-03
KOINUMA_TA RGETS_OF_S MAD2_OR_S MAD3	Genes with promoters occupied by SMAD2 or SMAD3 [GeneID=4087, 4088] in HaCaT cells (keratinocyte) according to a ChIP-chip analysis.	10	1.32E-05	4.27E-03
LIU_NASOPH ARYNGEAL_ CARCINOMA	Low abundance transcripts specific to nasopharyngeal carcinoma (NPC).	4	1.73E-05	5.16E-03
DACOSTA_U V_RESPONS E_VIA_ERCC 3_DN	Genes down-regulated in fibroblasts expressing mutant forms of ERCC3 [GeneID=2071] after UV irradiation.	10	1.81E-05	5.16E-03
WHITFIELD_ CELL_CYCLE _G1_S	Genes periodically expressed in synchronized HeLa cells (cervical carcinoma), with peak during the G1/S phase of cell cycle.	5	1.84E-05	5.16E-03
chr3q29	Genes in cytogenetic band chr3q29	4	1.94E-05	5.19E-03
CREIGHTON_ ENDOCRINE_ THERAPY_R ESISTANCE_ 1	The 'group 1 set' of genes associated with acquired endocrine therapy resistance in breast tumors expressing ESR1 and ERBB2 [GeneID=2099;2064].	8	2.12E-05	5.45E-03
MODULE_139	Genes in the cancer module 139.	4	2.80E-05	6.89E-03
TIEN_INTEST INE_PROBIO TICS_24HR_ UP	Genes up-regulated in Caco-2 cells (intestinal epithelium) after coculture with the probiotic bacteria L. casei for 24h.	8	3.10E-05	7.36E-03

Gene Set	Description	Count	p-value	FDR q-value
chr13q33	Genes in cytogenetic band chr13q33	3	3.51E-05	8.00E-03
LIM_MAMMARY_STEM_CELL_DN	Genes consistently down-regulated in mammary stem cells both in mouse and human species.	7	4.40E-05	9.68E-03
CREIGHTON_ENDOCRINE_THERAPY_RESISTANCE_4	The 'group 4 set' of genes associated with acquired endocrine therapy resistance in breast tumors expressing ESR1 but not ERBB2 [GeneID=2099;2064].	6	5.96E-05	1.27E-02
GENTILE_UV_HIGH_DOSE_DN	Selected genes down-regulated in WS1 (fibroblast) in response to irradiation with high dose UV-C.	6	6.51E-05	1.30E-02
MILI_PSEUDOPODIA_CHEMOTAXIS_DN	Transcripts depleted in pseudopodia of NIH/3T3 cells (fibroblast) in response to the chemotactic migration stimulus by lysophosphatidic acid (LPA) [PubChem=3988].	7	6.64E-05	1.30E-02
PYEON_CANCER_HEAD_AND_NECK_VS_CERVICAL_UP	Up-regulated genes in head and neck cancer compared to cervical carcinoma samples.	5	6.76E-05	1.30E-02
REACTOME_NUCLEAR_SIGNALING_BY_ERBB4	Genes involved in Nuclear signaling by ERBB4	3	7.98E-05	1.49E-02
CREIGHTON_ENDOCRINE_THERAPY_RESISTANCE_5	The 'group 5 set' of genes associated with acquired endocrine therapy resistance in breast tumors expressing ESR1 but not ERBB2 [GeneID=2099;2064].	7	9.24E-05	1.67E-02
PILON_KLF1_TARGETS_DN	Genes down-regulated in erythroid progenitor cells from fetal livers of E13.5 embryos with KLF1 [GeneID=10661] knockout compared to those from the wild type embryos.	14	9.52E-05	1.68E-02
GNF2_HDAC1	Neighborhood of HDAC1	4	1.02E-04	1.75E-02
DOANE_BREAST_CANCER_ESR1_UP	Genes up-regulated in breast cancer samples positive for ESR1 [GeneID=2099] compared to the ESR1 negative tumors.	4	1.09E-04	1.82E-02
RIGGINS_TAMOXIFEN_RESISTANCE_DN	Genes down-regulated SUM44/LCCTam cells (breast cancer) resistant to 4-hydroxytamoxifen [PubChem=63062] relative to the parental SUM44 cells sensitive to the drug.	5	1.25E-04	1.98E-02
LIM_MAMMARY_LUMINAL_MATURE_UP	Genes consistently up-regulated in mature mammary luminal cells both in mouse and human species.	4	1.25E-04	1.98E-02

Gene Set	Description	Count	p-value	FDR q-value
BRUNEAU_HEART_GREAT_VESSELS_AND_VALVULOGENESIS	Genes for which mutations result in developmental defects in the great vessels formation and valvulogenesis, a major class of congenital heart disease.	2	1.30E-04	2.00E-02
MODULE_180	Genes in the cancer module 180.	4	1.43E-04	2.15E-02
RICKMAN_TUMOR_DIFFERENTIATED_WELL_VS_POORLY_UP	Up-regulated genes that vary between HNSCC (head and neck squamous cell carcinoma) groups formed on the basis of their level of pathological differentiation: well vs poorly differentiated tumors.	5	1.73E-04	2.54E-02
THUM_SYSTOLIC_HEART_FAILURE_DN	Genes down-regulated in samples with systolic heart failure compared to normal hearts.	5	2.02E-04	2.90E-02
BENPORATH_SOX2_TARGETS	Set 'Sox2 targets': genes upregulated and identified by ChIP on chip as SOX2 [GeneID=6657] transcription factor targets in human embryonic stem cells.	8	2.09E-04	2.92E-02
MODULE_98	Genes in the cancer module 98.	6	2.28E-04	3.12E-02
OSMAN_BLADDER_CANCER_DN	Genes down-regulated in blood samples from bladder cancer patients.	6	2.71E-04	3.64E-02
MOHANKUMAR_TLX1_TARGETS_UP	Up-regulated in MCF7 cells (breast cancer) by TLX1 (HOX11) [GeneID=3195].	6	3.01E-04	3.95E-02
WEI_MIR34A_TARGETS	Potential direct target genes for MIR34A [GeneID=407040] microRNA in IMR32 cells (neuroblastoma).	4	3.19E-04	4.09E-02
MASSARWEH_RESPONSE_TO_ESTRADIOL	Genes rapidly up-regulated in breast cancer cell cultures by estradiol [PubChem=5757].	3	3.28E-04	4.13E-02
THUM_SYSTOLIC_HEART_FAILURE_UP	Genes up-regulated in samples with systolic heart failure compared to normal hearts.	6	3.38E-04	4.15E-02

Section E; Raw LFQ values for all mass spectrometry experiments

Below, in tables 1 – 4 E, the raw label free quantification (LFQ) values for all mass spectrometry experiments in chapter 4 of this study are reported.

Missing values in ERα IP lanes (ie 0) were imputed from a normal distribution to allow for 2-sided t-testing in chapter 4 of this study. Here, we report the raw values, not the imputed values.

Table 1E - +/- DOX, ERα D-12 antibody. All values are -log2 LFQ

Target name	DOX ER 1	DOX ER 2	DOX ER 3	DOX IGG 1	DOX IGG 2	DOX IGG 3	H2O ER 1	H2O ER 2	H2O ER 3	H2O IGG 1	H2O IGG 2	H2O IGG 3	Unique peptides	Seq. coverage
ADCK4	25.3071	0	0	0	0	0	25.9238	26.0292	26.0915	0	0	0	4	9
AES	25.6537	25.4665	25.5628	0	0	0	25.4966	25.4206	25.403	0	0	0	2	10.7
AHNAK2	26.3017	0	0	0	0	0	26.2421	26.2011	26.0978	0	0	0	4	5.6
ANK3	0	0	26.4291	0	0	26.4096	26.2391	26.0548	26.12	0	0	0	6	2.3
AP1M2;AP1M1	0	0	0	0	0	0	25.2572	25.178	25.4025	0	0	0	2	4.5
AP3B1	26.0466	25.865	26.21	0	0	0	25.9825	25.9974	25.9061	0	0	0	5	5.4
AP5Z1	26.209	25.9357	25.6285	0	0	0	26.8872	26.7576	26.9181	0	0	0	5	6.8
ARAF	26.345	26.124	26.5339	0	0	0	26.9012	26.6026	26.5715	0	0	26.1894	2	10.4
ARHGAP27	0	0	0	0	0	0	25.1381	25.8766	24.9802	0	0	0	4	4.4
ARID1A	30.4128	30.3822	30.3227	0	0	0	29.5868	29.4661	29.6042	0	0	0	9	8.1
ATRX	26.5651	26.6484	0	0	0	0	26.5704	26.572	26.3382	0	0	0	6	3.1
BCL7A	31.6071	31.6898	31.6775	0	0	0	31.1228	31.141	31.0713	0	0	0	7	53.3
BCL7B	31.2138	31.223	31.3929	0	0	0	30.6923	30.9078	30.7539	0	0	0	4	41.6
BCL7C	30.5411	30.6064	30.9854	0	0	0	30.5255	30.4551	30.3717	0	0	0	9	44.2
BNIPL	26.7	26.6375	26.3053	26.4099	0	0	26.6081	26.6061	26.8811	0	0	26.8236	3	10.6
BST2	0	26.446	26.5476	0	0	0	26.3852	26.4171	26.5203	0	0	0	2	13.9
C10orf76	25.2865	25.052	0	0	0	0	25.5611	25.9565	25.2178	0	0	0	2	3.5
CCNC	0	0	25.6135	0	0	0	25.4666	25.4846	25.4796	0	0	0	2	7.4
CDC42	24.2057	0	0	0	23.6776	0	24.5507	24.6707	24.5513	0	0	24.0323	2	11
CDK2AP1;CDK2AP2	26.0583	25.8515	0	0	0	24.4242	25.652	26.0512	25.5571	0	0	0	2	15.7
COMMD2	25.4518	25.6777	25.2497	0	0	26.3741	0	25.9565	25.6046	0	0	0	2	9.5
COPZ1	26.9555	27.2096	27.0929	0	0	0	27.2696	27.0935	0	0	0	0	2	11.9
CSNK2A1;CSNK2A3	26.2109	26.1903	0	0	0	0	26.3591	26.231	26.1669	0	0	0	5	17.6
DAB2IP	30.0677	29.584	29.2806	0	0	26.1652	29.0007	29.0726	29.0578	26.1241	0	0	14	16.9
DARS	25.77	0	26.1768	26.0584	0	0	25.8208	25.9159	25.8805	0	0	25.5098	7	13
DCP2	25.6073	25.7086	25.5624	0	0	0	25.7187	25.7609	26.1579	0	0	0	4	10.2
DDX27	26.2163	26.0884	26.2915	0	0	0	26.1605	25.9475	26.1495	0	0	0	6	7.2
DDX41	25.4149	25.8572	25.5655	0	0	0	25.7315	25.5113	25.2985	0	26.5872	0	7	13.5
DPF1	29.1321	29.1456	29.2244	0	0	0	28.9202	28.6583	28.9446	0	0	0	8	17.9
DPF2	33.2059	33.277	33.2311	0	0	0	32.7611	32.78	32.6933	0	0	0	24	59.8
DYNC1I2	26.6092	26.7133	26.6652	0	0	0	27.0251	26.9318	26.9536	0	0	26.5799	5	11.1
EFS	0	0	0	0	0	0	26.6466	26.3178	26.3994	0	26.7294	0	5	10.2
EHD4	27.4761	27.4332	27.4998	27.4702	0	0	27.1876	27.4259	27.4882	0	0	27.2676	7	21.3
EIF2S1	0	26.3763	0	0	0	0	26.2895	26.2568	26.0512	0	0	0	3	10.5
EIF2S2	24.4581	24.6587	0	0	0	0	24.5649	24.3951	24.9222	0	0	0	3	8.4
EIF6	0	26.1856	0	0	0	0	26.212	26.1292	25.9751	0	0	0	4	22.9
EMD	26.4107	26.4283	26.1691	0	0	0	26.3297	26.2624	26.1694	0	0	25.9671	3	15.4

Target name	DOX ER 1	DOX ER 2	DOX ER 3	DOX IGG 1	DOX IGG 2	DOX IGG 3	H2O ER 1	H2O ER 2	H2O ER 3	H2O IGG 1	H2O IGG 2	H2O IGG 3	Unique peptides	Seq. coverage
EPS8L2	26.3442	26.0971	26.2721	0	0	0	26.0629	26.2282	26.0238	0	0	0	4	7
FAM179B	27.505	27.4855	27.5465	0	0	0	27.2435	27.0372	27.1901	0	0	0	7	5.4
FAM45A;FAM45B	27.2518	27.2525	26.943	0	27.5789	0	26.7161	26.7046	26.6984	0	0	0	1	2.2
FAM50A	26.5058	0	0	0	0	0	26.5494	26.2707	26.3338	0	0	0	3	12.7
FTSJ3	26.4927	26.8398	26.5267	0	0	0	26.3912	26.6389	26.6058	25.9579	0	0	7	8.5
GAR1	0	0	0	0	0	0	25.1768	25.278	25.3417	0	0	0	3	11.5
GCAT	25.8292	25.9389	25.9302	0	0	0	26.0559	26.0234	26.4954	0	0	0	2	4.8
GLUD1;GLUD2	0	25.6703	26.101	0	0	0	25.9469	26.0548	26.2807	0	0	0	4	6.6
GNB1;GNB4;GNB2	0	0	0	0	0	0	26.0157	25.9433	25.6233	0	0	0	2	17.6
GRB7	24.6466	24.6099	24.6543	0	0	0	24.8129	24.7137	24.5703	24.6309	0	0	2	3.4
GREB1	26.8147	27.7173	27.1074	0	0	0	27.4557	27.5293	0	0	0	0	8	7.6
GREB1L	26.6084	26.2099	26.2096	0	0	0	26.6655	26.4452	25.979	0	0	0	3	2.7
GTF3C3	24.3179	0	0	0	0	0	24.6569	24.6453	24.6618	0	0	0	3	4.2
GTPBP6	0	0	26.6475	0	0	0	27.0946	26.8282	27.0222	0	0	26.5529	6	12
HECTD4	27.5341	27.6119	27.4815	0	0	0	0	26.723	0	0	0	0	4	1.4
HGS	27.4472	27.575	27.3454	0	0	0	28.0062	27.898	27.9532	0	0	0	10	12.6
INTS10	0	0	27.4532	0	0	0	27.655	28.1442	28.0405	0	0	0	3	5.2
IPO11	26.1172	26.0371	26.2509	0	0	0	25.9898	25.9278	25.7761	0	0	0	4	4.5
ITGA7	27.2109	27.2846	26.9111	0	0	0	0	0	27.7612	0	0	0	1	1.4
KIAA1033	0	0	0	0	0	0	25.496	25.3316	25.0402	0	0	0	2	1.6
KPNA2	27.5517	27.6582	27.404	0	0	0	28.0485	27.4895	27.2714	0	0	0	8	16.1
MED1	26.4781	0	0	0	0	0	26.5266	26.654	26.3336	0	0	0	8	7.4
MED13L	24.6733	24.7265	24.6141	0	0	0	25.529	0	0	0	0	24.2872	2	0.8
MED22	26.1728	26.2522	25.7723	0	0	0	26.1634	26.7005	26.0855	0	0	0	3	12
MED27	0	26.848	26.9183	0	0	0	27.1471	26.9719	27.3724	26.1923	0	0	3	10.6
MED30	0	0	0	0	0	0	25.6718	25.7001	25.5267	0	0	0	2	9.6
MRPS7	27.2326	27.0425	26.7948	0	0	0	27.4709	26.945	27.2746	0	0	0	5	21.5
MTPAP	26.7479	25.6194	25.9835	0	26.7158	0	26.2078	26.5789	26.0834	26.5529	0	0	5	7.4
MYO1B	0	0	0	0	0	0	25.3805	25.1997	25.2957	0	0	0	9	9.8
NUBP2	25.7535	25.6057	25.4583	0	0	0	0	0	25.8314	0	0	0	2	6.6
NUP88	0	0	25.2241	0	0	0	25.4853	25.5563	25.3673	0	0	0	2	3.2
PABPC4	25.833	25.7309	26.1985	0	0	0	0	0	25.7791	0	0	0	2	6.5
PARP1	26.3259	26.3127	26.3651	0	0	0	26.2066	26.2453	26.1806	0	0	0	6	7.5
PHF10	28.7685	28.5941	28.5357	0	0	0	27.9297	27.99	28.1128	0	0	0	6	11.4
PHF12	28.751	28.9065	28.4887	0	24.655	0	28.19	28.1128	27.2854	0	0	0	10	12.9
PPP1CA;PPP1CC	26.0146	26.2039	26.7102	0	0	0	26.6736	26.74	27.1095	26.4984	0	0	2	22.7
PPP1CB	26.189	26.2916	26.811	0	0	0	26.5906	26.8276	27.1844	0	0	0	1	19
RAB21	0	0	0	0	0	0	24.7701	24.7229	24.7624	0	0	0	2	8.9
RAB25	26.4007	26.2477	0	0	0	0	27.0777	27.2671	27.2225	0	0	0	2	13.1
RAB2A	0	24.7237	0	0	0	0	25.8677	26.538	25.8377	25.7976	0	0	4	19.3

Target name	DOX ER 1	DOX ER 2	DOX ER 3	DOX IGG 1	DOX IGG 2	DOX IGG 3	H2O ER 1	H2O ER 2	H2O ER 3	H2O IGG 1	H2O IGG 2	H2O IGG 3	Unique peptides	Seq. coverage
RAE1	0	0	0	0	0	0	25.9166	25.6612	25.587	0	25.1464	0	3	8.4
RAF1	26.0862	25.788	26.2552	0	26.1944	0	26.1425	26.1009	26.3703	25.969	0	0	2	13.3
RASAL2	29.8248	29.9038	29.7553	0	28.4717	0	29.5104	29.4146	29.1966	0	0	0	18	22.1
SCFD1	26.2456	26.2301	0	0	0	0	26.3799	26.0504	26.0737	0	0	0	4	9.3
SCYL1	26.1524	0	0	0	0	0	26.6802	26.0512	26.1035	0	0	26.2494	3	3.3
SEC14L1	26.0899	0	0	0	0	0	26.0194	25.8959	26.3232	0	0	0	2	3.8
SEC22B	0	0	27.0038	0	0	0	25.9765	26.2446	26.0763	25.8785	0	0	3	12.6
SEC31A	25.6549	25.6683	25.3159	0	0	0	0	26.1262	25.4174	0	0	0	4	3.6
SEH1L	25.0823	25.2272	24.953	0	24.9999	0	25.2704	25.4645	25.0709	0	0	0	3	8.1
SF3A3	25.5914	25.6411	25.762	0	0	0	25.6896	25.6308	25.4976	0	0	0	4	10.2
SH3YL1	25.4466	25.5225	25.5081	0	0	25.6411	25.8743	25.7633	26.4693	0	0	25.6597	2	5
SIN3B	28.4124	28.3719	28.2452	0	0	0	27.914	27.8703	27.7806	0	0	0	14	14.6
SKP1	26.2109	26.0405	25.917	0	0	0	0	26.0816	0	0	0	0	4	17.8
SMARCD1	31.7674	31.7925	31.7084	0	0	0	31.3839	31.2752	31.3457	0	0	0	19	38.1
SMC3	26.6144	26.4356	0	0	0	0	26.3633	26.7389	26.7961	0	0	0	7	8
SOWAHC	25.7632	25.7303	25.5859	0	0	0	25.7071	25.4744	25.8879	25.5863	0	0	4	10.5
SRSF11	26.348	26.2586	26.0473	0	0	0	26.6185	0	0	0	0	0	3	8.9
SS18	31.5134	31.4271	31.4452	0	0	0	30.6571	30.9546	31.1127	0	0	0	5	12.4
SS18L1	30.5251	30.4054	30.1268	0	0	0	30.2373	30.2748	30.0539	0	0	0	5	17.4
SSBP2;SSBP4;SSBP3	24.7769	0	0	0	0	0	24.7786	24.8177	24.5302	0	0	0	2	6.4
STK39	25.1509	25.117	24.9526	0	0	0	25.3387	25.3309	25.0472	25.3155	0	0	2	4.8
SUB1	0	25.8582	26.0168	26.8454	0	0	26.4733	25.7181	26.4978	0	0	26.0357	3	25.2
TBC1D30	0	0	0	0	0	0	26.6475	26.5378	26.571	0	0	0	3	3.4
TFRC	26.0833	0	25.9187	0	0	0	26.7827	26.0587	26.2185	0	0	0	8	12
TJP2	26.5062	0	0	0	0	0	26.6436	26.8861	26.5336	0	26.4148	0	10	10.1
TMED7-TICAM2;TMED7	0	0	0	0	0	0	26.1765	26.7521	26.9862	0	0	0	2	12.2
TMEM159	27.1527	27.2365	27.6642	0	0	0	27.3162	27.238	27.3984	0	0	0	4	19.3
TOMM70A	24.872	0	25.2601	0	0	0	25.1674	25.2168	25.3403	0	0	25.6068	5	9
TPD52L1	0	0	0	0	0	0	24.5888	24.4628	24.3964	0	24.8266	0	3	21.1
TRUB1	24.7538	25.0549	25.1244	0	0	0	25.6846	25.1657	25.9724	0	0	25.1147	3	9.2
UBTF	25.5096	25.47	0	0	0	0	25.4389	25.3799	25.3381	0	0	0	4	5.5
UQCRC2	0	27.3505	26.8003	0	0	27.7071	28.0751	27.214	27.227	0	0	0	12	31.6
VDAC1	0	25.4311	0	0	25.5485	0	25.3389	25.0029	24.8093	0	25.1601	0	4	15.9
VEZF1	0	0	0	0	0	0	24.6358	24.7491	24.4987	0	0	0	3	6.1
WDR5	26.6147	26.6471	26.4902	0	0	0	27.2212	27.1534	26.6476	0	0	0	4	19.2
WIZ	25.8934	25.7311	25.7334	0	0	0	0	0	0	0	0	0	2	1.6
XRCC5	25.9391	26.2725	26.2887	0	26.0434	0	25.9512	26.2405	26.4134	0	0	26.2495	6	9.6
YTHDC1	26.0388	25.8407	25.4688	0	0	0	0	26.2955	25.5552	0	0	26.1967	4	6.3
ZC3H18	25.9085	25.6718	25.8854	0	0	0	26.7956	25.9221	25.6463	0	0	26.0508	7	10.1
ZMYM3	25.2737	25.3983	25.5167	0	0	0	25.3711	25.379	25.3583	0	0	0	3	1.9

Table 2E. +/- E2, ERα D-12 antibody. All values are -log2 LFQ

Target name	E2 ER 1	E2 ER 2	E2 ER 3	E2 IGG 1	E2 IGG 2	E2 IGG 3	ETOH ER 1	ETOH ER 2	ETOH ER 3	ETOH IGG 1	ETOH IGG 2	ETOH IGG 3	Unique peptides	Seq. coverage
AP5Z1	25.5361	25.5462	0	0	25.8739	0	26.1651	26.6661	27.2861	0	0	0	5	6.8
ARID1A	30.5326	30.6312	30.5811	0	0	0	30.806	30.9144	30.8661	0	0	0	9	8.1
BCL7A	31.7591	31.7227	31.6949	0	0	0	31.6973	31.4949	31.4678	0	0	0	7	53.3
BCL7B	31.4763	31.3559	31.5116	0	0	0	30.8859	30.8717	30.9356	0	0	0	4	41.6
BCL7C	31.076	31.067	31.2209	0	0	0	31.1584	31.1582	30.996	0	0	0	9	44.2
BRD7	28.5255	27.8783	27.816	25.7778	0	0	28.1043	27.5341	28.0007	25.591	0	0	9	13.4
BRD9	0	0	0	0	0	0	26.6112	25.9605	26.0713	0	0	0	2	4.9
BST2	27.9392	27.7711	27.8511	0	0	0	0	0	0	0	0	27.1429	2	13.9
C14orf166	26.1333	26.1308	26.3733	0	0	0	26.137	26.4746	26.1225	26.0204	0	0	3	10.2
DEK	26.3358	26.0126	26.167	0	0	0	26.6144	0	26.7686	0	0	0	2	6.1
DPF1	29.6593	29.585	29.5182	0	0	0	29.2929	29.3036	29.2052	0	0	0	8	17.9
DPF2	33.3164	33.3882	33.3073	0	0	0	33.0877	33.1121	33.1166	0	0	0	24	59.8
FAM179B	27.8894	27.8699	27.5475	0	0	0	27.7573	27.6554	27.8617	0	0	0	7	5.4
FYTTD1	26.2638	26.105	26.2372	0	0	25.8008	26.0473	0	0	0	26.3028	0	6	16
GREB1L	0	0	0	0	0	0	26.1311	26.0562	26.1009	0	0	0	3	2.7
GTPBP6	25.596	26.0945	0	0	0	0	27.1294	26.9336	26.3517	0	0	0	6	12
HGS	28.14	27.7647	28.1193	0	26.1381	0	27.8866	27.9568	28.1982	0	0	0	10	12.6
MED1	0	26.4249	26.0065	26.6237	0	0	26.5951	26.9842	26.4998	0	0	0	8	7.4
MED15	0	0	0	0	0	0	25.9875	26.0146	25.8565	0	0	0	2	3.6
MED22	25.7512	25.6462	25.6265	0	0	0	26.2503	26.0893	26.0904	0	0	0	3	12
MED27	0	0	26.0873	0	0	26.068	26.7345	26.6987	26.7521	0	0	0	3	10.6
MORF4L1	25.8922	25.6657	25.7628	0	0	0	0	0	0	0	0	0	2	6.6
MT-CO2	26.5133	27.2378	27.3029	0	0	0	0	0	0	0	0	0	2	7.5
MYBBP1A	24.4708	25.4981	25.1873	0	0	0	0	0	0	0	0	0	4	3.3
PABPC4	26.0617	26.0196	26.214	0	0	0	26.462	25.724	26.5701	0	0	0	2	6.5
PDS5B	25.3489	25.4819	25.49	0	0	0	0	0	0	0	0	25.7915	1	1.6
PHF10	28.9468	28.8533	28.6814	0	0	0	28.7087	28.7941	28.6382	0	0	0	6	11.4
PHF12	27.6053	27.7584	27.7455	0	0	0	28.31	28.2644	28.2836	0	0	0	10	12.9
RASAL2	29.9494	29.7015	29.874	0	0	0	30.9106	30.218	30.1011	0	0	0	18	22.1
SIN3B	28.9342	28.7089	28.8093	0	0	0	28.5161	28.3921	28.5103	0	0	0	14	14.6
SMARCD1	32.0409	32.069	31.9934	0	0	0	31.8396	31.8806	31.919	0	0	0	19	38.1
SS18	31.5595	31.5065	31.5646	0	0	0	31.7873	31.6749	31.7168	0	0	0	5	12.4
SS18L1	31.0661	30.6247	30.6802	0	0	0	30.7213	30.7723	30.7903	0	0	0	5	17.4
TMEM159	27.3546	27.1775	27.3837	0	0	0	27.8196	27.8186	28.1237	0	0	0	4	19.3
TRRAP	27.5304	28.598	26.7604	0	0	0	0	0	0	0	0	26.5803	5	1.7
VDAC3	26.3019	26.7062	26.2226	0	27.8221	0	0	0	26	0	0	0	6	19.1

Table 3E, +/- DOX, ERα F-10 antibody. All values are -log2 LFQ

Target name	DOX ER 1	DOX ER 2	DOX ER 3	DOX IGG 1	DOX IGG 2	DOX IGG 3	H2O ER 1	H2O ER 2	H2O ER 3	H2O IGG 1	H2O IGG 2	H2O IGG 3	Unique peptides	Seq. coverage
AES	0	25.3286	25.2975	0	0	0	25.3758	25.4079	25.432	0	0	0	2	10.7
ANK3	26.0688	26.0034	0	0	0	26.4096	26.005	26.0415	26.148	0	0	0	6	2.3
AP5Z1	25.7357	0	25.4785	0	0	0	26.074	26.0972	25.9747	0	0	0	5	6.8
ARAF	26.4327	26.1454	26.2485	0	0	0	26.2238	0	26.0328	0	0	26.1894	2	10.4
ARID3A	26.4988	26.1175	26.234	0	26.6315	0	26.757	26.6155	26.9981	0	26.8046	0	4	9.6
ASTN2	28.4002	28.5288	28.5085	28.7068	0	0	28.3521	28.4254	28.4622	0	0	0	2	2.5
BNIPL	0	26.1495	0	26.4099	0	0	26.6228	26.5721	26.6818	0	0	26.8236	3	10.6
CALU	25.5681	25.4032	0	0	0	0	25.8673	25.4902	25.5285	0	0	0	3	11.4
DAB2IP	24.9627	25.1863	0	0	0	26.1652	26.1918	25.7577	26.8038	26.1241	0	0	14	16.9
DAZAP1	33.8189	33.9114	33.8729	0	0	0	34.4144	34.4729	34.432	0	0	0	9	22.6
DDX27	26.204	0	26.3293	0	0	0	25.9056	25.9107	25.9254	0	0	0	6	7.2
DDX41	26.0351	26.1452	26.2233	0	0	0	26.0013	26.148	26.1027	0	26.5872	0	7	13.5
DYNC1I2	26.6859	26.3754	26.4396	0	0	0	0	0	0	0	0	26.5799	5	11.1
EIF2S1	25.8183	25.8598	25.75	0	0	0	25.586	25.2124	0	0	0	0	3	10.5
EMD	26.3759	26.2987	26.663	0	0	0	26.1397	26.1253	0	0	0	25.9671	3	15.4
FTSJ3	26.5506	26.6773	26.6109	0	0	0	26.7626	0	0	25.9579	0	0	7	8.5
FXR2	0	0	0	0	0	0	26.5375	27.3177	27.1212	0	0	26.2525	1	3.9
GLUD1;GLUD2	25.7941	26.0343	25.6019	0	0	0	0	0	0	0	0	0	4	6.6
GREB1	27.8528	28.0897	28.1206	0	0	0	28.2966	28.2632	28.2128	0	0	0	8	7.6
GREB1L	27.1408	27.1059	26.969	0	0	0	28.4962	27.4496	27.4311	0	0	0	3	2.7
GTPBP6	26.1182	26.1373	26.0616	0	0	0	26.1268	26.3697	0	0	0	26.5529	6	12
IGLV2-11;IGLV2-8	28.5394	27.8143	28.9931	0	0	0	28.1972	29.4174	29.4088	0	0	0	1	10.9
KIDINS220	27.8323	27.7674	0	0	0	0	28.5357	28.0127	28.1527	0	0	0	2	1.2
LARP4B	30.3283	30.7802	29.8851	0	0	0	29.6527	29.4695	29.7995	0	29.3153	0	6	8.3
MMTAG2	25.9571	25.8401	25.8864	0	0	0	25.8879	0	25.9016	0	0	0	4	19.4
NLRP7;NLRP2	25.6214	25.5015	25.4438	0	0	0	0	0	0	0	0	0	3	3
NOC3L	25.1951	25.1637	25.1485	0	25.2944	0	0	0	0	25.3712	0	0	3	3.5
PARP1	0	0	0	0	0	0	26.3929	26.8531	26.1611	0	0	0	6	7.5
RAB25	0	0	0	0	0	0	26.3336	26.4031	26.4878	0	0	0	2	13.1
RBM45	32.9436	31.9307	31.2316	0	0	0	33.7267	33.2548	34.4963	0	0	0	24	41.8
RBM47	0	26.8367	0	0	0	0	27.0016	27.0366	27.2885	0	0	0	4	7.8
RPN2	27.2276	27.0574	27.0951	0	0	0	26.8138	0	0	26.6724	0	0	5	12.4
SEC22B	26.4356	0	26.097	0	0	0	26.0036	25.9647	26.2922	25.8785	0	0	3	12.6
SEC61A1;SEC61A2	27.0943	26.9797	26.9421	0	0	0	0	0	26.7103	0	0	0	4	8.6
SEP_10	25.7262	25.7657	0	0	0	25.7861	25.2418	24.9631	25.673	25.6266	0	0	9	20
SF3B6	26.238	25.9438	25.979	0	0	0	0	0	26.0984	0	25.7467	0	3	24.8
STT3A	25.5553	25.7083	25.5995	0	0	0	0	0	0	0	0	0	4	5

Target name	DOX ER 1	DOX ER 2	DOX ER 3	DOX IGG 1	DOX IGG 2	DOX IGG 3	H2O ER 1	H2O ER 2	H2O ER 3	H2O IGG 1	H2O IGG 2	H2O IGG 3	Unique peptides	Seq. coverage
TBC1D30	26.1409	0	26.2887	0	0	0	26.4654	26.3819	26.4872	0	0	0	3	3.4
TFRC	26.7886	26.8126	26.9829	0	0	0	0	26.7657	26.5292	0	0	0	8	12
TRUB1	24.4679	24.5631	24.4178	0	0	0	0	0	0	0	0	25.1147	3	9.2
WDR5	26.1854	26.3018	26.2751	0	0	0	26.428	26.4986	26.5022	0	0	0	4	19.2
XRCC5	26.0351	25.9759	25.948	0	26.0434	0	25.9069	26.0881	25.9082	0	0	26.2495	6	9.6
ZBTB44	27.8579	27.6389	27.8202	0	0	0	28.1126	27.9889	28.0354	0	0	0	4	10.4
ZNF385A	25.3728	25.5483	25.6388	0	0	0	25.6823	25.6402	25.5699	0	0	25.3608	3	7.5

Table 4E, +/- E2, ERα F-10 antibody. All values are -log2 LFQ

Target name	E2 ER 1	E2 ER 2	E2 ER 3	E2 IGG 1	E2 IGG 2	E2 IGG 3	ETOH ER 1	ETOH ER 2	ETOH ER 3	ETOH IGG 1	ETOH IGG 2	ETOH IGG 3	Unique peptides	Seq. coverage
ANXA2;ANXA2P2	25.9945	0	26.1605	0	0	0	25.6524	25.7046	25.8225	0	0	0	2	5.6
AP1G1	25.0011	24.998	25.0385	0	0	0	0	0	0	0	0	0	3	3.5
AP5Z1	25.9369	25.6402	25.8127	0	25.8739	0	26.0359	25.9511	25.9618	0	0	0	5	6.8
C14orf166	26.0511	26.1531	26.2827	0	0	0	26.2434	25.9326	26.153	26.0204	0	0	3	10.2
CCDC137	26.9261	26.8317	26.867	0	0	0	27.4433	0	0	0	0	0	1	3.1
CCDC47	26.7754	26.8405	26.738	0	0	0	26.5074	26.5356	26.505	0	26.1295	0	3	6.2
CHMP2A	25.8909	25.7983	25.7975	0	0	0	25.3914	25.3953	25.5016	0	0	0	3	11.7
DAZAP1	33.1078	33.1743	33.0185	0	0	0	33.2137	33.1899	33.2302	0	0	0	9	22.6
EIF2S1	26.9896	26.8798	27.1453	26.256	0	0	0	25.197	25.37	0	0	0	3	10.5
FYTTD1	25.7788	26.1462	26.6483	0	0	25.8008	26.0743	26.1196	26.6195	0	26.3028	0	6	16
GREB1	25.9579	25.8015	26.0554	0	28.7093	0	28.1218	27.5638	28.1094	0	0	0	8	7.6
GREB1L	0	0	0	0	0	0	26.6204	26.5248	26.8649	0	0	0	3	2.7
GTPBP6	0	0	25.6759	0	0	0	26.192	25.9509	26.3268	0	0	0	6	12
HEATR6	26.2422	26.3997	26.4662	0	26.8072	0	26.5159	26.38	26.6921	0	0	26.5054	4	6.3
IGLV2-11;IGLV2-8	0	26.8316	24.9862	0	0	0	25.799	28.5355	28.4896	0	0	0	1	10.9
MAGOH;MAGOHB	26.4798	26.3149	26.654	26.158	0	0	0	25.9358	0	0	0	0	3	28.8
MGP	27.2593	26.7715	27.1922	26.1142	0	0	0	25.8669	25.9576	0	0	0	2	19.4
MT-CO2	27.5308	27.4575	27.7455	0	0	0	0	0	0	0	0	0	2	7.5
MYBBP1A	25.559	25.3293	25.9668	0	0	0	25.3549	0	25.4278	0	0	0	4	3.3
NIPSNAP1	25.6668	25.421	25.1155	0	0	0	0	24.9608	0	0	0	0	2	8.8
NOC3L	0	0	25.232	0	0	0	25.2162	25.2144	25.7792	0	0	0	3	3.5
PABPC4	25.7585	26.2147	0	0	0	0	26.1378	25.9476	26.0432	0	0	0	2	6.5
PDS5B	26.1637	25.8821	25.9754	0	0	0	25.8746	25.7941	25.6787	0	0	25.7915	1	1.6
PPIG	26.6581	26.6915	26.714	0	0	26.2599	26.8379	27.0346	27.2083	0	0	26.8368	7	10.7
RAD21	31.1396	0	0	31.3151	0	0	31.1452	31.06	31.3368	0	0	31.2714	3	6.8
RANBP6	25.5522	25.9562	25.8424	0	0	0	25.9244	0	0	0	0	0	1	1.4
RBM45	29.7356	30.9259	31.5274	0	0	0	31.4772	31.5677	32.0813	0	0	25.9689	24	41.8
SEC61A1;SEC61A2	27.071	27.0227	26.9374	0	0	0	26.9784	26.8687	26.9807	0	0	0	4	8.6
SF3A3	26.3869	25.9587	25.8965	0	0	0	0	0	0	0	0	26.5204	4	10.2
SOD1	24.0504	23.989	24.2053	0	0	0	24.3831	24.557	24.3528	0	0	24.0851	2	15.6
STT3B	23.4339	22.8535	23.3148	0	0	0	0	0	0	0	0	0	3	3.6
THEM6	24.984	25.2422	25.2073	0	0	0	0	0	0	0	0	0	3	13
VDAC3	26.8531	27.653	27.047	0	27.8221	0	0	0	0	0	0	0	6	19.1
ZBTB44	26.2377	26.0171	26.1502	0	0	0	27.2082	27.0341	27.331	0	0	0	4	10.4
ZNF385A	25.3198	25.3032	25.2413	0	0	0	25.4281	25.131	25.2644	0	0	0	3	7.5

Bibliography

1983. Controlled trial of tamoxifen as adjuvant agent in management of early breast cancer. Interim analysis at four years by Nolvadex Adjuvant Trial Organisation. Lancet, 1, 257-61.

1997. Breast cancer and hormone replacement therapy: collaborative reanalysis of data from 51 epidemiological studies of 52,705 women with breast cancer and 108,411 women without breast cancer. Collaborative Group on Hormonal Factors in Breast Cancer. Lancet, 350, 1047-59.

2002. Breast cancer and breastfeeding: collaborative reanalysis of individual data from 47 epidemiological studies in 30 countries, including 50302 women with breast cancer and 96973 women without the disease. Lancet, 360, 187-95.

ABELS, M., RIVA, M., BENNET, H., AHLQVIST, E., DYACHOK, O., NAGARAJ, V., SHCHERBINA, L., FRED, R. G., POON, W., SORHEDE-WINZELL, M., FADISTA, J., LINDQVIST, A., KASK, L., SATHANOORI, R., DEKKER-NITERT, M., KUHAR, M. J., AHREN, B., WOLLHEIM, C. B., HANSSON, O., TENGHOLM, A., FEX, M., RENSTROM, E., GROOP, L., LYSSENKO, V. & WIERUP, N. 2016. CART is overexpressed in human type 2 diabetic islets and inhibits glucagon secretion and increases insulin secretion. Diabetologia, 59, 1928-37.

ABRAMS, E., NEIGEBORN, L. & CARLSON, M. 1986. Molecular analysis of SNF2 and SNF5, genes required for expression of glucose-repressible genes in Saccharomyces cerevisiae. Mol Cell Biol, 6, 3643-51.

ALAJEM, A., BIRAN, A., HARIKUMAR, A., SAILAJA, B. S., AARONSON, Y., LIVYATAN, I., NISSIM-RAFINIA, M., SOMMER, A. G., MOSTOSLAVSKY, G., GERBASI, V. R., GOLDEN, D. E., DATTA, A., SZE, S. K. & MESHORER, E. 2015. Differential association of chromatin proteins identifies BAF60a/SMARCD1 as a regulator of embryonic stem cell differentiation. Cell Rep, 10, 2019-31.

ALKNER, S., BENDAHL, P., GRABAU, D., MALMSTROM, P., FERNO, M. & RYDEN, L. 2013. The role of AIB1 and PAX2 in primary breast cancer: validation of AIB1 as a negative prognostic factor. Ann Oncol, 24, 1244-52.

ANAMPA, J., MAKOWER, D. & SPARANO, J. A. 2015. Progress in adjuvant chemotherapy for breast cancer: an overview. BMC Med, 13, 195.

ANDERSON, G. L. & NEUHOUSER, M. L. 2012. Obesity and the risk for premenopausal and postmenopausal breast cancer. Cancer Prev Res (Phila), 5, 515-21.

ANSARI, A., BOSE, S., YADAV, M. K., WANG, J. H., SONG, Y. K., KO, S. G. & KIM, H. 2016. CST, an Herbal Formula, Exerts Anti-Obesity Effects through Brain-Gut-Adipose Tissue Axis Modulation in High-Fat Diet Fed Mice. Molecules, 21.

ANTONIOU, A., PHAROAH, P. D., NAROD, S., RISCH, H. A., EYFJORD, J. E., HOPPER, J. L., LOMAN, N., OLSSON, H., JOHANNSSON, O., BORG, A., PASINI, B., RADICE, P., MANOUKIAN, S., ECCLES, D. M., TANG, N., OLAH, E., ANTON-CULVER, H., WARNER, E., LUBINSKI, J., GRONWALD, J., GORSKI, B., TULINIUS, H., THORLACIUS, S., EEROLA, H., NEVANLINNA, H., SYRJAKOSKI, K., KALLIONIEMI, O. P., THOMPSON, D., EVANS, C., PETO, J., LALLOO, F., EVANS, D. G. & EASTON, D. F. 2003. Average risks of breast and ovarian cancer associated

with BRCA1 or BRCA2 mutations detected in case Series unselected for family history: a combined analysis of 22 studies. Am J Hum Genet, 72, 1117-30.

ASNICAR, M. A., SMITH, D. P., YANG, D. D., HEIMAN, M. L., FOX, N., CHEN, Y. F., HSIUNG, H. M. & KOSTER, A. 2001. Absence of cocaine- and amphetamine-regulated transcript results in obesity in mice fed a high caloric diet. Endocrinology, 142, 4394-400.

BADVE, S., TURBIN, D., THORAT, M. A., MORIMIYA, A., NIELSEN, T. O., PEROU, C. M., DUNN, S., HUNTSMAN, D. G. & NAKSHATRI, H. 2007. FOXA1 expression in breast cancer--correlation with luminal subtype A and survival. Clin Cancer Res, 13, 4415-21.

BALDIN, V., LUKAS, J., MARCOTE, M. J., PAGANO, M. & DRAETTA, G. 1993. Cyclin D1 is a nuclear protein required for cell cycle progression in G1. Genes Dev, 7, 812-21.

BANTSCHEFF, M., HOPF, C., SAVITSKI, M. M., DITTMANN, A., GRANDI, P., MICHON, A. M., SCHLEGL, J., ABRAHAM, Y., BECHER, I., BERGAMINI, G., BOESCHE, M., DELLING, M., DUMPELFELD, B., EBERHARD, D., HUTHMACHER, C., MATHIESON, T., POECKEL, D., READER, V., STRUNK, K., SWEETMAN, G., KRUSE, U., NEUBAUER, G., RAMSDEN, N. G. & DREWES, G. 2011. Chemoproteomics profiling of HDAC inhibitors reveals selective targeting of HDAC complexes. Nat Biotechnol, 29, 255-65.

BARRETT, P., DAVIDSON, J. & MORGAN, P. 2002. CART gene promoter transcription is regulated by a cyclic adenosine monophosphate response element. Obes Res, 10, 1291-8.

BARSH, G. S. & SCHWARTZ, M. W. 2002. Genetic approaches to studying energy balance: perception and integration. Nat Rev Genet, 3, 589-600.

BASELGA, J., CARBONELL, X., CASTANEDA-SOTO, N. J., CLEMENS, M., GREEN, M., HARVEY, V., MORALES, S., BARTON, C. & GHAHRAMANI, P. 2005. Phase II study of efficacy, safety, and pharmacokinetics of trastuzumab monotherapy administered on a 3-weekly schedule. J Clin Oncol, 23, 2162-71.

BAUM, M., BRINKLEY, D. M., DOSSETT, J. A., MCPHERSON, K., PATTERSON, J. S., RUBENS, R. D., SMIDDY, F. G., STOLL, B. A., WILSON, A., LEA, J. C., RICHARDS, D. & ELLIS, S. H. 1983. Improved survival among patients treated with adjuvant tamoxifen after mastectomy for early breast cancer. Lancet, 2, 450.

BEATSON, G. ON THE TREATMENT OF INOPERABLE CASES OF CARCINOMA OF THE MAMMA: SUGGESTIONS FOR A NEW METHOD OF TREATMENT, WITH ILLUSTRATIVE CASES. The Lancet, 148, 162-165.

BECH, P., WINSTANLEY, V., MURPHY, K. G., SAM, A. H., MEERAN, K., GHATEI, M. A. & BLOOM, S. R. 2008. Elevated cocaine- and amphetamine-regulated transcript immunoreactivity in the circulation of patients with neuroendocrine malignancy. J Clin Endocrinol Metab, 93, 1246-53.

BEN-PORATH, I., THOMSON, M. W., CAREY, V. J., GE, R., BELL, G. W., REGEV, A. & WEINBERG, R. A. 2008. An embryonic stem cell-like gene expression signature in poorly differentiated aggressive human tumors. Nat Genet, 40, 499-507.

BERGH, J., JONSSON, P. E., LIDBRINK, E. K., TRUDEAU, M., EIERMANN, W., BRATTSTROM, D., LINDEMANN, J. P., WIKLUND, F. & HENRIKSSON, R. 2012. FACT: an open-label randomized phase III study of fulvestrant and anastrozole in combination compared with anastrozole

alone as first-line therapy for patients with receptor-positive postmenopausal breast cancer. J Clin Oncol, 30, 1919-25.

BERNS, E. M., VAN STAVEREN, I. L., KLIJN, J. G. & FOEKENS, J. A. 1998. Predictive value of SRC-1 for tamoxifen response of recurrent breast cancer. Breast Cancer Res Treat, 48, 87-92.

BERTUCCI, F., FINETTI, P. & BIRNBAUM, D. 2012. Basal breast cancer: a complex and deadly molecular subtype. Curr Mol Med, 12, 96-110.

BIAN, C., CHEN, Q. & YU, X. 2015. Correction: The zinc finger proteins ZNF644 and WIZ regulate the G9a/GLP complex for gene repression. Elife, 4.

BIEGEL, J. A., ZHOU, J. Y., RORKE, L. B., STENSTROM, C., WAINWRIGHT, L. M. & FOGELGREN, B. 1999. Germ-line and acquired mutations of INI1 in atypical teratoid and rhabdoid tumors. Cancer Res, 59, 74-9.

BIRCH, J. M., ALSTON, R. D., MCNALLY, R. J., EVANS, D. G., KELSEY, A. M., HARRIS, M., EDEN, O. B. & VARLEY, J. M. 2001. Relative frequency and morphology of cancers in carriers of germline TP53 mutations. Oncogene, 20, 4621-8.

BOSCH, A., EROLES, P., ZARAGOZA, R., VINA, J. R. & LLUCH, A. 2010. Triple-negative breast cancer: molecular features, pathogenesis, treatment and current lines of research. Cancer Treat Rev, 36, 206-15.

BRENNAN, D. J., O'CONNOR, D. P., LAURSEN, H., MCGEE, S. F., MCCARTHY, S., ZAGOZDZON, R., REXHEPAJ, E., CULHANE, A. C., MARTIN, F. M., DUFFY, M. J., LANDBERG, G., RYDEN, L., HEWITT, S. M., KUHAR, M. J., BERNARDS, R., MILLIKAN, R. C., CROWN, J. P., JIRSTROM, K. & GALLAGHER, W. M. 2012. The cocaine- and amphetamine-regulated transcript mediates ligand-independent activation of ERalpha, and is an independent prognostic factor in node-negative breast cancer. Oncogene, 31, 3483-94.

BRÜCKNER, A., POLGE, C., LENTZE, N., AUERBACH, D. & SCHLATTNER, U. 2009. Yeast Two-Hybrid, a Powerful Tool for Systems Biology. International Journal of Molecular Sciences, 10, 2763-2788.

BRUNNER, N., BOULAY, V., FOJO, A., FRETER, C. E., LIPPMAN, M. E. & CLARKE, R. 1993. Acquisition of hormone-independent growth in MCF-7 cells is accompanied by increased expression of estrogen-regulated genes but without detectable DNA amplifications. Cancer Res, 53, 283-90.

BRUNNER, N., BOYSEN, B., JIRUS, S., SKAAR, T. C., HOLST-HANSEN, C., LIPPMAN, J., FRANDSEN, T., SPANG-THOMSEN, M., FUQUA, S. A. & CLARKE, R. 1997. MCF7/LCC9: an antiestrogen-resistant MCF-7 variant in which acquired resistance to the steroidal antiestrogen ICI 182,780 confers an early cross-resistance to the nonsteroidal antiestrogen tamoxifen. Cancer Res, 57, 3486-93.

BRUNNER, N., FRANDSEN, T. L., HOLST-HANSEN, C., BEI, M., THOMPSON, E. W., WAKELING, A. E., LIPPMAN, M. E. & CLARKE, R. 1993. MCF7/LCC2: a 4-hydroxytamoxifen resistant human breast cancer variant that retains sensitivity to the steroidal antiestrogen ICI 182,780. Cancer Res, 53, 3229-32.

BURGHARDT, P. R., KROLEWSKI, D. M., DYKHUIS, K. E., CHING, J., PINAWIN, A. M., BRITTON, S. L., KOCH, L. G., WATSON, S. J. & AKIL, H. 2016. Nucleus accumbens cocaine-amphetamine regulated transcript mediates food intake during novelty conflict. Physiol Behav, 158, 76-84.

CASIMIRO, M. C., WANG, C., LI, Z., DI SANTE, G., WILLMART, N. E., ADDYA, S., CHEN, L., LIU, Y., LISANTI, M. P. & PESTELL, R. G. 2013. Cyclin D1 determines estrogen signaling in the mammary gland in vivo. Mol Endocrinol, 27, 1415-28.

CATALANO, S., MARSICO, S., GIORDANO, C., MAURO, L., RIZZA, P., PANNO, M. L. & ANDO, S. 2003. Leptin enhances, via AP-1, expression of aromatase in the MCF-7 cell line. J Biol Chem, 278, 28668-76.

CERAMI, E., GAO, J., DOGRUSOZ, U., GROSS, B. E., SUMER, S. O., AKSOY, B. A., JACOBSEN, A., BYRNE, C. J., HEUER, M. L., LARSSON, E., ANTIPIN, Y., REVA, B., GOLDBERG, A. P., SANDER, C. & SCHULTZ, N. 2012. The cBio cancer genomics portal: an open platform for exploring multidimensional cancer genomics data. Cancer Discov, 2, 401-4.

CHAMBLISS, K. L. & SHAUL, P. W. 2002. Estrogen modulation of endothelial nitric oxide synthase. Endocr Rev, 23, 665-86.

CHANG, L., CHEN, Y., LI, J., LIU, Z., WANG, Z., CHEN, J., CAO, W. & XU, Y. 2011. Cocaine-and amphetamine-regulated transcript modulates peripheral immunity and protects against brain injury in experimental stroke. Brain Behav Immun, 25, 260-9.

CHANG, M. 2012. Tamoxifen resistance in breast cancer. Biomol Ther (Seoul), 20, 256-67.

CHEN, M., CUI, Y.-K., HUANG, W.-H., MAN, K. & ZHANG, G.-J. 2013. Phosphorylation of estrogen receptor α at serine 118 is correlated with breast cancer resistance to tamoxifen. Oncology Letters, 6, 118-124.

CHIBA, H., MURAMATSU, M., NOMOTO, A. & KATO, H. 1994. Two human homologues of Saccharomyces cerevisiae SWI2/SNF2 and Drosophila brahma are transcriptional coactivators cooperating with the estrogen receptor and the retinoic acid receptor. Nucleic Acids Res, 22, 1815-20.

CHIU, H. Y., LIN, H. H. & LAI, C. C. 2010. Cocaine- and amphetamine-regulated transcript (CART) peptide activates ERK pathways via NMDA receptors in rat spinal cord dorsal horn in an age-dependent manner. Regul Pept, 164, 90-6.

CHO, H. D., LEE, J. E., JUNG, H. Y., OH, M.-H., LEE, J.-H., JANG, S.-H., KIM, K.-J., HAN, S. W., KIM, S. Y., KIM, H. J., BAE, S. B. & LEE, H. J. 2015. Loss of Tumor Suppressor ARID1A Protein Expression Correlates with Poor Prognosis in Patients with Primary Breast Cancer. Journal of Breast Cancer, 18, 339-346.

CICATIELLO, L., ADDEO, R., SASSO, A., ALTUCCI, L., PETRIZZI, V. B., BORGO, R., CANCEMI, M., CAPORALI, S., CARISTI, S., SCAFOGLIO, C., TETI, D., BRESCIANI, F., PERILLO, B. & WEISZ, A. 2004. Estrogens and progesterone promote persistent CCND1 gene activation during G1 by inducing transcriptional derepression via c-Jun/c-Fos/estrogen receptor (progesterone receptor) complex assembly to a distal regulatory element and recruitment of cyclin D1 to its own gene promoter. Mol Cell Biol, 24, 7260-74.

CIRIELLO, G., GATZA, M. L., BECK, A. H., WILKERSON, M. D., RHIE, S. K., PASTORE, A., ZHANG, H., MCLELLAN, M., YAU, C., KANDOTH, C., BOWLBY, R., SHEN, H., HAYAT, S., FIELDHOUSE, R., LESTER, S. C., TSE, G. M., FACTOR, R. E., COLLINS, L. C., ALLISON, K. H., CHEN, Y. Y., JENSEN, K., JOHNSON, N. B., OESTERREICH, S., MILLS, G. B., CHERNIACK, A. D., ROBERTSON, G., BENZ, C., SANDER, C., LAIRD, P. W., HOADLEY, K. A., KING, T. A. & PEROU, C. M. 2015. Comprehensive Molecular Portraits of Invasive Lobular Breast Cancer. Cell, 163, 506-19.

CIRUELOS, E., PASCUAL, T., ARROYO VOZMEDIANO, M. L., BLANCO, M., MANSO, L., PARRILLA, L., MUNOZ, C., VEGA, E., CALDERON, M. J., SANCHO, B. & CORTES-FUNES, H. 2014. The therapeutic role of fulvestrant in the management of patients with hormone receptor-positive breast cancer. Breast, 23, 201-8.

CLARKE, C. A., CANCHOLA, A. J., MOY, L. M., NEUHAUSEN, S. L., CHUNG, N. T., LACEY, J. V., JR. & BERNSTEIN, L. 2017. Regular and low-dose aspirin, other non-steroidal anti-inflammatory medications and prospective risk of HER2-defined breast cancer: the California Teachers Study. Breast Cancer Res, 19, 52.

CLOONAN, N., FORREST, A. R., KOLLE, G., GARDINER, B. B., FAULKNER, G. J., BROWN, M. K., TAYLOR, D. F., STEPTOE, A. L., WANI, S., BETHEL, G., ROBERTSON, A. J., PERKINS, A. C., BRUCE, S. J., LEE, C. C., RANADE, S. S., PECKHAM, H. E., MANNING, J. M., MCKERNAN, K. J. & GRIMMOND, S. M. 2008. Stem cell transcriptome profiling via massive-scale mRNA sequencing. Nat Methods, 5, 613-9.

COISY-QUIVY, M., DISSON, O., ROURE, V., MUCHARDT, C., BLANCHARD, J. M. & DANTONEL, J. C. 2006. Role for Brm in cell growth control. Cancer Res, 66, 5069-76.

CREIGHTON, C. J., MASSARWEH, S., HUANG, S., TSIMELZON, A., HILSENBECK, S. G., OSBORNE, C. K., SHOU, J., MALORNI, L. & SCHIFF, R. 2008. Development of resistance to targeted therapies transforms the clinically associated molecular profile subtype of breast tumor xenografts. Cancer Res, 68, 7493-501.

CURTIS, C., SHAH, S. P., CHIN, S.-F., TURASHVILI, G., RUEDA, O. M., DUNNING, M. J., SPEED, D., LYNCH, A. G., SAMARAJIWA, S., YUAN, Y., GRÄF, S., HA, G., HAFFARI, G., BASHASHATI, A., RUSSELL, R., MCKINNEY, S., GROUP, M., LANGERØD, A., GREEN, A., PROVENZANO, E., WISHART, G., PINDER, S., WATSON, P., MARKOWETZ, F., MURPHY, L., ELLIS, I., PURUSHOTHAM, A., BØRRESEN-DALE, A.-L., BRENTON, J. D., TAVARÉ, S., CALDAS, C. & APARICIO, S. 2012. The genomic and transcriptomic architecture of 2,000 breast tumours reveals novel subgroups. Nature, 486, 346.

DAHLMAN-WRIGHT, K., QIAO, Y., JONSSON, P., GUSTAFSSON, J. A., WILLIAMS, C. & ZHAO, C. 2012. Interplay between AP-1 and estrogen receptor alpha in regulating gene expression and proliferation networks in breast cancer cells. Carcinogenesis, 33, 1684-91.

DAVIES, C., PAN, H., GODWIN, J., GRAY, R., ARRIAGADA, R., RAINA, V., ABRAHAM, M., MEDEIROS ALENCAR, V. H., BADRAN, A., BONFILL, X., BRADBURY, J., CLARKE, M., COLLINS, R., DAVIS, S. R., DELMESTRI, A., FORBES, J. F., HADDAD, P., HOU, M. F., INBAR, M., KHALED, H., KIELANOWSKA, J., KWAN, W. H., MATHEW, B. S., MITTRA, I., MULLER, B., NICOLUCCI, A., PERALTA, O., PERNAS, F., PETRUZELKA, L., PIENKOWSKI, T., RADHIKA, R., RAJAN, B., RUBACH, M. T., TORT, S., URRUTIA, G., VALENTINI, M., WANG, Y. & PETO, R. 2013. Long-term effects of continuing adjuvant tamoxifen to 10 years versus stopping at 5 years after

diagnosis of oestrogen receptor-positive breast cancer: ATLAS, a randomised trial. Lancet, 381, 805-16.

DEL GIUDICE, E. M., SANTORO, N., CIRILLO, G., D'URSO, L., DI TORO, R. & PERRONE, L. 2001. Mutational screening of the CART gene in obese children: identifying a mutation (Leu34Phe) associated with reduced resting energy expenditure and cosegregating with obesity phenotype in a large family. Diabetes, 50, 2157-60.

DENG, L., SHANG, L., BAI, S., CHEN, J., HE, X., MARTIN-TREVINO, R., CHEN, S., LI, X. Y., MENG, X., YU, B., WANG, X., LIU, Y., MCDERMOTT, S. P., ARIAZI, A. E., GINESTIER, C., IBARRA, I., KE, J., LUTHER, T., CLOUTHIER, S. G., XU, L., SHAN, G., SONG, E., YAO, H., HANNON, G. J., WEISS, S. J., WICHA, M. S. & LIU, S. 2014. MicroRNA100 inhibits self-renewal of breast cancer stem-like cells and breast tumor development. Cancer Res, 74, 6648-60.

DEVITA, V. T., JR. & CHU, E. 2008. A history of cancer chemotherapy. Cancer Res, 68, 8643-53.

DEY, A., XHU, X., CARROLL, R., TURCK, C. W., STEIN, J. & STEINER, D. F. 2003. Biological processing of the cocaine and amphetamine-regulated transcript precursors by prohormone convertases, PC2 and PC1/3. J Biol Chem, 278, 15007-14.

DILWORTH, D. J., TACKETT, A. J., ROGERS, R. S., YI, E. C., CHRISTMAS, R. H., SMITH, J. J., SIEGEL, A. F., CHAIT, B. T., WOZNIAK, R. W. & AITCHISON, J. D. 2005. The mobile nucleoporin Nup2p and chromatin-bound Prp20p function in endogenous NPC-mediated transcriptional control. J Cell Biol, 171, 955-65.

DOBIN, A., DAVIS, C. A., SCHLESINGER, F., DRENKOW, J., ZALESKI, C., JHA, S., BATUT, P., CHAISSON, M. & GINGERAS, T. R. 2013. STAR: ultrafast universal RNA-seq aligner. Bioinformatics, 29, 15-21.

DOMINGUEZ, G., LAKATOS, A. & KUHAR, M. J. 2002. Characterization of the cocaine- and amphetamine-regulated transcript (CART) peptide gene promoter and its activation by a cyclic AMP-dependent signaling pathway in GH3 cells. J Neurochem, 80, 885-93.

DONG, D. D., JEWELL, C. M., BIENSTOCK, R. J. & CIDLOWSKI, J. A. 2006. Functional analysis of the LXXLL motifs of the human glucocorticoid receptor: association with altered ligand affinity. J Steroid Biochem Mol Biol, 101, 106-17.

DOUGLASS, J. & DAOUD, S. 1996. Characterization of the human cDNA and genomic DNA encoding CART: a cocaine- and amphetamine-regulated transcript. Gene, 169, 241-5.

DOUGLASS, J., MCKINZIE, A. A. & COUCEYRO, P. 1995. PCR differential display identifies a rat brain mRNA that is transcriptionally regulated by cocaine and amphetamine. J Neurosci, 15, 2471-81.

DOWSETT, M. & HAYNES, B. P. 2003. Hormonal effects of aromatase inhibitors: focus on premenopausal effects and interaction with tamoxifen. J Steroid Biochem Mol Biol, 86, 255-63.

DOWSETT, M., NIELSEN, T. O., A'HERN, R., BARTLETT, J., COOMBES, R. C., CUZICK, J., ELLIS, M., HENRY, N. L., HUGH, J. C., LIVELY, T., MCSHANE, L., PAIK, S., PENAULT-LLORCA, F., PRUDKIN, L., REGAN, M., SALTER, J., SOTIRIOU, C., SMITH, I. E., VIALE, G., ZUJEWSKI, J. A. &

HAYES, D. F. 2011. Assessment of Ki67 in breast cancer: recommendations from the International Ki67 in Breast Cancer working group. J Natl Cancer Inst, 103, 1656-64.

DWANE, L., GALLAGHER, W. M., NI CHONGHAILE, T. & O'CONNOR, D. P. 2017. The Emerging Role of Non-traditional Ubiquitination in Oncogenic Pathways. J Biol Chem, 292, 3543-3551.

EROLES, P., BOSCH, A., PEREZ-FIDALGO, J. A. & LLUCH, A. 2012. Molecular biology in breast cancer: intrinsic subtypes and signaling pathways. Cancer Treat Rev, 38, 698-707.

EWERTZ, M., DUFFY, S. W., ADAMI, H. O., KVALE, G., LUND, E., MEIRIK, O., MELLEMGAARD, A., SOINI, I. & TULINIUS, H. 1990. Age at first birth, parity and risk of breast cancer: a meta-analysis of 8 studies from the Nordic countries. Int J Cancer, 46, 597-603.

FELIPE LIMA, J., NOFECH-MOZES, S., BAYANI, J. & BARTLETT, J. M. 2016. EMT in Breast Carcinoma-A Review. J Clin Med, 5.

FIELDS, S. & SONG, O. 1989. A novel genetic system to detect protein-protein interactions. Nature, 340, 245-6.

FIGG, W. D., COOK, K. & CLARKE, R. 2014. Aromatase inhibitor plus ovarian suppression as adjuvant therapy in premenopausal women with breast cancer. Cancer Biology & Therapy, 15, 1586-1587.

FISHER, B., ANDERSON, S., BRYANT, J., MARGOLESE, R. G., DEUTSCH, M., FISHER, E. R., JEONG, J. H. & WOLMARK, N. 2002. Twenty-year follow-up of a randomized trial comparing total mastectomy, lumpectomy, and lumpectomy plus irradiation for the treatment of invasive breast cancer. N Engl J Med, 347, 1233-41.

FISHER, B., JEONG, J. H., ANDERSON, S., BRYANT, J., FISHER, E. R. & WOLMARK, N. 2002. Twenty-five-year follow-up of a randomized trial comparing radical mastectomy, total mastectomy, and total mastectomy followed by irradiation. N Engl J Med, 347, 567-75.

FISHER, B., REDMOND, C., BROWN, A., WICKERHAM, D. L., WOLMARK, N., ALLEGRA, J., ESCHER, G., LIPPMAN, M., SAVLOV, E., WITTLIFF, J. & ET AL., 1983. Influence of tumor estrogen and progesterone receptor levels on the response to tamoxifen and chemotherapy in primary breast cancer. J Clin Oncol, 1, 227-41.

FITZGERALD, L. M., BROWNE, E. P., CHRISTIE, K. D., PUNSKA, E. C., SIMMONS, L. O., WILLIAMS, K. E., PENTECOST, B. T., M. JAWALE, R., OTIS, C. N. & ARCARO, K. F. 2016. ELF5 and DOK7 regulation in anti-estrogen treated cells and tumors. Cancer Cell International, 16, 8.

FLAJOLLET, S., LEFEBVRE, B., CUDEJKO, C., STAELS, B. & LEFEBVRE, P. 2007. The core component of the mammalian SWI/SNF complex SMARCD3/BAF60c is a coactivator for the nuclear retinoic acid receptor. Mol Cell Endocrinol, 270, 23-32.

FREDRIKSSON, S., GULLBERG, M., JARVIUS, J., OLSSON, C., PIETRAS, K., GUSTAFSDOTTIR, S. M., OSTMAN, A. & LANDEGREN, U. 2002. Protein detection using proximity-dependent DNA ligation assays. Nat Biotechnol, 20, 473-7.

FUKUOKA, J., FUJII, T., SHIH, J. H., DRACHEVA, T., MEERZAMAN, D., PLAYER, A., HONG, K., SETTNEK, S., GUPTA, A., BUETOW, K., HEWITT, S., TRAVIS, W. D. & JEN, J. 2004. Chromatin

remodeling factors and BRM/BRG1 expression as prognostic indicators in non-small cell lung cancer. Clin Cancer Res, 10, 4314-24.

FUQUA, S. A., GU, G. & RECHOUM, Y. 2014. Estrogen receptor (ER) alpha mutations in breast cancer: hidden in plain sight. Breast Cancer Res Treat, 144, 11-9.

FUQUA, S. A., WILTSCHKE, C., ZHANG, Q. X., BORG, A., CASTLES, C. G., FRIEDRICHS, W. E., HOPP, T., HILSENBECK, S., MOHSIN, S., O'CONNELL, P. & ALLRED, D. C. 2000. A hypersensitive estrogen receptor-alpha mutation in premalignant breast lesions. Cancer Res, 60, 4026-9.

GAO, J., AKSOY, B. A., DOGRUSOZ, U., DRESDNER, G., GROSS, B., SUMER, S. O., SUN, Y., JACOBSEN, A., SINHA, R., LARSSON, E., CERAMI, E., SANDER, C. & SCHULTZ, N. 2013. Integrative analysis of complex cancer genomics and clinical profiles using the cBioPortal. Sci Signal, 6, pl1.

GARCIA-PEDRERO, J. M., KISKINIS, E., PARKER, M. G. & BELANDIA, B. 2006. The SWI/SNF chromatin remodeling subunit BAF57 is a critical regulator of estrogen receptor function in breast cancer cells. J Biol Chem, 281, 22656-64.

GARCIA-PEDRERO, J. M., KISKINIS, E., PARKER, M. G. & BELANDIA, B. 2006. The SWI/SNF chromatin remodeling subunit BAF57 is a critical regulator of estrogen receptor function in breast cancer cells. J Biol Chem, 281, 22656-64.

GELMON, K., DENT, R., MACKEY, J. R., LAING, K., MCLEOD, D. & VERMA, S. 2012. Targeting triple-negative breast cancer: optimising therapeutic outcomes. Ann Oncol, 23, 2223-34.

GERTZ, J., SAVIC, D., VARLEY, K. E., PARTRIDGE, E. C., SAFI, A., JAIN, P., COOPER, G. M., REDDY, T. E., CRAWFORD, G. E. & MYERS, R. M. 2013. Distinct properties of cell type-specific and shared transcription factor binding sites. Molecular cell, 52, 10.1016/j.molcel.2013.08.037.

GIESSRIGL, B., SCHMIDT, W. M., KALIPCIYAN, M., JEITLER, M., BILBAN, M., GOLLINGER, M., KRIEGER, S., JÄGER, W., MADER, R. M. & KRUPITZA, G. 2013. Fulvestrant induces resistance by modulating GPER and CDK6 expression: implication of methyltransferases, deacetylases and the hSWI/SNF chromatin remodelling complex. British Journal of Cancer, 109, 2751-2762.

GIRAULT, I., LEREBOURS, F., AMARIR, S., TOZLU, S., TUBIANA-HULIN, M., LIDEREAU, R. & BIECHE, I. 2003. Expression analysis of estrogen receptor alpha coregulators in breast carcinoma: evidence that NCOR1 expression is predictive of the response to tamoxifen. Clin Cancer Res, 9, 1259-66.

GIROTTI, M. R., GREMEL, G., LEE, R., GALVANI, E., ROTHWELL, D., VIROS, A., MANDAL, A. K., LIM, K. H., SATURNO, G., FURNEY, S. J., BAENKE, F., PEDERSEN, M., ROGAN, J., SWAN, J., SMITH, M., FUSI, A., OUDIT, D., DHOMEN, N., BRADY, G., LORIGAN, P., DIVE, C. & MARAIS, R. 2016. Application of Sequencing, Liquid Biopsies, and Patient-Derived Xenografts for Personalized Medicine in Melanoma. Cancer Discov, 6, 286-99.

GLAROS, S., CIRRINCIONE, G. M., MUCHARDT, C., KLEER, C. G., MICHAEL, C. W. & REISMAN, D. 2007. The reversible epigenetic silencing of BRM: implications for clinical targeted therapy. Oncogene, 26, 7058-66.

GOODMAN, L. S., WINTROBE, M. M. & ET AL., 1946. Nitrogen mustard therapy; use of methyl-bis (beta-chloroethyl) amine hydrochloride and tris (beta-chloroethyl) amine hydrochloride for Hodgkin's disease, lymphosarcoma, leukemia and certain allied and miscellaneous disorders. J Am Med Assoc, 132, 126-32.

GOZGIT, J. M., PENTECOST, B. T., MARCONI, S. A., OTIS, C. N., WU, C. & ARCARO, K. F. 2006. Use of an aggressive MCF-7 cell line variant, TMX2-28, to study cell invasion in breast cancer. Mol Cancer Res, 4, 905-13.

GRAESSMANN, M., BERG, B., FUCHS, B., KLEIN, A. & GRAESSMANN, A. 2007. Chemotherapy resistance of mouse WAP-SVT/t breast cancer cells is mediated by osteopontin, inhibiting apoptosis downstream of caspase-3. Oncogene, 26, 2840-50.

GREMEL, G., LEE, R. J., GIROTTI, M. R., MANDAL, A. K., VALPIONE, S., GARNER, G., AYUB, M., WOOD, S., ROTHWELL, D. G., FUSI, A., WALLACE, A., BRADY, G., DIVE, C., DHOMEN, N., LORIGAN, P. & MARAIS, R. 2016. Distinct subclonal tumour responses to therapy revealed by circulating cell-free DNA. Ann Oncol, 27, 1959-65.

GUERARDEL, A., BARAT-HOUARI, M., VASSEUR, F., DINA, C., VATIN, V., CLEMENT, K., EBERLE, D., VASSEUR-DELANNOY, V., BELL, C. G., GALAN, P., HERCBERG, S., HELBECQUE, N., POTOCZNA, N., HORBER, F. F., BOUTIN, P. & FROGUEL, P. 2005. Analysis of sequence variability in the CART gene in relation to obesity in a Caucasian population. BMC Genet, 6, 19.

GUTIERREZ, M. C., DETRE, S., JOHNSTON, S., MOHSIN, S. K., SHOU, J., ALLRED, D. C., SCHIFF, R., OSBORNE, C. K. & DOWSETT, M. 2005. Molecular changes in tamoxifen-resistant breast cancer: relationship between estrogen receptor, HER-2, and p38 mitogen-activated protein kinase. J Clin Oncol, 23, 2469-76.

GUTSCHNER, T., HAMMERLE, M., EISSMANN, M., HSU, J., KIM, Y., HUNG, G., REVENKO, A., ARUN, G., STENTRUP, M., GROSS, M., ZORNIG, M., MACLEOD, A. R., SPECTOR, D. L. & DIEDERICHS, S. 2013. The noncoding RNA MALAT1 is a critical regulator of the metastasis phenotype of lung cancer cells. Cancer Res, 73, 1180-9.

HALSTED, W. S. 1894. I. The Results of Operations for the Cure of Cancer of the Breast Performed at the Johns Hopkins Hospital from June, 1889, to January, 1894. Ann Surg, 20, 497-555.

HANAHAN, D. & WEINBERG, R. A. 2011. Hallmarks of cancer: the next generation. Cell, 144, 646-74.

HAQUE, A., ENGEL, J., TEICHMANN, S. A. & LÖNNBERG, T. 2017. A practical guide to single-cell RNA-sequencing for biomedical research and clinical applications. Genome Medicine, 9, 75.

HEEBOLL, S., BORRE, M., OTTOSEN, P. D., ANDERSEN, C. L., MANSILLA, F., DYRSKJOT, L., ORNTOFT, T. F. & TORRING, N. 2008. SMARCC1 expression is upregulated in prostate cancer and positively correlated with tumour recurrence and dedifferentiation. Histol Histopathol, 23, 1069-76.

HEHIR, M. P., LAURSEN, H., HIGGINS, M. F., BRENNAN, D. J., O'CONNOR, D. P. & MCAULIFFE, F. M. 2012. Maternal and fetal cocaine- and amphetamine-regulated transcript in diabetic and non-diabetic pregnancy. Gynecol Endocrinol, 28, 682-5.

HEIN, M. Y., HUBNER, N. C., POSER, I., COX, J., NAGARAJ, N., TOYODA, Y., GAK, I. A., WEISSWANGE, I., MANSFELD, J., BUCHHOLZ, F., HYMAN, A. A. & MANN, M. 2015. A human interactome in three quantitative dimensions organized by stoichiometries and abundances. Cell, 163, 712-23.

HERSCHKOWITZ, J. I., SIMIN, K., WEIGMAN, V. J., MIKAELIAN, I., USARY, J., HU, Z., RASMUSSEN, K. E., JONES, L. P., ASSEFNIA, S., CHANDRASEKHARAN, S., BACKLUND, M. G., YIN, Y., KHRAMTSOV, A. I., BASTEIN, R., QUACKENBUSH, J., GLAZER, R. I., BROWN, P. H., GREEN, J. E., KOPELOVICH, L., FURTH, P. A., PALAZZO, J. P., OLOPADE, O. I., BERNARD, P. S., CHURCHILL, G. A., VAN DYKE, T. & PEROU, C. M. 2007. Identification of conserved gene expression features between murine mammary carcinoma models and human breast tumors. Genome Biol, 8, R76.

HODGES, C., KIRKLAND, J. G. & CRABTREE, G. R. 2016. The many roles of BAF (mSWI/SNF) and PBAF complexes in cancer. Cold Spring Harbor perspectives in medicine, 6, a026930.

HODI, F. S., O'DAY, S. J., MCDERMOTT, D. F., WEBER, R. W., SOSMAN, J. A., HAANEN, J. B., GONZALEZ, R., ROBERT, C., SCHADENDORF, D., HASSEL, J. C., AKERLEY, W., VAN DEN EERTWEGH, A. J., LUTZKY, J., LORIGAN, P., VAUBEL, J. M., LINETTE, G. P., HOGG, D., OTTENSMEIER, C. H., LEBBE, C., PESCHEL, C., QUIRT, I., CLARK, J. I., WOLCHOK, J. D., WEBER, J. S., TIAN, J., YELLIN, M. J., NICHOL, G. M., HOOS, A. & URBA, W. J. 2010. Improved survival with ipilimumab in patients with metastatic melanoma. N Engl J Med, 363, 711-23.

HOLMES, M. D., CHEN, W. Y., LI, L., HERTZMARK, E., SPIEGELMAN, D. & HANKINSON, S. E. 2010. Aspirin intake and survival after breast cancer. J Clin Oncol, 28, 1467-72.

HONG, C. F., LIN, S. Y., CHOU, Y. T. & WU, C. W. 2016. MicroRNA-7 Compromises p53 Protein-dependent Apoptosis by Controlling the Expression of the Chromatin Remodeling Factor SMARCD1. J Biol Chem, 291, 1877-89.

HOU, J., ZHENG, D. Z., ZHOU, J. Y. & ZHOU, S. W. 2010. Orexigenic effect of cocaine- and amphetamine-regulated transcript (CART) after injection into hypothalamic nuclei in streptozotocin-diabetic rats. Clin Exp Pharmacol Physiol, 37, 989-95.

HOWELL, A., CUZICK, J., BAUM, M., BUZDAR, A., DOWSETT, M., FORBES, J. F., HOCTIN-BOES, G., HOUGHTON, J., LOCKER, G. Y. & TOBIAS, J. S. 2005. Results of the ATAC (Arimidex, Tamoxifen, Alone or in Combination) trial after completion of 5 years' adjuvant treatment for breast cancer. Lancet, 365, 60-2.

HOWELL, A., PIPPEN, J., ELLEDGE, R. M., MAURIAC, L., VERGOTE, I., JONES, S. E., COME, S. E., OSBORNE, C. K. & ROBERTSON, J. F. 2005. Fulvestrant versus anastrozole for the treatment of advanced breast carcinoma: a prospectively planned combined survival analysis of two multicenter trials. Cancer, 104, 236-9.

HOWELL, A., ROBERTSON, J. F., ABRAM, P., LICHINITSER, M. R., ELLEDGE, R., BAJETTA, E., WATANABE, T., MORRIS, C., WEBSTER, A., DIMERY, I. & OSBORNE, C. K. 2004. Comparison of fulvestrant versus tamoxifen for the treatment of advanced breast cancer in postmenopausal women previously untreated with endocrine therapy: a multinational, double-blind, randomized trial. J Clin Oncol, 22, 1605-13.

HSIAO, P. W., FRYER, C. J., TROTTER, K. W., WANG, W. & ARCHER, T. K. 2003. BAF60a mediates critical interactions between nuclear receptors and the BRG1 chromatin-remodeling complex for transactivation. Mol Cell Biol, 23, 6210-20.

HURTADO, A., HOLMES, K. A., ROSS-INNES, C. S., SCHMIDT, D. & CARROLL, J. S. 2011. FOXA1 is a key determinant of estrogen receptor function and endocrine response. Nat Genet, 43, 27-33.

IOANNIDES, S. J., BARLOW, P. L., ELWOOD, J. M. & PORTER, D. 2014. Effect of obesity on aromatase inhibitor efficacy in postmenopausal, hormone receptor-positive breast cancer: a systematic review. Breast Cancer Res Treat, 147, 237-48.

ISBEL, L., PROKOPUK, L., WU, H., DAXINGER, L., OEY, H., SPURLING, A., LAWTHER, A. J., HALE, M. W. & WHITELAW, E. 2016. Wiz binds active promoters and CTCF-binding sites and is required for normal behaviour in the mouse. Elife, 5.

JARHULT, J., LANDERHOLM, K., FALKMER, S., NORDENSKJOLD, M., SUNDLER, F. & WIERUP, N. 2010. First report on metastasizing small bowel carcinoids in first-degree relatives in three generations. Neuroendocrinology, 91, 318-23.

JAWORSKI, J. N., HANSEN, S. T., KUHAR, M. J. & MARK, G. P. 2008. Injection of CART (Cocaine- and Amphetamine- Regulated Transcript) peptide into the nucleus accumbens reduces cocaine self-administration in rats. Behavioural brain research, 191, 266-271.

JAWORSKI, J. N., KIMMEL, H. L., MITRANO, D. A., TALLARIDA, R. J. & KUHAR, M. J. 2007. Intra-VTA CART 55-102 reduces the locomotor effect of systemic cocaine in rats: an isobolographic analysis. Neuropeptides, 41, 65-72.

JAWORSKI, J. N., KOZEL, M. A., PHILPOT, K. B. & KUHAR, M. J. 2003. Intra-accumbal injection of CART (cocaine-amphetamine regulated transcript) peptide reduces cocaine-induced locomotor activity. J Pharmacol Exp Ther, 307, 1038-44.

JENSEN, P. B., KRISTENSEN, P., CLAUSEN, J. T., JUDGE, M. E., HASTRUP, S., THIM, L., WULFF, B. S., FOGED, C., JENSEN, J., HOLST, J. J. & MADSEN, O. D. 1999. The hypothalamic satiety peptide CART is expressed in anorectic and non-anorectic pancreatic islet tumors and in the normal islet of Langerhans. FEBS Lett, 447, 139-43.

JESELSOHN, R., BUCHWALTER, G., DE ANGELIS, C., BROWN, M. & SCHIFF, R. 2015. ESR1 mutations-a mechanism for acquired endocrine resistance in breast cancer. Nat Rev Clin Oncol, 12, 573-83.

JESELSOHN, R., YELENSKY, R., BUCHWALTER, G., FRAMPTON, G., MERIC-BERNSTAM, F., GONZALEZ-ANGULO, A. M., FERRER-LOZANO, J., PEREZ-FIDALGO, J. A., CRISTOFANILLI, M., GOMEZ, H., ARTEAGA, C. L., GILTNANE, J., BALKO, J. M., CRONIN, M. T., JAROSZ, M., SUN, J., HAWRYLUK, M., LIPSON, D., OTTO, G., ROSS, J. S., DVIR, A., SOUSSAN-GUTMAN, L., WOLF, I., RUBINEK, T., GILMORE, L., SCHNITT, S., COME, S. E., PUSZTAI, L., STEPHENS, P., BROWN, M. & MILLER, V. A. 2014. Emergence of constitutively active estrogen receptor-alpha mutations in pretreated advanced estrogen receptor-positive breast cancer. Clin Cancer Res, 20, 1757-1767.

JIA, J., CHEN, X., ZHU, W., LUO, Y., HUA, Z. & XU, Y. 2008. CART protects brain from damage through ERK activation in ischemic stroke. Neuropeptides, 42, 653-61.

JIANG, J., SARWAR, N., PESTON, D., KULINSKAYA, E., SHOUSHA, S., COOMBES, R. C. & ALI, S. 2007. Phosphorylation of estrogen receptor-alpha at Ser167 is indicative of longer disease-free and overall survival in breast cancer patients. Clin Cancer Res, 13, 5769-76.

JIRSTROM, K., RYDEN, L., ANAGNOSTAKI, L., NORDENSKJOLD, B., STAL, O., THORSTENSON, S., CHEBIL, G., JONSSON, P. E., FERNO, M. & LANDBERG, G. 2005. Pathology parameters and adjuvant tamoxifen response in a randomised premenopausal breast cancer trial. J Clin Pathol, 58, 1135-42.

JOB, M. O. & KUHAR, M. J. 2012. Intraperitoneal Administration of CART 55-102 Inhibits Psychostimulant-Induced Locomotion. J Drug Alcohol Res, 1.

JOB, M. O., PERRY, J., SHEN, L. L. & KUHAR, M. J. 2014. Cocaine-and-Amphetamine Regulated Transcript (CART) peptide attenuates dopamine- and cocaine-mediated locomotor activity in both male and female rats: lack of sex differences. Neuropeptides, 48, 75-81.

JOB, M. O., SHEN, L. L. & KUHAR, M. J. 2013. The inhibition of cocaine-induced locomotor activity by CART 55-102 is lost after repeated cocaine administration. Neurosci Lett, 550, 179-83.

JONES, D. C., LAKATOS, A., ROGGE, G. A. & KUHAR, M. J. 2009. Regulation of cocaine- and amphetamine-regulated transcript mRNA expression by calcium-mediated signaling in GH3 cells. Neuroscience, 160, 339-47.

JORDAN, V. C. 2008. Tamoxifen: catalyst for the change to targeted therapy. Eur J Cancer, 44, 30-8.

JORDAN, V. C. & DOWSE, L. J. 1976. Tamoxifen as an anti-tumour agent: effect on oestrogen binding. J Endocrinol, 68, 297-303.

JUNE, C. H., WARSHAUER, J. T. & BLUESTONE, J. A. 2017. Is autoimmunity the Achilles' heel of cancer immunotherapy? Nat Med, 23, 540-547.

KALYUGA, M., GALLEGO-ORTEGA, D., LEE, H. J., RODEN, D. L., COWLEY, M. J., CALDON, C. E., STONE, A., ALLERDICE, S. L., VALDES-MORA, F., LAUNCHBURY, R., STATHAM, A. L., ARMSTRONG, N., ALLES, M. C., YOUNG, A., EGGER, A., AU, W., PIGGIN, C. L., EVANS, C. J., LEDGER, A., BRUMMER, T., OAKES, S. R., KAPLAN, W., GEE, J. M., NICHOLSON, R. I., SUTHERLAND, R. L., SWARBRICK, A., NAYLOR, M. J., CLARK, S. J., CARROLL, J. S. & ORMANDY, C. J. 2012. ELF5 suppresses estrogen sensitivity and underpins the acquisition of antiestrogen resistance in luminal breast cancer. PLoS Biol, 10, e1001461.

KARMAKAR, S., FOSTER, E. A., BLACKMORE, J. K. & SMITH, C. L. 2011. Distinctive functions of p160 steroid receptor coactivators in proliferation of an estrogen-independent, tamoxifen-resistant breast cancer cell line. Endocrine-related cancer, 18, 113-127.

KARNIK, P. S., KULKARNI, S., LIU, X. P., BUDD, G. T. & BUKOWSKI, R. M. 1994. Estrogen receptor mutations in tamoxifen-resistant breast cancer. Cancer Res, 54, 349-53.

KAWAI, H., LI, H., CHUN, P., AVRAHAM, S. & AVRAHAM, H. K. 2002. Direct interaction between BRCA1 and the estrogen receptor regulates vascular endothelial growth factor (VEGF) transcription and secretion in breast cancer cells. Oncogene, 21, 7730-9.

KAYA, E., GOZEN, O., UGUR, M., KOYLU, E. O., KANIT, L. & BALKAN, B. 2016. Nicotine regulates cocaine-amphetamine-Regulated Transcript (Cart) in the mesocorticolimbic system. Synapse, 70, 283-92.

KIM, J. H., CREEKMORE, E. & VEZINA, P. 2003. Microinjection of CART peptide 55-102 into the nucleus accumbens blocks amphetamine-induced locomotion. Neuropeptides, 37, 369-73.

KIMMEL, H. L., GONG, W., VECHIA, S. D., HUNTER, R. G. & KUHAR, M. J. 2000. Intra-ventral tegmental area injection of rat cocaine and amphetamine-regulated transcript peptide 55-102 induces locomotor activity and promotes conditioned place preference. J Pharmacol Exp Ther, 294, 784-92.

KLINGE, C. M. 2008. Estrogenic Control of Mitochondrial Function and Biogenesis. Journal of cellular biochemistry, 105, 1342-1351.

KLOK, M. D., JAKOBSDOTTIR, S. & DRENT, M. L. 2007. The role of leptin and ghrelin in the regulation of food intake and body weight in humans: a review. Obes Rev, 8, 21-34.

KRISTENSEN, P., JUDGE, M. E., THIM, L., RIBEL, U., CHRISTJANSEN, K. N., WULFF, B. S., CLAUSEN, J. T., JENSEN, P. B., MADSEN, O. D., VRANG, N., LARSEN, P. J. & HASTRUP, S. 1998. Hypothalamic CART is a new anorectic peptide regulated by leptin. Nature, 393, 72-6.

KRUMBHAAR, E. B. & KRUMBHAAR, H. D. 1919. The Blood and Bone Marrow in Yelloe Cross Gas (Mustard Gas) Poisoning: Changes produced in the Bone Marrow of Fatal Cases. J Med Res, 40, 497-508.3.

LAKATOS, A., PRINSTER, S., VICENTIC, A., HALL, R. A. & KUHAR, M. J. 2005. Cocaine- and amphetamine-regulated transcript (CART) peptide activates the extracellular signal-regulated kinase (ERK) pathway in AtT20 cells via putative G-protein coupled receptors. Neurosci Lett, 384, 198-202.

LAMB, J., LADHA, M. H., MCMAHON, C., SUTHERLAND, R. L. & EWEN, M. E. 2000. Regulation of the functional interaction between cyclin D1 and the estrogen receptor. Mol Cell Biol, 20, 8667-75.

LAMBERT, P. D., COUCEYRO, P. R., MCGIRR, K. M., DALL VECHIA, S. E., SMITH, Y. & KUHAR, M. J. 1998. CART peptides in the central control of feeding and interactions with neuropeptide Y. Synapse, 29, 293-8.

LANDERHOLM, K., FALKMER, S. E., JARHULT, J., SUNDLER, F. & WIERUP, N. 2011. Cocaine- and amphetamine-regulated transcript in neuroendocrine tumors. Neuroendocrinology, 94, 228-36.

LANDERHOLM, K., SHCHERBINA, L., FALKMER, S. E., JARHULT, J. & WIERUP, N. 2012. Expression of cocaine- and amphetamine-regulated transcript is associated with worse survival in small bowel carcinoid tumors. Clin Cancer Res, 18, 3668-76.

LATCHMAN, D. S. 2001. Transcription factors: bound to activate or repress. Trends Biochem Sci, 26, 211-3.

LEE, R. J., GREMEL, G., MARSHALL, A., MYERS, K. A., FISHER, N., DUNN, J., DHOMEN, N., CORRIE, P. G., MIDDLETON, M. R., LORIGAN, P. & MARAIS, R. 2017. Circulating tumor DNA predicts survival in patients with resected high risk stage II/III melanoma. Ann Oncol.

LEE, S. J., VERMA, S., SIMONDS, S. E., KIRIGITI, M. A., KIEVIT, P., LINDSLEY, S. R., LOCHE, A., SMITH, M. S., COWLEY, M. A. & GROVE, K. L. 2013. Leptin stimulates neuropeptide Y and cocaine amphetamine-regulated transcript coexpressing neuronal activity in the dorsomedial hypothalamus in diet-induced obese mice. J Neurosci, 33, 15306-17.

LEO, A. D., JERUSALEM, G., PETRUZELKA, L., TORRES, R., BONDARENKO, I. N., KHASANOV, R., VERHOEVEN, D., PEDRINI, J. L., SMIRNOVA, I., LICHINITSER, M. R., PENDERGRASS, K., MALORNI, L., GARNETT, S., RUKAZENKOV, Y. & MARTIN, M. 2014. Final Overall Survival: Fulvestrant 500mg vs 250mg in the Randomized CONFIRM Trial. JNCI Journal of the National Cancer Institute, 106, djt337.

LI, B., NI CHONGHAILE, T., FAN, Y., MADDEN, S. F., KLINGER, R., O'CONNOR, A. E., WALSH, L., O'HURLEY, G., MALLYA UDUPI, G., JOSEPH, J., TARRANT, F., CONROY, E., GABER, A., CHIN, S. F., BARDWELL, H. A., PROVENZANO, E., CROWN, J., DUBOIS, T., LINN, S., JIRSTROM, K., CALDAS, C., O'CONNOR, D. P. & GALLAGHER, W. M. 2017. Therapeutic Rationale to Target Highly Expressed CDK7 Conferring Poor Outcomes in Triple-Negative Breast Cancer. Cancer Res, 77, 3834-3845.

LI, W., HU, Y., OH, S., MA, Q., MERKURJEV, D., SONG, X., ZHOU, X., LIU, Z., TANASA, B., HE, X., CHEN, A. Y., OHGI, K., ZHANG, J., LIU, W. & ROSENFELD, M. G. 2015. Condensin I and II Complexes License Full Estrogen Receptor alpha-Dependent Enhancer Activation. Mol Cell, 59, 188-202.

LIAO, Y., SMYTH, G. K. & SHI, W. 2014. featureCounts: an efficient general purpose program for assigning sequence reads to genomic features. Bioinformatics, 30, 923-30.

LIN, Y., HALL, R. A. & KUHAR, M. J. 2011. CART Peptide Stimulation of G Protein-Mediated Signaling in Differentiated PC12 Cells: Identification of PACAP 6-38 as a CART Receptor Antagonist. Neuropeptides, 45, 351-358.

LIST, H. J., LAURITSEN, K. J., REITER, R., POWERS, C., WELLSTEIN, A. & RIEGEL, A. T. 2001. Ribozyme targeting demonstrates that the nuclear receptor coactivator AIB1 is a rate-limiting factor for estrogen-dependent growth of human MCF-7 breast cancer cells. J Biol Chem, 276, 23763-8.

LIST, H. J., REITER, R., SINGH, B., WELLSTEIN, A. & RIEGEL, A. T. 2001. Expression of the nuclear coactivator AIB1 in normal and malignant breast tissue. Breast Cancer Res Treat, 68, 21-8.

LIU, H. S., SHEN, H., LUO, Y., HOFFER, B. J., WANG, Y. & YANG, Y. 2016. Post-treatment with cocaine- and amphetamine-regulated transcript enhances infarct resolution, reinnervation, and angiogenesis in stroke rats - an MRI study. NMR Biomed, 29, 361-70.

LIU, T., YU, J., DENG, M., YIN, Y., ZHANG, H., LUO, K., QIN, B., LI, Y., WU, C., REN, T., HAN, Y., YIN, P., KIM, J., LEE, S., LIN, J., ZHANG, L., ZHANG, J., NOWSHEEN, S., WANG, L., BOUGHEY, J., GOETZ, M. P., YUAN, J. & LOU, Z. 2017. CDK4/6-dependent activation of DUB3 regulates cancer metastasis through SNAIL1. Nat Commun, 8, 13923.

LOINDER, K. & SODERSTROM, M. 2004. Functional analyses of an LXXLL motif in nuclear receptor corepressor (N-CoR). J Steroid Biochem Mol Biol, 91, 191-6.

LOVE, M. I., HUBER, W. & ANDERS, S. 2014. Moderated estimation of fold change and dispersion for RNA-seq data with DESeq2. Genome Biol, 15, 550.

LOVEN, J., HOKE, H. A., LIN, C. Y., LAU, A., ORLANDO, D. A., VAKOC, C. R., BRADNER, J. E., LEE, T. I. & YOUNG, R. A. 2013. Selective inhibition of tumor oncogenes by disruption of super-enhancers. Cell, 153, 320-34.

LUO, Y., SHEN, H., LIU, H. S., YU, S. J., REINER, D. J., HARVEY, B. K., HOFFER, B. J., YANG, Y. & WANG, Y. 2013. CART peptide induces neuroregeneration in stroke rats. J Cereb Blood Flow Metab, 33, 300-10.

LV, L., JIMENEZ-KRASSEL, F., SEN, A., BETTEGOWDA, A., MONDAL, M., FOLGER, J. K., LEE, K. B., IRELAND, J. J. & SMITH, G. W. 2009. Evidence supporting a role for cocaine- and amphetamine-regulated transcript (CARTPT) in control of granulosa cell estradiol production associated with dominant follicle selection in cattle. Biol Reprod, 81, 580-6.

MA, X., HAYES, E., PRIZANT, H., SRIVASTAVA, R. K., HAMMES, S. R. & SEN, A. 2016. Leptin-Induced CART (Cocaine- and Amphetamine-Regulated Transcript) Is a Novel Intraovarian Mediator of Obesity-Related Infertility in Females. Endocrinology, 157, 1248-57.

MALOVANNAYA, A., LANZ, R. B., JUNG, S. Y., BULYNKO, Y., LE, N. T., CHAN, D. W., DING, C., SHI, Y., YUCER, N., KRENCIUTE, G., KIM, B. J., LI, C., CHEN, R., LI, W., WANG, Y., O'MALLEY, B. W. & QIN, J. 2011. Analysis of the human endogenous coregulator complexome. Cell, 145, 787-99.

MAMO, A., CAVALLONE, L., TUZMEN, S., CHABOT, C., FERRARIO, C., HASSAN, S., EDGREN, H., KALLIONIEMI, O., ALEYNIKOVA, O., PRZYBYTKOWSKI, E., MALCOLM, K., MOUSSES, S., TONIN, P. N. & BASIK, M. 2012. An integrated genomic approach identifies ARID1A as a candidate tumor-suppressor gene in breast cancer. Oncogene, 31, 2090-100.

MAO, P., ARDESHIRI, A., JACKS, R., YANG, S., HURN, P. D. & ALKAYED, N. J. 2007. Mitochondrial mechanism of neuroprotection by CART. The European journal of neuroscience, 26, 624-632.

MAO, P., MESHUL, C. K., THUILLIER, P., GOLDBERG, N. R. & REDDY, P. H. 2012. CART peptide is a potential endogenous antioxidant and preferentially localized in mitochondria. PLoS One, 7, e29343.

MASSARWEH, S., OSBORNE, C. K., CREIGHTON, C. J., QIN, L., TSIMELZON, A., HUANG, S., WEISS, H., RIMAWI, M. & SCHIFF, R. 2008. Tamoxifen resistance in breast tumors is driven by growth factor receptor signaling with repression of classic estrogen receptor genomic function. Cancer Res, 68, 826-33.

MATHEW, R., SEILER, M. P., SCANLON, S. T., MAO, A. P., CONSTANTINIDES, M. G., BERTOZZI-VILLA, C., SINGER, J. D. & BENDELAC, A. 2012. BTB-ZF factors recruit the E3 ligase cullin 3 to regulate lymphoid effector programs. Nature, 491, 618-21.

MATSEN, C. B. & NEUMAYER, L. A. 2013. Breast cancer: a review for the general surgeon. JAMA Surg, 148, 971-9.

MCCARTHY, D. J., CHEN, Y. & SMYTH, G. K. 2012. Differential expression analysis of multifactor RNA-Seq experiments with respect to biological variation. Nucleic Acids Res, 40, 4288-97.

MCDERMOTT, D. F., DRAKE, C. G., SZNOL, M., CHOUEIRI, T. K., POWDERLY, J. D., SMITH, D. C., BRAHMER, J. R., CARVAJAL, R. D., HAMMERS, H. J., PUZANOV, I., HODI, F. S., KLUGER, H.

M., TOPALIAN, S. L., PARDOLL, D. M., WIGGINTON, J. M., KOLLIA, G. D., GUPTA, A., MCDONALD, D., SANKAR, V., SOSMAN, J. A. & ATKINS, M. B. 2015. Survival, Durable Response, and Long-Term Safety in Patients With Previously Treated Advanced Renal Cell Carcinoma Receiving Nivolumab. J Clin Oncol, 33, 2013-20.

MCINERNEY, E. M., ROSE, D. W., FLYNN, S. E., WESTIN, S., MULLEN, T.-M., KRONES, A., INOSTROZA, J., TORCHIA, J., NOLTE, R. T., ASSA-MUNT, N., MILBURN, M. V., GLASS, C. K. & ROSENFELD, M. G. 1998. Determinants of coactivator LXXLL motif specificity in nuclear receptor transcriptional activation. Genes & Development, 12, 3357-3368.

MEI, S., QIN, Q., WU, Q., SUN, H., ZHENG, R., ZANG, C., ZHU, M., WU, J., SHI, X., TAING, L., LIU, T., BROWN, M., MEYER, C. A. & LIU, X. S. 2017. Cistrome Data Browser: a data portal for ChIP-Seq and chromatin accessibility data in human and mouse. Nucleic Acids Res, 45, D658-d662.

MOHAMMED, H., D'SANTOS, C., SERANDOUR, A. A., ALI, H. R., BROWN, G. D., ATKINS, A., RUEDA, O. M., HOLMES, K. A., THEODOROU, V., ROBINSON, J. L., ZWART, W., SAADI, A., ROSS-INNES, C. S., CHIN, S. F., MENON, S., STINGL, J., PALMIERI, C., CALDAS, C. & CARROLL, J. S. 2013. Endogenous purification reveals GREB1 as a key estrogen receptor regulatory factor. Cell Rep, 3, 342-9.

MOHAMMED, H., RUSSELL, I. A., STARK, R., RUEDA, O. M., HICKEY, T. E., TARULLI, G. A., SERANDOUR, A. A., BIRRELL, S. N., BRUNA, A., SAADI, A., MENON, S., HADFIELD, J., PUGH, M., RAJ, G. V., BROWN, G. D., D'SANTOS, C., ROBINSON, J. L., SILVA, G., LAUNCHBURY, R., PEROU, C. M., STINGL, J., CALDAS, C., TILLEY, W. D. & CARROLL, J. S. 2015. Progesterone receptor modulates ERalpha action in breast cancer. Nature, 523, 313-7.

MOHAMMED, H., TAYLOR, C., BROWN, G. D., PAPACHRISTOU, E. K., CARROLL, J. S. & D'SANTOS, C. S. 2016. Rapid immunoprecipitation mass spectrometry of endogenous proteins (RIME) for analysis of chromatin complexes. Nat Protoc, 11, 316-26.

MORIMOTO, L. M., WHITE, E., CHEN, Z., CHLEBOWSKI, R. T., HAYS, J., KULLER, L., LOPEZ, A. M., MANSON, J., MARGOLIS, K. L., MUTI, P. C., STEFANICK, M. L. & MCTIERNAN, A. 2002. Obesity, body size, and risk of postmenopausal breast cancer: the Women's Health Initiative (United States). Cancer Causes Control, 13, 741-51.

MORIN, R., BAINBRIDGE, M., FEJES, A., HIRST, M., KRZYWINSKI, M., PUGH, T., MCDONALD, H., VARHOL, R., JONES, S. & MARRA, M. 2008. Profiling the HeLa S3 transcriptome using randomly primed cDNA and massively parallel short-read sequencing. Biotechniques, 45, 81-94.

MORTAZAVI, A., WILLIAMS, B. A., MCCUE, K., SCHAEFFER, L. & WOLD, B. 2008. Mapping and quantifying mammalian transcriptomes by RNA-Seq. Nat Methods, 5, 621-8.

MURPHY, L. C., NIU, Y., SNELL, L. & WATSON, P. 2004. Phospho-serine-118 estrogen receptor-alpha expression is associated with better disease outcome in women treated with tamoxifen. Clin Cancer Res, 10, 5902-6.

MYERS, E., HILL, A. D., KELLY, G., MCDERMOTT, E. W., O'HIGGINS, N. J., BUGGY, Y. & YOUNG, L. S. 2005. Associations and interactions between Ets-1 and Ets-2 and coregulatory proteins, SRC-1, AIB1, and NCoR in breast cancer. Clin Cancer Res, 11, 2111-22.

NAGALAKSHMI, U., WANG, Z., WAERN, K., SHOU, C., RAHA, D., GERSTEIN, M. & SNYDER, M. 2008. The Transcriptional Landscape of the Yeast Genome Defined by RNA Sequencing. Science (New York, N.Y.), 320, 1344-1349.

NAGELOVA, V., PIRNIK, Z., ZELEZNA, B. & MALETINSKA, L. 2014. CART (cocaine- and amphetamine-regulated transcript) peptide specific binding sites in PC12 cells have characteristics of CART peptide receptors. Brain Res, 1547, 16-24.

NJIAJU, U. O. & OLOPADE, O. I. 2012. Genetic determinants of breast cancer risk: a review of current literature and issues pertaining to clinical application. Breast J, 18, 436-42.

OH, J., SOHN, D. H., KO, M., CHUNG, H., JEON, S. H. & SEONG, R. H. 2008. BAF60a interacts with p53 to recruit the SWI/SNF complex. J Biol Chem, 283, 11924-34.

ONATE, S. A., TSAI, S. Y., TSAI, M. J. & O'MALLEY, B. W. 1995. Sequence and characterization of a coactivator for the steroid hormone receptor superfamily. Science, 270, 1354-7.

O'REILLY, E. A., GUBBINS, L., SHARMA, S., TULLY, R., GUANG, M. H., WEINER-GORZEL, K., MCCAFFREY, J., HARRISON, M., FURLONG, F., KELL, M. & MCCANN, A. 2015. The fate of chemoresistance in triple negative breast cancer (TNBC). BBA Clin, 3, 257-75.

OSBORNE, C. K., BARDOU, V., HOPP, T. A., CHAMNESS, G. C., HILSENBECK, S. G., FUQUA, S. A., WONG, J., ALLRED, D. C., CLARK, G. M. & SCHIFF, R. 2003. Role of the estrogen receptor coactivator AIB1 (SRC-3) and HER-2/neu in tamoxifen resistance in breast cancer. J Natl Cancer Inst, 95, 353-61.

OSBORNE, C. K. & SCHIFF, R. 2011. Mechanisms of endocrine resistance in breast cancer. Annu Rev Med, 62, 233-47.

PAGANI, O., REGAN, M. M., WALLEY, B. A., FLEMING, G. F., COLLEONI, M., LANG, I., GOMEZ, H. L., TONDINI, C., BURSTEIN, H. J., PEREZ, E. A., CIRUELOS, E., STEARNS, V., BONNEFOI, H. R., MARTINO, S., GEYER, C. E., JR., PINOTTI, G., PUGLISI, F., CRIVELLARI, D., RUHSTALLER, T., WINER, E. P., RABAGLIO-PORETTI, M., MAIBACH, R., RUEPP, B., GIOBBIE-HURDER, A., PRICE, K. N., BERNHARD, J., LUO, W., RIBI, K., VIALE, G., COATES, A. S., GELBER, R. D., GOLDHIRSCH, A. & FRANCIS, P. A. 2014. Adjuvant exemestane with ovarian suppression in premenopausal breast cancer. N Engl J Med, 371, 107-18.

PAL, S., YUN, R., DATTA, A., LACOMIS, L., ERDJUMENT-BROMAGE, H., KUMAR, J., TEMPST, P. & SIF, S. 2003. mSin3A/histone deacetylase 2- and PRMT5-containing Brg1 complex is involved in transcriptional repression of the Myc target gene cad. Mol Cell Biol, 23, 7475-87.

PARKER, J. S., MULLINS, M., CHEANG, M. C., LEUNG, S., VODUC, D., VICKERY, T., DAVIES, S., FAURON, C., HE, X., HU, Z., QUACKENBUSH, J. F., STIJLEMAN, I. J., PALAZZO, J., MARRON, J. S., NOBEL, A. B., MARDIS, E., NIELSEN, T. O., ELLIS, M. J., PEROU, C. M. & BERNARD, P. S. 2009. Supervised risk predictor of breast cancer based on intrinsic subtypes. J Clin Oncol, 27, 1160-7.

PAVLIDES, S., TSIRIGOS, A., VERA, I., FLOMENBERG, N., FRANK, P. G., CASIMIRO, M. C., WANG, C., PESTELL, R. G., MARTINEZ-OUTSCHOORN, U. E., HOWELL, A., SOTGIA, F. & LISANTI, M. P. 2010. Transcriptional evidence for the "Reverse Warburg Effect" in human breast cancer tumor stroma and metastasis: Similarities with oxidative stress,

inflammation, Alzheimer's disease, and "Neuron-Glia Metabolic Coupling". Aging (Albany NY), 2, 185-199.

PEREIRA, B., CHIN, S.-F., RUEDA, O. M., VOLLAN, H.-K. M., PROVENZANO, E., BARDWELL, H. A., PUGH, M., JONES, L., RUSSELL, R., SAMMUT, S.-J., TSUI, D. W. Y., LIU, B., DAWSON, S.-J., ABRAHAM, J., NORTHEN, H., PEDEN, J. F., MUKHERJEE, A., TURASHVILI, G., GREEN, A. R., MCKINNEY, S., OLOUMI, A., SHAH, S., ROSENFELD, N., MURPHY, L., BENTLEY, D. R., ELLIS, I. O., PURUSHOTHAM, A., PINDER, S. E., BØRRESEN-DALE, A.-L., EARL, H. M., PHAROAH, P. D., ROSS, M. T., APARICIO, S. & CALDAS, C. 2016. The somatic mutation profiles of 2,433 breast cancers refine their genomic and transcriptomic landscapes. Nature Communications, 7, 11479.

PEROU, C. M., SORLIE, T., EISEN, M. B., VAN DE RIJN, M., JEFFREY, S. S., REES, C. A., POLLACK, J. R., ROSS, D. T., JOHNSEN, H., AKSLEN, L. A., FLUGE, O., PERGAMENSCHIKOV, A., WILLIAMS, C., ZHU, S. X., LONNING, P. E., BORRESEN-DALE, A. L., BROWN, P. O. & BOTSTEIN, D. 2000. Molecular portraits of human breast tumours. Nature, 406, 747-52.

PETRELLI, A., CAROLLO, R., CARGNELUTTI, M., IOVINO, F., CALLARI, M., CIMINO, D., TODARO, M., MANGIAPANE, L. R., GIAMMONA, A., CORDOVA, A., MONTEMURRO, F., TAVERNA, D., DAIDONE, M. G., STASSI, G. & GIORDANO, S. 2015. By promoting cell differentiation, miR-100 sensitizes basal-like breast cancer stem cells to hormonal therapy. Oncotarget, 6, 2315-2330.

PETRUCELLI, N., DALY, M. B. & FELDMAN, G. L. 2010. Hereditary breast and ovarian cancer due to mutations in BRCA1 and BRCA2. Genetics In Medicine, 12, 245.

PFISTER, N. T., FOMIN, V., REGUNATH, K., ZHOU, J. Y., ZHOU, W., SILWAL-PANDIT, L., FREED-PASTOR, W. A., LAPTENKO, O., NEO, S. P., BARGONETTI, J., HOQUE, M., TIAN, B., GUNARATNE, J., ENGEBRAATEN, O., MANLEY, J. L., BORRESEN-DALE, A. L., NEILSEN, P. M. & PRIVES, C. 2015. Mutant p53 cooperates with the SWI/SNF chromatin remodeling complex to regulate VEGFR2 in breast cancer cells. Genes Dev, 29, 1298-315.

PLEVIN, M. J., MILLS, M. M. & IKURA, M. 2005. The LxxLL motif: a multifunctional binding sequence in transcriptional regulation. Trends Biochem Sci, 30, 66-9.

PRAT, A., PARKER, J. S., KARGINOVA, O., FAN, C., LIVASY, C., HERSCHKOWITZ, J. I., HE, X. & PEROU, C. M. 2010. Phenotypic and molecular characterization of the claudin-low intrinsic subtype of breast cancer. Breast Cancer Res, 12, R68.

PRATT, W. B. & TOFT, D. O. 1997. Steroid receptor interactions with heat shock protein and immunophilin chaperones. Endocr Rev, 18, 306-60.

QIN, L., LIU, Z., CHEN, H. & XU, J. 2009. The steroid receptor coactivator-1 regulates twist expression and promotes breast cancer metastasis. Cancer Res, 69, 3819-27.

QING, K. & CHEN, Y. 2007. Central CART gene delivery by recombinant AAV vector attenuates body weight gain in diet-induced-obese rats. Regul Pept, 140, 21-6.

QUÉNET, D., MCNALLY, J. G. & DALAL, Y. 2012. Through thick and thin: the conundrum of chromatin fibre folding in vivo. EMBO Reports, 13, 943-944.

RAJENDRAN, B. K. & DENG, C. X. 2017. Characterization of potential driver mutations involved in human breast cancer by computational approaches. Oncotarget, 8, 50252-50272.

RAMACHANDRAN, R., BECH, P., MURPHY, K. G., CAPLIN, M. E., PATEL, M., VOHRA, S., KHAN, M. S., DHILLO, W. S., SHARMA, R., PALAZZO, F. F., WIN, Z., TAN, T., KHOO, B., MEERAN, K., FRILLING, A., GHATEI, M. A., BLOOM, S. R. & MARTIN, N. M. 2015. Comparison of the utility of Cocaine- and Amphetamine-Regulated Transcript (CART), chromogranin A, and chromogranin B in neuroendocrine tumor diagnosis and assessment of disease progression. J Clin Endocrinol Metab, 100, 1520-8.

RANPURA, V., HAPANI, S. & WU, S. 2011. Treatment-related mortality with bevacizumab in cancer patients: a meta-analysis. Jama, 305, 487-94.

REDMOND, A. M., BANE, F. T., STAFFORD, A. T., MCILROY, M., DILLON, M. F., CROTTY, T. B., HILL, A. D. & YOUNG, L. S. 2009. Coassociation of estrogen receptor and p160 proteins predicts resistance to endocrine treatment; SRC-1 is an independent predictor of breast cancer recurrence. Clin Cancer Res, 15, 2098-106.

REINERT, T., SAAD, E. D., BARRIOS, C. H. & BINES, J. 2017. Clinical Implications of ESR1 Mutations in Hormone Receptor-Positive Advanced Breast Cancer. Frontiers in Oncology, 7, 26.

REISMAN, D. N., SCIARROTTA, J., WANG, W., FUNKHOUSER, W. K. & WEISSMAN, B. E. 2003. Loss of BRG1/BRM in human lung cancer cell lines and primary lung cancers: correlation with poor prognosis. Cancer Res, 63, 560-6.

RENEHAN, A. G., SOERJOMATARAM, I., TYSON, M., EGGER, M., ZWAHLEN, M., COEBERGH, J. W. & BUCHAN, I. 2010. Incident cancer burden attributable to excess body mass index in 30 European countries. Int J Cancer, 126, 692-702.

RINGNÉR, M., FREDLUND, E., HÄKKINEN, J., BORG, Å. & STAAF, J. 2011. GOBO: Gene Expression-Based Outcome for Breast Cancer Online. PLoS ONE, 6, e17911.

ROBERTS, C. W. & BIEGEL, J. A. 2009. The role of SMARCB1/INI1 in development of rhabdoid tumor. Cancer Biol Ther, 8, 412-6.

ROBINSON, D. R., WU, Y. M., VATS, P., SU, F., LONIGRO, R. J., CAO, X., KALYANA-SUNDARAM, S., WANG, R., NING, Y., HODGES, L., GURSKY, A., SIDDIQUI, J., TOMLINS, S. A., ROYCHOWDHURY, S., PIENTA, K. J., KIM, S. Y., ROBERTS, J. S., RAE, J. M., VAN POZNAK, C. H., HAYES, D. F., CHUGH, R., KUNJU, L. P., TALPAZ, M., SCHOTT, A. F. & CHINNAIYAN, A. M. 2013. Activating ESR1 mutations in hormone-resistant metastatic breast cancer. Nat Genet, 45, 1446-51.

ROBINSON, M. D., MCCARTHY, D. J. & SMYTH, G. K. 2010. edgeR: a Bioconductor package for differential expression analysis of digital gene expression data. Bioinformatics, 26, 139-40.

ROGGE, G., JONES, D., HUBERT, G. W., LIN, Y. & KUHAR, M. J. 2008. CART peptides: regulators of body weight, reward and other functions. Nat Rev Neurosci, 9, 747-58.

ROGGE, G. A., SHEN, L.-L. & KUHAR, M. J. 2010. Chromatin immunoprecipitation assays revealed CREB and serine 133 phospho-CREB binding to the CART gene proximal promoter. Brain research, 1344, 1-12.

ROSS-INNES, C. S., STARK, R., TESCHENDORFF, A. E., HOLMES, K. A., ALI, H. R., DUNNING, M. J., BROWN, G. D., GOJIS, O., ELLIS, I. O., GREEN, A. R., ALI, S., CHIN, S. F., PALMIERI, C., CALDAS, C. & CARROLL, J. S. 2012. Differential oestrogen receptor binding is associated with clinical outcome in breast cancer. Nature, 481, 389-93.

SABNIS, G. J., GOLOUBEVA, O., CHUMSRI, S., NGUYEN, N., SUKUMAR, S. & BRODIE, A. M. H. 2011. Functional activation of the estrogen receptor-α and aromatase by the HDAC inhibitor, entinostat, sensitizes of ER-negative tumors to letrozole. Cancer research, 71, 1893-1903.

SARNOWSKA, E., GRATKOWSKA, D. M., SACHAROWSKI, S. P., CWIEK, P., TOHGE, T., FERNIE, A. R., SIEDLECKI, J. A., KONCZ, C. & SARNOWSKI, T. J. 2016. The Role of SWI/SNF Chromatin Remodeling Complexes in Hormone Crosstalk. Trends Plant Sci, 21, 594-608.

SARWAR, N., KIM, J. S., JIANG, J., PESTON, D., SINNETT, H. D., MADDEN, P., GEE, J. M., NICHOLSON, R. I., LYKKESFELDT, A. E., SHOUSHA, S., COOMBES, R. C. & ALI, S. 2006. Phosphorylation of ERalpha at serine 118 in primary breast cancer and in tamoxifen-resistant tumours is indicative of a complex role for ERalpha phosphorylation in breast cancer progression. Endocr Relat Cancer, 13, 851-61.

SATHANOORI, R., OLDE, B., ERLINGE, D., GÖRANSSON, O. & WIERUP, N. 2013. Cocaine- and Amphetamine-regulated Transcript (CART) Protects Beta Cells against Glucotoxicity and Increases Cell Proliferation. The Journal of Biological Chemistry, 288, 3208-3218.

SCHAUFELE, F., CHANG, C. Y., LIU, W., BAXTER, J. D., NORDEEN, S. K., WAN, Y., DAY, R. N. & MCDONNELL, D. P. 2000. Temporally distinct and ligand-specific recruitment of nuclear receptor-interacting peptides and cofactors to subnuclear domains containing the estrogen receptor. Mol Endocrinol, 14, 2024-39.

SCHIFF, R., MASSARWEH, S. A., SHOU, J., BHARWANI, L., MOHSIN, S. K. & OSBORNE, C. K. 2004. Cross-talk between estrogen receptor and growth factor pathways as a molecular target for overcoming endocrine resistance. Clin Cancer Res, 10, 331s-6s.

SEN, A., BETTEGOWDA, A., JIMENEZ-KRASSEL, F., IRELAND, J. J. & SMITH, G. W. 2007. Cocaine- and amphetamine-regulated transcript regulation of follicle-stimulating hormone signal transduction in bovine granulosa cells. Endocrinology, 148, 4400-10.

SHADEO, A., CHARI, R., LONERGAN, K. M., PUSIC, A., MILLER, D., EHLEN, T., VAN NIEKERK, D., MATISIC, J., RICHARDS-KORTUM, R., FOLLEN, M., GUILLAUD, M., LAM, W. L. & MACAULAY, C. 2008. Up regulation in gene expression of chromatin remodelling factors in cervical intraepithelial neoplasia. BMC Genomics, 9, 64.

SHCHERBINA, L., EDLUND, A., ESGUERRA, J. L., ABELS, M., ZHOU, Y., OTTOSSON-LAAKSO, E., WOLLHEIM, C. B., HANSSON, O., ELIASSON, L. & WIERUP, N. 2017. Endogenous beta-cell CART regulates insulin secretion and transcription of beta-cell genes. Mol Cell Endocrinol, 447, 52-60.

SHEN, J., XIAO, Z., WU, W. K., WANG, M. H., TO, K. F., CHEN, Y., YANG, W., LI, M. S., SHIN, V. Y., TONG, J. H., KANG, W., ZHANG, L., LI, M., WANG, L., LU, L., CHAN, R. L., WONG, S. H., YU,

J., CHAN, M. T., CHAN, F. K., SUNG, J. J., CHENG, A. S. & CHO, C. H. 2015. Epigenetic silencing of miR-490-3p reactivates the chromatin remodeler SMARCD1 to promote Helicobacter pylori-induced gastric carcinogenesis. Cancer Res, 75, 754-65.

SHEN, J., XIAO, Z., WU, W. K., WANG, M. H., TO, K. F., CHEN, Y., YANG, W., LI, M. S., SHIN, V. Y., TONG, J. H., KANG, W., ZHANG, L., LI, M., WANG, L., LU, L., CHAN, R. L., WONG, S. H., YU, J., CHAN, M. T., CHAN, F. K., SUNG, J. J., CHENG, A. S. & CHO, C. H. 2015. Epigenetic silencing of miR-490-3p reactivates the chromatin remodeler SMARCD1 to promote Helicobacter pylori-induced gastric carcinogenesis. Cancer Res, 75, 754-65.

SIMON, J. M., PARKER, J. S., LIU, F., ROTHBART, S. B., AIT-SI-ALI, S., STRAHL, B. D., JIN, J., DAVIS, I. J., MOSLEY, A. L. & PATTENDEN, S. G. 2015. A Role for Widely Interspaced Zinc Finger (WIZ) in Retention of the G9a Methyltransferase on Chromatin. The Journal of Biological Chemistry, 290, 26088-26102.

SINGHAI, R., PATIL, V. W., JAISWAL, S. R., PATIL, S. D., TAYADE, M. B. & PATIL, A. V. 2011. E-Cadherin as a diagnostic biomarker in breast cancer. N Am J Med Sci, 3, 227-33.

SINGLETARY, S. E., PATEL-PAREKH, L. & BLAND, K. I. 2005. Treatment trends in early-stage invasive lobular carcinoma: a report from the National Cancer Data Base. Ann Surg, 242, 281-9.

SKAAR, J. R., PAGAN, J. K. & PAGANO, M. 2014. SCF ubiquitin ligase-targeted therapies. Nat Rev Drug Discov, 13, 889-903.

SLATTERY, M. L., LUNDGREEN, A., HINES, L., WOLFF, R. K., TORRES-MEJIA, G., BAUMGARTNER, K. N. & JOHN, E. M. 2015. Energy homeostasis genes and breast cancer risk: The influence of ancestry, body size, and menopausal status, the breast cancer health disparities study. Cancer epidemiology, 39, 1113-1122.

SMITH, C. L., NAWAZ, Z. & O'MALLEY, B. W. 1997. Coactivator and corepressor regulation of the agonist/antagonist activity of the mixed antiestrogen, 4-hydroxytamoxifen. Mol Endocrinol, 11, 657-66.

SORLIE, T., PEROU, C. M., TIBSHIRANI, R., AAS, T., GEISLER, S., JOHNSEN, H., HASTIE, T., EISEN, M. B., VAN DE RIJN, M., JEFFREY, S. S., THORSEN, T., QUIST, H., MATESE, J. C., BROWN, P. O., BOTSTEIN, D., LONNING, P. E. & BORRESEN-DALE, A. L. 2001. Gene expression patterns of breast carcinomas distinguish tumor subclasses with clinical implications. Proc Natl Acad Sci U S A, 98, 10869-74.

SORLIE, T., TIBSHIRANI, R., PARKER, J., HASTIE, T., MARRON, J. S., NOBEL, A., DENG, S., JOHNSEN, H., PESICH, R., GEISLER, S., DEMETER, J., PEROU, C. M., LONNING, P. E., BROWN, P. O., BORRESEN-DALE, A. L. & BOTSTEIN, D. 2003. Repeated observation of breast tumor subtypes in independent gene expression data sets. Proc Natl Acad Sci U S A, 100, 8418-23.

SOTIRIOU, C., NEO, S. Y., MCSHANE, L. M., KORN, E. L., LONG, P. M., JAZAERI, A., MARTIAT, P., FOX, S. B., HARRIS, A. L. & LIU, E. T. 2003. Breast cancer classification and prognosis based on gene expression profiles from a population-based study. Proc Natl Acad Sci U S A, 100, 10393-8.

SPARANO, J. A., GRAY, R. J., MAKOWER, D. F., PRITCHARD, K. I., ALBAIN, K. S., HAYES, D. F., GEYER, C. E., JR., DEES, E. C., PEREZ, E. A., OLSON, J. A., JR., ZUJEWSKI, J., LIVELY, T., BADVE, S. S., SAPHNER, T. J., WAGNER, L. I., WHELAN, T. J., ELLIS, M. J., PAIK, S., WOOD, W. C.,

RAVDIN, P., KEANE, M. M., GOMEZ MORENO, H. L., REDDY, P. S., GOGGINS, T. F., MAYER, I. A., BRUFSKY, A. M., TOPPMEYER, D. L., KAKLAMANI, V. G., ATKINS, J. N., BERENBERG, J. L. & SLEDGE, G. W. 2015. Prospective Validation of a 21-Gene Expression Assay in Breast Cancer. N Engl J Med, 373, 2005-14.

SPARANO, J. A. & PAIK, S. 2008. Development of the 21-gene assay and its application in clinical practice and clinical trials. J Clin Oncol, 26, 721-8.

STEIN, J., SHAH, R., STEINER, D. F. & DEY, A. 2006. RNAi-mediated silencing of prohormone convertase (PC) 5/6 expression leads to impairment in processing of cocaine- and amphetamine-regulated transcript (CART) precursor. Biochem J, 400, 209-15.

STEIN, J., STEINER, D. F. & DEY, A. 2006. Processing of cocaine- and amphetamine-regulated transcript (CART) precursor proteins by prohormone convertases (PCs) and its implications. Peptides, 27, 1919-25.

STEINBERG, M. D., JULIANO, M. A. & WISE, L. 1985. Psychological outcome of lumpectomy versus mastectomy in the treatment of breast cancer. Am J Psychiatry, 142, 34-9.

STREUBEL, G., FITZPATRICK, D. J., OLIVIERO, G., SCELFO, A., MORAN, B., DAS, S., MUNAWAR, N., WATSON, A., WYNNE, K., NEGRI, G. L., DILLON, E. T., JAMMULA, S., HOKAMP, K., O'CONNOR, D. P., PASINI, D., CAGNEY, G. & BRACKEN, A. P. 2017. Fam60a defines a variant Sin3a-Hdac complex in embryonic stem cells required for self-renewal. Embo j, 36, 2216-2232.

SU, Q., HU, S., GAO, H., MA, R., YANG, Q., PAN, Z., WANG, T. & LI, F. 2008. Role of AIB1 for tamoxifen resistance in estrogen receptor-positive breast cancer cells. Oncology, 75, 159-68.

SUN, A., TAWFIK, O., GAYED, B., THRASHER, J. B., HOESTJE, S., LI, C. & LI, B. 2007. Aberrant expression of SWI/SNF catalytic subunits BRG1/BRM is associated with tumor development and increased invasiveness in prostate cancers. Prostate, 67, 203-13.

SUN, X., WANG, S. C., WEI, Y., LUO, X., JIA, Y., LI, L., GOPAL, P., ZHU, M., NASSOUR, I., CHUANG, J. C., MAPLES, T., CELEN, C., NGUYEN, L. H., WU, L., FU, S., LI, W., HUI, L., TIAN, F., JI, Y., ZHANG, S., SOROURI, M., HWANG, T. H., LETZIG, L., JAMES, L., WANG, Z., YOPP, A. C., SINGAL, A. G. & ZHU, H. 2017. Arid1a Has Context-Dependent Oncogenic and Tumor Suppressor Functions in Liver Cancer. Cancer Cell, 32, 574-589.e6.

SWAIN, S. M., KIM, S. B., CORTES, J., RO, J., SEMIGLAZOV, V., CAMPONE, M., CIRUELOS, E., FERRERO, J. M., SCHNEEWEISS, A., KNOTT, A., CLARK, E., ROSS, G., BENYUNES, M. C. & BASELGA, J. 2013. Pertuzumab, trastuzumab, and docetaxel for HER2-positive metastatic breast cancer (CLEOPATRA study): overall survival results from a randomised, double-blind, placebo-controlled, phase 3 study. Lancet Oncol, 14, 461-71.

SZKLARCZYK, D., MORRIS, J. H., COOK, H., KUHN, M., WYDER, S., SIMONOVIC, M., SANTOS, A., DONCHEVA, N. T., ROTH, A., BORK, P., JENSEN, L. J. & VON MERING, C. 2017. The STRING database in 2017: quality-controlled protein-protein association networks, made broadly accessible. Nucleic Acids Res, 45, D362-d368.

THIM, L., KRISTENSEN, P., NIELSEN, P. F., WULFF, B. S. & CLAUSEN, J. T. 1999. Tissue-specific processing of cocaine- and amphetamine-regulated transcript peptides in the rat. Proc Natl Acad Sci U S A, 96, 2722-7.

TING, H. J., BAO, B. Y., HSU, C. L. & LEE, Y. F. 2005. Androgen-receptor coregulators mediate the suppressive effect of androgen signals on vitamin D receptor activity. Endocrine, 26, 1-9.

TOYOSHIMA, M., ASAKAWA, A., FUJIMIYA, M., INOUE, K., INOUE, S., KINBOSHI, M. & KOIZUMI, A. 2007. Dimorphic gene expression patterns of anorexigenic and orexigenic peptides in hypothalamus account male and female hyperphagia in Akita type 1 diabetic mice. Biochem Biophys Res Commun, 352, 703-8.

TRAN, B. & BEDARD, P. L. 2011. Luminal-B breast cancer and novel therapeutic targets. Breast Cancer Res, 13, 221.

TRAVIS, R. C. & KEY, T. J. 2003. Oestrogen exposure and breast cancer risk. Breast Cancer Res, 5, 239-47.

TROTTER, K. W. & ARCHER, T. K. 2008. The BRG1 transcriptional coregulator. Nucl Recept Signal, 6, e004.

TYANOVA, S., TEMU, T. & COX, J. 2016. The MaxQuant computational platform for mass spectrometry-based shotgun proteomics. Nat Protoc, 11, 2301-2319.

TYANOVA, S., TEMU, T., SINITCYN, P., CARLSON, A., HEIN, M. Y., GEIGER, T., MANN, M. & COX, J. 2016. The Perseus computational platform for comprehensive analysis of (prote)omics data. Nat Methods, 13, 731-40.

UPADHYA, M. A., SHELKAR, G. P., SUBHEDAR, N. K. & KOKARE, D. M. 2016. CART modulates the effects of levodopa in rat model of Parkinson's disease. Behav Brain Res, 301, 262-72.

VIEDMA-RODRIGUEZ, R., BAIZA-GUTMAN, L., SALAMANCA-GOMEZ, F., DIAZ-ZARAGOZA, M., MARTINEZ-HERNANDEZ, G., RUIZ ESPARZA-GARRIDO, R., VELAZQUEZ-FLORES, M. A. & ARENAS-ARANDA, D. 2014. Mechanisms associated with resistance to tamoxifen in estrogen receptor-positive breast cancer (review). Oncol Rep, 32, 3-15.

VILARINO-VARELA, M., CHIN, Y. S. & MAKRIS, A. 2009. Current indications for post-mastectomy radiation. Int Semin Surg Oncol, 6, 5.

WALSH, C. A., QIN, L., TIEN, J. C.-Y., YOUNG, L. S. & XU, J. 2012. The Function of Steroid Receptor Coactivator-1 in Normal Tissues and Cancer. International Journal of Biological Sciences, 8, 470-485.

WANG, C., FAN, S., LI, Z., FU, M., RAO, M., MA, Y., LISANTI, M. P., ALBANESE, C., KATZENELLENBOGEN, B. S., KUSHNER, P. J., WEBER, B., ROSEN, E. M. & PESTELL, R. G. 2005. Cyclin D1 antagonizes BRCA1 repression of estrogen receptor alpha activity. Cancer Res, 65, 6557-67.

WANG, W. 2013. Radiotherapy in the management of early breast cancer. J Med Radiat Sci, 60, 40-6.

WANG, X., LI, J., DUAN, Y., WU, H., XU, Q. & ZHANG, Y. 2017. Whole genome sequencing analysis of lung adenocarcinoma in Xuanwei, China. Thorac Cancer, 8, 88-96.

WANG, Y., QIU, B., LIU, J., ZHU, W. G. & ZHU, S. 2014. Cocaine- and amphetamine-regulated transcript facilitates the neurite outgrowth in cortical neurons after oxygen and glucose deprivation through PTN-dependent pathway. Neuroscience, 277, 103-10.

WANG, Y., ZHANG, T., KWIATKOWSKI, N., ABRAHAM, B. J., LEE, T. I., XIE, S., YUZUGULLU, H., VON, T., LI, H., LIN, Z., STOVER, D. G., LIM, E., WANG, Z. C., IGLEHART, J. D., YOUNG, R. A., GRAY, N. S. & ZHAO, J. J. 2015. CDK7-dependent transcriptional addiction in triple-negative breast cancer. Cell, 163, 174-86.

WANG, Z., GERSTEIN, M. & SNYDER, M. 2009. RNA-Seq: a revolutionary tool for transcriptomics. Nature reviews. Genetics, 10, 57-63.

WARBURG, O., WIND, F. & NEGELEIN, E. 1927. THE METABOLISM OF TUMORS IN THE BODY. J Gen Physiol, 8, 519-30.

WEIGELT, B., MACKAY, A., A'HERN, R., NATRAJAN, R., TAN, D. S., DOWSETT, M., ASHWORTH, A. & REIS-FILHO, J. S. 2010. Breast cancer molecular profiling with single sample predictors: a retrospective analysis. Lancet Oncol, 11, 339-49.

WEINER, M., SKOOG, L., FORNANDER, T., NORDENSKJÖLD, B., SGROI, D. C. & STÅL, O. 2013. Oestrogen receptor co-activator AIB1 is a marker of tamoxifen benefit in postmenopausal breast cancer. Annals of Oncology, 24, 1994-1999.

WEISSMAN, B. & KNUDSEN, K. E. 2009. Hijacking the chromatin remodeling machinery: impact of SWI/SNF perturbations in cancer. Cancer Res, 69, 8223-30.

WHITFIELD, M. L., SHERLOCK, G., SALDANHA, A. J., MURRAY, J. I., BALL, C. A., ALEXANDER, K. E., MATESE, J. C., PEROU, C. M., HURT, M. M., BROWN, P. O. & BOTSTEIN, D. 2002. Identification of Genes Periodically Expressed in the Human Cell Cycle and Their Expression in Tumors. Molecular Biology of the Cell, 13, 1977-2000.

WIERUP, N., BJORKQVIST, M., KUHAR, M. J., MULDER, H. & SUNDLER, F. 2006. CART regulates islet hormone secretion and is expressed in the beta-cells of type 2 diabetic rats. Diabetes, 55, 305-11.

WIERUP, N., KUHAR, M., NILSSON, B. O., MULDER, H., EKBLAD, E. & SUNDLER, F. 2004. Cocaine- and amphetamine-regulated transcript (CART) is expressed in several islet cell types during rat development. J Histochem Cytochem, 52, 169-77.

WIERUP, N., RICHARDS, W. G., BANNON, A. W., KUHAR, M. J., AHREN, B. & SUNDLER, F. 2005. CART knock out mice have impaired insulin secretion and glucose intolerance, altered beta cell morphology and increased body weight. Regul Pept, 129, 203-11.

WILHELM, B. T., MARGUERAT, S., WATT, S., SCHUBERT, F., WOOD, V., GOODHEAD, I., PENKETT, C. J., ROGERS, J. & BAHLER, J. 2008. Dynamic repertoire of a eukaryotic transcriptome surveyed at single-nucleotide resolution. Nature, 453, 1239-43.

WOLCHOK, J. D., KLUGER, H., CALLAHAN, M. K., POSTOW, M. A., RIZVI, N. A., LESOKHIN, A. M., SEGAL, N. H., ARIYAN, C. E., GORDON, R. A., REED, K., BURKE, M. M., CALDWELL, A., KRONENBERG, S. A., AGUNWAMBA, B. U., ZHANG, X., LOWY, I., INZUNZA, H. D., FEELY, W., HORAK, C. E., HONG, Q., KORMAN, A. J., WIGGINTON, J. M., GUPTA, A. & SZNOL, M. 2013. Nivolumab plus ipilimumab in advanced melanoma. N Engl J Med, 369, 122-33.

WU, J. N. & ROBERTS, C. W. M. 2013. ARID1A Mutations in Cancer: Another Epigenetic Tumor Suppressor? Cancer discovery, 3, 35-43.

WU, L., WU, Y., GATHINGS, B., WAN, M., LI, X., GRIZZLE, W., LIU, Z., LU, C., MAO, Z. & CAO, X. 2003. Smad4 as a transcription corepressor for estrogen receptor alpha. J Biol Chem, 278, 15192-200.

XU, Y., ZHANG, W., KLAUS, J., YOUNG, J., KOERNER, I., SHELDAHL, L. C., HURN, P. D., MARTINEZ-MURILLO, F. & ALKAYED, N. J. 2006. Role of cocaine- and amphetamine-regulated transcript in estradiol-mediated neuroprotection. Proc Natl Acad Sci U S A, 103, 14489-94.

YAMASHITA, H., NISHIO, M., TOYAMA, T., SUGIURA, H., KONDO, N., KOBAYASHI, S., FUJII, Y. & IWASE, H. 2008. Low phosphorylation of estrogen receptor alpha (ERalpha) serine 118 and high phosphorylation of ERalpha serine 167 improve survival in ER-positive breast cancer. Endocr Relat Cancer, 15, 755-63.

YANG, Y. S., KORNELIUS, E., CHIOU, J. Y., LAI, Y. R., LO, S. C., PENG, C. H. & HUANG, C. N. 2017. Low-Dose Aspirin Reduces Breast Cancer Risk in Women with Diabetes: A Nationwide Retrospective Cohort Study in Taiwan. J Womens Health (Larchmt).

YANIK, T., DOMINGUEZ, G., KUHAR, M. J., DEL GIUDICE, E. M. & LOH, Y. P. 2006. The Leu34Phe ProCART mutation leads to cocaine- and amphetamine-regulated transcript (CART) deficiency: a possible cause for obesity in humans. Endocrinology, 147, 39-43.

YERMOLAIEVA, O., CHEN, J., COUCEYRO, P. R. & HOSHI, T. 2001. Cocaine- and amphetamine-regulated transcript peptide modulation of voltage-gated Ca2+ signaling in hippocampal neurons. J Neurosci, 21, 7474-80.

YU, C. H., CHU, S. C., CHEN, P. N., HSIEH, Y. S. & KUO, D. Y. 2017. Participation of ghrelin signalling in the reciprocal regulation of hypothalamic NPY/POMC-mediated appetite control in amphetamine-treated rats. Appetite, 113, 30-40.

YUAN, J., HEGDE, P. S., CLYNES, R., FOUKAS, P. G., HARARI, A., KLEEN, T. O., KVISTBORG, P., MACCALLI, C., MAECKER, H. T., PAGE, D. B., ROBINS, H., SONG, W., STACK, E. C., WANG, E., WHITESIDE, T. L., ZHAO, Y., ZWIERZINA, H., BUTTERFIELD, L. H. & FOX, B. A. 2016. Novel technologies and emerging biomarkers for personalized cancer immunotherapy. J Immunother Cancer, 4, 3.

ZHANG, F., WANG, Y., WANG, L., LUO, X., HUANG, K., WANG, C., DU, M., LIU, F., LUO, T., HUANG, D. & HUANG, K. 2013. Poly(ADP-ribose) polymerase 1 is a key regulator of estrogen receptor alpha-dependent gene transcription. J Biol Chem, 288, 11348-57.

ZHANG, Q. X., BORG, A., WOLF, D. M., OESTERREICH, S. & FUQUA, S. A. 1997. An estrogen receptor mutant with strong hormone-independent activity from a metastatic breast cancer. Cancer Res, 57, 1244-9.

ZHANG, X., ZHANG, Y., YANG, Y., NIU, M., SUN, S., JI, H., MA, Y., YAO, G., JIANG, Y., SHAN, M., ZHANG, G. & PANG, D. 2012. Frequent low expression of chromatin remodeling gene ARID1A in breast cancer and its clinical significance. Cancer Epidemiol, 36, 288-93.

ZHOU, W. & SLINGERLAND, J. M. 2014. Links between oestrogen receptor activation and proteolysis: relevance to hormone-regulated cancer therapy. Nat Rev Cancer, 14, 26-38.

ZHOU, W., SRINIVASAN, S., NAWAZ, Z. & SLINGERLAND, J. M. 2014. ERalpha, SKP2 and E2F-1 form a feed forward loop driving late ERalpha targets and G1 cell cycle progression. Oncogene, 33, 2341-53.

ZHOU, X., LIU, S., CAI, G., KONG, L., ZHANG, T., REN, Y., WU, Y., MEI, M., ZHANG, L. & WANG, X. 2015. Long Non Coding RNA MALAT1 Promotes Tumor Growth and Metastasis by inducing Epithelial-Mesenchymal Transition in Oral Squamous Cell Carcinoma. Scientific Reports, 5, 15972.

ZHU, P., BAEK, S. H., BOURK, E. M., OHGI, K. A., GARCIA-BASSETS, I., SANJO, H., AKIRA, S., KOTOL, P. F., GLASS, C. K., ROSENFELD, M. G. & ROSE, D. W. 2006. Macrophage/cancer cell interactions mediate hormone resistance by a nuclear receptor derepression pathway. Cell, 124, 615-29.